HEAVY METAL/POLYACID INTERACTION

An electrochemical study of the binding of Cd(II), Pb(II) and Zn(II) to polycarboxylic and humic acids

Promotor: dr. J. Lyklema
hoogleraar in de fysische en kolloïdchemie
Co-promotor: dr. H.P. van Leeuwen
hoofdmedewerker

Rob. F.M.J. Cleven

HEAVY METAL/POLYACID INTERACTION

An electrochemical study of the binding of Cd(II), Pb(II) and Zn(II) to polycarboxylic and humic acids

Proefschrift
ter verkrijging van de graad van
doctor in de landbouwwetenschappen,
op gezag van de rector magnificus,
dr. C.C. Oosterlee,
in het openbaar te verdedigen
op vrijdag 26 oktober 1984
des namiddags te vier uur in de aula
van de Landbouwhogeschool te Wageningen

STELLINGEN

1. Polyelectrolyteffecten dragen substantieel bij tot de binding van zware-metaalionen aan humuszuren onder natuurlijke omstandigheden.

   Dit proefschrift, hoofdstuk 7.

2. De beide modellen, door Buscall & Corner gehanteerd voor de interpretatie van de concentratieafhankelijkheid van de schijnbare dissociatieconstante van respectievelijk polyacrylzuur in oplossing en polyacrylzuur aan polystyreenlatex gebonden, bevatten essentiële onjuistheden.

   Buscall, R. & Corner, T., 1982. Polyelectrolyte stabilised latices. Part 2: Characterisation and colloidal behaviour. Colloids and Surfaces 5: 333-351.

3. Bij het verklaren van de verschillen in viscositeitsgemiddelde molekuulmassa's van metaal-fulvinezuurcomplexen bij diverse metaal/fulvinezuur concentratieverhoudingen, gaan Ghosh & Schnitzer ten onrechte voorbij aan de invloed van de hoeveelheid gebonden metaalionen.

   Ghosh, K. & Schnitzer, M., 1981. Fluorescence excitation spectra and viscosity behavior of a fulvic acid and its copper and iron complexes. Soil Sci. Soc. Am. J. 45: 25-29.

4. De door Anderson & Sioda gegeven verklaring van de effectiviteit van elektrolytische preconcentratie van metalen is onvoldoende onderbouwd, en is zeker niet van toepassing bij gebruik van kwikelektroden.

   Anderson, J.L. & Sioda, R.E., 1983. Electro-deposition as a preconcentration step in analysis of multicomponent solutions of metallic ions. Talanta 30: 627-629.

5. Vanwege de posities van de elektroden en de afwezigheid van een voorziening om elektrodepolarisatie-effecten te bepalen, is de methode van Carius & Dobiás niet geschikt voor nauwkeurige meting van stromingsstromen.

   Carius, W. & Dobiás, B., 1981. Semi-automatic apparatus for the measurement of streaming potential and streaming current. Colloid & Polymer Sci. 259: 470-471.

6. De correctie, toegepast door Kvastek & Horvat, voor de invloed van de oppervlakteruwheid op de impedantie van polykristallijne zilverjodide-elektroden, leidt tot fysisch irrealistische conclusies.

   Kvastek, K. & Horvat, V., 1983. Analysis of the Ag/AgI electrode impedance. J. Electroanal. Chem. 147: 83-96.

7. De suggestie dat bronnen voor groeistappen op lage-index vlakken van silicium worden gegenereerd door de oppervlaktereconstructie zoals voorgesteld door van Vechten, is in haar algemeenheid onwaarschijnlijk, en is zeker niet van toepassing bij de gebruikelijke groeitemperaturen.

van Vechten, J.A., 1977. Surface reconstruction as a source of growth steps. J. Crystal Growth 38: 139-142.

8. Tegen de achtergrond van het feit dat de afmetingen van de basis-eenheidscel in de superstructuur van natief B-type zetmeel zijn gerelateerd aan de hoeveelheid in de structuur opgenomen water, kan een aardappelzetmeelkorrel worden beschouwd als een bijzondere vorm van een gemoduleerd kristal.

Cleven, R., van den Berg, C. & van der Plas, L., 1978. Crystal structure of hydrated potato starch. Starch/Stärke 30: 223-228.

9. De mate van structuurbevordering in zetmelen door opgenomen kleine molekulen wordt voor een groot gedeelte sterisch bepaald: ze is groter voor B-type zetmeel vergeleken met het compactere A-type, en ze neemt af in de serie water > methanol > ethanol.

Cleven, R., 1978. Ongepubliceerd werk.

10. Ontogenetische symmetriebeschouwingen van anatomie en fysiologie van het menselijk lichaam kunnen waardevolle inzichten opleveren, en verdienen meer aandacht in de geneeskunde.

11. Het voornemen van de regering om het tegengaan van ongerechtvaardigd onderscheid van personen op grond van geslacht, homofilie en huwelijkse staat een breed wettelijk kader te geven, dient gepaard te gaan met een voornemen om ongevraagde registraties van geslacht, geslachtelijke voorkeur of huwelijkse staat te beëindigen en/of te ontmoedigen.

Voorontwerp van een wet gelijke behandeling, 1981.

12. Het verschil tussen apparaat en machine is aan slijtage onderhevig.

13. De groeiende belangstelling, zeker die van wetenschappelijke zijde, naar een gedetailleerd beeld van het leven op aarde na een nucleair conflict, is een maat voor de acceptatie van de realiseringskans van zo'n conflict.

Rob. F.M.J. Cleven
Heavy metal/polyacid interaction
Wageningen, 26 oktober 1984

ABSTRACT

Cleven, Rob.F.M.J. (Laboratory for Physical and Colloid Chemistry, Agricultural University Wageningen, The Netherlands), 1984.
HEAVY METAL/POLYACID INTERACTION; an electrochemical study of the binding of Cd(II), Pb(II) and Zn(II) to polycarboxylic and humic acids. Thesis, Agricultural University, Wageningen, 225 + 9 pp., 90 figs., 22 tables, 443 refs., English and Dutch summaries.

Polyelectrolyte effects in the interaction of heavy metal ions with model polycarboxylic acids have been described, in order to establish the relevance of these effects in the interaction of heavy metal ions with naturally occurring humic and fulvic acids. The model systems consisted of Cd(II), Pb(II) or Zn(II) nitrates in combination with partially neutralized poly(acrylic acid), poly(methacrylic acid) or partially esterified poly(methacrylic acid). Metal binding characteristics have been investigated as a function of the metal/polyion ratio, the degree of neutralization, and the concentration of added 1:1 salt, and have been determined applying normal pulse polarography, conductometry and potentiometry. Covalent and electrostatic contributions to the binding have been disentangled, and discussed in terms of intrinsic binding constants and effective polyion charge densities. It is concluded that polyelectrolyte effects play an important role in heavy metal/humic acid systems at natural pH levels.

CONTENTS page

'Even the scientist who is convinced of the validity of deterministic descriptions would probably hesitate to imply that at the very moment of the Big Bang, the moment of the creation of the universe as we know it, the date of the publication of this book was already inscribed in the laws of nature'

Ilya Prigogine & Isabelle Stengers (1984)

1 INTRODUCTION

1.1 PURPOSE OF THIS STUDY

The present thesis deals with the challenging problem of the interactions of divalent metal ions with polyelectrolytes. This issue is of a great practical and theoretical importance.

The relevance for practice originates from the fact that in soils and natural waters the transport and the bio-availability of heavy metal ions are drastically influenced by the presence of *humic* substances. These natural macromolecules, having many binding sites per molecule, may be considered as polyelectrolytes.

Theoretically, the problem of properly accounting for the chemical *and* physical contributions to the association of metal ions with polyelectrolytes is largely unsolved, notwithstanding considerable attention paid to these phenomena over the past few decades. One of the reasons for the incomplete understanding is the lack of sufficiently detailed data.

In the *present* study, complete sets of data on metal ion association with natural *and* synthetic polyelectrolytes are systematically established, by using different electrochemical techniques and an appropriate experimental strategy. These data will contribute to the solution of a number of theoretical and practical questions, including the defining of polyelectrolytic effects in the association of heavy metal ions with humic substances.

1.2 GENERAL BACKGROUND

1.2.1 Polyacids: features & current topics

Polyelectrolytes have originally been defined by *Fuoss* (1948) as substances of high molecular mass which are simultaneously electrolytes. More recent definitions stress the dissociation products in solution: multiply charged polyions and counterions of small charge and opposite sign (*IUPAC*, 1952; *Marinsky*, 1966; *Manning*, 1979b).

Physico-chemical features of polyacids are markedly different from those of non-ionic polymers and monomeric acids. Two classic examples are:

- Upon dilution of a partially neutralized polyacid solution, the reduced specific viscosity increases dramatically (*Eisenberg & Fuoss*,

1954). Only at extremely low polyelectrolyte concentrations a maximum is reached (*Eisenberg*, 1977).
- Upon neutralization of weak polyacids the apparent dissociation constant decreases by orders of magnitude (*Katchalsky & Spitnik*, 1947).

In the presence of simple salts, these effects are suppressed or even absent (*Richards*, 1980). The cited features are now well understood (*Overbeek*, 1976).

Central concepts in the understanding of polyelectrolyte behaviour are:

i The strong mutual electrical interaction of the charges on the polyion, and the response of the small ions to the high electrical field around the polyion.

ii The morphological response of the polymer chain segments to the local charge distribution in the solution.

Metal ion association

An important feature of polyacids is the strong association with metal ions that may persist even at high dilution (*Oosawa*, 1971). Crucial characteristics of this association still lack complete understanding. Some current issues are:

i The development of models to describe the association.

ii The evaluation of the nature of the association: localized or delocalized 'binding'.

iii The discrimination between ion-specific and generic electrostatic effects.

iv The distribution of metal ions of different valence over the 'bound' states: competition effects in mixed systems.

v The cooperativity of the binding sites.

vi The occurrence of polyelectrolyte effects, i.e. those effects provoked by the charge density of the polyion, in natural systems containing polymeric acid such as humic acid.

vii The response of various analytical methods to associated metal ions.

In the *present* work, all of these issues will be highlighted. Results were achieved by measuring counterion binding in various metal/polyacid systems using *different*:
- polycarboxylic acids,
- divalent metal nitrates,

- metal/polyacid concentration ratios,
- charge densities of the polyions,
- concentrations added 1:1 salt,
- electrochemical analytical methods,
- concepts in data treatment.

Central concepts in the understanding of metal ion association with polyacids are:

i Physical: a high local concentration of metal ions in the vicinity of the polyion due to coulombic attraction.

ii Chemical: complex formation with functional groups due to covalent binding.

Against the background of classic theories of electrolytes, polymer physics and metal complexation, new theories had to be developed to describe the behaviour of polyelectrolytes, and the notion of 'binding' had to be reconsidered.

Pioneering investigations of the physical chemistry of polyelectrolytes by *Staudinger* in the twenties and *Kern* in the thirties, were followed, after World War II, by more systematic studies by *Katchalsky* in Jerusalem and *Fuoss* in Yale. The early investigations of synthetic polyacids were restricted to poly(acrylic acid) and poly(methacrylic acid). These polyelectrolytes are still frequent model substances, like in the *present* work.

Since 1946, a number of polyelectrolyte theories have been developed. Some recent theories on metal ion association lead, on main issues, to controversies, to be discussed in chapter 2. For example the counterion '*condensation*' theory of *Manning* (1969a) in which molecular thermodynamics is applied on a line charge model, and the counterion '*accumulation*' theory of *Guéron & Weisbuch* (1979), in which electrostatics is applied on a curved charged plane model.

In the *present* work, a number of predictions by these two theories will be compared with the results in the chapters 4-6.

Applications

Among the oldest applications of polyelectrolytes is the agricultural use of poly(acrylic acid) and its derivatives, such as '*Krilium*' and '*Rohagit*' as soil conditioners (*Eisenberg & Fuoss*, 1954; *Kretz & Völker*, 1964). The fertilizing properties of these products, like those of humus, are based on cation exchange processes and stabiliza-

tion of the clay structure.

Acrylic polyacids are also used in medicine, as drug carriers (*Kreuter*, 1983) and in dental cements (*Wiegman-Ho & Ketelaar*, 1983), and in technology, for example in the removal of heavy metal ions from effluents (*Jellinek & Sangal*, 1972), and as a main component of ion-exchange resins (*Marinsky*, 1966).

Generally, applications of polyelectrolytes are based on their binding power for ionic species, or on adsorption on colloidal particles or emulsion droplets. Depending on the conditions, adsorption may have a strong stabilizing action against flocculation, or it may evoke flocculation due to bridging. Other applications involve suppression of turbulence in flow, prevention of scale growth in heat exchangers, and the formation of hyperfiltration membranes (*Eldridge*, 1973).

The future use of polyelectrolytes as 'catalysts' in a variety of chemical reactions is very promising (*Tsuchida & Nishide*, 1977; *Ise*, 1978; *Tondre*, 1982; *Ise et al.*, 1982). Reactions between ionic species of the same sign are enhanced due to the high local concentrations of the reactants near polyions of opposite sign. In reactions with uncharged reactants, steric and specific effects attributed to the polymeric ligands play a leading role in the 'catalytic' activities (*Kanedo & Tsuchida*, 1981). Metal complexes of synthetic poly(amino acid) may be model substances in the study of enzymatic activities of metal complexes of natural polypeptides.

Natural polyelectrolytes

Generally, metal ions associated to *bio*polyelectrolytes, such as proteins, nucleic acids and acidic polysaccharides, play a vital role in biological functions in living tissue (*Williams*, 1971; *Muzarelli*, 1973; *Daune*, 1974). The interaction of metal ions with DNA is frequently studied. The structure of this polyacid is well-known, and the distance separating the phosphate groups, projected on the double-helix axis in native DNA, is fixed and very short: 0.17 nm. A high charge density results. Because of the stiff helical conformation, DNA is often used as a model polyelectrolyte (*Manning*, 1979a, 1981a).

In the case of proteins, bearing both acidic and alkaline groups, the conformation may be dependent on the medium. Consequently, the effective charge is often low, the charge separations may not be fixed, and the interpretation of polyelectrolyte effects is correspondingly difficult.

Polyacidic organic material in soils and natural waters is of agricultural importance. This type of *geo*polymer comprises a wide variety of similar compounds, often collectively known as humic acid. They are formed by the decomposition of dead vegetable matter, and they are among the most abundantly and most widely occurring natural products on earth (*Schnitzer & Ghosh*, 1979). Humic acid plays a crucial role in the mobilization and transport of heavy metal ions in soils and natural waters (*DHaese*, 1977).

The chemical nature of humic acid is poorly defined (*Schnitzer & Khan*, 1976). To a complex skeleton of aliphatic and aromatic structures, many functional groups, predominantly carboxylic, are attached. The humic acid molecules show some flexibility (*Hayano et al.*, 1982).

Polyelectrolyte behaviour of humic material is difficult to ascertain because of the irregular structure and mixture of components present even in purified samples. The divergency in apparent association constants of similar metal/humic acid systems has generally been attributed to *mixture* effects, whereas *electrostatic* effects may also be involved.

Literature on metal association with humic acid is very abundant, and has frequently been reviewed (*Flaig et al.*, 1975; *Schnitzer & Khan*, 1976; *Mantoura*, 1981). Nevertheless, studies of electrostatic effects in the association are relatively scarce (*Arai & Kumada*, 1977a,b; *Marinsky et al.*, 1980, 1982; *Young et al.*, 1982).

Knowledge of the polyelectrolyte character of the metal association with humic acid is important in metal speciation studies and modelling of ecosystems: electrostatic binding and chemical binding obey different laws, and lead to different speciation patterns. Successful predictions and control of pathways of toxic metals in the environment are dependent on the proper understanding of the nature of the interaction.

In the *present* work, the polyelectrolytic nature of metal/humics interaction is studied on the analogy of, and referring to the preceding study of the interaction of metal ions with synthetic polyacids.

1.2.2 Heavy metals: environmental aspects

The equivocal term 'heavy metals', suggesting a physical classification, is generally used where there are connotations with toxicity (*Nieboer & Richardson*, 1980). Topics at the biennial conferences on 'Heavy metals in the Environment' stress this connection. The toxicity

of heavy metals is related to their ability to form complexes with biomolecules. In such complexes, essential functional groups may be blocked, other essential metal ions displaced, and active conformations modified.

In soils and natural waters, heavy metals are distributed over many different species, of which the aquo-complexes are generally considered to be the most toxic (*Hart*, 1981). Binding to organic matter decreases the toxicity of heavy metal ions, but it increases their mobility and often their bio-availability. The uptake of heavy metal ions by roots, and the plant physiology are influenced by the presence of organic ligands and by the concentrations of the metal ions in the soil (*Schnitzer & Khan*, 1976; *van der Werff*, 1981). It is not yet fully understood how the processes of metal uptake depend on speciation, concentrations and kinetic factors (*Zunino et al.*, 1975).

Accumulation factors for heavy metals in micro-organisms, fossil substances and in sediments, by natural and man-made processes, can exceed 100,000 (*Szalay & Szilágyi*, 1969; *Martell*, 1975; *World Health Organization*, 1982).

A number of heavy metals, such as Co, Cr, Cu, Fe and Zn, are essential constituents of the human body. Both deficiencies and overdoses are hazardous. A general toxicity sequence for mammals is (*Venugopal & Luckey*, 1975): Ag, Hg, Tl, Cd > Cu, Pb, Co, Sn > Mn, Zn, Ni, Fe, Cr. Antagonistic effects and synergisms are possible: e.g. the toxicity of Pb and Cd is decreased in the presence of Zn (*Vogelaar*, 1980), probably because of competition for the same sites.

Toxicity sequences have been linked to chemical classifications of heavy metals. The 'hard acid', or A-type metal ions are generally less toxic than the 'soft acid', or B-type metal ions. This classification is based on *trends* in the equilibrium constants for the formation of complexes, generally with inorganic ligands. Recently, a more generally applicable 'covalence index' was proposed (*Nieboer & Richardson*, 1980). This index is the ratio of the squared *Pauling* electronegativity and the crystal ionic radius of the metal ion. For a given metal ion it is considered to be a measure of the importance of covalent interactions relative to ionic interactions.

Cadmium, lead and zinc

For the metal ions investigated in the *present* study, Cd^{2+}, Pb^{2+} and Zn^{2+}, the covalence indices are 2.9, 3.3 and 2.2, respectively. This means that the tendency to form covalent bonds usually de-

creases in the order Pb>Cd>Zn.

The average content in soils amounts to 0.06, 10 and 50 mg/kg for Cd, Pb and Zn, respectively. The toxicity for plants of these metals, that increasingly occur in the ecosystems of industrialized societies, and their uptake by roots, have been demonstrated (*van der Werff*, 1981; *Jones et al.*, 1981; *World Health Organization*, 1982).

1.3 SCOPE OF THE PRESENT WORK

1.3.1 Objectives

The *present* electrochemical study of the interaction of Cd(II), Pb(II) and Zn(II) with a number of polycarboxylic acids is focussed on two main objectives:

i The physico-chemical description of polyelectrolyte effects in the association of heavy metal ions with model polycarboxylic acids of well-defined composition and structure.

ii The assessment of polyelectrolyte effects in the association of heavy metal ions with humic acid.

Interactions of Cd(II), Pb(II) and Zn(II) with simple carboxylic ligands are mainly covalent, whereas in those with *poly*carboxylic ligands strong electrostatic effects may be additionally manifest. Therefore, variables controlling the electrical field around the polyion were selected to be studied. In addition, monomer-like ligands were also investigated.

The objectives were achieved by determinations of free M^{2+}- and H^{+}-ions in the metal/polyacid systems. As the response to free M^{2+}-ions in the electrochemical analyses may depend on the polyelectrolytic nature of the ligand, three independent methods, viz. polarography, potentiometry and conductometry, were used.

Against the background of the current issues on metal ion association with polyelectrolytes, actual questions to be answered are:

i How do the metal/polyacid equilibria depend on:
   - the concentration ratio of the reactants;
   - the charge density of the polyacid;
   - the concentration 1:1 salt?

ii Is it possible to separate ion-specific and generic electrostatic effects, and how do Cd, Pb and Zn differ in this respect? Do simple relations exist with intrinsic chemical properties of metal-carboxylates?

iii Does the protolytic dissociation interfere with the metal ion complexation?

iv What is the applicability of current models of metal ion association with polyanions to the systems investigated?

v Do the polyanionic sites show cooperativity in the binding of metal ions?

vi Is a polyelectrolyte effect also manifest in the metal ion association with humic acid? Can it be quantified and taken into account in speciation?

1.3.2 Selection of materials & methods

To produce meaningful experimental results on the physical chemistry of the interaction of heavy metal ions with polycarboxylic acids, careful selections have to be made with respect to materials and methods.

Materials

The study of polyelectrolyte effects in the association of metal ions with humic material is one of our main objectives. Two samples of humics of a different origin were selected: a soil-derived sample, here named humic acid, HA, and a water-derived, fulvic acid, FA. The former was obtained after soil extraction procedures, the latter was in a natural state.

To characterize polyelectrolyte effects in general, three synthetic polyacids were studied. Their functional group was the same as the dominant functional group in humics, namely the carboxylate anion. Polycarboxylic acids are frequently used as model substances for humic acid (*Khalaf et al.*, 1975; *Anderson & Russell*, 1976; *Arai & Kumada*, 1977a; *Young et al.*, 1981, 1982).

Samples of a differing molecular mass of the simplest of this series, poly(acrylic acid), PAA, were used. In addition, poly(methacrylic acid), PMA, was studied. An additional methyl group in PMA, that is missing in PAA, generates a slightly different chemical environment for the functional group. Moreover, at low charge densities, PMA retains a more compact conformation than PAA, due to the methyl group (*Arnold & Overbeek*, 1950; *Leyte & Mandel*, 1964; *Ben-Naim*, 1980). Finally, a copolymer of methacrylic acid and its methyl ester was investigated. This substance, which may also be considered partially esterified poly(methacrylic acid) and will henceforth be abbreviated

as PMApe, has a lower average charge density than PMA, at the same degrees of neutralization. This copolymer has been studied previously in this laboratory by potentiometric titration methods and rheological techniques (*Böhm & Lyklema*, 1975; *van Vliet & Lyklema*, 1978, 1979; *Ralston et al.*, 1981).

By way of comparison, low molecular mass analogues of the acrylic polyacids, viz. 2-methylpropanoic and butanedioic acid, were also tested as ligands in heavy metal complexation.

The heavy metal ions of Cd, Pb and Zn were selected because they are:

i detectable by polarographic techniques;
ii of environmental importance;
iii able to form complexes.

Generally, the complexation behaviour of Cd(II) is much the same as that of Zn(II), whereas for Pb(II) it is rather different. Other metals, viz. Ag(I), Ba(II), Cu(II) and Al(III), were incidentally studied for comparison. All metals were used in the form of their nitrates.

Methods

A wide variety of techniques can be employed to study metal/polyelectrolyte interaction. Electroanalytical methods were selected because of their special suitability for speciation, down to low concentration levels: Among these methods, voltammetric techniques such as normal pulse polarography, are distinguished by their very high sensitivity and selectivity.

Although the (pulse) polarographic response to metal ions in the presence of simple ligands is well understood, the presence of *polymeric* ligands may give rise to a less clear-cut interpretation. Complications are connected with the binding mechanism involved, experimental limitations, and polymer adsorption. Additional independent information was obtained by conductometry and potentiometry (to determine H^+- and Cd^{2+}-activities) in similar systems.

Polarography selectively detects a fraction of the metal ions, and interferes with the equilibria in the sample solution. Conductometry responds to net effects of all ionic species in solution, and does not disturb the equilibria. Potentiometry measures the activity of one particular ion only, without affecting the equilibria in the solution.

The different methods yield complementary information, so that their combined use strengthens the basis of our conclusions.

Viscosimetry and spectroscopic techniques were used in a limited number of auxiliary measurements to check the relative viscosity of some sample solutions, to determine the carbon content of the humic material, and to ensure the absence of interfering multivalent metal ions in the natural fulvic acid sample.

1.3.3 Variables investigated

The selected systems were systematically studied with respect to three variables:

i the metal/ligand concentration ratio, M/L;
ii the degree of neutralization of the polyacid, α_n;
iii the concentration of added 1:1 salt, c_1.

These variables control the electrostatic effects exerted by the polyions.

Association of a metal ion M with a charged functional group L will decrease the effective charge of the polyion. Therefore a subsequently added metal ion may be associated less firmly if electrostatic attraction is involved. Such a decrease is studied by changing the M/L ratio.

The charge of a polycarboxylic acid molecule is directly related to the number of carboxylic groups that have been deprotonated. In this respect, α_n is a master variable.

For polyacids, the effect of added 1:1 salt on the metal ion association is more complicated than for simple ligand systems. The distances separating the charged sites on a polyion are often small, and more or less fixed, not dependent on the concentration of simple salt. But the *Debye-Hückel* screening parameter, a measure of the extent of mutual electrostatic interaction, is affected by the concentration of simple salt. Therefore, the screened coulombic fields of the individual groups on the polyion will overlap even at high c_1. Due to this persisting overlap, the classic *Debye-Hückel* approach for activity coefficients is not valid in the case of ion-polyion interaction. In systems with added 1:1 salt, the effective charge density of the polyion may also be decreased by association of monovalent metal ions. These interferences with divalent metal ion association were studied by changing c_1.

1.3.4 Description of contents

Chapter 2 contains a concise survey of current concepts and models in metal ion association with polyelectrolytes. Two competing electrostatic models are described in more detail: the '*condensation*' model by *Manning*, and the '*accumulation*' model by *Guéron & Weisbuch*. Information is given on the heavy metal ions and the synthetic polycarboxylic acids used. A review of relevant literature, up to and including 1982, on divalent metal/polyacid interaction is also incorporated in this chapter.

In chapter 3, the materials used and the experimental strategy are described. Fundamentals of the electroanalytical methods are explained, and interpretations of the responses are considered.

In the chapters 4-6, the experimental results for the *synthetic* polyacids are presented and discussed. Chapter 4 is predominantly focussed on the effects of M/L variation. Chapter 5 is mainly devoted to the influence of α_n, and chapter 6 comprises the results of changing c_l. The results are discussed against the background of polyelectrolyte effects.

Chapter 7 is dedicated to the interaction of heavy metal ions with *humic* and *fulvic acid*. The experimental results are discussed with respect to the nature of the interaction.

Chapter 8 contains a recapitulation of the main results.

2 M(II)/POLYECTROLYTES: THEORY & LITERATURE

2.1 GENERAL

2.1.1 Interactions in metal/polyacid solutions

In the present study, the samples typically are dilute aqueous solutions containing a partially neutralized polycarboxylic acid, a divalent metal nitrate and/or a monovalent metal nitrate. Thus, *schematically*, a sample may contain the following basic species:

(1) $-COO^-$, (2) -COOH, (3) R-, (4) M^{2+}, (5) M^+,
(6) H^+, (7) H_2O, (8) OH^-, (9) NO_3^- (2.1)

In this series, R- represents the alkyl part of the repeating unit. Interactions that are relevant in the physico-chemical characterization of the association of M^{2+} with $-COO^-$ will be considered briefly.

(1) $-COO^-$

The intramolecular charge-charge interaction between the carboxylate groups is most important. In common polyelectrolytes, the charge spacing is so short that the electric fields around the groups overlap substantially, even at high ionic strengths. By definition, polyelectrolyte effects originate from this type of interaction.

The overlapping fields give rise to a high potential at the polyion. As a result, counterions are attracted to the polyion, and their concentration may reach dramatically high local values (*Manning*, 1978b; *Guéron & Weisbuch*, 1980). Another consequence is the stretching of the polymer due to the mutual repulsion of the charges. This change affects both the charge spacing and the chemical micro-environment of the functional groups.

(2) -COOH

The weakly acidic carboxyl group, in which the proton is covalently bound (*Manning*, 1981b), is uncharged. As a result of the deprotonation of -COOH by added KOH, the functional group becomes charged. Covalent binding of K^+ with $-COO^-$ is essentially absent (*Mandel*, 1967; *Koda et al.*, 1982). Thus, the degree of neutralization is a variable to control the charge of polycarboxylic acids.

(3) R-

Alkyl side chains of the polyacid can interact, and form hydrophobic bonds. Generally, the longer the alkyl group, the stronger this type of bonding (*Dubin & Strauss*, 1975). Hydrophobic bonding can result in hypercoiling, that is the formation of a conformation more compact than the random coil. A more compact conformation implies a shorter charge spacing, and thus a higher local potential.

(4) M^{2+}

The interaction between metal ions M^{2+} and COO^- groups of the polyacid may range from purely electrostatic to fully covalent. The distinction between both types of interaction is not unambiguous. The convention is adopted here, that the free energy change of the association of M^{2+} can be written as the sum of two contributions. ΔG_{int} and ΔG_{el}: the former, corresponding with the intrinsic binding, is a constant for a given system, whereas the latter, referring to the electrostatic interaction, is a function of the polyion potential.

There is no agreement in literature on the definition of 'bound' counterions in polyelectrolyte solutions (*Dolar & Peterlin*, 1969; *Manning*, 1979b). Although a spectrum of binding types exists (*Eldridge*, 1973), a *two-state* approach is generally employed. In this approach, the metal ions are considered to be either bound or free (*Manning*, 1978a; *Oosawa*, 1971). Anticipating further discussion of the concepts of 'binding', in § 2.2.1, the definition is adopted here, that 'bound' counterions are those of which the self-diffusion coefficient is observed to be equal to that of the much larger polyion (*Magdalenat et al.*, 1974; *Manning*, 1979b).

(5) M^+

The interaction of M^+ with the charged species in the samples is two-fold. If M^+ is present in excess over M^{2+}, the ionic strength is dominated by the monovalent ions. As a consequence, they control the magnitude of the *Debye-Hückel* screening length κ^{-1}, which is a measure of the distance over which charged groups 'feel' each other. For a 1:1 salt solution, κ^{-1} is given by:

$$\kappa^{-1} = \left(\frac{\varepsilon \, k \, T}{4 \, \pi \, e^2} \right)^{-\frac{1}{2}} \cdot c_1^{-\frac{1}{2}} \qquad (2.2)$$

where ε is the dielectric constant of the solvent, k the *Boltzmann* constant, T is the *Kelvin* temperature, e the elementary charge, and c_1 the concentration 1:1 salt. In water, at 25°C, the screening length κ^{-1} is given (in nm) by:

$$\kappa^{-1} = 9.6 \cdot c_1^{-\frac{1}{2}} \qquad (2.3)$$

with c_1 in $mol.m^{-3}$. For poly(meth)acrylates, the charge spacing is about 0.24 nm, and thus at ionic strengths up to 10^3 $mol.m^{-3}$ polyelectrolyte effects are still expected. The activity coefficient of free M^{2+} is also related to κ^{-1}, through c_1.

The second function of M^+ is their electrostatic interaction with the polycarboxylate ion, in competition with M^{2+}. Upon binding of M^{2+}, bound M^+ ions may be liberated. There is no agreement on the stoichiometry of this exchange process (*Miyamoto & Imai*, 1980a,b; *Shimizu et al.*, 1981).

(6) H^+

Protons interact with $-COO^-$, in competition with M^{2+} and M^+. Upon binding of M^{2+}, the pH will change. The pH of a polycarboxylic acid solution is a function of the *intrinsic* acid strength of the RCOOH group, and the *effective* charge of the polyion (*Nagasawa*, 1971; *Manning*, 1981b). The effective charge is the result of both the degree of neutralization and the association of M^{2+} and M^+ with $-COO^-$. In the case of a (partially) covalent binding of M^{2+} with $-COO^-$, the charge of the polyion will also decrease, and the intrinsic acid strength of neighbouring functional groups may be affected. Thus the change in pH upon binding of M^{2+} with $-COO^-$ may be caused by different concurrent processes.

(7) H_2O

Generally, ionic species are hydrated in water. For polycarboxylates, the amount of structure water, in which the dipoles are highly oriented, is 10-20 cm^3 per mole $RCOO^-$, whereas for divalent metal ions values up to 100 $cm^3.mol^{-1}$ have been determined (*Conway*, 1981).

Intimate metal/polyion association requires (partial) dehydration of the reactants, resulting in a gain in entropy (*Crescenzi et al.*, 1974; *Delben & Paoletti*, 1974). Moreover, partial dehydration is expected because of the very large local concentrations of bound metal ions.

(8) OH^-

Relevant functions of OH^- are the neutralization of -COOH, and the possible hydroxide formation with M^{2+}.

(9) NO_3^-

Coions are expelled from the polyion domain. Insofar the NO_3^- ions are not involved in inorganic complex formation with M^{n+}, they have no direct consequences for the metal/polyion interaction (*Manning & Zimm*, 1965).

2.1.2 Polyion models

Polyelectrolytes are more or less randomly coiled in solution. The charges are fixed on the polymer chain. If the ionic strength is not too large and not extremely small, overlapping electrical fields around the charges may be approximated as an overall cylindrical potential distribution (*Manning*, 1972). The latter condition is generally obeyed because of the polyelectrolyte concentration only. In the case of high ionic strength, the approximation with smeared out charges may fail (*Nagasawa*, 1974).

For the binding of counterions, only a short section of the chain needs to be considered, so that the coiling of the polyion may be neglected. In this case, the *cylinder* model is generally considered to be appropriate (*Strauss*, 1958; *Katchalsky*, 1971; *Manning*, 1972; *Nagasawa*, 1974; *Stigter*, 1975; *van der Drift*, 1975). In this model, the polyion is considered to be a thread or rod of infinite length. Calculated counterion binding parameters are, as also experimentally observed, independent of the molecular mass (*Nagasawa*, 1974).

For a limited number of phenomena, such as polyion expansion, diffusion and complex-coacervation, the coiled conformation is important. In these cases, a *sphere* model is more appropriate (*Nagasawa*, 1974; *Overbeek*, 1976). In this model, the whole molecule is circumscribed by a sphere. However, assuming a uniform distribution of charges in the sphere, calculated counterion distribution around the sphere generally depends on the molecular mass (*Nagasawa*, 1974).

2.2 COUNTERION ASSOCIATION

2.2.1 Definitions of binding

With respect to counterion association, three classes of metal ions can be distinguished in solutions with charged polycarboxylic acids:

i Ions that are fixed to functional groups by chemical linkage(s): these ions have completely *lost* their original mobility. In the present study, ions in this class will be identified as *covalently bound*. Sometimes, terms such as site-bound, complexed or specifically bound are synonymously used in the literature. Obviously, the diffusion coefficient of covalently bound metal ions is equal to that of the polyion. Metal ions in this class (i) may reduce the polyion charge in the same way as bound protons do. The formation of a covalent complex is primarily described by a coordination number j and an intrinsic binding constant K_{int}, that is independent of the polyion charge. In addition there will be electrostatic contributions to the overall binding constant. Frequently, covalent bonds can be detected spectroscopically without ambiguity (*Nagasawa*, 1974).

ii Ions of which the mobility is *restricted* as compared to the polyacid-free but otherwise identical solution: a spectrum of mobilities may exist, ranging from almost completely immobile to virtually 'free'. This behaviour of the metal ions is mainly attributed to electrostatic field effects. Depending on the polyion charge, the counterion distribution may range from a diffuse *Debye* atmosphere (or *Gouy* diffuse layer) to a compact *Bjerrum* or *Stern*-like layer. The ions in class (ii) may be partially (de)hydrated. They retain their full charge, and are associated with the polyion as a whole rather than with certain carboxylate groups.

Some authors consider class (ii) ions as 'free', because of the (limited) mobility or the absence of significant covalency (*Marinsky*, 1976; *Guéron & Weisbuch*, 1980). Other authors consider all class (ii) ions as 'bound' in a thermodynamic sense (*Record et al.*, 1976, 1978), or a certain part of class (ii) ions as 'bound' (*Magdalenat et al.*, 1974). This matter will be treated in some detail in the discussion of the two-state approach. In the *present* study, class (ii) ions are subdivided by a simple distribution over two groups ('two-state approach'): a fraction of ions of which the diffusion coefficient is considered to be equal to that of the

much larger polyion, denoted as *electrostatically bound*, and a fraction of ions which are considered to be *free*. By proposing this subdivision, it is accepted that it is in principle possible that different analytical methods see different bound and free fractions. Sometimes, the electrostatically bound ions are called 'condensed' (*Oosawa*, 1971), 'territorially bound' (*Manning*, 1979b) or 'atmospherically trapped' (*Spegt & Weill*, 1976).

iii Ions of which the mobility is virtually *equal* to that in a poly-acid-free but otherwise identical solution: class (iii) metal ions are *free*.

In connotation with the distribution of the three classes of ions over two states, the *effective charge* of the polyion is defined as the charge on the polyion together with that of the bound metal ions.

The two-state approach

The two-state approach is widely accepted (*Anderson & Record*, 1980). Despite its rather approximative character, such an approach is claimed to function well (*Delville & Laszlo*, 1983). In many discussions on thermodynamic properties of polyelectrolytes it was pointed out that part of the counterions behave *as if* those ions had reacted with fixed charges to form associated groups, even though they are believed to be completely dissociated (*Nagasawa*, 1974).

It generally appears from theoretical considerations of the counter-ion distribution around a polyion, that the concentration c (of class (ii) ions) decreases sharply with the radial distance x from the poly-ion cylinder surface. In the accumulation theory of *Guéron & Weisbuch* (1980), which is not a two-state theory, the concentration c initially decreases almost linearly with x. At x=0, the concentration is called CIV, the Concentration In the Vicinity of the polyion. The condensation theory of *Manning* (1969a) is based on a two-state concept: the local concentration of electrostatically bound ions ('condensed' ions) c_{loc} does not change with x up to R_M, the radius of the cylindrical volume around the polyion in which all condensed ions are present. These theories will be discussed briefly in § 2.2.4. Anticipating that discussion, fig. 2.1 represents schematically the counterion distributions of the not-covalently bound ions in a 'continuous' and a 'two-state' approach.

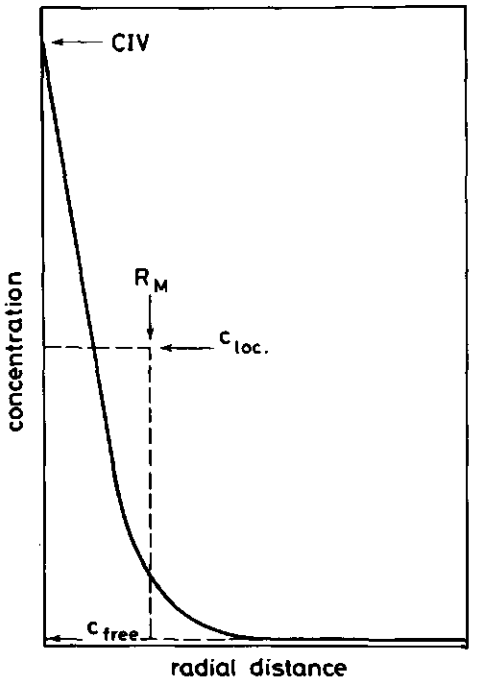

FIGURE 2.1 Counterion distributions, schematically represented, of not-covalently bound metal ions.
Solid curve: continuous distribution;
Dotted curve: two-state approach.

From an experimental point of view, the two-state approach is often the only option to define a degree of metal ion association. Most analytical techniques cannot discriminate between counterions with different distances to the polyion, and the degree of metal ion binding is usually determined by measuring the amount of free ions. Only in some applications of NMR, bound ions can be operationally defined as those which are within a certain distance from the polyion (*Gunnarsson & Gustavsson*, 1982). In the present study, in which polarography, conductometry and a Cd-selective electrode are applied, the change of the limiting current, the conductivity and the electrode potential, as compared to the same quantities in polyacid-free solution, are interpreted in terms of the degree of ion binding. These interpretations will be discussed in chapter 3. The experimental parameters relevant for these methods are the diffusion coefficient, the conductance and the activity coefficient, respectively. They are interrelated through the *Nernst-Einstein* equation. The parameters are affected by the binding of the metal ions with the polyion, each in a specific way. Consequently, the methods may yield different results. Therefore, the bound

metal ions, as determined by the techniques mentioned, will be distinguished as polarographically, conductometrically and potentiometrically bound, respectively.

2.2.2 Metal-polyion equilibria

The interaction of a divalent metal ion M with carboxylate groups L of a partially neutralized polycarboxylic acid HL in the presence of monovalent metal ions K, may result in covalent and electrostatic binding of M, and in the release of bound K and bound H.

At present, there is no theory for the distribution of bound counterions over the subpopulations: covalently and electrostatically bound (*Manning*, 1977a, 1979b).

The present experimental study of M/polycarboxylic acid systems is focussed on the unravelling of the covalent contribution *and* the characteristics of the electrostatic contribution to the binding of M. The former aim will be achieved considering a covalent binding model, to be discussed in § 2.2.3, in which the effect of the electric field of the polyion is treated as a non-ideality of the system. The latter purpose will be achieved by considering the experimental results for the highly charged polyions against predictions of purely electrostatic theories, in § 2.2.4, in which covalent contributions are neglected.

Although both modes of metal binding and the release of both K and H are phenomena that occur simultaneously, there are specific ranges of experimental conditions with respect to the variables M/L, α_n and c_l, under which each of the phenomena can be separately analysed.

It is well-known that the apparent acid strengths of highly charged polycarboxylic acids are much lower than those of the corresponding simple acids (*Arnold*, 1957; *Kagawa & Gregor*, 1957). Anticipating the results, we shall base the following analyses on the finding that the release of H^+ upon binding of M^{2+} by highly charged polyacids at low M/L ratio, is negligible. Under this condition, the exchange reaction for the binding of a divalent metal ion M^{2+} with a polyion of v charged ligands L to which u K^+ ions are bound, can be written schematically as:

$$M^{2+} + K_u L_v^{u-v} \rightleftharpoons MK_{u-w}L_v^{2+u-v-w} + wK^+ \qquad (2.4)$$

For low concentrations of the reactants, the equilibrium constant of

this exchange reaction is (charges omitting):

$$K_{ex} = \frac{[MK_{u-w}L_v][K]^w}{[M][K_uL_v]} \qquad (2.5)$$

where brackets denote concentrations.
K_{ex} applies to a certain state of the polyion, viz. it must have a charge density at which u ions K are bound.

There is sufficient evidence in the literature that alkali metal ions interact almost purely electrostatically with polycarboxylic acids (*Koda et al.*, 1982; *Gunnarsson & Gustavsson*, 1982). With this finding, the formation of the *covalent* complex ML_j(int) as a result of intrinsic binding of M with j carboxylate groups on an otherwise *uncharged* polyacid, is conventionally written as:

$$M + jL \rightleftharpoons ML_j(int) \qquad (2.6)$$

The intrinsic binding constant for reaction (2.6) is given by:

$$K_{int,j} = \frac{(ML_j)_{int}}{(M)(L)^j} \qquad (2.7)$$

where parentheses denote activities. It should be noted that in eq. (2.7) the effects of monovalent metal ions are incorporated via the activity coefficients of the reactants. Evidently, the ligands are also involved in the acid/base equilibrium.

The apparent metal association constant, as directly derived from experimental data, is defined as:

$$K_{app,j} = \frac{[M]_{total} - [M]_{free}}{[M]_{free} \cdot [L]^j_{free}} \qquad (2.8)$$

where in brackets concentrations are denoted. The numerator of the r.h.s. of eq. (2.8) is equal to the concentration of bound M. $[L]_{free}$ can be identified with $v \cdot [K_uL_v]$.

For dilute systems, and high polyion charge, $K_{app,j}$ can be related to K_{ex}. For j=1:

$$K_{app,1} \cong \frac{1}{v} \cdot K_{ex} \cdot [K]^{-w} \qquad (2.9)$$

For dilute systems, and negligibly small degree of acid dissociation α_d:

$$K_{app,j}\ (\alpha_d \to 0) \cong K_{int,j} \tag{2.10}$$

2.2.3 Covalent binding

In § 2.2.1 the convention was adopted that the change in free energy of the association of heavy metal ions with polycarboxylic acids can be written as the sum of a constant (intrinsic) term and an electrostatic term that depends on the electrical potential at the locus of the binding. Consequently, log $K_{app,j}$ is given by:

$$\log K_{app,j} = \log K_{int,j} + \Delta \log K \tag{2.11}$$

where Δ log K represents the potential-dependent term. The potential at the binding site of M is dependent on α_d, and on the composition of the solution. In principle, log $K_{int,j}$ can be determined by measuring log $K_{app,j}$ at different values of α_d and extrapolation to $\alpha_d = 0$ (*James & Parks*, 1982).

A method to evaluate Δ log K is to consider this term as a measure of the electrical work to bring a divalent ion from infinity to the surface of the polyion, where the electrical potential is ψ_s:

$$2.3\ \Delta \log K = -2e\psi_s/kT \tag{2.12}$$

An alternative way to formulate this method is to consider *local* equilibria between metal ions M in the thermodynamically bound and free states (*Marinsky*, 1976). The local concentration in the 'free' state $[M]_{loc}$ is assumed to be given through the *Boltzmann* equation:

$$[M]_{loc} = [M] \cdot \exp(-2e\psi/kT) \tag{2.13}$$

where ψ is the potential at the locus of the binding. Going to the polyion surface, $\psi \to \psi_s$, and the fraction of the bound ions that is covalently bound becomes unity.

Starting from the *Poisson* equation, a number of approximations of ψ_s have been made (*Katchalsky*, 1971; *Stigter*, 1975; *Delville*, 1980; *Anderson & Record*, 1980; *Guéron & Weisbuch, 1980; Gunnarsson & Gustavsson*, 1982; *Bratko & Vlachy*, 1982). According to *Marinsky* (1976) the term $2e\psi_s/kT$ in eq. (2.12) can be experimentally determined at any α_d value, from the electric contribution to the free energy of the proton

binding, as measured from the acid-base titration. In this approximation, it is assumed that ψ_s is the same for the proton and the metal ion binding. The acid/base titration will be discussed in § 2.3.2. In § 5.3.2 the applicability of the approximation

$$\Delta G_{el}\ (M^{2+}) \cong 2 \cdot \Delta G_{el}\ (H^{+}) \qquad (2.14)$$

will be discussed against the background of the experimental results.

A second, more approximative method to determine $K_{int,j}$ experimentally, will be applied in chapter 4, on the results of M/L variation. The method will be discussed in detail in § 4.1.1. The basic concept is that at sufficiently large M/L, the effective charge of the polyion is low, as a result of the binding of M. Under these conditions, the polyacid behaves *as if* it is not a polyelectrolyte. Then, the change in pH is interpreted as the result of the substitution of covalently bound protons by covalently bound metal ions.

2.2.4 Electrostatic binding

For the association of metal ions with highly charged polycarboxylic acids, the electrostatic contribution to the free energy may be much higher than the covalent contribution. Under these conditions, the dependence of the experimentally observed binding on α_d, M/L and c_1 can be compared, in selected cases, with the theoretical results from purely electrostatic models.

In the development of polyelectrolyte theories, two different models are currently employed to account for counterion binding. One model starts from the concept of counterion condensation (CC), and the other from the *Poisson-Boltzmann* (PB) equations. The *basic* assumptions, characteristics and results of CC, as elaborated by *Manning* (1969a,b,c) and those of PB, as elaborated by *Guéron & Weisbuch* (1980), will be briefly reviewed below. A full survey of CC has been given by *Manning* (1978b), and of PB by *Guéron & Weisbuch* (1979, 1980) and *Weisbuch & Guéron* (1981). Short reviews have also been published (*Manning*, 1972, 1979b; *Guéron & Weisbuch*, 1981; *Guéron*, 1982).

For the cylindrical polyion, both theories rely on the dimensionless line charge density parameter ξ, given by:

$$\xi = \frac{e^2}{4\pi\varepsilon kTb} \qquad (2.15)$$

where e is the elementary charge, ε is the bulk dielectric constant, k the *Boltzmann* constant, T the *Kelvin* temperature, and b the linear charge spacing along the polyion chain.

Counterion condensation

The counterion condensation theory of *Manning* is based on the following assumptions.

i Systems for which ξ exceeds a certain critical value ξ_{crit} are thermodynamically unstable: counterions will 'condense' onto the polyion in order to reduce the value of ξ effectively to ξ_{crit}. For systems containing only one type of metal ion, with charge z, ξ_{crit} is given by:

$$\xi_{crit} = \frac{1}{z} \tag{2.16}$$

If the number of ions condensed per charged group is θ_z for z-valent ions, the maximum value of θ_z is:

$$\theta_z = \frac{1}{z} \left(1 - \frac{1}{z \cdot \xi}\right) \tag{2.17}$$

ii Condensed counterions are present in a cylindrical volume around the polyion. The local concentration of the condensed ions $c_{loc,z}$ in the condensation volume V_p per group, is independent of the distance x to the polyion, and is given by:

$$c_{loc,z} = \frac{\theta_z}{V_p} \tag{2.18}$$

The diffusion coefficient of the condensed ions is assumed to be equal to that of the polyion.

iii For the remaining effective charge on the polyion, the *Debye-Hückel* theory is applicable, to calculate the electrostatic free energy of the system.

By minimization of the sum of the mixing and electrostatic free energy contributions with respect to θ_z, expressions for θ_z and V_p as a function of ξ, z and c_1 for systems with 1:1 salt are derived. A number of these expressions are given and applied in § 4.4.2.

A remarkable prediction of the CC theory is the occurrence of critical values of ξ for different valences of counterions. Consider a

highly charged polyion ($\xi > 1$) in a solution in which initially only monovalent metal ions are present. Some monovalent ions are condensed, until $\xi_{eff} = 1$. Upon addition of a divalent metal salt to the solution, three regions can be recognized:

1. $\xi_{eff} = 1$. If the amount of divalent metal ions M is sufficiently low, all M ions are condensed, and a number of monovalent metal ions K may be condensed, to keep $\xi_{eff} = 1$;
2. $0.5 < \xi_{eff} < 1$. All M ions are condensed, no K ions are condensed;
3. $\xi_{eff} = 0.5$. No K ions are condensed, and a fraction of the M ions is condensed, sufficient to establish $\xi_{eff} = 0.5$.

Poisson-Boltzmann

Guéron and *Weisbuch* introduced the CIV, already mentioned in § 2.2.1, and assumed that the *Boltzmann* equation is applicable throughout:

$$CIV_z = c_z \cdot \exp(-ze\psi_s/kT) \qquad (2.19)$$

where c_z is the bulk concentration of the z-valent ions. The second assumption is that also the *Poisson* equation is applicable throughout. The accumulated ions are considered to be mobile. The CIV is dependent both on ξ and the radius a of the polyion cylinder.

The PB differential equation has been numerically solved, using a fourth order *Runge-Kutta* method. From the results, presented by *Guéron* and *Weisbuch*, it appears that the local concentration of the metal ions initially decreases sharply and linearly with x, down to a concentration of about 0.25 CIV. A remarkable result is the sum-rule, valid at $\xi > 0.5$: the sum of the CIV values of the ions with different valence is a constant at a given charge density. The fact that the *total* CIV is independent of the counterion valence is explained by the better screening of the more strongly attracted ions with higher valence. In an approximative formula, valid for a cylindrical polyion in low 1:1 salt, the sum is given by:

$$CIV = CIV_1 + CIV_2 + \ldots + CIV_z \cong \frac{\xi}{2\pi a^2 b} \exp(-2.3/\xi) \qquad (2.20)$$

The sum-rule, in combination with eq. (2.19), directly implies that no critical values for ξ are foreseen. In mixed systems, no discontinuities at $\xi = 1$ are predicted.

A scheme to calculate the values of CIV_1 and CIV_2 at a given set ξ, a, and concentrations c_1 and c_2 in the bulk has been published by *Weisbuch & Guéron* (1981).

Comparison of the theories

A number of results from the two theories are *mutatis mutandis* the same: for example, preferential accumulation (or: condensation) of divalent over monovalent cations is predicted by both. Moreover, in systems with only one type of metal ion, both CIV and c_{loc} are claimed to be rather insensitive to the concentration of the metal ions in the bulk. Both CIV and c_{loc} may become very large, up to the molar region. Activity coefficients of metal ions in polyelectrolyte solutions, as predicted by the two theories, do not differ significantly.

Differences between the models relevant for the present work concern the distribution of counterions around the polyion, the im/mobility of the condensed/accumulated counterions, the occurrence of critical values of ξ in CC and the sum-rule in PB.

The counterion distributions, as assumed in CC and calculated in PB, have been sketched in fig. 2.1. It is obvious that for high CIV, the metal ions will form a rather 'condense' layer around the polyion. The concept of condensation has been corroborated by authors applying statistical mechanics (*Ramanathan & Woodbury*, 1982), different elaborations of solutions of the PB equations (*Anderson & Record*, 1980; *Delville*, 1980; *Odijk*, 1983), and the Monte Carlo method (*leBret & Zimm*, 1984) to the problem of the counterion distribution. According to the last-mentioned authors, counterion condensation is a necessary consequence of the proper evaluation of the PB equations.

If the assumption that condensed ions are immobilized is correct, and if covalent interaction is negligible, the amount of bound metal ions as experimentally determined, would correspond to the amount of condensed ions. In that case, the occurrence of critical values of ξ can be established experimentally. A confirmation of condensation would imply that the sum-rule is not generally valid. The existence of some ξ_{crit} should also have consequences for the dependence of $\log K_{app,a}$ on α_d: a discontinuity would exist. However, no discrete values of ξ_{crit} are foreseen in the case of excess 1:1 salt (*Manning*, 1974). Thus, the most direct observation of the condensation phenomenon may be made for the conductometrically studied salt-free systems rather than for the polarographically studied solutions.

2.3 CHARACTERISTICS OF THE REACTANTS

2.3.1 PAA, PMA, PMApe

The structural formulas of poly(acrylic acid), PAA, and poly(methacrylic acid), PMA, are given in fig. 2.2. In PMApe, a partially esterified version of PMA, about one-third of the carboxyl groups had been randomly converted into methylester groups.

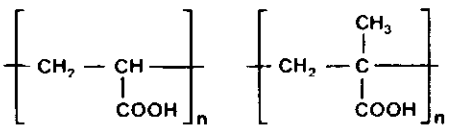

PAA PMA

FIGURE 2.2 Structural formulas of PAA and PMA.

Detailed descriptions of the synthesis and properties of these polyacids have been given by *Böhm* (1974).

Dimensions

It follows from molecular models that in the stretched conformation of isotactic and syndiotactic PAA, the monomer length b is 0.22 and 0.26 nm, respectively (*Sasaki & Minakata*, 1980), whereas for PMA the corresponding values are 0.23 and 0.24 nm (*van der Drift*, 1975). The radii of the unhydrated polyion chains are ∿ 0.3 nm for PAA and ∿ 0.4 nm for PMA. Because of hydration of polycarboxylates (*Begala & Strauss*, 1972; *Conway*, 1981; *Ueberreiter*, 1982), the effective radius is larger than the anhydrous radius. Sometimes, it is set at 0.5 nm (*Sasaki & Minakata*, 1980). The partial volume of unhydrated PAA is about 40 cm^3 per mole monomer, slightly dependent on α_d. For PMA it is about 44 $cm^3 \cdot mol^{-1}$ at $\alpha_d = 1$, but it decreases significantly with α_d (*Conway*, 1981).

In the present study, the measurements were frequently performed with a polyacid concentration of ∿ 2.5 moles functional groups per m^3, and ∿ 50 $mol \cdot m^{-3}$ added 1:1 salt. Assuming a regular packing of parallel cylinders, the distance separating the cylinders is about 28 nm. For comparison: the radius of the condensation volume is predicted to be ∿ 1.5 nm at $\alpha_d = 1.0$ (*Manning*, 1977b), and κ^{-1} is 1.4 nm.

Conformations

The conformational transition of PMA and PMApe (and its absence for PAA) from a compact to an extended structure, at a certain charge density, is well-known, and has been extensively described (*Leyte & Mandel*, 1964; *Böhm*, 1974; *Dubin & Strauss*, 1975; *Gustavsson et al.*, 1978; *Ben-Naim*, 1980). Hydrophobic forces originating from the methyl side chains promote a compact polymer conformation, whereas repulsive electrostatic forces conduce the expansion. The enthalpy of the transition is increasingly positive with temperature, demonstrating the hydrophobic character of the interaction (*Delben et al.*, 1972). Adsorption of the polymer may facilitate the transition to the expanded form (*van Vliet & Lyklema*, 1978). According to *Nagasawa et al.* (1965), PMA is less flexible than PAA as a result of the more hydrophobic character of the former.

Recently, it has been discovered that PAA shows a gradual change in conformation with α_d (*Koda et al.*, 1982; *Gunnarsson & Gustavsson*, 1982). This finding would agree with the observation that often the charge density of PAA appears to be larger than ξ_{str}, that is the structural charge density calculated on the basis of the stretched conformation (*Liquori et al.*, 1959).

2.3.2 Protolytic properties

General

The neutralization of polycarboxylic acids with bases yields polyions which become increasingly charged, expanded, hydrated, and associated with counterions as the deprotonation proceeds. All of these processes are interrelated and influence the dissociation equilibrium. The apparent acid dissociation constant is defined as:

$$pK_{app,a} = pH + \log \frac{1 - \alpha_d}{\alpha_d} \qquad (2.21)$$

where α_d is the degree of dissociation. In the case of polycarboxylic acids, $pK_{app,a}$ is not a true constant. Experimentally, $pK_{app,a}$ is found to be dependent on α_d (*Arnold*, 1957), the polymer concentration c_p (*Nagasawa et al.*, 1965), the 1:1 salt concentration c_1 (*Oth & Doty*, 1952), the composition of the polymer backbone and side-chains (*Bloys van Treslong*, 1978), the valence (*Katchalsky & Spitnik*, 1947) and the nature (*Kagawa & Gregor*, 1957) of the cations present. Generally, $pK_{app,a}$

is split up in a constant term pK_a and a term ΔpK_a accounting for the variable factors:

$$pK_{app,a} = pK_a + \Delta pK_a \qquad (2.22)$$

where K_a is the acid dissociation constant for $\alpha_d \to 0$. K_a is conventionally defined as:

$$K_a = \frac{[RCOO^-](H^+)}{[RCOOH]} \; ; \; \alpha_d \to 0 \qquad (2.23)$$

where in brackets the concentration, and in parentheses the activity is denoted. At low c_p and c_1, K_a can be identified with the intrinsic acid dissociation constant of the monomeric unit.

The non-ideality term ΔpK_a comprises all the factors that are directly or indirectly dependent on the polyion charge, i.e. it includes both long-range and short-range coulombic effects.

The α_d dependence of $pK_{app,a}$

According to *Nagasawa* (1971), ΔpK_a is a measure of the electrical work per mole, ΔG_{el} to remove a proton from the surface of the polyion to infinity. At any α_d value:

$$2.3 \cdot \Delta pK_a \cong \Delta G_{el}/RT \qquad (2.24)$$

where R is the gas constant. Alternatively, ΔpK_a can be expressed by:

$$2.3 \cdot \Delta pK_a \cong -e\psi_s/kT \qquad (2.25)$$

where ψ_s is the potential at the proton binding site. Eq. (2.25) demonstrates that the titration with base is an experimental procedure of charging a polycarboxylic acid molecule. Eq. (2.25) has been used by *Torrence et al.* (1971) to calculate activity coefficients of polyions, and by *Marinsky* (1976) to assess the accumulation of metal ions in the vicinity of the polyion. We will use eq. (2.25) in comparison with eq. (2.12), for example to calculate coordination numbers in the metal complexation (§ 4.4.1), to estimate the covalent contribution in the complex formation (§ 5.3.1), and to assess the polyelectrolyte effect of humic acids (§ 7.4.1).

A number of theoretical models have been applied to calculate ΔpK_a or ψ_s as a function of α_d. For the cylinder model of the polyion, the

Poisson-Boltzmann equation (*Kagawa & Gregor*, 1957; *Kotin & Nagasawa*, 1962), a site-binding model (*Sasaki & Minakata*, 1980) and the condensation concept (*Manning*, 1981b) have been applied. A remarkable feature of the results of the condensation theory is the predicted discontinuity in the increase of $pK_{app,a}$ with α_d, at a certain critical α_d value, whereas other models formulate a monotonous increase.

From empirical models (*Katchalsky & Spitnik*, 1947; *Mandel*, 1970) it appeared that, for a given c_p and c_1, two adjustable constants are usually sufficient to yield reasonable fits to the experimental data. Frequently employed is the extended *Henderson-Hasselbalch* (HH) equation:

$$pH = pK_{av} - m \cdot \log \frac{1 - \alpha_d}{\alpha_d} \qquad (2.26)$$

where K_{av} and m are constants. This equation can, *mutatis mutandis*, be applied to describe the binding of M^{2+} instead of H^+. In § 4.4.2 a modification of eq. (2.26) will be used to interpret the results of metal ion titrations in polyacid solutions. Eq. (2.26) has been employed by *Gregor et al.* (1955a) to calculate the free ligand concentration at any value of the pH of a metal/polyacid system, applying the results of the acid/base titration of the metal-free system as a reference. This *Gregor* method has frequently been applied in calculations of binding constants and coordination numbers of metal-polyacid complexes from potentiometric data only. The method has a number of serious drawbacks and will not be applied in the present work.

The c_1 and c_p dependencies of $pK_{app,a}$

At high α_d and low c_p, $pK_{app,a}$ should decrease linearly with log c_1, with a slope of unity (*Manning & Holtzer*, 1973). In the absence of 1:1 salt, the same type of dependence would be valid for c_p, because of the contribution of the charged groups to the ionic strength.

Polycarboxylic acids

PMApe is a weaker acid than PMA (*Böhm*, 1974), and PMA is weaker than PAA (*Arnold*, 1957), probably due to the inductive effect of the methyl groups (*Gregor et al.*, 1955a,b). Moreover, isotactic PMA (b = 0,23 nm) is weaker than atactic PMA (b = 0.24 nm) (*Loebl & O'Neill*, 1960).

Literature values of pK_a show considerable spread. Usually, pK_a

values range from 4-5. The slight dependence of pK_a on concentration, polyacid side-chain composition and ionic strength is not yet clearly established (*Arnold*, 1957; *Nagasawa & Holtzer*, 1964; *Mandel*, 1970). The extrapolation of $pK_{app,a}$ to $\alpha_d \to 0$ to determine pK_a is difficult, and different methods yield different results (*Arnold*, 1957).

The dramatic increase of $pK_{app,a}$ with α_d, for PMA and PMApe, at low α_d values, is attributed to the occurrence of a compact conformation (*Leyte & Mandel*, 1964). In the region of conformational transition, $dpK_{app,a}/d\alpha_d$ becomes smaller, and may be even negative.

The free energy of dissociation of PAA and PMA is dominated by a negative entropy term. Although the enthalpy becomes more negative with increasing α_d, the entropy decreases more rapidly, leading to increasing values of $pK_{app,a}$ (*Crescenzi et al.*, 1972, 1973; *Olofsson & Vlasenko*, 1982). In the region of the conformational transition of PMA the enthalpy of dissociation is positive (*Crescenzi et al.*, 1972).

For PAA, PMA and PMApe, $pK_{app,a}$ decreases with increasing c_p and c_1 (*Arnold*, 1957; *Kagawa & Gregor*, 1957; *Nagasawa et al.*, 1965; *Böhm*, 1974). The value of $pK_{app,a}$ may also vary with the type of metal hydroxide used (*Gregor et al.*, 1957; *Plochocka & Wojnarovski*, 1971). From the group of alkali metal ions, only Li^+ is involved in some covalent binding with $RCOO^-$ (*Koda et al.*, 1982). However, K^+ (*Koda et al.*, 1982) and Na^+ (*Gunnarsson & Gustavsson*, 1982) only interact electrostatically with PAA. Differences in the interaction of PAA with Na^+, K^+ and Cs^+ were not found by *Olofsson & Vlasenko* (1982).

2.3.3 Cd(II), Pb(II), Zn(II)

The electron configurations of the outer electrons of Cd, Pb and Zn are $5s^24d^{10}$, $5d^{10}6p^2$, and $4s^23d^{10}$, respectively. The electronegativities on the *Little & Jones* scale are 1.46, 1.55 and 1.66, respectively. The ionic radii of the corresponding unhydrated divalent cations are 0.097, 0.094 and 0.074 nm, respectively. These data often explain a number of the complex formation characteristics of these metals.

In contrast to the situation with Pb, the d-orbitals of Cd and Zn are not involved in any bond formation. The chemistry of Cd and Zn is much the same, although the tendency to form complexes is slightly larger for Cd (*Durrant & Durrant*, 1970). Pb possesses more possibilities to form complexes than Cd and Zn. The order in tendency of complex formation Pb > Cd ≅ Zn is also applicable to carboxylates as ligands in low molecular mass complexes (*Sillén & Martell*, 1964, 1971).

The three metal ions studied assume intermediate positions on the *Lewis* scale of acidity, being neither 'hard' nor 'soft' acids.

According to *Conway* (1981), *Stokes'* law is surprisingly well applicable to the hydrated radii of a number of metal ions, Cd, Pb and Zn included. We will use this feature in the evaluation of the polarographic results, to be pointed out in § 3.3.3.

2.4 LITERATURE

2.4.1 M/polycarboxylic acids

A number of experimentally observed properties of metal/polycarboxylic acid systems relevant for the present study will now be briefly described.

It has been demonstrated by *Mandel* (1967) that different methods may be sensitive to different aspects of the metal-polyion association. For instance, in otherwise identical solutions of Cu/PMA and Ba/PMA, the same decrease in specific viscosity is observed as compared to the metal-free solutions, whereas the potentiometric behaviour of the samples differs markedly, due to difference in the 'chemical part' of the associations.

Copper

The most widely studied metal ion is Cu^{2+}. It forms largely covalent complexes with PMA (*Mandel & Leyte*, 1964b; *Marinsky & Ansprach*, 1975; *O'Neill et al.*, 1965) and PAA (*Yamashita et al.*, 1979a). For both systems, coordination numbers j of 1, 2 and 4 have been reported (*Kotliar & Morawetz*, 1955; *Kolawole & Mathieson*, 1977; *Noji & Yamaoka*, 1979; *Marinsky*, 1982).

According to *Eldridge & Treloar* (1976), Cu^{2+} is able to provoke a redistribution of charged and uncharged groups in PAA, to create adjacent binding sites, whereas $Co(NH_3)_6^{3+}$ appeared to be unable to do so. Moreover, *Leyte et al.* (1968) claimed that a binuclear copper complex exists in the interaction product with PMA, and *Yamashita et al.* (1979a) reported that the intrinsic binding constant for Cu/PAA changes with α_d. The occurrence of large values of j, polyion charge redistribution, binuclear complexes and the change of K_{int}(M/PAA) have not been reported for other metal ions.

Chemical binding

Evidence for chemical interactions, in addition to electrostatic ones, in metal/polycarboxylic acid systems, have also been reported for other metals than Cu, such as: Ag (*Khalaf et al.*, 1975), Ca (*Travers & Marinsky*, 1974), Cd (*Mandel & Leyte*, 1964a), Co (*Spegt et al.*, 1973), La (*Khalaf et al.*, 1975), Li (*Quadrifoglio et al.*, 1973), Mg (*Begala & Strauss*, 1972), Mn (*Karenzi et al.*, 1979), Ni (*Ansprach & Marinsky*, 1975), Pb (*van Leeuwen et al.*, 1981), Tb (*Nagata & Okamoto*, 1983) and Zn (*Yamashita et al.*, 1979b). The chemical contribution is small for Co, Li, Mg and Mn.

For a number of metal ions, such as Co, Cd, Ni and Zn, both j=1 (*Travers & Marinsky*, 1974; *Ansprach & Marinsky*, 1975) and j=2 (*Mandel & Leyte*, 1964a) have been indicated as the coordination number of the predominant complex.

Although no significant chemical binding was found for the alkali metals, except for Li, the electrostatic interaction with polycarboxylate ions has been reported to decrease in the order Li > Na > K > Rb (*Crescenzi et al.*, 1959, 1960; *Eldridge & Treloar*, 1970; *Nagata & Okamoto*, 1983), that is with increasing radius of the unhydrated metal ion. Consequently, partial dehydration would be expected to occur.

The binding strength with PMApe decreases, according to *Ralston et al.* (1981), in the order Cd > Ni > Mn > Ca. For maleic acid copolymers, the sequence Cu > Cd > Mn > Ni > Zn > Co was found (*Felber et al.*, 1968; *Felber & Purdie*, 1971). However, *Yamashita et al.* (1979b) claim for maleic acid polymers: Cu > Zn > Ni ≅ Co ≅ Mn, whereas for PMA an order Co > Ni > Cu has been advocated by *Constantino et al.* (1967). The well-known order of *Irving & Williams* (1948,1953) for metal complexation is not generally observed.

According to *Paoletti et al.* (1976) the interaction of Ba with polycarboxylates is almost purely electrostatic.

PAA versus PMA

The binding of Cu^{2+} to PAA is stronger than to PMA (*Yamashita et al.*, 1979a), and it is stronger with linear than with branched polycarboxylic acids (*Gregor et al.*, 1955a,b). Stronger association with PAA, as compared to PMA, has also been reported for Tb^{3+} (*Nagata & Okamoto*, 1983) and Na^{+} (*Crescenzi et al.*, 1959, 1960). *Loebl et al.* (1955) suggested that a stronger interaction may be related to a larger flexibility of the polymer.

Polyion conformational changes may influence the metal ion associa-

tion with polymaleic copolymers (*Yamashita et al.*, 1979b), with PMA (*Gustavsson et al.*, 1978) and with PAA (*Yamashita et al.*, 1979a). *Kotliar & Morawetz* (1955) related the change of K_{int} for Cu/PMA to the α_d range in which the conformation of PMA is assumed to change. However, according to *Jakubowski* (1975), the compact conformation of PMA is stabilized by the interaction Cu/PMA.

Enthalpy and entropy

According to *Loebl et al.* (1955), *Felber et al.* (1968) and *Paoletti et al.* (1976) the metal ion association with polycarboxylate systems is mainly entropically driven. The changes in enthalpy upon binding of Cu, Ni and Ba to maleic acid copolymers (*Crescenzi et al.*, 1974; *Delben & Paoletti*, 1974) and that of Cu and La to PAA and PMA (*Khalaf et al.*, 1975) are endothermic, thus emphasizing the entropically driven character. It has been suggested that the increase in entropy upon binding is partially attributed to the release of hydrated water from polyion and metal ion (*Begala & Strauss*, 1972; *Crescenzi et al.*, 1974; *Delben & Paoletti*, 1974).

2.4.2 Cd, Pb, Zn/PAA, PMA, PMApe

Several authors have published experimental results for systems analogous to those investigated in the present study. Conclusions derived from those results appear to be partly contradictory.

In a potentiometric study, *Mandel & Leyte* (1964a), using a modified *Gregor* method, claimed that j=2 for Cd/PMA and Zn/PMA.

Travers & Marinsky (1974), applying isotope labelling in Zn/PMA and Zn/PAA, and *Jakubowski* (1975), applying polarography in Zn/PMA, found j=1 for these systems. These authors also used the acid/base titration in the absence of M^{2+} as a reference. However, ΔpK_a was used as a measure of the non-ideality of the polyion in the metal containing systems. In addition, it has been claimed that the intrinsic binding constants are identifiable with those of 'monomeric' organic complexes.

Bolewski & Lubina (1969, 1970) studied Cd/PMA and Zn/PMA polarographically. It was found that j=2 in both systems. However, the electrostatic character of the binding was not considered at all.

Lapanje (1964) and *Lapanje & Oman* (1965) determined polarographically the degree of ion binding in a Cd/PAA system in the presence and in the absence of excess of KCl. It was found that in the system without KCl, the binding of Cd is almost complete, and that the character

of the binding is partly covalent.

Yamashita et al. (1976) used a Cd-selective electrode to study Cd/PAA. Using a modification of *Gregor*'s reference method, an average coordination number j=1.5 was given, but values of the equilibrium constants appeared to be dependent on α_d, and were not given for that reason.

Kurenkov et al. (1979) investigated Cd/PAA with and without 1:1 salt, using polarography. It was demonstrated that, in the absence of 1:1 salt, the diffusion currents decrease to a plateau value with increasing concentration PAA, and increase linearly with α_n at a ratio $[PAA]_T/[Cd]_T = 2$. The authors claim that the use of NaOH (instead of KOH) to neutralize PAA, leads to stronger binding of Cd^{2+}. This observation is not in agreement with the results obtained by *Crescenzi et al.* (1959, 1960), indicating that the binding strength M^+/PAA decreases in the order Na > K.

Kolawole & Bello (1980) and *Kolawole & Olayemi* (1981), using different techniques, investigated Zn/PMA, and concluded that j=2 at low, and j=1 at high concentrations of Zn.

Ralston et al. (1981) studied rheological properties of oil in water emulsions, stabilized by PMApe in the presence of Cd^{2+}. It was advocated that only at intermediate values of α_n, considerable interparticle interaction occurs due to Cd-PMApe bridging. Independently, potentiometric titrations of Cd/PMApe in solution were carried out, going from $\alpha_n = 1.00$ downward. It was claimed that the range of α_n values where the conformational transition occurs, is the same as in the case of Na/PMApe. However, for other divalent metal ions, such as Ca, Mn and Ni, at otherwise identical conditions, that range appeared to be shifted to higher values of α_n.

Van Leeuwen et al. (1981) concluded from the results of an exploratory study preceding the present investigations, that the metal ion binding in Cd/PMApe and Pb/PMApe systems can only be explained by a combination of covalent and electrostatic interaction.

3 EXPERIMENTAL: MATERIALS & METHODS

3.1 GENERAL

3.1.1 Experimental strategy

As described in § 1.2.3, the variables studied are the metal ligand concentration ratio, M/L, where L represents a carboxyl*ate* group, the degree of neutralization α_n, and the concentration of added 1:1 salt c_1.

Changes in M/L can be brought about in several ways. For example:

i Addition of polyacid to a metal nitrate solution. In this case, the overall polyacid concentration c_p will change also, which may complicate the results (*Saar*, 1980).

ii Addition of base to a metal/polyacid system: α_n will change simultaneously.

iii Mixing metal/polyacid solutions of different M/L. However, the solutions with high M/L tend to coagulate, thus rendering all mixtures less defined.

iv Addition of metal salt to a polyacid solution, up to incipient coagulation.

In our study, the last-mentioned strategy was applied. Essential feature of this strategy is the constant distance of separation of the charged sites on the polyacid. Dilution of the sample is controlled and limited by the use of metal nitrate solutions of relatively high concentration. Series of this type will be called here: *M/L-titrations*.

Variation of α_n was achieved either by adding aliquots of a KOH solution, or by mixing metal/polyacid solutions of the same metal ion and the same polyacid concentrations at different degrees of neutralization. By using sufficiently low metal ion concentrations, coagulation is prevented. Series of varying α_n will be called: *α_n-titrations*.

Effects of added 1:1 salt were studied using either an addition- or a mixing strategy, so far as coagulation could be avoided. Generally, KNO_3 was used, but a number of addition series were repeated using $CsNO_3$ or $LiNO_3$. Series of varying 1:1 salt concentration will be called: *c_1-titrations*.

Approximately 200 different titration series were performed. In a series, either the polarographic (P) response, or the conductometric (C), or the Cd-ion selective electrode (I) response was determined. The pH-response was determined for nearly every sample solution in all

the titrations. About 125 single M/L titrations were performed for different metal/acid combinations, α_n- and c_1-values. The distribution over the analytical techniques was 50-P, 50-C and 25-I. About 50 (15-P, 35-C) single α_n-titrations, and about 25 (20-P, 5-C) single c_1-titrations completed the systematic experiments.

3.1.2 Conditions & procedures

In this paragraph the experimental conditions and procedures are described that have been generally observed. Experimental conditions and arrangements especially referring to particular analytical techniques will be described in the corresponding sections.

Water

The only solvent used was water. Employing a Millipore Super-Q system, tap water was demineralized by reverse osmosis. Subsequently it passed, in several cycles, over an activated charcoal column and a mixed bed ion exchanger. In the purification system, the water never contacted metal-containing parts. After degassing traces of CO_2, the resulting purified water, with pH = 6, had a conductivity less than 0.5 $\mu S \cdot cm^{-1}$.

Temperature

Generally, titrations were performed at 25.0 °C. Only the c_1-titrations of the Cd/PMApe systems were performed at 20.0 °C. Haake thermostats were used.

Concentration

The analytical concentration of a polyacid solution, c_p, is expressed as the volumic number of functional groups (protonated *and* deprotonated), in $mol \cdot m^{-3}$, as determined in protolytic titrations.

For the various metal ion detecting techniques applied in the *present* study, the detection limit is about 10^{-3} $mol \cdot m^{-3}$ under the experimental conditions observed. Interesting values for the metal/polyacid concentration ratio are those not exceeding unity. Therefore, the initial polyacid concentration was generally set in the range 1-3 $mol \cdot m^{-3}$.

Higher concentrations could lead to disadvantages: the viscosity of the polymer solution could rise to levels at which the diffusion coefficient of the free metal ions is seriously reduced, the discrepancy with natural levels of humic material would become too large, and our

data would be less suited to check the various polyelectrolyte theories that have been derived for dilute solutions only.

For the synthetic polyacid, the humic acid and the fulvic acid sample solutions, the initial c_p values were chosen at about 2.5 ± 0.2, 2.0 ± 0.1 and 1.0 ± 0.1 mol·m^{-3}, respectively.

To obtain ionic strengths below 0.01 mol·dm^{-3}, levels comparable to some natural conditions and interesting for theoretical reasons, the initial c_p values in the c_l-titrations of the Cd/PMApe and the Pb/PMApe systems were set at 0.15 and 0.3 mol·m^{-3}, respectively.

Nitrogen

Traces of oxygen that disturb the polarographic currents, and traces of carbon dioxide that may obscure the pH- and conductometric responses, were removed by passing purified nitrogen through the sample solutions: at least 8 minutes for each 5 ml of a fresh sample, and 4 minutes after each addition. During the measurements, the sample solutions were blanketed by a nitrogen stream.

The nitrogen was purified in a washing-bottle train, in 5 stages. In the first, an alkaline solution of pyrogallol absorbed oxygen. In the second, concentrated sulphuric acid dried the gas to avoid poisoning of the reducing catalyst in the third stage. The BTS catalyst, containing Cu(I) on a carrier, removed any remaining traces of oxygen. In the fourth, carbon dioxide was removed by potassium hydroxide pellets, and in the fifth, the gas was humidified to avoid evaporation in the titration vessel.

Procedures

Polyacid solutions were prepared by dilution to the desired concentrations of the stock solutions, and stored in the dark at 4 °C. Subsequently, two of the three variables, M/L, α_n and c_l, were adjusted.

Typical experiments in the M/L-titration series consisted of either spiking the sample with aliquots of a metal nitrate solution of relatively high molarity, usually 10 mol·m^{-3}, or preparing a series of batches with increasing M/L ratio. The latter procedure was adopted in those cases where the former gave less reproducible results, for example in the metal/humics systems and in the Pb/PAA experiments. These batches were allowed to stand overnight for equilibration. Typical experiments in the α_n-titrations and the c_l-titrations were *mutatis mutandis* the same. If the mixing procedure was adopted, two bat-

ches were prepared by addition, all others were obtained by mixing these two batches in different proportions.

Some series have been completely reproduced. For other series, random tests of the reproducibility were performed.

Aliquots of metal nitrate- or base solutions were added with Pipetman of Eppendorf pipettes. Only those pipettes were used that, according to the manufacturer, had an accuracy of 0.6%. All volume increments were recorded, to account for the small dilution effect.

During the degassing stage, the solutions were magnetically stirred prior to the conductometric and potentiometric measurements. During the actual measurements, the solutions were *not* stirred.

After the degassing, a short waiting period was observed. Then, the polarogram was recorded, or the conductivity read. To determine the potentiometric readings, a longer waiting period (1-30 minutes) was needed, in order to allow the pH- or the Cd-selective electrode to equilibrate. In those cases where the pH electrode attained equilibrium very slowly, the pH was recorded as a function of time. Due to the necessary waiting periods, single titrations could take 5 hours.

During the pH measurements, neither the mercury electrode, nor the Cd-selective electrode, nor the platinum electrodes of the conductometric cell were connected with the corresponding instruments. During the other measurements, the pH-potentiometer was set in a stand-by position, to avoid interference of the different electrometric set-ups.

Concentrations of the polyacid solutions c_p were determined by conductometric and potentiometric proton titrations, using 100 $mol \cdot m^{-3}$ KOH.

3.2 CHEMICALS

3.2.1 General

Except for the humic material, all chemicals were analytical grade. They were used without further purificiation.

List of chemicals: Fulvic acid solution (obtained by courtesy of *Dr. J. Buffle*, Analytical Chemistry Department of the University of Geneva); humic acid and barium hydroxide (both: Fluka); poly(acrylic acid) solutions (Polysciences); poly(methacrylic acid) solution, and lead nitrate (both: BDH); 2,1-copolymer of methacrylic acid and the methyl ester of methacrylic acid: Rohagit S hv (Röhm); cadmium nitrate, zinc

nitrate, barium nitrate, pyrogallol, isobutyric acid, and succinic acid (all: Baker); silver nitrate (UCB); aluminium nitrate, potassium nitrate, cesium nitrate, lithium nitrate, Titrisol pH buffers 4, 7 and 10, potassium hydroxide pellets, Titrisol potassium hydroxide solutions, Titrisol nitric acid solutions, mercury polarographically-pure quality, sulphuric acid and BTS catalyst (all: Merck); Dowex ion exchanger AG 50 W-X4 50-100 mesh (Bio-Rad).

Metal nitrate stock solutions were prepared by dissolving weighed amounts in water. Dilutions of the stock solutions were stored in polyethylene bottles.

The concentrations of the Titrisol KOH and HNO_3 solutions were incidentally checked. The specified concentrations of 100 $mol \cdot m^{-3}$ turned out to be accurate within 0.5%.

Alkaline solutions of pyrogallol were prepared by dissolving 100 grams of pyrogallol and 300 grams KOH per litre of water.

Before use, the green BTS catalyst pellets were transformed into their active black state, by reducton in a hydrogen gas stream at 130 °C.

3.2.2 Poly(acrylic acid)

The three poly(acrylic acid) solutions as received were clear, yellowish and highly viscous. They contained 25% solids in water. Molecular masses as specified by Polysciences were 50,000 $g \cdot mol^{-1}$, 150,000 $g \cdot mol^{-1}$ and 300,000 $g \cdot mol^{-1}$. The lot/product numbers of these solutions were 11951/0627, 2043/4550 and 4-1681/4551, respectively. Stock solutions of about 10 $mol \cdot m^{-3}$ were prepared by dilution with water. The molecular mass of a PAA monomer unit is 72 $g \cdot mol^{-1}$.

3.2.3 Poly(methacrylic acid)

The poly(methacrylic acid) solution as received was a clear colourless, highly viscous 20% w/w solution in water. The average molecular mass according to BDH was 26,000 $g \cdot mol^{-1}$. The lot and product numbers were 1056920 and 29805, respectively.

A stock solution of about 100 $mol \cdot m^{-3}$ was prepared by dilution with water.

The molecular mass of a PMA monomer unit is 86 $g \cdot mol^{-1}$.

3.2.4 Partially esterified poly(methacrylic acid)

The copolymer of methacrylic acid and the methyl ester of methacrylic acid, Rohagit S hv, was received as a white powder. According to Röhm the viscosity average molecular mass of this high viscosity version was about 10^6 g·mol^{-1}. The acid capacity was given as 405-440 mg KOH·g^{-1}, indicating a degree of esterification of 29-35%. The product number was 1/96740. The properties of PMApe have been described by *Völker* (1961a,b) and *Böhm* (1974).

To prepare the PMApe stock solution, about 1.5 g of the powder was very slowly added, in the dark, to one litre of a solution containing 50 mol·m^{-3} KOH in water, at 70 °C, under continuous stirring.

Subsequently, α_n was reduced by adding slowly a HNO_3 solution, until α_n = 0.032. Below this value coagulation sets in.

The solution obtained was dialysed against pure water until the conductivity of the dialysate remained constant at about 2 μS·cm^{-1}. From this stock solution, sample solutions were prepared by dilution with water.

The molecular mass of a PMApe unit that contains on the average one carboxylic group, is 128-139 g·mol^{-1}. Henceforth we will take the carboxylic/ester group ratio to be 2, resulting in a molecular mass of 136 g·mol^{-1} for the averaged 'monomeric unit'.

3.2.5 Humic acid

The humic acid used was a commercial sample from Fluka. It was prepared from sodium humates, extracted from the top layer of a brown coal area. The brown-black powder was partly soluble in water.

Although the manufacturer gave a molecular mass range of 600-1000 g·mol^{-1}, we will argue in chapter 7 that, after the purification and fractionation applied, under the experimental conditions observed, ten times this value is more realistic. The lot and product numbers were 191699116 and 53680, respectively.

Reference samples of humic and fulvic material are not yet available. However, on the 'International Symposium on Complexation of Trace Metals in Natural Waters' (Texel, May 2-6, 1983), it was announced by *R.F.C. Mantoura*, that in 1984 the production of reference material will begin. At present, extraction and purification procedures are not standardized: in literature, very different pH values during extraction have been applied (*Flaig et al.*, 1975).

The difference between humic acid and fulvic acid is not sharp. Frequently, the molecular mass range is invoked as a criterion to discriminate: up to about 5000 $g \cdot mol^{-1}$ the name fulvic acid is preferred. Since the high molecular mass range is only soluble in alkaline solutions, and the low molecular mass range is also soluble in acidic solutions, adjustment of the pH is generally used as a means to control the fraction humic material.

The pH chosen to bring humic material in solution is often high: 11 (*Bovendeur et al.*, 1982) or pH > 11 (*Arai & Kumada*, 1981). Very high pH levels may result in decomposition of the humic material due to saponification and auto-oxidation (*Schnitzer & Khan*, 1976). Therefore we chose pH = 9.0 in the dissolution phase.

On the acid side in the fractionation procedure, pH values were set as low as 1.5 (*Holtzclaw & Sposito*, 1979). Very low pH levels will result in solutions containing only 'small' fulvic acid molecules: the fraction in solution would be less representative for humic acid. Besides, the comparison with model polyelectrolytes would become less justified: to study polyelectrolyte effects, large molecules are mandatory. For these reasons, we maintained pH = 3.0 in the fractionation phase.

To prepare a stock solution, 10 g of the Fluka humic acid was added to 1 litre of water. By additions of aliquots of a 3 $mol \cdot dm^{-3}$ KOH solution, the pH was set, and maintained at 9.0. After shaking the mixture for 24 hours, the pH was reduced, by slowly adding a 3 $mol \cdot dm^{-3}$ HNO_3 solution, to pH = 3.0, under continuous stirring of the mixture. After leaving the mixture standing for 24 hours, the precipitate was centrifugated at 18,000 r.p.m. for 40 minutes.

The pH of the decanted supernatant was brought to pH = 7, to prevent further coagulation. The solution obtained was dialysed against conductivity water, using a Spectrapor tubing with a molecular mass cut-off of 3,500. Dialysis was continued until the conductivity of the refreshed dialysate remained constant at about 7 $\mu S \cdot cm^{-1}$. The dialysed solution, with a pH of 6.8 and a conductivity of κ_s = 770 $\mu S \cdot cm^{-1}$, was subsequently treated with an ion exchanger of the type AG 50W-X4 from Bio-Rad, to transfer the material into the acid form.

The pH of the final stock solution was 2.83, and the conductivity κ_s = 560 $\mu S \cdot cm^{-1}$. The dry mass content was 3.90 $kg \cdot m^{-3}$, of which 4.8% ashes. Hence, the stock solution contained 3.71 $kg \cdot m^{-3}$ organic material. The dissolved organic carbon (DOC) content was determined as 2.06 $kg \cdot m^{-3}$, being 56% of the organic material, which is in accordance

with literature data (*Schnitzer & Khan*, 1976).

The stock solution was stored in the dark, at 4 °C. The concentration of carboxylic groups was determined by potentiometric and conductometric acid/base titrations, and appeared to be 18.5 $mol \cdot m^{-3}$, or 9.0 mol per kg DOC. About 10-fold dilutions of the stock solution were used in the metal complexation experiments.

3.2.6 Fulvic acid

The original material was sampled by *Buffle et al.*, on September 12th 1981, from the 'Mare aux Evées', a pond near Fontainebleau (France). The original material was considered to be a water leachable fraction of soil fulvic acids. Analysis reports have been published (*Buffle et al.*, 1982; *Buffle & Deladoey*, 1982). In these reports the number of the sample concerned is 50a. The original, sampled solution was filtered on 8 μ and 0.45 μ membranes, and 10-fold concentrated by freeze drying. The total organic carbon (TOC) content of the solution obtained in this way was 0.2 $kg \cdot m^{-3}$. The contents of total iron and calcium in the concentrate were about 0.02 and 5 $mol \cdot m^{-3}$, respectively. Since about 70% of the organic matter was retained between PM10 and UM05 Amicon membranes, the average molecular mass of this fulvic material is estimated to be about 2000 $g \cdot mol^{-1}$.

Because of some coagulation, the concentrate as received was filtered on a Büchner funnel prior to dialysis of the FA solution against pure water, until the refreshed dialysate showed a constant conductivity of about 1 $\mu S \cdot cm^{-1}$. The molecular mass cut-off of the cellulose dialysis tube was 1,000.

The dialysed solution, with a pH of 4.1 and a conductivity of κ_s = 59 $\mu S \cdot cm^{-1}$, was treated with AG 50W-X4 ion exchanger to transfer the fulvic material into the acid form. The pH of the final stock solution was 3.31, and the conductivity κ_s = 179 $\mu S \cdot cm^{-1}$.

The concentration of carboxylic groups of the FA stock solution appeared to be 1.188 $mol \cdot m^{-3}$, in the potentiometric and conductometric acid/base titrations.

The effectivity of the dialysis and ion exchange for removing iron and calcium was checked by Atomic Absorption Spectroscopy (AAS). No detectable iron could be found with flameless-ASS, at 248.5 nm. With flame-AAS, at 422 nm, the concentration of calcium found was 0.1 $g \cdot m^{-3}$.

After slight dilution, the stock solution was used in the metal complexation experiments. The DOC content of a sample solution with a con-

centration of 0.952 $mol \cdot m^{-3}$ FA was determined as 0.063 $kg \cdot m^{-3}$, which agreed with the value of 0.065 $kg \cdot m^{-3}$ obtained by *Buffle* for the same sample. Apparently, a substantial loss of material occurred in the purification process. From these data the concentration of carboxylic groups appears to be 15 mol per kg DOC. This value is usually about twice that for HA (*Schnitzer & Ghosh*, 1979).

3.3 POLAROGRAPHY

3.3.1 Introduction

In voltammetry the current i at a working electrode is measured as a function of the applied potential E. The term polarography is used when the working electrode is a mercury drop. The high overvoltage for hydrogen at the Hg electrode allows the application of potentials that are sufficiently negative to reduce cadmium, lead and zinc ions.

Generally the current consists of a non-faradaic ('charging') component, due to the (dis)charging of the interfacial double layer without charge transfer, and faradaic components, due to electrode reactions. The application of classic polarography was limited by difficulties in unravelling these two contributions. With new polarographic techniques, viz. pulse polarography (PP) - see 3.3.2, and new polarographic instrumentation, viz. the static mercury drop electrode (SMDE) - see 3.3.6, the charging current can be separated more effectively from the faradaic components, and a high sensitivity can be achieved.

Voltammetric techniques are increasingly used in trace metal speciation of natural water systems, where concentrations levels down to 10^{-8} $mol \cdot m^{-3}$ are to be detected (*Nürnberg*, 1978; *Buffle et al.*, 1976; *Buffle*, 1979; *Florence*, 1982; *Valenta & Nürnberg*, 1980).

To measure metal ion concentrations below 10^{-4} $mol \cdot m^{-3}$, a preconcentration procedure must be applied. Generally, an electrolysis period is observed preceding an anodic stripping process, employing a hanging mercury drop. The detection limit can be lowered by using a mercury film electrode and employing pulsed potential steps during stripping. This is the most sensitive technique available (*Flato*, 1972).

A large variety of potential-time functions is currently employed in polarography (*Bond*, 1980). As a rule, the more simple the applied E-t function, the more established is the theoretical expression of the i-E relation. Hence, in physicochemical studies, where precise

measurements and straightforward i-E relations are required, preconcentration steps should be avoided (*Nürnberg & Valenta*, 1975; *Saar & Weber*, 1982).

A number of studies on the physical chemistry of macromolecules in solution, using polarography, have been reported in literature. *Paleček* (1981) reviewed those where the macromolecule acts as the electroactive species. In table 3.1 a collection of literature entries is presented in which a macromolecule is involved in a complexation equilibrium and polarography has been used. Trace metal analysis studies are not included in table 3.1.

TABLE 3.1 A collection of entries into polarographic studies of interactions with macromolecules in solution

metal	macromolecule	reference	
Cd	Bovine serum albumin	TANFORD	1951
Hg, Zn	Bovine serum albumin	SAROFF & MARK	1953
Cu	Poly(acrylic acid)	WALL & GILL	1954
Cd, Zn	Bovine serum albumin	RAO & LAL	1958
Cd	Poly(styrene sulphonate)	LAPANJE & OMAN	1962
Cd, Tl	Pepsin	LAPANJE	1964,1966
Cd, Tl	Poly(acrylic acid)	LAPANJE & OMAN	1965
Cd, Cu	Poly(vinylpyridine)	FREI & MILLER	1965
Co, Cu, Ni	Humics	ORLOV & EROSICEVA	1967
Cd, Cu	Deoxyribonucleic acid	BACH & MILLER	1967
Cd, Cu	Deoxyribonucleic acid	MILLER & BACH	1968
Cd, Cu, Zn	Poly(methacrylic acid)	BOLEWSKI & LUBINA	1969,1970
Cu	Poly(α,L-glutamic acid)	INOUE ET AL.	1971
(polyamines)	Poly(adenylic acid)	JANIK & SOMMER	1973
Cu, Zn	Poly(methacrylic acid)	JAKUBOWSKI	1975
Cu	Poly(methacrylic acid)	MARINSKY & ANSPRACH	1975
Co, Ni	Poly(methacrylic acid)	ANSPRACH & MARINSKY	1975
Cd, Cu, Pb, Zn	Humics	ERNST ET AL.	1975
Cd	Poly(acrylic acid)	MYAGCHENKOV & KURENKOV	1976
In	Poly(methacrylic acid)	MYAGCHENKOV ET AL.	1977
In	Poly(styrene sulphonic acid)	KURENKOV ET AL.	1977
Cd	Poly(styrene sulphonic acid)	MYAGCHENKOV ET AL.	1978
Cd	Carboxymethylcellulose	TRIVEDI ET AL.	1978
(H)	Humics	GREEN & MANAHAN	1979
Cd, Zn	Humics	SAHA ET AL.	1979
Cd	Poly(acrylic acid)	KURENKOV	1979
Pb	Humics	BUFFLE & GRETER	1979
Cu, Fe	Humics	FRIMMEL	1979a,b
Cd, Cu, Ni, Pb, Zn	Humics	WILSON ET AL.	1980
Cd, Cu, Pb	Humics	SKOGERBOE ET AL.	1980
Cd	Humics	VAN LEEUWEN	1980
Cd, Pb	Poly(methacrylic acid)	VAN LEEUWEN ET AL.	1981
Fe	Humics	FRIMMEL ET AL.	1981
Cd	Acrylamide/acrylic acid copol.	AKHMED'YANOVA ET AL.	1981
Cd	Acrylamide/styrene sulphonic acid copol.	KURENKOV ET AL.	1981
Al	Humics	RITCHIE ET AL.	1981,1982
Cd	Humics	BHAT & WEBER	1982

Table 3.1 reflects the well-known renaissance of polarographic methods about 1970 (*Flato*, 1972) also in macromolecular science. Still, the use of a dynamic method such as some forms of polarography, may be limited by typical complications. Examples for the *present* study of *poly*electrolytes:

- The correct interpretation of the observed i-E characteristics (see 3.3.3).
- Complications in the range of low 1:1 salt levels (see 3.3.4).
- Difficulties emerging from the adsorption of macromolecules at the mercury-solution interface (see 3.3.5).

The metal ions investigated are known to produce reversible, diffusion-controlled currents in the presence of a number of both high and low molecular mass complexing agents, including acrylic polyacids and humic acids, using appropriate supporting electrolytes (*Kolthoff & Lingane*, 1952; *Bolewski & Lubina*, 1969, 1970; *Jakubowski*, 1975; *Oyama et al.*, 1977a,b; *Saha et al.*, 1979; *Sharma et al.*, 1978). Zinc ions may show quasi-reversible and irreversible polarographic waves (*Subrahmanya*, 1960).

In table 3.2, values of polarographically relevant parameters for Cd^{2+}, Pb^{2+} and Zn^{2+} are collected. The second column contains the forward rate constant k_r for the electrode reaction at the Hg electrode:

$$M^{2+}_{aq} + 2e(Hg) \overset{k_r}{\rightleftharpoons} M(Hg) \qquad (3.1)$$

The polarographic reduction of Zn^{2+} is slower than that of Cd^{2+} and Pb^{2+}, probably due to hampered amalgam formation (*Tamamushi*, 1980). Consideration of intermediate oxidation states is not necessary for Cd, Pb and Zn (*Ficker et al.*, 1978). The third column presents pK_h values for the first hydrolysis step of the metal ions:

$$M^{2+}(H_2O)_j \rightleftharpoons M^{+}(H_2O)_{j-1}OH + H^{+} \qquad (3.2)$$

Because of this hydrolysis, the pH range over which M^{2+}_{aq} is the dominant species is limited. In literature, allowed pH values at low ionic strength have been given ranging up to about 9, 6.5 and 9 for Cd-, Pb- and Zn-containing systems, respectively (*Subrahmanya*, 1957; *Ernst et al.*, 1975; *James et al.*, 1975; *Lind*, 1978; *Sohn & Hughes*, 1981).

In the fourth and the fifth column examples are given of half-wave potentials $E_{1/2}$ with respect to the $Ag/AgCl,KCl_{sat}$ reference electrode,

and values of diffusion coefficients, respectively.

In the present study, the polarographic measurements of the M/L- and α_n-titrations were usually performed using 50 $mol \cdot m^{-3}$ KNO_3 as the supporting electrolyte. The point of zero charge (p.z.c.) of the mercury electrode at this KNO_3 concentration is -470 mV vs. $Ag/AgCl,KCl_{sat}$ at different pH values (*Ritchie et al.*, 1981).

TABLE 3.2 Values of polarographically relevant parameters for Cd^{2+}, Pb^{2+} and Zn^{2+}

metal ion	log k_R	pK_h	$-E_{\frac{1}{2}}$/V vs. $Ag/AgCl,KCl_{sat}$	$10^6 \cdot D$ $cm^2 \cdot s^{-1}$
Cd^{2+}	0 (1)	9.8 (2)	0.60 (4)	7.4 (6)
Pb^{2+}	0.17 (1)	6.2 (3)	0.44 (5)	9.4 (7)
Zn^{2+}	- 2,4 (1)	9.7 (3)	1.04 (5)	7.1 (7)

(1) TAMAMUSHI, 1980; averages for different media; $cm \cdot s^{-1}$ values
(2) JAMES ET AL., 1975; ionic strength 0.01 $mol \cdot dm^{-3}$
(3) SILLÉN & MARTELL, 1971; zero ionic strength, 25 °C
(4) KELKAR & NEMADE, 1979; 2.0 $mol \cdot dm^{-3}$ $NaClO_4$, 30 °C
(5) KOLTHOFF & LINGANE, 1952; 0.1 $mol \cdot dm^{-3}$ KCl, 25 °C
(6) IKEUCHI ET AL., 1979; 0.1 $mol \cdot dm^{-3}$ KNO_3, 25 °C
(7) WANG, 1954; < 0.1 $mol \cdot dm^{-3}$ KCl, 25 °C

Both the dropping mercury electrode (DME) and the static mercury drop electrode (SMDE) were used. With the former the drop grows, while with the latter the drop size is constant during the measurement of the polarographic current.

3.3.2 Normal Pulse Polarography

The idea of Pulse Polarography (PP) was introduced by *Barker* (1958) as an extension of his work on square wave polarography. The general principles of PP were discussed by *Barker & Gardner* (1960). *Parry & Osteryoung* (1965) exploited PP as an analytical tool, and *Osteryoung et al.* (1975) described applications.

In Normal Pulse Polarography (NPP), sometimes called Integral Pulse Polarography, successive potential pulses of increasingly more negative amplitude are applied to the Hg electrode. Except during the duration of the pulse, the potential is maintained at an initially preset value E_i, chosen to the anodic side of the reduction wave. The pulses are synchronized so as to occur once, at a definite time, in

the life of each Hg drop, at the end of the drop life t_d. In fig. 3.1 the potential-time behaviour is depicted.

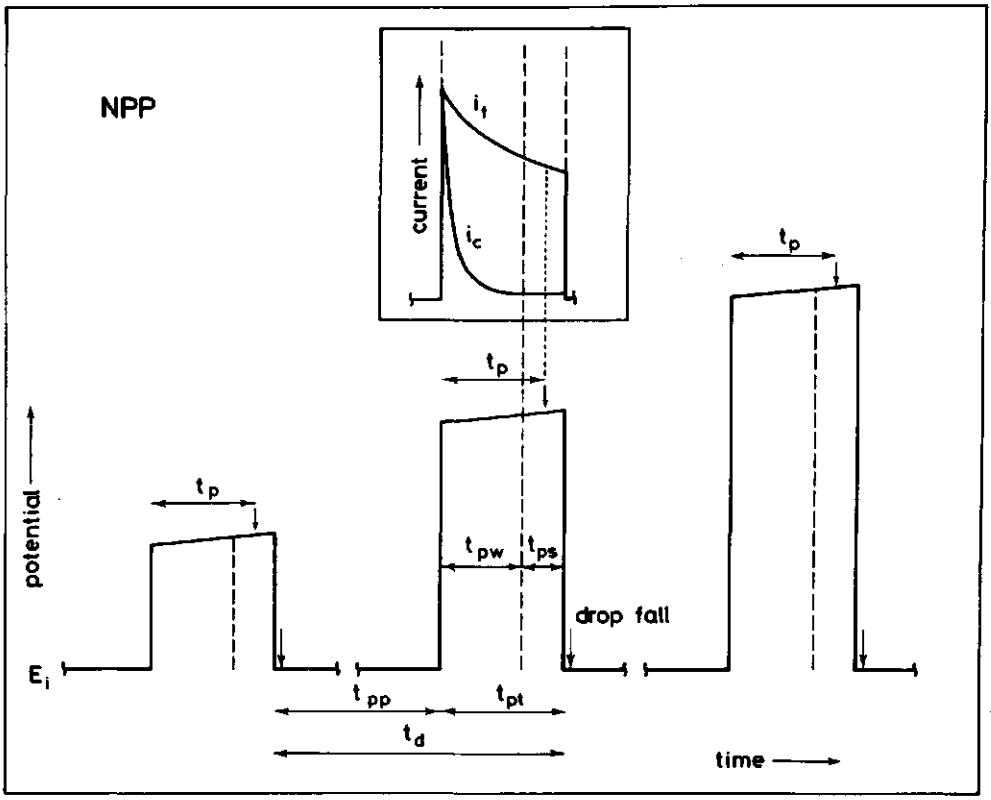

FIGURE 3.1 NPP potential-time behaviour and the corresponding current response for a single pulse in the potential region where a faradaic reaction is occurring. E_i = initial potential; i_f = faradaic current; i_c = charging current; t_d = drop period; t_{pp} = pre-pulse period; t_{pt} = total pulse period; t_{pw} = waiting period before current sampling; t_{ps} = sampling period; t_p = effective pulse period.

During the pre-pulse period t_{pp}, a drop is formed (SMDE), or allowed to grow (DME). The current is sampled during a period t_{ps} at the end of the total pulse period t_{pt}. In the waiting period t_{pw}, the initial part of t_{pt}, the charging current i_c decays to a negligible value after a few milliseconds.

Thus $$t_d = t_{pp} + t_{pt} \qquad (3.3)$$

and $$t_{pt} = t_{pw} + t_{ps} \qquad (3.4)$$

If diffusion-controlled, the faradaic current i_f decays during t_{ps}

as $t^{\frac{1}{2}}$ (*Bond*, 1980).

As the average of the sampled current over t_{ps} is actually recorded, the effective pulse period t_p is given by:

$$t_p^{-\frac{1}{2}} = \frac{1}{t_{ps}} \int_{t_{ps}} t^{-\frac{1}{2}}\, dt \qquad (3.5)$$

The resulting polarograms resemble the conventional DC polarograms, which explains the use of the word 'normal'.

If the initial potential is chosen well before the reduction wave, the i-E relationship for a non-expanding plane electrode is (*Parry & Osteryoung*, 1965):

$$i = -\pi^{-\frac{1}{2}} \cdot n \cdot F \cdot A \cdot D^{+\frac{1}{2}} \cdot c_d^* \cdot t_p^{-\frac{1}{2}} (1 + P)^{-1} \qquad (3.6)$$

where $P = \exp[(nF/RT)(E - E_{\frac{1}{2}})]$, E is the pulse potential, $E_{\frac{1}{2}}$ is the - reversible - NPP half-wave potential, n is the number of electrons transferred per ion reduced in the electrode reaction, F is the *Faraday* constant, T is the *Kelvin* temperature, A is the surface area of the drop, D is the diffusion coefficient of the electroactive species (the depolarizer), c_d^* is the bulk concentration of the depolarizer, and t_p is the effective pulse period.

For potentials sufficiently more negative than $E_{\frac{1}{2}}$, where P approaches zero, the limiting current obtained is given by the *Cottrell* equation:

$$i_\ell = -\pi^{-\frac{1}{2}} \cdot n \cdot F \cdot A \cdot D^{+\frac{1}{2}} \cdot c_d^* \cdot t_p^{-\frac{1}{2}} \qquad (3.7)$$

From the demonstrated applicability of the *Cottrell* equation (*Parry & Osteryoung*, 1965; *Fonds et al.*, 1967) it appears that in NPP the growing Hg drop can be approximated by the stationary plane model. Differences between observed and calculated i_ℓ values are usually attributed to the sphericity of the Hg electrode, the growth of the drop and the shielding by the capillary tip (*Brinkman & Los*, 1964, 1967). These three effects, partially compensating each other, would increase the limiting current, in extreme cases - small A, large t_p - up to c. 5%. However, the magnitude of the generally small net effect varies about linearly with D and with c_d^* (*Brinkman & Los*, 1967). Hence, by using *calibration* plots, these effects can be cancelled out for the major part.

On the basis of the E-t and the i-t characteristics, a number of advantages of the NPP mode can be considered with respect to our subject:

i At appropriate choices for A and t_p, a high sensitivity can be achieved, and low metal ion concentrations can be measured. Employing low metal ion concentrations allows the use of a low concentration of supporting electrolyte which must exceed that of the reducible species by a factor of 25-50. In this study, a concentration of 50 $mol \cdot m^{-3}$ KNO_3 is frequently employed. At 1:1 salt levels below 100 $mol \cdot m^{-3}$, D values of Cd^{2+}, Pb^{2+} and Zn^{2+} are hardly affected by the ionic strength (*Wang*, 1954; *Bhattacharya*, 1972; *Bolzan*, 1975), and impurities are of minor importance. Besides, the *Debye* screening length κ^{-1} is, for 50 $mol \cdot m^{-3}$ KNO_3, about 1.4 nm, which is favourable in polyelectrolyte investigations, because the charge effects of the polyions are not suppressed. Moreover, as natural waters and soils can have ionic strengths down to 10 $mol \cdot m^{-3}$ (*Davison & Whitfield*, 1977), experiments at low salt levels are of environmental interest.

ii A criterion for the diffusion-controlled character of the limiting current is provided by eq. (3.7): For a given solution and drop size, a *Cottrell* plot of i_ℓ vs. $t_p^{-\frac{1}{2}}$ should give a straight line through the origin. In practice, a small intercept on the i_ℓ-axis is usually observed, mainly due to the sphericity effect. A deviation from linearity indicates influences on mass transport due to e.g. coupled homogeneous reactions ('kinetic currents') (*van Leeuwen*, 1979b). A straight *Cottrell* plot, but with a *large* intercept on the i_ℓ-axis, is indicative for reactant adsorption (*van Leeuwen*, 1980). Thus, variation of t_p is a diagnostic tool. As reactant adsorption may readily occur in metal/polyacid systems and substantially influence i_ℓ and $E_{\frac{1}{2}}$, this phenomenon will be separately discussed in § 3.3.5.
Variation of E_i is sometimes a remedial tool to avoid adsorption effects (*van Leeuwen et al.*, 1981).

iii In NPP, E_i is somewhere to the anodic side of the reduction wave, and pulse potentials are increasingly more negative. Thus the charge of the electrode can be controlled, to a limited extent, in the pre-pulse period. If $E_{\frac{1}{2}}$ would be chosen to the cathodic side, and the pulse potentials made increasingly more positive ('scan reversal'), then a limiting current is flowing during the pre-pulse periods. This application of PP is termed Reverse Pulse Po-

larography (RPP). In RPP reactant adsorption during t_{pp} is effectively prevented. On the other hand, any information from adsorption effects is also lost.

For reversible red/ox reactions at the electrode the NPP and the RPP polarograms show the same $E_{\frac{1}{2}}$ value and the same shape, and differ only with respect to the zero of current (*Osteryoung & Kirowa-Eisner*, 1980). In the present study RPP was incidentally applied to test the corresponding NPP limiting currents.

3.3.3 Association constant determination

The overall association reaction between a metal (aquo)ion M and a ligand L may generally be written as:

$$M + jL \underset{k_d}{\overset{k_a}{\rightleftharpoons}} ML_j \qquad (3.8)$$

where j is the coordination number, k_a and k_d are the rate constants for the association and dissociation, respectively.

Polarographic studies of the association constant K_{ML_j} for reaction (3.8), where M is the *reducible* species, are generally based on the elaboration of the shift in the half-wave potential $\Delta E_{\frac{1}{2}}$ and/or the change of the limiting current Δi_ℓ of the metal ions in the presence of ligands (*Crow*, 1969).

The following subjects will now be successively discussed:

i Whether, for the systems to be investigated, $\Delta E_{\frac{1}{2}}$ *or* Δi_ℓ is the more appropriate parameter. It will be argued that in the case of polymeric ligands it is Δi_ℓ, whereas in the case of monomeric ligands $\Delta E_{\frac{1}{2}}$ is to be employed.

ii The interpretation of Δi_ℓ *in the case of polymeric ligands*. It will be demonstrated that Δi_ℓ is the result of the reduction of the mean diffusion coefficient $\bar{D}$ of the reducible species due to the presence of the polycarboxylate ligand.

iii *The mean diffusion coefficient.* $\bar{D}$ will be elaborated in terms of the diffusion coefficients and concentrations of the free and bound metal ions.

iv The interpretation of $\Delta E_{\frac{1}{2}}$ *in the case of monomeric ligands*. The conventional *DeFord-Hume* method is briefly described.

$\Delta E_{\frac{1}{2}}$ *or* Δi_ℓ

Generally, the use of $\Delta E_{\frac{1}{2}}$ to calculate K_{ML_j} requires the following conditions to be satisfied:

i The electrode reaction should be electrochemically reversible.

ii The limiting currents should be diffusion-controlled.

iii The association equilibrium should be polarographically labile, meaning that, for an effective pulse period in NPP, t_p:

$$k_d \cdot k_a^{-\frac{1}{2}} \cdot t_p^{-\frac{1}{2}} \gg 1 \qquad (3.9)$$

iv There should be a large excess of ligand.

v The values of $\Delta E_{\frac{1}{2}}$ should be sufficiently large, at least more than 25 mV (*Bach & Miller*, 1967).

vi The values of $\Delta E_{\frac{1}{2}}$ should be sufficiently accurate.

vii For a given coordination number j, K_{ML_j} should be independent of the M/L ratio.

In metal/polyacid systems, conditions iv-vii are not generally satisfied.

Viscosity limits prevent the use of a large excess of ligand. Besides, values of M/L > 0.5 are also of interest in this study.

Under the experimental conditions, values of $\Delta E_{\frac{1}{2}}$ were generally lower than 50 mV. Values of $\Delta E_{\frac{1}{2}}$ are less accurate in polyelectrolyte solutions, as compared to simple electrolyte solutions. The charge on the polyion introduces a liquid junction potential at the reference electrode, of which the magnitude may depend on the M/L ratio. This phenomenon will be discussed, in another context, in § 3.4.3. Finally, the dependence of K_{ML_j} on M/L is one of the items in this study.

In recent literature, only *Jakubowski* (1975) used $\Delta E_{\frac{1}{2}}$ values in the study of Zn/PMA and Cu/PMA. The maximum value of $\Delta E_{\frac{1}{2}}$ in the former system was 9.5 mV, and in the latter 52.7 mV. His results on Cu/PMA were contradicted by *Slota* (1979), using potentiometry for the same system.

Because of the above-mentioned reasons, we will generally not use $\Delta E_{\frac{1}{2}}$ for the polymeric systems, except by way of comparison in the α_n-titrations. Fortunately, Δi_ℓ values for the metal/polyacid systems are sufficiently large, and can be determined accurately.

In the case of the monomeric ligands investigated, viz. 2-methylpropanoic and butanedioic acid, all conditions i-vii can be satisfied, as will be illustrated in the results. In this case, Δi_ℓ values are very small, as the diffusion coefficients of the complexed and uncom-

plexed metal ions do not differ much.

Literature data on complex formation of Cd^{2+}, Pb^{2+} and Zn^{2+}, with mono- and dicarboxylic acids, support the use of $\Delta E_{\frac{1}{2}}$ for these systems (*Klemencić & Filipović*, 1958; *Yadav et al.*, 1973; *Sharma et al.*, 1979).

Δi_ℓ in the case of polymeric ligands

The correct interpretation of the reduction of i_ℓ of metal ions due to the presence of polyacids requires information on the character of the current measured, and on the character of the association equilibrium involved. The reversibility of the electrode reaction is irrelevant for the interpretation of Δi_ℓ (*Crow*, 1982).

Anticipating the results in the next chapters, we state already that over a wide range of experimental conditions the limiting currents are *diffusion-controlled*. Literature data on the association of heavy metal ions, including Cd^{2+}, Pb^{2+} and Zn^{2+}, with polycarboxylic acids, including poly(methacrylic) and humic acids, support this finding (*Bach & Miller*, 1967; *Bolewski & Lubina*, 1969; *Inoue et al.*, 1971; *Jakubowski*, 1975; *Saha et al.*, 1979; *Buffle & Greter*, 1979; *Frimmel*, 1981).

The diffusion coefficients of the free metal ions will not be significantly influenced by the slight change in viscosity of the solutions due to the presence of the polyelectrolytes (*Doty & Ehrlich*, 1952). From preliminary experiments with PMA at about 3 $mol \cdot m^{-3}$, it appeared that over a wide pH range the relative viscosity never exceeded that of pure water by more than 10%. Upon addition of 2:1 salts, the relative viscosity of the PMA solution generally decreases.

The diffusion-controlled character of i_ℓ allows the application of the *Cottrell* equation (3.7). It also allows us to conclude that the association equilibria are either labile (see eq. 3.9) or non-labile. The latter means that the equilibrium can be considered to be frozen at any time and place in the experiment, to be expressed by

$$k_d \cdot k_a^{-\frac{1}{2}} \cdot t_p^{-\frac{1}{2}} \ll 1 \qquad (3.10)$$

In the intermediate case ('quasi-lability') the *Cottrell* plot is not a straight line (*van Leeuwen*, 1979b). For labile equilibria $\Delta E_{\frac{1}{2}}$ generally increases systematically with decreasing M/L, whereas for non-labile equilibria there is generally no such shift of $E_{\frac{1}{2}}$.

Anticipating the results, we will consider the metal/polycarboxylic acid systems investigated as labile, for sufficiently low M/L values. As the polymer coil tends to become progressively compact with increas-

ing degree of association (*Kanedo & Tsuchida*, 1981; *Kowblansky & Zema*, 1981), a growing degree of polarographic non-lability may develop with increasing M/L under some conditions.

Literature data on the kinetics of counterion interaction with polyelectrolytes support very often the assumption of lability. According to *Manning* (1978b), electrostatic binding of metal ions to polyelectrolytes is characterized by high exchange rates. Data of *Linse et al.* (1981) for Cd/poly(styrenesulphonate) and *Nishikawa & Tsuchida* (1976) for Cu/PAA confirm the high exchange rates, although for the latter systems an additional slower reaction may also occur (*Yamada et al.*, 1982).

The systems Zn/PMA, Cu/PMA and Cu/PAA are polarographically labile, according to *Jakubowski* (1975): shifts in $E_{\frac{1}{2}}$ were determined and the diffusion-controlled character of the limiting currents was verified over a range of electrolysis periods. In addition, the kinetics of proton-transfer reactions of PMA and PAA are fast (*Weiss et al.*, 1971), in comparison with the polarographic time scale. With respect to M/HA interactions, it has been reported for Cd^{2+}, Cu^{2+}, Pb^{2+} and Zn^{2+}, that bound metal ions contribute to the limiting currents, but there is no agreement on the degree of lability (*Ernst et al.*, 1975; *Frimmel*, 1979b; *Buffle & Greter*, 1979; *Saha et al.*, 1979).

In the case of a pulse polarographically labile complex, a metal ion is over any arbitrarily chosen time interval $\tau << t_p$ for a certain fraction, τ_f, of this interval in the free, and during the remaining fraction, τ_b, in the bound state. Therefore, when a current is flowing, *all* reducible metal ions within the diffusion layer δ show a net diffusion towards the Hg drop.

The diffusion layer in NPP is given by:

$$\delta = (\pi \cdot \bar{D} \cdot t_p)^{+\frac{1}{2}} \qquad (3.11)$$

where $\bar{D}$ is some mean diffusion coefficient of the reducible species.

Then, the limiting current is related to $\bar{D}$ and the *total* concentration of the reducible metal ions in the bulk, c_T^*:

$$i_\ell = B' \cdot \bar{D}^{+\frac{1}{2}} \cdot c_T^* \qquad (3.12)$$

where $B' = -\pi^{-\frac{1}{2}} \cdot n \cdot F \cdot A \cdot t_p^{-\frac{1}{2}}$, in the case of NPP.

Expression (3.12), elaborated first by *Kačena & Matoušek* (1953) for systems with small ligands, has been used for Cd/DNA and Cu/DNA,

by *Bach & Miller* (1967).

For Cd/PMA, Cu/PMA and Zn/PMA (*Bolewski & Lubina*, 1969, 1970), and for Cd/PMApe and Pb/PMApe (*van Leeuwen et al.*, 1981), the following expression for i_ℓ has been used:

$$i_\ell = B' \cdot D_f^{+\frac{1}{2}} \cdot c_f^* + B' \cdot D_b^{+\frac{1}{2}} \cdot c_b^* \qquad (3.13)$$

where D_f and D_b are the diffusion coefficients, and c_f^* and c_b^* the bulk concentrations of the free and bound metal ions, respectively.

Eq. (3.13) generally holds in the case of a non-labile equilibrium, where the complex is also electro-active. However, eq. (3.13) needs to be considered also for labile complexes *if* the degree of complexation is independent of the concentration free metal ions. This will only be the case at very low concentrations added 1:1 salt, and at high M/L values. We will return to this point in the discussion of the results.

For Cd/HA and Zn/HA, *Saha et al.* (1979) used:

$$i_\ell = B' \cdot D_f^{+\frac{1}{2}} \cdot (c_f^* + b_1 \cdot c_b^*) \qquad (3.14)$$

where b_1 is some fractional coefficient, used as an adjustable parameter to account for the contribution of bound metal ions to the limiting current. The physical meaning of b_1 is not well-defined, but will be related to the degree of (non-)lability of the equilibria. Eq. (3.14) has also been used in polarographic studies of Cd(II) and Zn(II) complexes with proteins (*Tanford*, 1951; *Saroff & Mark*, 1953; *Rao & Lal*, 1958). The degree of (non-)lability of systems in which humic acids or proteins are the ligands will depend on the particular sample compositions.

The mean diffusion coefficient

To elaborate $\bar{D}$, we will consider - as stated in chapter 2 - a metal ion 'bound', if the self-diffusion coefficient of the metal ion is observed to be equal to that of the much larger polyion (*Magdalenat et al.*, 1974; *Manning*, 1979b).

For high exchange rates between 'free' and 'bound' metal ions, no deviations from the Fickian processes will show up (*Nallet et al.*, 1982), and thus the r.h.s. of the *Einstein-Smoluchowski* equation for $\langle x^2 \rangle$, the mean-square displacement of a metal ion during a time interval τ:

$$\langle x^2 \rangle = 2 \cdot \bar{D} \cdot \tau \qquad (3.15)$$

can be written as:

$$2 \cdot \bar{D} \cdot (\tau_f + \tau_b) = 2 \cdot D_f \cdot \tau_f + 2 \cdot D_b \cdot \tau_b \qquad (3.16)$$

The time intervals τ_f and τ_b are related to the concentrations c_f and c_b through:

$$\frac{\tau_f}{\tau_f + \tau_b} = \frac{c_f}{c_f + c_b} \quad ; \quad \frac{\tau_b}{\tau_f + \tau_b} = \frac{c_b}{c_f + c_b} \qquad (3.17)$$

Using eqs. (3.17) for the bulk concentrations, eq. (3.16) is rewritten as:

$$\bar{D} = D_f \cdot \frac{c_f^*}{c_T^*} + D_b \cdot \frac{c_b^*}{c_T^*} \qquad (3.18)$$

As D_f and D_b differ largely in the case of polymeric ligands, $\bar{D}$ can be used to determine the fraction 'free' and 'bound' metal ions.

Within the diffusion layer, the *local* concentration c_T will be different at every distance x from the electrode. To calculate c_f^* from the experimentally determined $\bar{D}$, using eq. (3.18), the ratios c_f/c_T and c_b/c_T are assumed to be constant over the diffusion layer. Generally, this assumption is a good approximation if excess of ligand is present (*Crow*, 1969). Using the results to be obtained with respect to c_f^*/c_T^* for different c_T^*, the validity of the assumption will be reconsidered.

A theoretical treatment of the variation of the local concentrations, as far as i_ℓ is concerned, is complicated. The variation is dependent on the association mechanism involved: delocalized (atmospheric) binding or localized (site) binding. In the latter case, it is also dependent on the coordination number j. *Elenkova & Nedelcheva* (1976) gave such treatments for low molecular mass complexes, where $D_f = D_b$, which are not applicable to the present cases. In the case of excess metal ions, they predicted that the polarographic wave will be split up.

Miller & Bach (1968) suggested a correction for the variation of c_f/c_T within the diffusion layer. For j = 1 complexes they assume that the $\bar{D}$ value observed is approximately the same as that for an average

degree of complexation $\bar{\theta}_n$ of the polyion over the diffusion layer, given by:

$$\bar{\theta}_n = 0.5 \cdot \theta_n \text{ (bulk)} \tag{3.19}$$

In principle, the choice of the factor 0.5 is arbitrary, as the average is not weighted.

To determine $\bar{D}$ experimentally, we applied eq. (3.12). Denoting the limiting currents for the sample solution and the corresponding blank solution ($c_f^* = c_T^*$) as i_ℓ and i_o, respectively, then, with A and t_p constant, it follows that:

$$\frac{i_\ell^2}{i_o^2} = \frac{\bar{D}}{D_f} \tag{3.20}$$

Eq. (3.18) and eq. (3.20) can be combined to:

$$\frac{i_\ell^2}{i_o^2} = \frac{c_f^*}{c_T^*} + \frac{D_b}{D_f} \cdot \frac{c_b^*}{c_T^*} \tag{3.21}$$

Using eq. (3.21), c_f^* and c_b^* can be calculated, taking into account the limitations inherent to the original equations.

In the presence of 1:1 salt in excess over c_f^*, the D_f values for the sample and the blank solution will be the same. According to the definition of 'binding', D_b is equal to the diffusion coefficient of the polymeric ligand.

The use of eq. (3.21) is based on the very great difference between the diffusion coefficients D_f and D_b. For DNA, D_b has been set zero by *Bach & Miller* (1967), just as for PMA, with $\bar{M}$ = 500,000, by *Bolewski & Lubina* (1969). In our study, the small D_b/D_f values were estimated on the basis of the radii involved (*Crow*, 1968, 1982). Both the acrylic and humic substances are assumed to have approximately spherical shapes in solution (*Richards*, 1980; *Visser*, 1982; *Ritchie & Posner*, 1982). Applying the *Stokes-Einstein* relation to the ratio of the radius of the free aquo-ions, r_f, (*Conway*, 1981) and the radius of gyration of the polymer, r_p, (*Morawetz*, 1965) it follows that:

$$\frac{D_b}{D_f} = \frac{r_f}{r_p} \tag{3.22}$$

The effective radii of the three metal ions concerned are very close, 0.15 ± 0.01 nm (*Creighton*, 1935; *Hunt*, 1963). Tabulated values for the radii of gyration for different molecular mass samples of - uncharged - PAA (*Brandrup & Immergut*, 1965; *Corner*, 1981), were used, and the values for the PMA(pe) samples were calculated using *Mark-Houwink* constants, for PAA and PMA (*Baxendale et al.*, 1946; *Takahashi et al.*, 1957). The r_p values reported for humic acid fractions of appropriate molecular mass, were used for the HA and FA samples (*Ghosh & Schnitzer*, 1980; *Thurman et al.*, 1982).

In table 3.3 the D_b/D_f values calculated are collected. Experimental tests of the order of magnitude of the calculated values will be discussed together with the results.

TABLE 3.3 D_b/D_f values calculated from literature data

polyacid	$\bar{M}$	D_b/D_f
PMApe	1000,000	0.002
PAA	300,000	0.01
PAA	150,000	0.01
PAA	50,000	0.02
PMA	26,000	0.02
HA	10,000	0.05
FA	2,000	0.07

As both acrylic and humic polyacids are assumed to be more or less flexible coils (*Richards*, 1980; *Rajalakshmi et al.*, 1959; *Hayano et al.*, 1983), due to electrostatic forces, the coils will expand with increasing charge and with decreasing salt concentration. According to *Chien & Isihara* (1976) these expansion effects can be described by:

$$\alpha_s^2 = 1 + b_2 \cdot \frac{\bar{M}^{\frac{1}{2}}}{c_1^{\frac{1}{2}}} \qquad (3.23)$$

where α_s is the linear expansion coefficient, and b_2 is a proportionality constant. Due to these effects, D_b/D_f values may be lower than those in table 3.3.

$\Delta E_{\frac{1}{2}}$ in the case of 'monomeric' ligands

According to the method of *DeFord & Hume* (1951), a shift in $E_{\frac{1}{2}}$ is interpreted as the result of a lowered $[M^{n+}(\text{free})]/[M(Hg)]$ ratio at

the mercury electrode surface, due to the complexation reaction, as compared to the corresponding ligand-free solution. Using the *Nernst* equation, $\Delta E_{\frac{1}{2}}$ can be expressed in terms of the free ligand concentration [L], the conditional association constants K_{ML_j}, the diffusion coefficient of the free metal ion D_f and the average diffusion coefficient of the metal ions in the presence of ligand $\bar{D}$: (*Crow*, 1969):

$$\Delta E_{\frac{1}{2}} = \frac{2.3RT}{nF} \log \left[\frac{\bar{D}^{+\frac{1}{2}}}{D_f^{+\frac{1}{2}}} \sum_j K_{ML_j} \cdot [L]^j \right] \qquad (3.24)$$

It is assumed that the electrode reaction is electrochemically reversible, the equilibria involved are labile, M/L is very small, and that $\bar{D}$ is not much smaller than D_f.

In the rearranged form of eq. (3.24):

$$\text{antilog} \left[\frac{nF}{2.3RT} \cdot \Delta E_{\frac{1}{2}} + \log \frac{D_f^{+\frac{1}{2}}}{\bar{D}^{+\frac{1}{2}}} \right] = \sum_j K_{ML_j} \cdot [L]^j \qquad (3.25)$$

the l.h.s. is usually written as $F_0[L]$ to emphasize that it is a function of the free ligand concentration.

The $F_0[L]$ function can be written as:

$$F_0[L] = 1 + K_{ML_1}[L] + K_{ML_2}[L]^2 + ... + K_{ML_j}[L]^j \qquad (3.26)$$

To determine the values of K_{ML_j}, a graphical method advised by *Leden* (1941) was applied to the experimentally determined values of $F_0[L]$. A graph of $F_0[L]$ versus [L] must have a limiting slope of K_{ML_1} for [L] approaching zero. A preliminary value of K_{ML_1} is thus obtained immediately. A new function $F_1[L]$ is then defined by:

$$F_1[L] = \frac{F_0[L] - 1}{[L]} \qquad (3.27)$$

A plot of $F_1[L]$ values against corresponding values of [L] must have a limiting slope of K_{ML_2}, as [L] tends to zero, and an intercept on the $F_1[L]$ axis of K_{ML_1}. Thus a confirmative estimation of K_{ML_1} is possible and, in addition, a preliminary value of K_{ML_2} is obtained.

New functions are defined similarly, for example:

$$F_2[L] = \frac{F_1[L] - K_{ML_1}}{[L]} \qquad (3.28)$$

The procedure is continued until the final function $F_j[L]$ has been reached. The final function should be independent of the ligand concentration.

3.3.4 Conduction currents

In the absence of excess inert salt, NPP limiting currents are not diffusion controlled. For a limited number of measurements, in the c_1-titration series of the Cd/PMApe and Pb/PMApe systems, the condition of excess inert salt was not satisfied. Therefore, a correction was applied to the measured i_ℓ, in order to obtain the diffusion controlled part i_d for which the *Cottrell* equation can be used.

In a solution without convection, ion transport occurs because of a gradient in electrochemical potential. According to the *Nernst-Planck* equation, the current carried by an ion r, in a dilute solution without convection, is for linear mass transfer given by:

$$i_r = - z \cdot F \cdot A \cdot D_r \frac{\partial c_r}{\partial x} - z^2 \cdot F^2 \cdot A \cdot \frac{D_r}{RT} \cdot c_r \frac{\partial \phi}{\partial x} \qquad (3.29)$$

where $\partial\phi/\partial x$ is the potential gradient, and all other symbols have their usual meaning.

The first term on the r.h.s. is the diffusion contribution $i_{d,r}$ and the second term is the conduction (or: migration) contribution $i_{m,r}$. In multi-component systems, expressions for i_r are coupled through the potential distribution, which is a function of all the species in solution. *Okada et al.* (1959) demonstrated that no explicit expression for $i_{m,r}$ is available in the case of simultaneously flowing conduction and diffusion currents. Only for small conduction contributions to the limiting current (*Kharkats*, 1978), the empirical expression by *Heyrovský* is valid (*Ilkovič*, 1934):

$$i_{m,r} = t_r \cdot i_\ell \qquad (3.30)$$

where t_r is the transference number of r.

Eq. (3.30) has been used by *Lapanje & Oman* (1965) and by *Myagchenkov & Kurenkov* (1976), in both cases with respect to Cd/PAA systems without inert salt.

The conduction contribution to i_ℓ is dependent on the bulk concentrations of all ionic species. In the case of a single type of reducible cation, i_ℓ/i_d is a convenient measure for the conduction current i_m (*Newman*, 1966, 1973). To correct for the conduction contribution to i_ℓ of the Cd/PMApe and Pb/PMApe sample solutions, we measured i_ℓ/i_d of blank solutions of approximately the same concentration levels $Cd(NO_3)_2$ and $Pb(NO_3)_2$ as those for the samples, for different concentrations KNO_3, $LiNO_3$ and $CsNO_3$. The composition of the blank solutions was expressed by

$$R = \frac{[M^+]}{[M^+] + 2[M^{2+}]} \qquad (3.31)$$

Excess of inert salt, where $i_\ell = i_d$, was operationally defined at $R = 0.996$.

In fig. 3.2, curves of i_ℓ/i_d versus $R^{+\frac{1}{2}}$ are depicted for KNO_3 as the inert salt. A square-root scale is used on the abscissa axis since only a small amount of supporting electrolyte causes considerable reduction of i_ℓ.

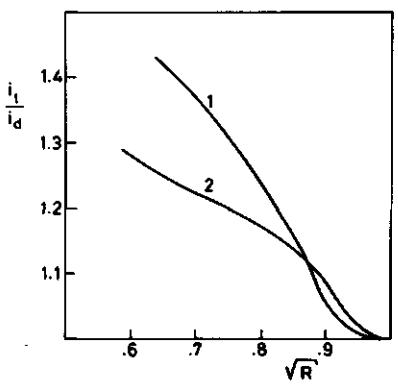

FIGURE 3.2 Calibration graphs for the conduction contribution to the limiting current, for (1) lead nitrate and (2) cadmium nitrate solutions as a function of the relative concentration R of inert salt. i_ℓ/i_d is the ratio of the limiting current observed, and the diffusion current in the case of excess inert salt ($R \to 1$).
1. $[Pb^{2+}] = 0.3$ mol·m^{-3}; $t_p = 48$ ms; pH = 6;
2. $[Cd^{2+}] = 0.1$ mol·m^{-3}; $t_p = 175$ ms; pH = 6.

Application of the curves, for calibration of i_m of the sample solutions, implies the following assumptions:

i Diffusion and conduction currents are additive.

ii The PMApe complexes contribute neither to the diffusion, nor to the conduction currents, because of the low D_b values.

iii For every R, the diffusion coefficient of the free metal ions is not altered by the presence of the polymer complex. For very low R values, where this assumption may be approximately correct, the calculated fraction bound metal ions may be too large, and the corresponding association constants overestimated.

To determine i_d from i_ℓ of the sample solutions, using the calibration plots, an iterative procedure had to be followed, since the bound metal ions were assumed not to contribute to i_ℓ. After a first assessment of the free metal ion concentration $[M]_{f,1}$, R_1 can be calculated. Using this R value, an improved $[M]_{f,2}$ can be found using the calibration plot. From this, an improved value R_2 is obtained, and so on.

Due to the necessary additions of KOH, to adjust α_n, R values below 0.5 were never reached.

3.3.5 Adsorption phenomena

Reactant adsorption onto the mercury electrode may cause substantial enhancement of the peak-shaped current response in Differential Pulse Polarography (*Jacobsen & Lindseth*, 1976; *Flanagan et al.*, 1977a), Anodic Stripping Voltammetry (*Brezonik et al.*, 1976; *Bhat et al.*, 1981) and Single Drop Square Wave Polarography (*Ramaley et al.*, 1981). Usually, the shape of the peak is not significantly affected, and the adsorption may not be noticed as such. Characteristic potentials may shift to move negative values, and overestimation of association constants results (*Bond & Hefter*, 1971).

Natural and synthetic polymeric ligands are known to adsorb at the mercury-water interface (*Frei & Miller*, 1965; *Buffle et al.*, 1978; *van Leeuwen et al.*, 1981; *Dunsch et al.*, 1983). Non-reducible ligands may induce adsorption of electro-active metal ions. In NPP, as contrasted with DPP, notable effects of induced adsorption are a maximum on the polarographic wave, and a possible depression of the limiting current. Overestimation of association constants will result. In NPP, the occurrence of a maximum suggests a possible adsorption effect on i_ℓ, although the absence of such a maximum does not warrant absence of adsorption (*Barker & Bolzan*, 1966; *Flanagan et al.*, 1977b; *van Leeuwen*, 1982). A decisive diagnostic tool is the intercept of the i_ℓ-axis of the *Cottrell* plot: in the case of induced adsorption this intercept is enlarged (*van Leeuwen*, 1979a, 1980).

The decrease of i_ℓ as a result of reactant adsorption in NPP has

been described on the basis of digital simulation by *Flanagan et al.* (1977b) and on the basis of an analytical theory by *van Leeuwen et al.* (1982). The origin of the depression of i_ℓ is the depletion of the adsorbing reactant near the electrode surface outside the adsorbed layer, as a result of the adsorption process during the pre-pulse period t_{pp}. Generally, the effect of the depletion is larger for larger t_{pp}/t_p or t_d/t_p ratio. Ultimately, Sampled Direct Current (SDC), where $t_{pt} = t_d$, can be used to avoid depression of i_ℓ.

A better alternative to avoid complications due to adsorption would be the using of RPP, where the flow of a limiting current during the pre-pulse period prevents accumulation of depolarizer at the electrode surface. Application of RPP is preferred over SDC because the advantages of short t_p values remain viable.

An additional complication due to adsorption is the hindrance of the diffusion of the depolarizer through the adsorbed layer, in the case of high surface coverages (*Kodama & Murray*, 1965; *Miller*, 1965).

Fig. 3.3 illustrates some effects of reactant adsorption on the polarographic waves, all for the *same* Pb/FA solution. NPP polarograms (A1-A4; B1-B4) and RPP polarograms (A5-A8; B5-B8) are shown for corresponding t_p-t_d combinations. The polarograms start at the initial potentials indicated in the caption.

Generally, the adsorption of ionic ligands is governed by both electrostatic and chemical factors. Hence, the dependency of the adsorption on the applied potential may be complicated (*Janik & Sommer*, 1973; *Berg & Horn*, 1981). The water dipoles are also oriented in the electrical field near the electrode, and their replacement upon adsorption of a ligand depends on the electric field (*Parsons*, 1980). Moreover, adsorbed trains of polyions are within the compact part of the double layer, while the loops are outside it. In NPP, where the electrode potential in the pre-pulse period may be chosen freely, sufficiently positive from $E_{\frac{1}{2}}$, initial potentials are sometimes encountered where the effects of induced adsorption are negligible (*van Leeuwen et al.*, 1981). Complications may arise if the adsorbed (negatively charged) ligand desorbs at sufficiently negative pulse potentials: an additional i_ℓ decrease may result.

In the case of long drop periods, the depletion of adsorbing reactant just outside the adsorbed layer would become smaller, due to sufficient supply from the bulk. The amount adsorbed would become in equilibrium with the bulk concentration of adsorbing reactant.

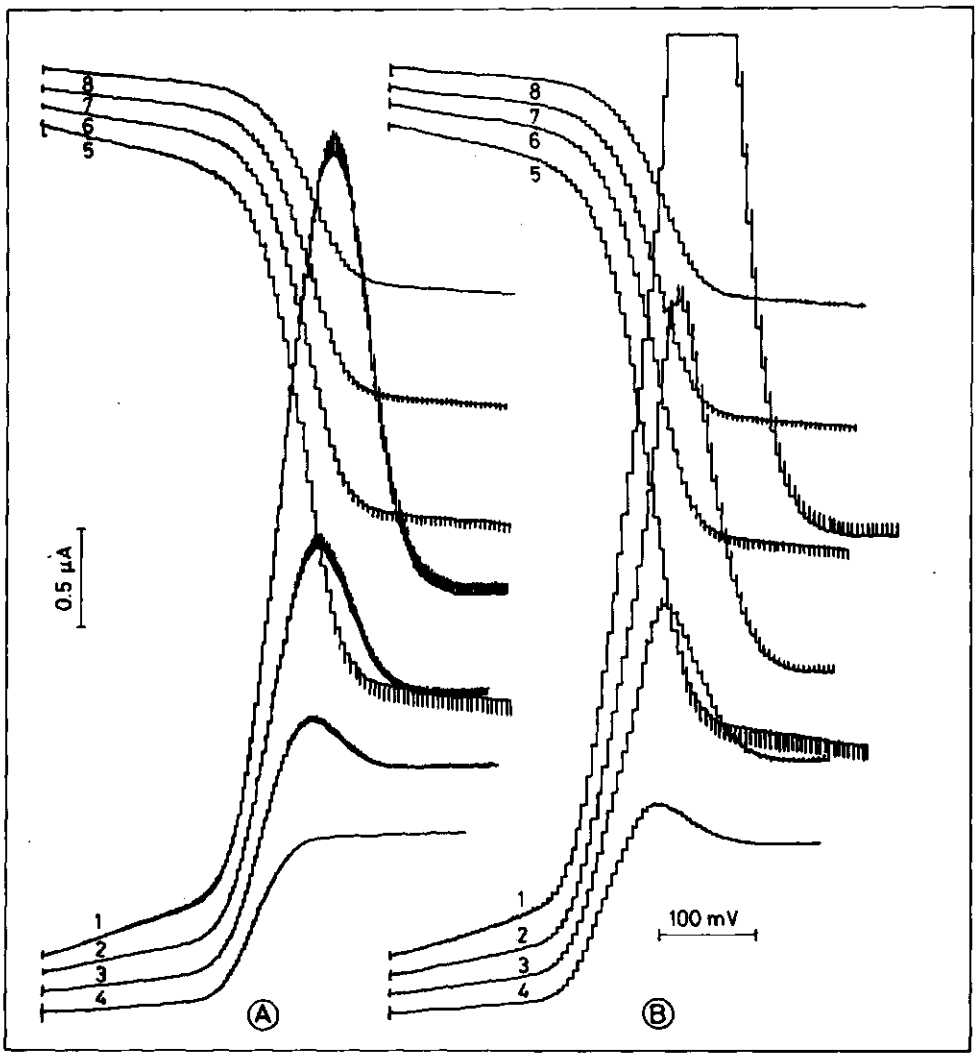

FIGURE 3.3 Effects of reactant adsorption on the polarographic waves for a Pb/FA solution. From left to right: increasing pulse amplitudes.

$[FA]_T$= 0.995 mol·m^{-3}; $[Pb^{2+}]_T$ = 0.249 mol·m^{-3}; α_n = 0.8; $[KNO_3]$ = 50 mol·m^{-3}.

A: t_d = 0.5 s; B: t_d = 1 s.

NPP (1-4): E_i = -300 mV vs $Ag/AgCl,KCl_{sat}$;

RPP (5-8): E_i = -800 mV vs $Ag/AgCl,KCl_{sat}$;

t_p: 25.3 ms (1,5); 48.7 ms (2,6); 84.9 (3,7); 174.9 (4,8).

However, with respect to the drop periods applied (0.5-2 s), this equilibrium will generally not be reached at the low concentrations of polyacid ($\sim$ 2 mol·m^{-3}) and the low values of the diffusion coefficients concerned ($\sim 10^{-7}$ cm^2·s^{-1}).

3.3.6 Experimental

All polarograms were obtained using modified PAR Model 174A polarographic analyzers from EG&G. The modification allowed variation of the effective pulse period t_p. The NPP mode was employed for all the sample solutions. In some instances the SDC mode was also used.

For all measurements, except for the c_l-titrations of Pb/PMApe, static mercury drop electrodes SMDE PAR Model 303 from EG&G were used. A basic feature of this electrode is that the mercury is dispensed very rapidly. A drop is formed within at most 0.2 s, and then left hanging stationary at the capillary tip until the current measurement is made. Three different drop sizes can be employed. The ratio of their surface areas is approximately 2.6 : 1.6 : 1. The drop size is slightly dependent on the capillary used.

The SMDE is equipped with a fixed $Ag/AgCl,KCl_{sat}$ reference electrode, provided with a porous Vycor frit to contact the test solution. The counter electrode is a fixed platinum wire. We modified the electrode block to allow a pH microelectrode to be inserted into the solution. The potentialities of the SMDE have been described by *Schmidtpott* (1980) and by *Bond & Jones* (1980).

Only in the case of the c_l-titrations of the Pb/PMApe system, a dropping mercury electrode (DME) was used. It was synchronized with the polarographic analyzer through a PAR Model 174/70 drop timer. The height of the mercury column was fixed at such a value that the drop area, at the moment of dislodgement, was 0.66 mm^2. An Electrofact Model R113 Saturated Calomel Electrode was used as the reference electrode. The counter electrode was a platinum wire.

X-Y recorders Hewlett Packard Model 7040A, Houston Model 2200-3-3 and PAR Model RE0074 were employed.

The relative error in the determination of polarographic limiting currents has been reported to be between 0.1% and 3%, depending on the concentration level and the technique used (*Meites et al.*, 1977). From repeated measurements, we concluded that the relative error in i_ℓ is about 1% on the average in our measurements; it is lower for the higher concentrations (free) metal ions.

In table 3.4, typical ranges of apparatus settings are collected. Relevant particular combinations of settings will be given along with the results in the chapters 4, 5, 6 and 7.

TABLE 3.4 Ranges of apparatus settings used in the polarographic analyses

control	settings
operation mode	NPP; SDC
current range	0.02 μA - 1 mA
initial potential	in V versus $Ag/AgCl,KCl_{sat}$
Cd^{2+}	NPP: -0.50; RPP: -1.1
Pb^{2+}	NPP: -0.30; RPP: -0.9
Zn^{2+}	NPP: -0.90; RPP: -1.5
drop time t_d	0.5; 1; 2 s
pulse duration t_p	25 - 500 ms
potential scan range	0.75; 1.5 V
potential scan rate	2; 5; 10 $mV \cdot s^{-1}$
drop size DME	0.66 mm^2
SMDE	small : ∿ 0.8 mm^2
	medium: ∿ 1.4 mm^2
	large : ∿ 2.3 mm^2
low pass filter	off
sample period t_{ps}	16.2 ms
sample volume	5; 10 ml
recorder	10 inch: full current range
	15 inch: full potential scan

3.4 POTENTIOMETRY

3.4.1 Glass electrode

In metal complexation studies, the pH is usually controlled at a prefixed value. The idea is that, at a particular ionic strength, for a wide range of pH values, the acid dissociation reaction is completely described by a specific dissociation constant. Then a constant pH implies a constant degree of dissociation α_d.

For polyacids, however, the observed dissociation constant is dependent on the charge density of the polyion, and, hence, it depends on α_d, on the degree of metal ion association, on the concentration and the conformation of the polyacid (*Katchalsky & Spitnik*, 1947; *Mandel*, 1970;

Manning & Holtzer, 1973; *Young et al.*, 1981), as described in chapter 2.

To study charge effects in metal ion association with polyacids, we preferred to keep the initial degree of neutralization, α_n, constant in the M/L titrations, rather than the pH.

The degree of dissociation α_d was calculated from the continuously monitored pH value and α_n:

$$\alpha_n = \frac{[KOH]_a}{c_p} \; ; \; \alpha_d = \frac{[KOH]_a + [H^+] - [OH^-]}{c_p} \tag{3.32}$$

where $[KOH]_a$ is the concentration of KOH added.

Corresponding values for pH and α_d were used in the α_n-titrations to calculate the apparent dissociation constant $pK_{app,a}$ of the polyacid according to the definition:

$$pK_{app,a} = pH + \log \frac{1 - \alpha_d}{\alpha_d} \tag{3.33}$$

From the variation of $pK_{app,a}$ with α_d, the effect of the metal association on the charge of the polyion can be elucidated.

With respect to the M/L-titrations, the pH measurements were used to calculate the amounts of protons released upon increasing metal association. Then, proton release can be attributed either to dissociation of the polyacid because of a lowered effective charge density of the polyion, or to substitution of bound protons by metal ions.

For a glass electrode, the measured pH is related to the potential difference ΔE between two reference electrodes, one on each side of a proton-sensitive glass membrane:

$$\Delta E = \frac{2.3RT}{F} \log \frac{(H^+)_0}{(H^+)_i} \tag{3.34}$$

where $(H^+)_0$ and $(H^+)_i$ are the proton activities outside and inside the glass bulb, respectively.

In the familiar design, where the proton activity inside has a fixed value, eq. (3.34) can be written as:

$$E = E_{st} + \frac{2.3RT}{F} \log (H^+) \tag{3.35}$$

where E_{st} represents a standard potential of the particular cell.

Since the outer reference electrode is inserted in the solution through a KCl salt bridge, a diffusion- or liquid junction potential is part of E_{st}. Calibration of the glass electrode in buffer solutions of known proton activity will only work perfectly if E_{st} has the same value in the buffers and in the solutions.

For solutions with highly charged, unscreened particles, such as some clay-suspensions, the diffusion potentials may differ from those in the buffers (*Overbeek*, 1976). This effect is called 'suspension effect'. Because of it, for negatively charged particles, the observed pH is *lower* than the real pH (*Schwabe et al.*, 1980). Thus, in the case of high charge density (high α_d, low M/L, low c_1), the pH values read may be underestimations.

In section 3.4.3 an equation will be derived to estimate the maximum error in the pH due to the suspension effect, in the acrylic polyacid systems. At a 1:1 salt concentration level of 50 $mol \cdot m^{-3}$, the suspension effect is vanished, at the polyacid concentrations applied (*Lichtenbelt*, 1972).

3.4.2 Cd solid state electrode

For a number of Cd/PMA and Cd/HA systems, bound fractions were determined using a Cd-selective solid state electrode.

The theoretical relationship between the potential difference with respect to a reference electrode, and the Cd^{2+} concentration is:

$$E = E_{st} + \frac{2.3RT}{2F} \log \gamma_{Cd^{2+}} + \frac{2.3RT}{2F} \log [Cd^{2+}]_v \qquad (3.36)$$

where $\gamma_{Cd^{2+}}$ is the activity coefficient, and $[Cd^{2+}]_v$ the value of the Cd^{2+} concentration in $mol \cdot dm^{-3}$. Plots of E versus log $[Cd^{2+}]_v$ appeared to be linear for the ionic strength levels applied, and $[Cd^{2+}]$ ranging from 10^{-3} to 10^{-5} $mol \cdot dm^{-3}$. According to *Gardiner* (1974a) this linearity continues down to 10^{-6} $mol \cdot dm^{-3}$ for the particular type of electrode used.

Values for the constants A'' and B'' in the operational equation:

$$E = A'' + B'' \cdot \log [Cd^{2+}]_v \qquad (3.37)$$

were for $[KNO_3]$ = 50 mol·m^{-3}: -85.41 and 29.10, and for $[KNO_3]$ = 200 mol·m^{-3}: -89.89 and 29.83 mV, respectively.

Since the response time of the electrode in the polyacid systems investigated appeared to be long, the potential readings were not more accurate than ± 0.5 mV, which results in an uncertainty in the Cd^{2+} concentration of ∿ 8%.

The CdS/Ag_2S mixture that forms the membrane of the electrode, is sensitive to light (*Veselý et al.*, 1978). The electrode shows a day-to-day drift in the potential readings. Polishing reduced this drift.

Operating the electrode was claimed to be impractical when the Cd^{2+} concentration is changed from high to low (*Cheam & Gamble*, 1974). Also *Saar* (1980) claimed results differing between Cd in HA, and HA in Cd titrations, but attributed this observation to an intrinsic property of the Cd/HA system.

With respect to the SCE reference electrode, the junction with the sample solution introduces an additional potential jump, the liquid junction potential, which is incorporated in A''. In the presence of highly charged polyelectrolytes, this quantity needs closer discussion, see next paragraph.

3.4.3 Suspension effect

The suspension effect is the difference in pH when the reference electrode is positioned in a suspension and when it is in the equilibrium solution of that suspension, irrespective of the position of the glass electrode.

The suspension effect corresponds to the liquid junction potential E_ℓ between the salt bridge of the reference electrode and the suspension. The effect generally occurs where the pH in the presence of highly charged particles is measured.

According to *Overbeek* (1953), E_ℓ is identical to the *Donnan*-potential over a dialysis membrane separating the polyelectrolyte solution from its equilibrium solution. In formula:

$$pH = pH_{observed} - \frac{E_D \cdot F}{2.3 \cdot RT} \qquad (3.38)$$

where E_D, the *Donnan*-potential, has the same sign as the charge of the polyion.

The general expression for the liquid junction potential, for a reference electrode with a saturated KCl solution, is:

$$E_\ell = -\frac{1}{F} \cdot \int_{\text{sat.KCl}}^{\text{solution}} \sum_r \frac{t_r d\mu_r}{z_r} \qquad (3.39)$$

where for each ionic species r, the charge z_r, the transference number t_r and the chemical potential μ_r are to be inserted.

If the charge on the polyions is high, the differences in mobility of the small ions are the dominant factor in E_ℓ. For that case, eq. (3.39) may be approximated by (*Overbeek*, 1953):

$$E_D = \frac{RT}{F} \cdot \ln \frac{\text{conductance suspension}}{\text{conductance solution}} \qquad (3.40)$$

In a partially neutralized polyacid solution, the mobility of the counterions is slowed down much more than that of the coions (*Manning*, 1972). Hence, for highly charged ions, eq. (3.40) may be reduced to:

$$E_D = \frac{2.3RT}{F} \cdot \log \frac{D_c}{D_o} \qquad (3.41)$$

where D_c and D_o are the self-diffusion coefficients of the counterion in the presence and in the absence of the polyacid, respectively.

The ratio D_c/D_o has been given by *Manning* (1974) for monovalent counterions:

$$D_c/D_o = 0.87 \cdot \xi^{-1} \; ; \; \xi > 1 \qquad (3.42)$$

where ξ is the charge density parameter discussed in chapter 2. For PMA and PAA is:

$$\xi = 2.85 \cdot \alpha_d \qquad (3.43)$$

Consequently, for $\alpha_d > 0.3$:

$$E_D = \frac{2.3RT}{F} \log (0.3 \cdot \alpha_d^{-1}) \; ; \; \Delta pH(max) = \log (0.3 \cdot \alpha_d^{-1}) \qquad (3.44)$$

In practice, the error is generally smaller than that given in eq.

(3.44) (*Overbeek*, 1953).

For α_d = 0.5, E_D = -13 mV. This value is different from E_D = -18 mV, measured for NaPMA at α_d = 0.5 at very low NaBr concentrations, in dialysis experiments (*Lichtenbelt*, 1972).

In the absence of added salt, $-E_D$ values for acrylic polyacids may rise to 30 mV at α_d = 1, corresponding with 0.5 pH unit. For the humics, the ΔpH values are much less.

For metal/polyacid systems in which divalent metal ions are also present, E_D will be smaller than the value given by eq. (3.44). The polyion charge density will decrease, and the monovalent ions will regain their normal diffusion rate (*Magdelenat et al.*, 1974).

3.4.4 Experimental

Potentiometric measurements were carried out with an Electrofact Model 36060 or a Model 36200 potentiometer.

The glass electrodes used were Electrofact and Schott combination electrodes with Ag/AgCl,KCl_{sat} references. Before each titration, the potentiometer settings were calibrated with buffers of pH = 4.0, 7.0 and 10.0. In case of any conductometrically measurable leakage through the diaphragm, the pH-electrode was replaced, and the titration repeated.

The cadmium selective solid state electrode used was an Orion Model 94-48A in combination with an Electrofact Model R113 SCE electrode. Calibration was carried out with solutions of known concentrations of $Cd(NO_3)_2$ adjusted to the desired ionic strength.

3.5 CONDUCTOMETRY

3.5.1 Conductivity of polyelectrolyte solutions

Conductometry is increasingly used to study properties of polyelectrolyte solutions: transference phenomena (*Joshi & Kwak*, 1980), counter ion association (*Kwak & Hayes*, 1975; *Rinando & Milas*, 1970), self-diffusion of counterions (*Manning*, 1975; *Yoshida*, 1978; *Miyamoto*, 1979). Classical work has been reviewed by *Kurucsev & Steel* (1967). Humic acids were studied conductometrically with the purpose to analyse functional groups (*Ghosh & Mukherjee*, 1972; *Arai & Kumada*, 1977a,b) to study the interactions with clays (*Adhikari et al.*, 1976) and those with metal ions (*van Dijk*, 1960).

The limiting law, generally applied for the equivalent conductivity of *pure* polyelectrolytes can be written as:

$$\Lambda = f\ (\lambda_c^\circ + \lambda_p) \tag{3.45}$$

where λ_c° is the equivalent conductivity of the counterion, in pure solvent, λ_p is the equivalent conductivity of the polyionic species (per equivalent charged monomer) in the solution, and f is a parameter related to the fraction of counterions that is not bound.

According to *Huizinga et al.* (1950) and *Miyamoto* (1979) f can be assumed to represent the fraction 'free' counterions. *Manning* (1969a) advocates that the fraction 'free' is given by $|z_c^{-1}| \cdot \xi^{-1}$, where z_c is the counterion valency. For $\xi > |z_c^{-1}|$ he derived (*Manning*, 1975):

$$f = 0.87 \cdot |z_c^{-1}| \cdot \xi^{-1} \tag{3.46}$$

Ise & Okubo (1978) stated that *Manning*s interpretation of f agreed with their experimental data for NaPAA, for high values of ξ. *Yoshida* (1982), using a different theoretical concept came to a constant of 0.77 instead of 0.87 in eq. (3.46).

Values for Λ in polysalt solutions have been claimed to be independent of the polymer concentration (*Miyamoto*, 1979). However, *Vink* (1982) observed for very dilute systems an increase with decreasing concentration, in polyacrylate and polymethacrylate systems.

Values for λ_p are independent of macromolecular mass (*Nagasawa*, 1974), but may change with charge density (*Eisenberg*, 1958; *van der Drift*, 1975; *Arai & Kumada*, 1977a).

Manning (1975) derived a theoretical expression for λ_p, using the 'infinite cylinder' model discussed in chapter 2, for polysalt solutions:

$$\lambda_p = \frac{279 \cdot A' \cdot |z_c^{-1}| \cdot |\ln \kappa \cdot a|}{1 + 43.2 \cdot A' \cdot (|z_c| \lambda_c^\circ)^{-1} \cdot |\ln \kappa \cdot a|} \tag{3.47}$$

where κ is the Debye screening parameter, a is the radius of the polyion cylinder, and $A' = \varepsilon kT/3\pi\eta e$, in which ε is the bulk dielectric constant and η the bulk viscosity.

According to eq. (3.47), λ_p is dependent on the type of counterion. Such a dependence has been found for PSS salts (*Szymczak et al.*, 1975), but not for PMA salts (*Eisenberg*, 1958; *van der Drift*, 1975).

Literature values for λ_p of acrylic polyacids in solutions without added salt are in between 40 and 60 $S \cdot cm^2 \cdot eq^{-1}$ at low α_d values (*Gregor et al.*, 1957; *Arai & Kumada*, 1977a; *Vink*, 1981). There is no agreement on the dependence of λ_p on α_d, probably due to the different models employed to calculate λ_p from the Λ values of different salts. According to *van der Drift* (1975) and *Vink* (1981) a very small change with α_d at higher α_d values is observed for PMA and PAA, respectively. Older literature data reported an increase for PAA (*Wall & Doremus*, 1954) and a decrease for PMA (*Gregor et al.*, 1957). For humic acid, the λ_p values given by *Arai & Kumada* (1977b) are between 45 and 55 $S \cdot cm^2 \cdot eq^{-1}$.

It is remarkable that the λ_p values for the different types of polycarboxylic acids are all very close, at about 50 $S \cdot cm^2 \cdot eq^{-1}$, not too far from the value of λ for the acetate ion: 41 $S \cdot cm^2 \cdot mol^{-1}$.

According to *van der Drift* (1975), the λ_p value of PMA decreases rapidly with increasing concentration added 1:1 salt.

To assess the association of divalent metal ions with polyacids, we determined the change in conductivity, $\Delta\kappa_p$ of the polyacid solutions upon addition of metal nitrates, for given values of α_n. Moreover, we determined the change in conductivity in the absence of polyacid, $\Delta\kappa_b$.

The change in the conductivity of a solution upon any addition is generally given by:

$$\Delta\kappa = \sum_r \lambda_r \cdot \Delta[r] \qquad (3.48)$$

where $\Delta[r]$ is the change in concentration of any ionic species r, and $\Delta\kappa$ is the resulting change in conductivity of the solution. For λ_r in $S \cdot cm^2 \cdot mol^{-1}$, and $[r]$ in $mol \cdot m^{-3}$, $\Delta\kappa$ has the dimension $\mu S \cdot cm^{-1}$. At the low concentration levels, and within the small concentration ranges considered in the *present* study, the concentration dependence of λ_r appeared to be negligibly small.

Applying eq. (3.48) for the *blank* titration:

$$\Delta\kappa_b = \lambda_M \cdot \Delta[M]_a + \lambda_{NO_3} \cdot \Delta[NO_3]_a \qquad (3.49)$$

where $\Delta[M]_a$ and $\Delta[NO_3]_a$ are the changes in the concentration of the metal- and nitrate ions added, respectively.

For the titration of the *polyacid* solution eq. (3.48) will give:

$$\Delta\kappa_p = \lambda'_M \cdot \Delta[M]_f + \lambda'_{NO_3} \cdot \Delta[NO_3]_a + \lambda'_K \cdot \Delta[K]_f + \lambda_p \cdot \Delta[L]_f + \lambda'_H \cdot \Delta[H]_f + \lambda'_{OH} \cdot \Delta[OH]_f \qquad (3.50)$$

where L is a carboxylate group, λ'_r is the equivalent ionic conductivity of species r in the presence of the polyacid, and $\Delta[M]_f$, $\Delta[K]_f$ and $\Delta[H]_f$ are the changes in the concentrations of the *free* cations M^{n+}, K^+ and H^+, respectively. Eq. (3.50) includes no contribution of bound metal ions. It is assumed that in the contact of a bound metal ion with the polyion, the charges of M^{n+} and nL^- are effectively compensated. Eq. (3.50) is, in combination with eq. (3.49) very helpful in the interpretation of the results of the M/L-titrations in chapter 4.

Generally, the *difference* between $\Delta\kappa_b$ and $\Delta\kappa_p$ will be plotted versus the concentration divalent metal nitrate:

$$\Delta\kappa_T = \Delta\kappa_b - \Delta\kappa_p \qquad (3.51)$$

This difference will be called the *conductivity excess*.

Over the range of pH values between 5.5 and 9, the contributions of H^+- and OH^- ions are negligible. Nitrate ions are pushed away from the negatively charged polyion. They will not be associated, and retain approximately their original mobility: $\lambda'_{NO_3} \cong \lambda_{NO_3}$. With these considerations, eq. (3.51) can be written as:

$$\Delta\kappa_T = \lambda_M \cdot \Delta[M]_a - \lambda'_M \cdot \Delta[M]_f - \lambda_p \cdot \Delta[L]_f - \lambda'_K \cdot \Delta[K]_f \qquad (3.52)$$

To calculate amounts bound heavy metal ions, approximations have to be made with respect to values of λ_M, λ_p, λ'_K, $[L]_f$ and $[K]_f$, and the changes of these values in the course of the titration. These approximations depend on the α_n- and M/L values, and will be discussed in chapter 4.

3.5.2 Acid/base titrations

Conductometric acid/base titrations were carried out to determine the concentration of carboxylic groups in the polyacid solutions. Fig. 3.4 gives, by way of example, the titration of a PAA stock solution. A plot of the observed pH versus α_n is included.

It is clear that the conductometrically determined endpoint is well-defined, contrary to the inflexion point in the pH curve. Using high

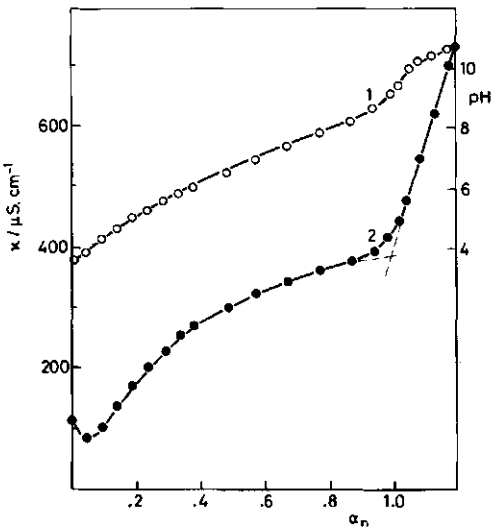

FIGURE 3.4 Conductometric and potentiometric acid/base titration curves for [PAA] = 10.39 mol·m^{-3}; $\bar{M}$ = 300,000; base: KOH; no added salt; (1) pH; (2) conductivity.

salt levels, the sharpness of the pH inflexion point can be improved. The conductometric endpoint was sufficiently sharp for all the polyacids used.

Other features of the acid/base titrations will be discussed in chapter 5, especially the changes in the titration curves in the presence of divalent metal ions.

3.5.3 Experimental

The conductometric measurements were carried out with a conductometer WTW Model LF530. The accuracy, as given by the manufacturer, was ± 0.5% of the reading, in μS·cm^{-1} or mS·cm^{-1}. The apparatus was equipped with a temperature measuring device WTW Model TFK530. A fixed frequency of 4 kHz was applied. It has been reported (*Eisenberg*, 1958; *Vink*, 1981) that λ_p of PMA and PAA is not dependent on the applied frequency.

The conductometric cells used, WTW Model LTA01, equipped with blank platinum electrodes, had cell constants of 0.102 cm^{-1} and 0.109 cm^{-1}. Sample volumes employed were 20 and 40 ml.

4 INFLUENCE METAL/POLYION RATIO

4.1 CONDUCTOMETRY

The results of the conductometric M/L-titrations will be represented as graphs* of the conductivity excess $\Delta\kappa_T$, defined in eq. (3.51), versus the amount of added metal nitrate. In this way, the *difference* between the *change* of the conductivity of metal nitrate solutions in the absence of polyacid and the same with polyacid is expressed. Apart from a slight dilution effect, $\Delta\kappa_T$ expresses metal/polyion interaction. In addition, the corresponding graphs of the proton production $\Delta[H^+]$ versus the amount of metal nitrate are given.

It is noted that *no* KNO_3 was added to the sample solutions. K^+ ions present in the samples originate from the partial neutralization of the polyacid with KOH.

4.1.1 Zn, Cd, Pb/PMApe

Zn/PMApe

In fig. 4.1.a, graphs of $\Delta\kappa_T$ are given for the Zn/PMApe titrations at five different α_n values, respectively. This figure will be discussed in detail.

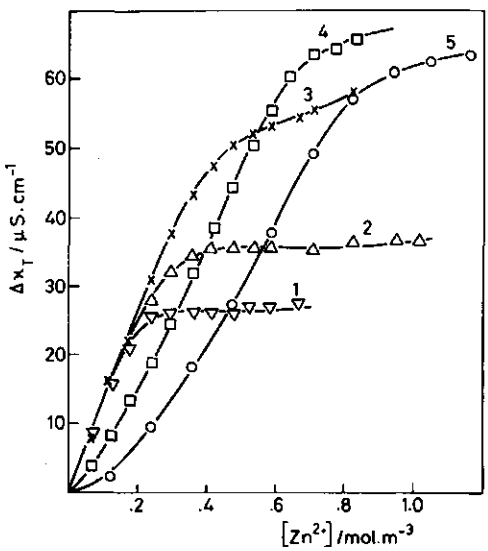

FIGURE 4.1.a The conductivity excess $\Delta\kappa_T$ versus the concentration $Zn(NO_3)_2$. $[PMApe]_i$ = 2.38 mol·m^{-3}. α_n = 0.23 (1), 0.33 (2), 0.43 (3), 0.63 (4), 0.83 (5).

* The numerical data of these and all other graphs in this work are available on request.

Curve 1. This curve is characterized by three parts: an initial linear steep increase of $\Delta\kappa_T$, a rounding off of the curve, and a second linear part with almost zero slope. The second linear part begins at the point where the sum of the charges of added zinc ions is approximately equal to the sum of the carboxylate charges: $2\cdot[Zn]_a \cong \alpha_n\cdot c_p$. This suggests charge equivalence, since the proton production is still very low at that point.

The initial linear part has a slope β of 130 $S\cdot cm^2\cdot mol^{-1}$. In chapter 3, eq. (3.52) has been derived to express the relative contributions of the ionic species to $\Delta\kappa_T$ over the range of pH values in which $[H^+]$ and $[OH^-]$ are too small to contribute measurably to the conductivity. Considering eq. (3.52), let us assume the extreme case that all zinc ions are conductometrically bound. Then, it follows that $\Delta[Zn]_f = 0$, and consequently $\Delta[L] = -2\cdot[Zn]_a$. A provisional assumption is further that for low α_n no conductometric binding occurs of alkali ions, and thus $\Delta[K]_f = 0$. With these assumptions, and applying eq. (3.52), the initial slope β is given by:

$$\beta = \frac{\Delta\kappa_T}{\Delta[Zn]_a} \cong \lambda_{Zn} + 2\cdot\lambda_p \qquad (4.1)$$

Using $\Lambda_{Zn(NO_3)_2} = 227\ S\cdot cm^2\cdot mol^{-1}$ and $\Lambda_{KPMApe}(\alpha_n = 0.23) = 90\ S\cdot cm^2\cdot mol^{-1}$, measured under appropriate experimental conditions, and using literature data of the ratios of the limiting equivalent conductivities $\lambda^\circ_{Zn}/2\cdot\lambda^\circ_{NO_3} = 0.74$ (*Robinson & Stokes*, 1955) and $\lambda^\circ_K/\lambda^\circ_p = 1.47$ (*Vink*, 1981), it follows that $\lambda_{Zn} \cong 96\ S\cdot cm^2\cdot mol^{-1}$ and $\lambda_p = 36\ S\cdot cm^2\cdot mol^{-1}$. Using these values in eq. (4.1), the slope would be $\beta \cong 168\ S\cdot cm^2\cdot mol^{-1}$. Two refinements can be applied. The mobility of the K^+ ions is limited by the polyion field. Upon association of Zn^{2+}, λ'_K will increase, finally approaching its normal value λ_K. According to *Manning* (1974), $\lambda'_K \cong 0.9\ \lambda_K$ for K/PMApe at $\alpha_n = 0.23$. Thus an improved approximation would be $\beta \cong 168 - 0.1\cdot\lambda_K\cdot[K]_f$, resulting in $\beta \cong 164\ S\cdot cm^2\cdot mol^{-1}$ for curve 1. Second, λ_p is dependent on the counterion valency (*Manning*, 1975). According to eq. (3.47) this dependency is approximately an inverse proportionality. Thus λ_p may be reduced to about 50%. Due to this effect, the calculated value of β is further reduced to about 128 $S\cdot cm^2\cdot mol^{-1}$, a value that agrees with the measured one. This elaboration illustrates that in the absence of 1:1 salt, the association of Zn^{2+} with PMApe will be complete, at low M/L. With re-

spect to the nature of the association, it is noted that generally the stability constants for the chemical binding of Zn^{2+} with low molecular mass carboxylic acids are low (*Sillén & Martell*, 1964, 1971). Moreover, the value of the initial slope β, as determined from the M/L-titration of the Zn/isobutyric acid system at $\alpha_n = 0.4$ and a concentration of titratable groups of 2.5 $mol \cdot m^{-3}$, was very small, i.e. about 20 $S \cdot cm^2 \cdot mol^{-1}$. These data suggest that the Zn/PMApe interaction may be predominantly electrostatic.

At a certain value of $[Zn]_a$, the slope of the curve begins to diminish: the rounding off of the curve sets in. We will call the ratio [M]/[L] at the onset of the decrease of the slope the critical ratio R_c. At values of [Zn]/]L] > R_c, the association of Zn^{2+} will be less than complete. Then, $[Zn]_f$ and λ'_{Zn} will gradually increase upon further addition of $Zn(NO_3)_2$. Properties of R_c for the systems investigated will be discussed in § 4.1.4.

The second linear part shows a very small slope, due to the slight dilution effect with respect to $[K]_f$ and $[L]_f$. These concentrations become gradually smaller, and $\Delta\kappa_T$ increases correspondingly.

Curves 2 and 3. For these curves, α_n is 0.33 and 0.43, respectively. The initial linear parts show the same slope as in curve 1 for α_n = 0.23. Thus, at low M/L, the association of Zn^{2+} with PMApe will be complete. The range of M/L values where full association occurs increases with α_n.

The initial values of $[K]_f$ and $[L]_f$ increase with α_n. Consequently, the dilution effect increases and the slope of the terminating part increases with α_n. Continuation of the M/L-titration to large values of M/L, not shown in the figure, would show an increasing slope as a result of the dilution. From the same curves for other systems, i.e. for Zn/PMA by *Kolawole & Olayemi* (1981) and for Cu/PMA by *Kolawole & Mathieson* (1977), it was concluded that intersection points at M/L ≅ 0.5 and M/L ≅ 1 are equivalence points for the formation of ML_2 and ML complexes, respectively. These conclusions must be erroneous.

Curves 4 and 5. In these curves, for which α_n is 0.63 and 0.83, respectively, the initial values of $\Delta\kappa_T$ are lower than those in curves 1-3. It is reasonable to assume that at these values of α_n, complete association of Zn^{2+} initially occurs. Considering eq. (3.52), the interpretation must now be that $\Delta[K]_f$ is positive at the onset of the titrations. This indicates that K^+ ions were conductometrically bound to the polyacid in the Zn^{2+}-free solutions. Upon addition of $Zn(NO_3)_2$, conductometrically bound K^+ exchanges with Zn^{2+}. If the number of K^+

ions bound per $RCOO^-$ group was θ_1, the slope β at the onset of the titration is in this case approximated by:

$$\beta \cong \lambda_{Zn} + 2(1 - \theta_1) \cdot \lambda_p - 2 \cdot \theta_1 \cdot \lambda'_K \qquad (4.2)$$

As discussed before, the factor of 2 in the second term on the r.h.s. of eq. (4.2) may decrease, whereas λ'_K may increase as the titration proceeds. In any case, an increase of β must be due to a decrease of θ_1. Comparing curve 4 with curve 5 and with the curves 1-3, the model elaborated leads to the following indications:

i $\theta_1 \cong 0$ below a certain value of α_n;
ii if $\theta_1 > 0$, θ_1 increases with increasing α_n;
iii if $\theta_1 > 0$, θ_1 decreases with increasing M/L.

There is no agreement in the literature with respect to the exchange ratio of bound M^+ and bound M^{2+} in polyelectrolyte solutions. Obviously, considering 'bound' in a thermodynamic sense, that ratio is two. In a conductometric sense, the binding of one M^{2+} would result, according to *Miyamoto* (1981), in the release of one bound M^+ if the interaction with the polyacid is purely electrostatic. However, the release of two M^+ has been predicted by *Miyamoto & Imai* (1980) in the case of covalent M^{2+}/polyacid interaction. According to *Manning* (1978b), that ratio depends on the values of ξ and c_1. Ion specific effects on the exchange ratio bound M^+/M^{2+} have been demonstrated by *Rinando & Milas* (1972) and *Joshi & Kwak* (1981). For complete association of M^{2+}, the exchange ratio is given by $2 \cdot \theta_1$. Because of the approximative character of eq. (4.2), this equation will not be quantitatively used to estimate θ_1. In chapter 6, values of θ_1 will be given, calculated from results of c_1-titrations.

From curves 4 and 5 it is evident that β is initially small. However, it rapidly increases to a value close to that initially found in the curves 1-3. This suggests that θ_1 becomes zero at high M/L: all bound K^+ will have been exchanged by Zn^{2+}.

In fig. 4.1.b, the decrease of the pH is given in curves 1-5 for the titrations presented in fig. 4.1.a.

For all values of α_n, the trend is: an initially small decrease of the pH, followed by a large decrease at values of $[Zn]_a$ at which the association of Zn^{2+} ceases to be complete. The latter decrease fades out at higher M/L. It is noted that at all values of the pH in fig. 4.1.b, the corresponding values of α_n and α_d are virtually equal.

The initial decrease of the pH will primarily be due to the decrease

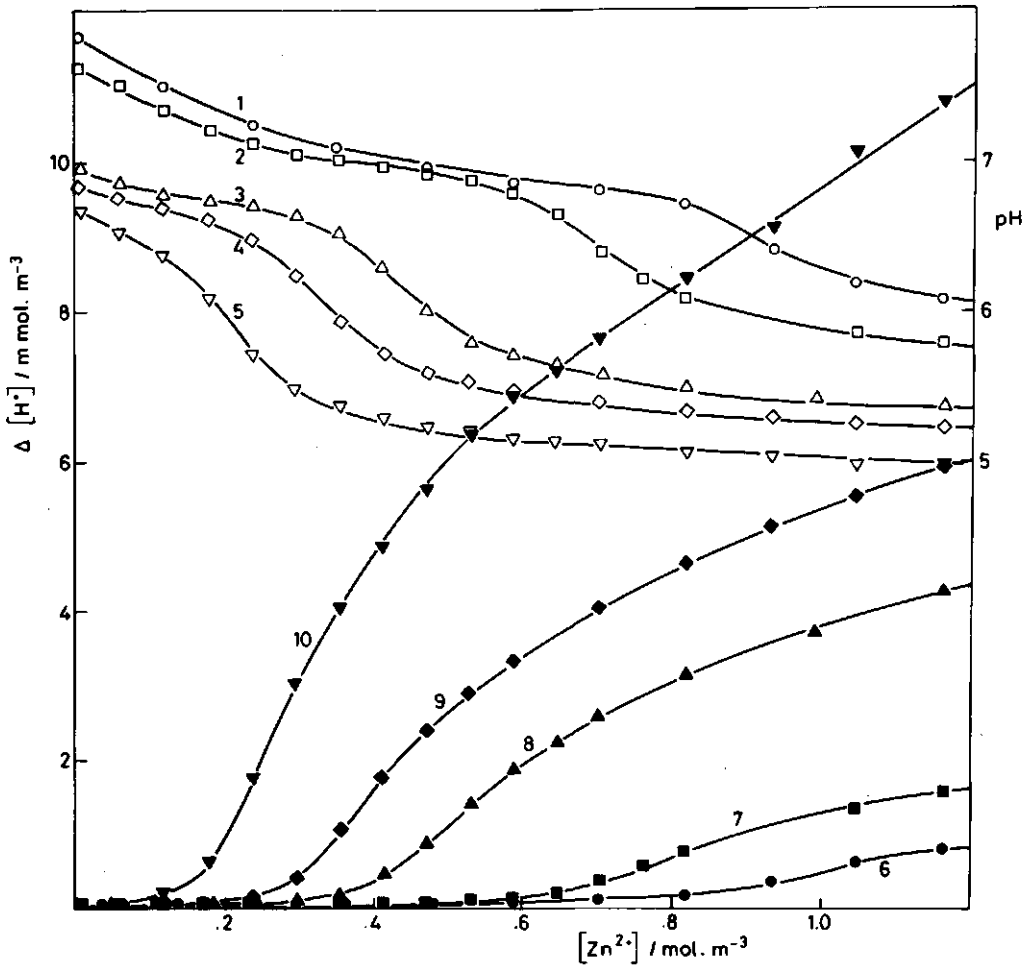

FIGURE 4.1.b. The concentration of released protons, and the pH versus the concentration $Zn(NO_3)_2$.
α_n = 0.23 (5,10), 0.33 (4,9), 0.43 (3,8), 0.63 (2,7), 0.83 (1,6).

of the strength of the electrical field around the polyion. However, the subsequent larger decrease of the pH must be due primarily to the chemical binding of Zn^{2+} with the polyacid, since the larger decrease occurs at values of $[Zn]_a$ at which the effective charge density of the polyacid is low.

The events are much better expressed by plotting the proton produc-

tion $\Delta[H^+]$ versus the amount added metal nitrate. $\Delta[H^+]$ is defined as the difference of the proton concentration in the sample and the same in the M^{2+}-free but otherwise identical solution. In the calculation of $\Delta[H^+]$ from pH values, activity coefficients were neglected. The $\Delta[H^+]$ curves 6-10 correspond to the curves 1-5, respectively.

To estimate the intrinsic binding constant, defined in eq. (2.7), of the Zn/PMApe interaction, three difficulties arise:

i The reaction stoichiometry must be known. In section 4.4.1 we will demonstrate, on the basis of polarographic results, that a 1:1 complex ZnL is predominantly formed. A coordination number j of unity is also supported by literature data (*Travers & Marinsky*, 1974; *Jakubowski*, 1975).

ii The acid dissociation constant of the acid groups involved in the interaction with Zn^{2+} must be known, to determine the concentration of L involved. However, the apparent acid strength is a function of α_d and the sample composition. The Gregor-method, discussed in § 2.3.2, to evaluate [L], will not be used because of the fundamental criticism of the method (*Marinsky*, 1976). A rather different method to estimate [L] appropriately will be proposed below.

iii The concentration of intrinsically bound zinc, $[ZnL]_{int}$, must be known. With the experimental methods applied, this concentration is not directly accessible: an approximation must be applied.

To estimate the intrinsic binding constant K_{int} of the formation of the complex ZnL, the following provisional model is applied:
Consider the *chemical* reaction:

$$Zn + HL \rightleftharpoons ZnL + H \qquad (4.3)$$

Eq. (4.3) is an appropriate description of the Zn/PMApe interaction only if the effective charge of the polyion is very low. This will be the case at values of $[Zn]_a$ at which $\Delta[H^+]$ increases rapidly. At the particular value of $[Zn]_a$ at which the increase of $\Delta[H^+]$ is maximal, it is assumed that:

i If *further* binding of zinc ions occurs upon addition of $Zn(NO_3)_2$, the concentration of the zinc complex formed is $[ZnL]_{int} \cong [H]$;

ii For low values of $[ZnL]_{int}$: $d[Zn] \cong d[Zn]_a$;

iii The effective charge of the polyion is so low, that the intrinsic dissociation constant K_a and α_d determine the ligand concentration: $[L] = K_a \cdot (1 - \alpha_d) \cdot c_p \cdot [H]^{-1}$.

Using the model elaborated, to calculate K_{int}, it follows that:

$$K_{int} \cong \frac{[H]^2 \cdot K_a^{-1}}{[Zn] \cdot (1 - \alpha_d) \cdot c_p} \qquad (4.4)$$

Multiplying both sides of eq. (4.4) with [Zn], differentiating with respect to [Zn], and applying $d[Zn] = d[Zn]_a$ yields in a general form:

$$K_{int} \cong \left[\frac{d[H]}{d[M]_a}\right]_m \cdot \frac{2 \cdot [H] \cdot K_a^{-1}}{(1 - \alpha_d) \cdot c_p} \qquad (4.5)$$

where $(d[H]/d[M]_a)_m$ is the maximal slope S_m in the $\Delta[H^+]$ curve. In chapter 5, it will be demonstrated that pK_a(PMApe) = 5.3.

In table 4.1, the results for some α_n values are collected. The data illustrate a small but definite covalent character in the Zn/PMApe interaction. At low M/L, eletrostatic effects dominate. The downward trend of K_{int} with α_n is due to the fact that one feature of the model, the use of K_a, is less appropriate at high charge densities.

TABLE 4.1 Intrinsic association constant K_{int} for ZnPMApe from conductometry and potentiometry

α_n	$\left[\frac{d[H]}{d[Zn]_a}\right]_m$	pH	K_{int}*
0.33	0.012	6.4	1.2
0.43	0.008	6.5	0.9
0.63	0.006	6.6	0.7

* for convenience, values of K_{int} are calculated on the basis of $mol^{-1} \cdot dm^{+3}$ units

Cd, Pb/PMApe

In figs 4.2.a and 4.2.b, graphs of $\Delta\kappa_T$ and $\Delta[H^+]$ are given at α_n = 0.43, for Pb, Cd and, by way of comparison, again for Zn.

Fig. 4.2.a shows no difference between Cd and Zn, whereas the increase of $\Delta\kappa_T$ is larger for Pb. The ratios of λ_M° for Cd, Zn and Pb are 1:1:1.35, respectively. Considering eq. (4.1), the larger value of λ_{Pb} accounts for the larger initial slope β. For Pb, the increase of $\Delta\kappa_T$ extends over a larger range of $[M]_a$, as compared to Cd and Zn. This may be explained by a more extensive covalent binding in the case of Pb.

Fig. 4.2.b demonstrates the partially covalent character of the

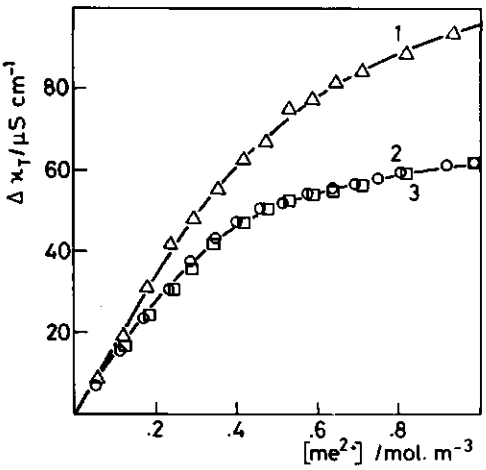

FIGURE 4.2.a The conductivity excess $\Delta\kappa_T$ versus the concentration $M(NO_3)_2$, at α_n = 0.43. $[PMApe]_i$ = 2.38 mol·m^{-3}. (1) Pb^{2+}; (2) Cd^{2+}; (3) Zn^{2+}.

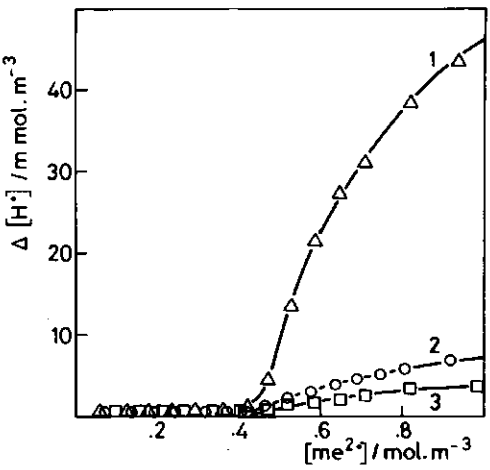

FIGURE 4.2.b The concentration of released protons versus the concentration $M(NO_3)_2$, at α_n = 0.43. $[PMApe]_i$ = 2.38 mol·m^{-3}. (1) Pb^{2+}; (2) Cd^{2+}; (3) Zn^{2+}.

Pb/PMApe interaction: a pronounced H^+-production, as compared to that for Cd and Zn. For Cd, it is slightly larger than for Zn. Applying eq. (4.5) it follows that K_{int}(PbPMApe) ≅ 28 and K_{int}(CdPMApe) ≅ 1.7. Thus the order of decreasing K_{int} for MPMApe is: Pb > Cd > Zn. This order agrees with that of the decreasing covalence index of these metal ions according to *Nieboer & Richardson* (1980).

An interesting feature of the $\Delta[H^+]$ curves is that, due to the difference in covalent binding between K^+ and H^+ with $RCOO^-$ groups, the exchange processes M^{2+}/K^+ and M^{2+}/H^+ apparently occur largely subsequently. As a consequence, the *effects* of the electrostatic and covalent binding of M^{2+} with PMApe are correspondingly separated.

4.1.2 Zn, Cd, Pb, Al, Cu, Ag/PMA

Zn/PMA

In figs 4.3.a and 4.3.b, $\Delta\kappa_T$ and the corresponding $\Delta[H^+]$ curves are given for Zn/PMA, at four different values of α_n.

All trends observed in the Zn/PMApe system are also found for the present Zn/PMA system:

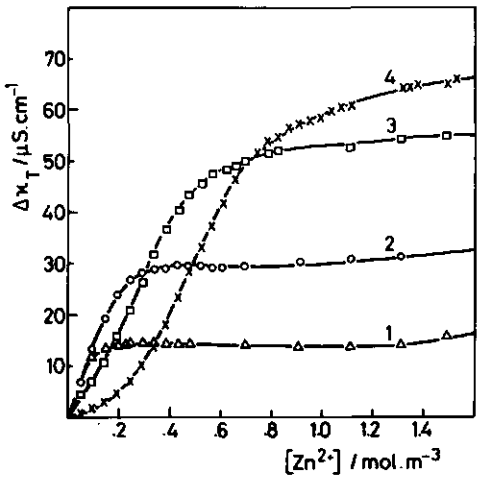

FIGURE 4.3.a The conductivity excess $\Delta\kappa_T$ versus the concentration $Zn(NO_3)_2$. $[PMA]_i$ = 2.50 mol·m^{-3}. α_n = 0.15 (1), 0.25 (2), 0.50 (3), 0.70 (4).

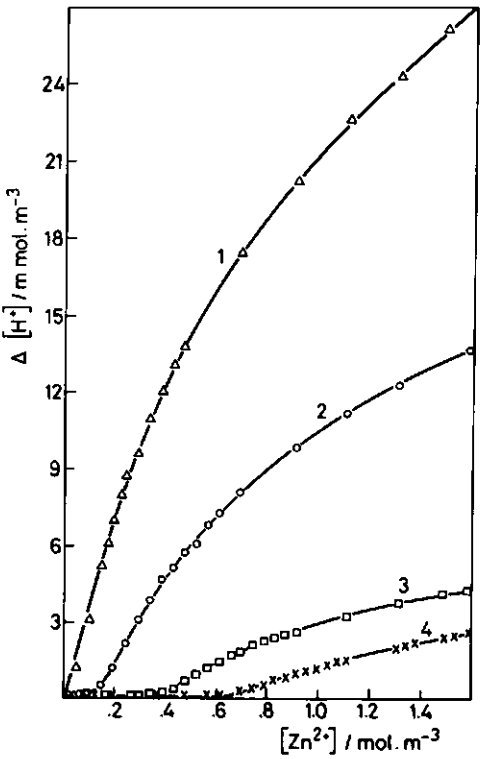

FIGURE 4.3.b The concentration of released protons versus the concentration $Zn(NO_3)_2$. $[PMA]_i$ = 2.50 mol·m^{-3}. α_n = 0.15 (1), 0.25 (2), 0.50 (3), 0.70 (4).

i An initial slope $\beta \cong 130$ S·cm^2·mol^{-1} at low α_n, indicating complete association of Zn^{2+};

ii The rounding off of the curves, just before charge neutralization;

iii Low values of the slope β for [Zn]/[L] > 0.5;

iv At higher values of α_n, the initial slope decreases with α_n, indicating the exchange reaction of conductometrically bound K^+/Zn^{2+}.

The large difference in molecular mass between the PMApe and the PMA samples does not give rise to differences in the observed trends. This is in agreement with literature data (*Oosawa*, 1971).

The curves of the proton production in fig. 4.3.b corroborate the similarity of the Zn/PMA and Zn/PMApe systems. However, the slight difference between the chemical environment of the functional groups in PMA and PMApe is expected to cause differences in K_a, and in K_{int}. In chapter 5, it will be demonstrated that for PMA the value of K_a is 4.85. Using this K_a value in eq. (4.5), it appears that the values of K_{int} for ZnPMA are approximately equal to those for ZnPMApe, at corresponding values of α_n.

Cd/PMA

In figs 4.4.a and 4.4.b, $\Delta\kappa_T$ and the corresponding $\Delta[H^+]$ values are pictured for Cd/PMA at different values of α_n.

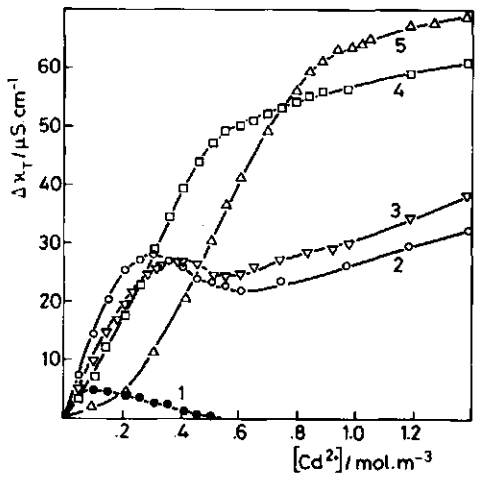

FIGURE 4.4.a The conductivity excess $\Delta\kappa_T$ versus the concentration $Cd(NO_3)_2$. $[PMA]_i$ = 2.50 mol·m^{-3}. α_n = 0.10 (1), 0.25 (2), 0.35 (3), 0.50 (4), 0.75 (5).

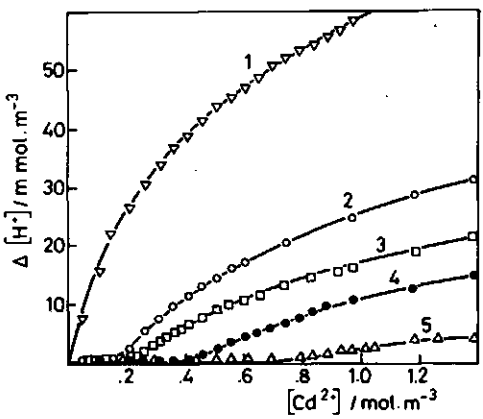

FIGURE 4.4.b The concentration of released protons versus the concentration $Cd(NO_3)_2$. $[PMA]_i$ = 2.50 mol·m^{-3}. α_n = 0.10 (1), 0.25 (2), 0.35 (3), 0.50 (4), 0.75 (5).

The curves 1-3 in fig. 4.4.a differ from the corresponding curves in fig. 4.3.a. For Cd/PMA, there exists a range of values of $[Cd]_a$ where $\Delta\kappa_T$ *decreases*. The reason for this decrease is a considerable proton production. The term $\lambda_H^1 \cdot \Delta[H]$ in eq. (3.50) is sufficiently

large to be effective. For instance, during the M/L-titration at α_n = 0.25 up to $[M]_a \cong 0.4$ mol·m^{-3}, the pH decreases from about 6.3 to 4.9 in the Cd/PMA system, whereas in the Zn/PMA system, the pH decreases to 5.3 over the same range. At values of pH < 5.5, H^+ ions start to contribute measurably to $\Delta\kappa_T$. For the higher values of α_n in fig. 4.4.a, the pH remains at values that do not give rise to a decrease of $\Delta\kappa_T$.

The initial slope $\beta \cong 130$ S·cm^2·mol^{-1}, in curve 2, is the same as that for Cd/PMApe. Thus, at low M/L, complete association is likely. The larger proton production at high M/L, as compared to the Cd/PMApe or Zn/PMA systems, and the complete association at low M/L, seem independent phenomena.

The proton production curves are given in fig. 4.4.b. Application of eq. (4.5) results in values of K_{int}(CdPMA) that are slightly larger than those of K_{int}(CdPMApe), for all values of α_n. Apparently, the absence of the ester groups in PMA favours complexation of Cd^{2+} with $RCOO^-$.

Pb/PMA

In figs 4.5.a and 4.5.b, $\Delta\kappa_T$ and the corresponding $\Delta[H^+]$ are presented for Pb/PMA at different values of α_n.

The initial slope $\beta \cong 180$ S·cm^2·mol^{-1} of curve 2 in fig. 4.5.a is the same as the corresponding slope for Pb/PMApe. This indicates complete association of Pb^{2+} with PMA at low M/L. The effect of the covalent character of the Pb/PMA interaction, as observed in the $\Delta\kappa_T$ curves is dramatic: the curves show a pronounced maximum. The maxima occur slightly before the point of charge neutralization by Pb^{2+}. The decrease of $\Delta\kappa_T$ is less strong at high M/L due to the diminishing rise in the proton production, and the more pronounced dilution effect.

In fig. 4.5.b, the values of the maximum slope S_m are large. For instance, in curve 1, $S_m \cong 0.90$. This means that at $\alpha_n = 0.1$ the maximum exchange ratio bound H/Pb is approximately unity. Application of eq. (4.5) is now limited by the inequality $d[Pb] < d[Pb]_a$. For $\alpha_n = 0.40$, $S_m \cong 0.28$ at pH = 5.4. These data yield: log K_{int}(PbPMA) > 2.

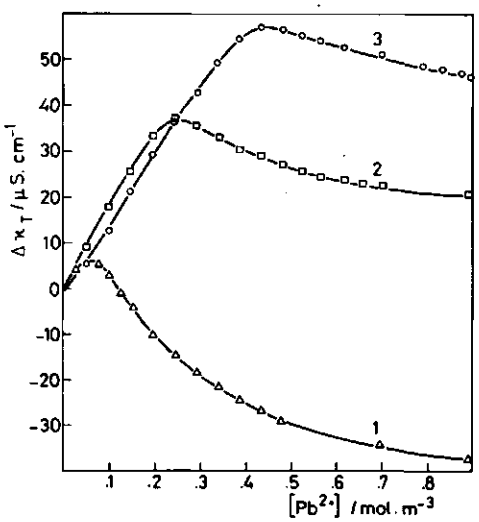

FIGURE 4.5.a The conductivity excess $\Delta\kappa_T$ versus the concentration $Pb(NO_3)_2$. $[PMA]_i$ = 2.50 mol·m^{-3}. α_n = 0.10 (1), 0.25 (2), 0.40 (3).

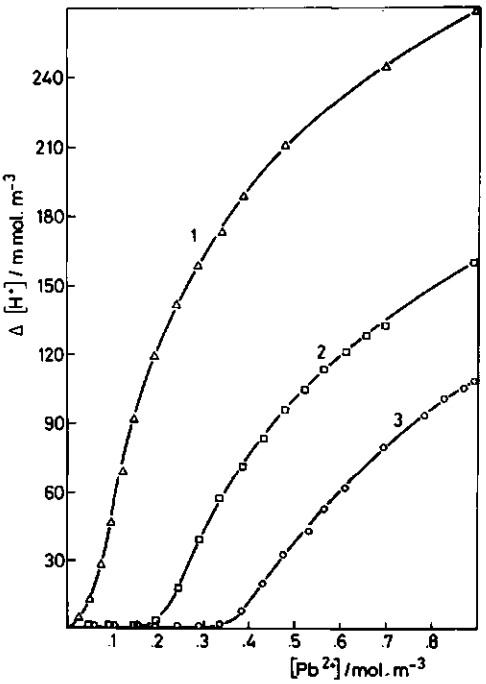

FIGURE 4.5.b The concentration of released protons versus the concentration $Pb(NO_3)_2$. $[PMA]_i$ = 2.50 mol·m^{-3}. α_n = 0.10 (1), 0.25 (2), 0.40 (3).

Al/PMA

In figs 4.6.a and 4.6.b, $\Delta\kappa_T$ and the corresponding $\Delta[H^+]$ are given for Al/PMA at different values of α_n.

The aluminium ion is highly charged, and generally binds strongly to oxygen-containing ligands. The main trends observed in the series Zn, Cd, Pb/PMA with respect to the character of the interactions are also very clearly observed with Al/PMA.

The maximum value of the slope $\beta \cong 200$ S·cm^2·mol^{-1}, at α_n = 0.25 in fig. 4.6.a, indicates complete association of Al^{3+} at low M/L. Up to the critical ratio R_c, no substantial proton production is observed in fig. 4.6.b. At higher values of α_n, the maximum slope β is observed at higher $[Al]_a$ because of the exchange of conductometrically bound K^+/Al^{3+}. A rapid increase of $\Delta[H^+]$ starts at about charge neutralization by Al^{3+}. Due to the rapid increase of the proton production, the $\Delta\kappa_T$

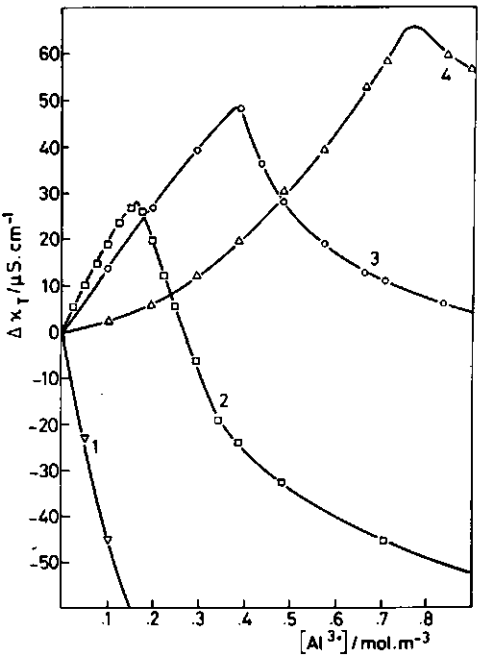

FIGURE 4.6.a The conductivity excess $\Delta\kappa_T$ versus the concentration $Al(NO_3)_3$. $[PMA]_i$ = 2.50 mol·m^{-3}. α_n = 0.0 (1), 0.25 (2), 0.50 (3), 1.0 (4).

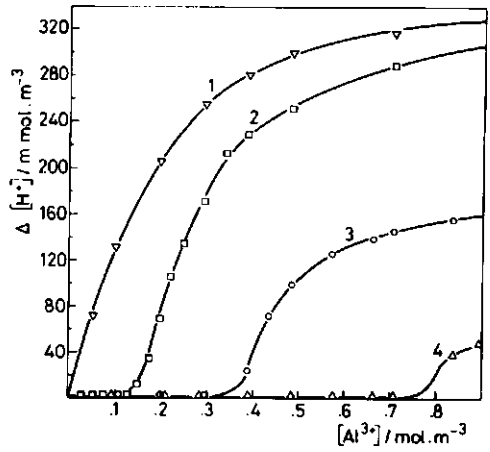

FIGURE 4.6.b The concentration of released protons versus the concentration $Al(NO_3)_3$. $[PMA]_i$ = 2.50 mol·m^{-3}. α_n = 0.0 (1), 0.25 (2), 0.50 (3), 1.0 (4).

curves show a peak. The peaks sharply separate the regions where Al^{3+} interacts predominantly with $L^-(K^+)$ and LH, respectively. At α_n values of 0.0 and 0.25, the maximum slope $S_m = (d[H]/d[Al]_a)_m$ appears to be about 1.5, suggesting a dimer structure of the Al-complex.

M/PMA

In figs 4.7.a and 4.7.b, $\Delta\kappa_T$ and the corresponding $\Delta[H^+]$ are again collected for Zn, Cd, Pb, Al/PMA, together with those for Cu/PMA and Ag/PMA, all at α_n = 0.25.

For the monovalent silver ions, only slight interaction seems to occur. The initial slope β of 20 S·cm^2·mol^{-1} cannot be explained by extensive association. The fact that $\lambda'_{Ag} < \lambda_{Ag}$ and the dilution effect account for the increase of $\Delta\kappa_T$. All the $\Delta\kappa_T$ curves for the multivalent ion systems start with an approximately linear increase, the slopes of the curves being related to the ionic conductivities of the metal ions.

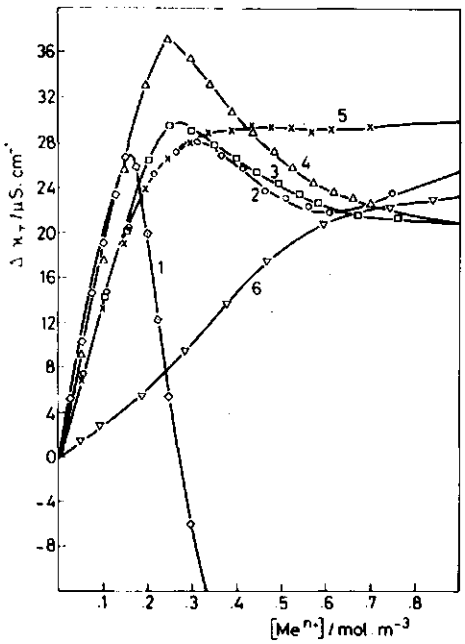

FIGURE 4.7.a The conductivity excess $\Delta\kappa_T$ versus the concentration $M(NO_3)_n$ at α_n = 0.25. $[PMA]_i$ = 0.25 mol·m^{-3}. (1) Al^{3+}; (2) Cd^{2+}; (3) Cu^{2+}; (4) Pb^{2+}; (5) Zn^{2+}; (6) Ag^+.

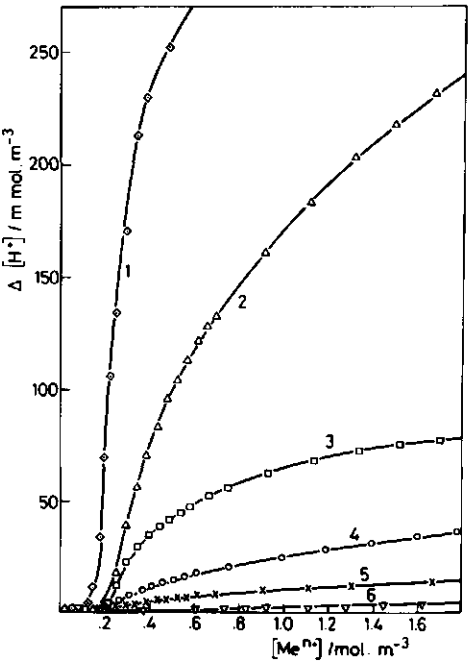

FIGURE 4.7.b The concentration of released protons versus the concentration $M(NO_3)_n$ at α_n = 0.25. $[PMA]_i$ = 0.25 mol·m^{-3}. (1) Al^{3+}; (2) Pb^{2+}; (3) Cu^{2+}; (4) Pb^{2+}; (5) Zn^{2+}; (6) Ag^+.

Maxima of increasing sharpness are observed in the order: Cd, Cu, Pb, Al. The sharper the maximum, the lower the concentration of $[M]_a$ at which it occurs, the larger the proton production.

In fig. 4.7.b, the differences in proton production reflect the differences in covalent character of the binding. In table 4.2, the maximum slopes S_m of the curves are collected, together with the corresponding values of the pH. For the divalent metal systems, the values of log K_{int}(MPMA) have been calculated for α_n = 0.25, applying eq. (4.5). The larger the value of K_{int} calculated using eq. (4.5), the larger its underestimation. Thus the order of increasing covalent character in the M/PMA interaction is: Zn < Cd < Cu < Pb.

TABLE 4.2 Maximum slope of the proton production in M/PMA systems at $\alpha_n = 0.25$, and the corresponding values of pH and log K_{int}(MPMA)

metal	$\left[\frac{d[H]}{d[M]_a}\right]_m$	pH	log K_{int}(MPMA)
Al	1.50	4.2	-
Pb	0.40	5.3	2.19
Cu	0.23	5.4	1.85
Cd	0.06	5.9	0.74
Zn	0.02	6.1	0.04
Ag	0.005	6.1	-

4.1.3 Cd, Ba, Zn, Pb/PAA

The results of the M/PAA series are given in figs 4.8.a,b and 4.9.a,b. The molecular mass of the sample in this series was 300,000.

Cd/PAA

In figs 4.8.a and 4.8.b, $\Delta\kappa_T$ and the corresponding values of $\Delta[H^+]$ are represented for Cd/PAA at different values of α_n.

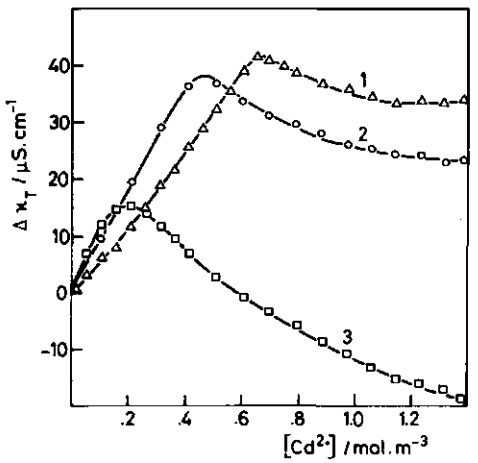

FIGURE 4.8.a The conductivity excess ΔK_T versus the concentration $Cd(NO_3)_2$. $[PAA]_i$ = 2.50 mol·m^{-3}. α_n = 0.60 (1), 0.40 (2), 0.20 (3).

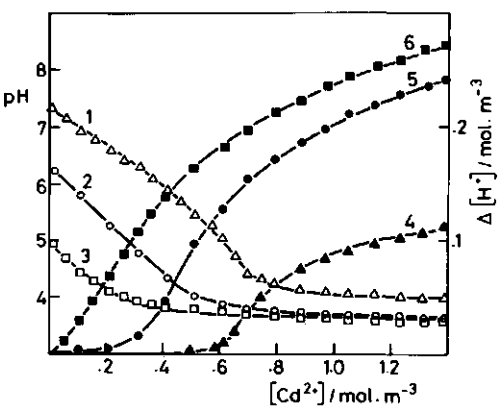

FIGURE 4.8.b The concentration of released protons, and the pH versus the concentration $Cd(NO_3)_2$. $[PAA]_i$ = 2.50 mol·m^{-3}. α_n = 0.60 (1,4), 0.40 (2,5), 0.20 (3,6).

Comparing the $\Delta\kappa_T$ curves for Cd/PAA with those for Cd/PMA - in fig. 4.4.a - it is evident that for Cd/PAA the distinct peaks reflect a larger proton production. The maximum slope β in fig. 4.8.a is about 130 $S \cdot cm^2 \cdot mol^{-1}$, the same value as found in fig. 4.4.a. This demonstrates the equivalency of the electrostatic contributions, whereas the covalent contributions are different.

In fig. 4.8.b, $\Delta[H^+]$ and the corresponding values of the pH are given. Obviously, the proton production is larger for Cd/PAA as compared with Cd/PMA. In chapter 5, it will be demonstrated that pK_a(PAA) = 4.72, whereas pK_a(PMA) = 4.85 and pK_a(PMApe) = 5.30. However, the lower value for PAA cannot quantitatively account for the increase in the proton production. At α_n = 0.40, the maximum slope $(d[H]/d[Cd]_a)_m$ is about 0.4. Applying eq. (4.5), it appears that log K_{int}(CdPAA) $\cong$ 2.96, whereas log K_{int}(CdPMA) is 0.32, at the same value of α_n.

M/PAA

In figs 4.9.a and 4.9.b, $\Delta\kappa_T$ and the corresponding $\Delta[H^+]$ are collected for the Ba, Zn, Pb/PAA systems, and again for Cd/PAA, all at α_n = 0.40.

In fig. 4.9.a, the curves for M/PAA follow the same pattern as those for M/PMA in fig. 4.7.a. The initial rise in $\Delta\kappa_T$ can be explained by com-

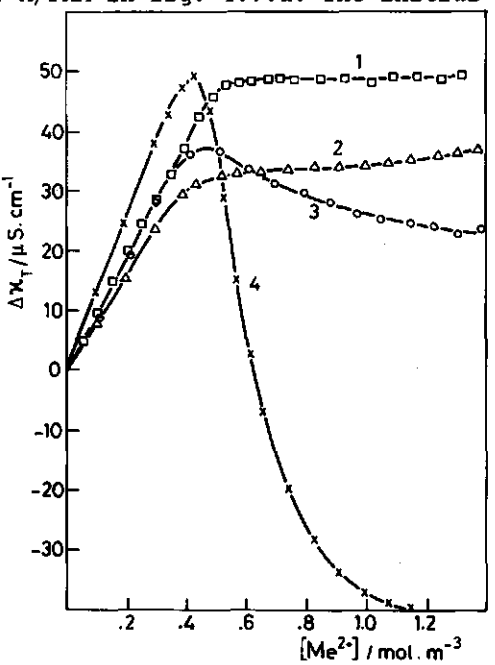

FIGURE 4.9.a The conductivity excess $\Delta\kappa_T$ versus the concentration $M(NO_3)_2$, at α_n = 0.40. $[PAA]_i$ = 2.50 $mol \cdot m^{-3}$. (1) Ba^{2+}; (2) Zn^{2+}; (3) Cd^{2+}; (4) Pb^{2+}.

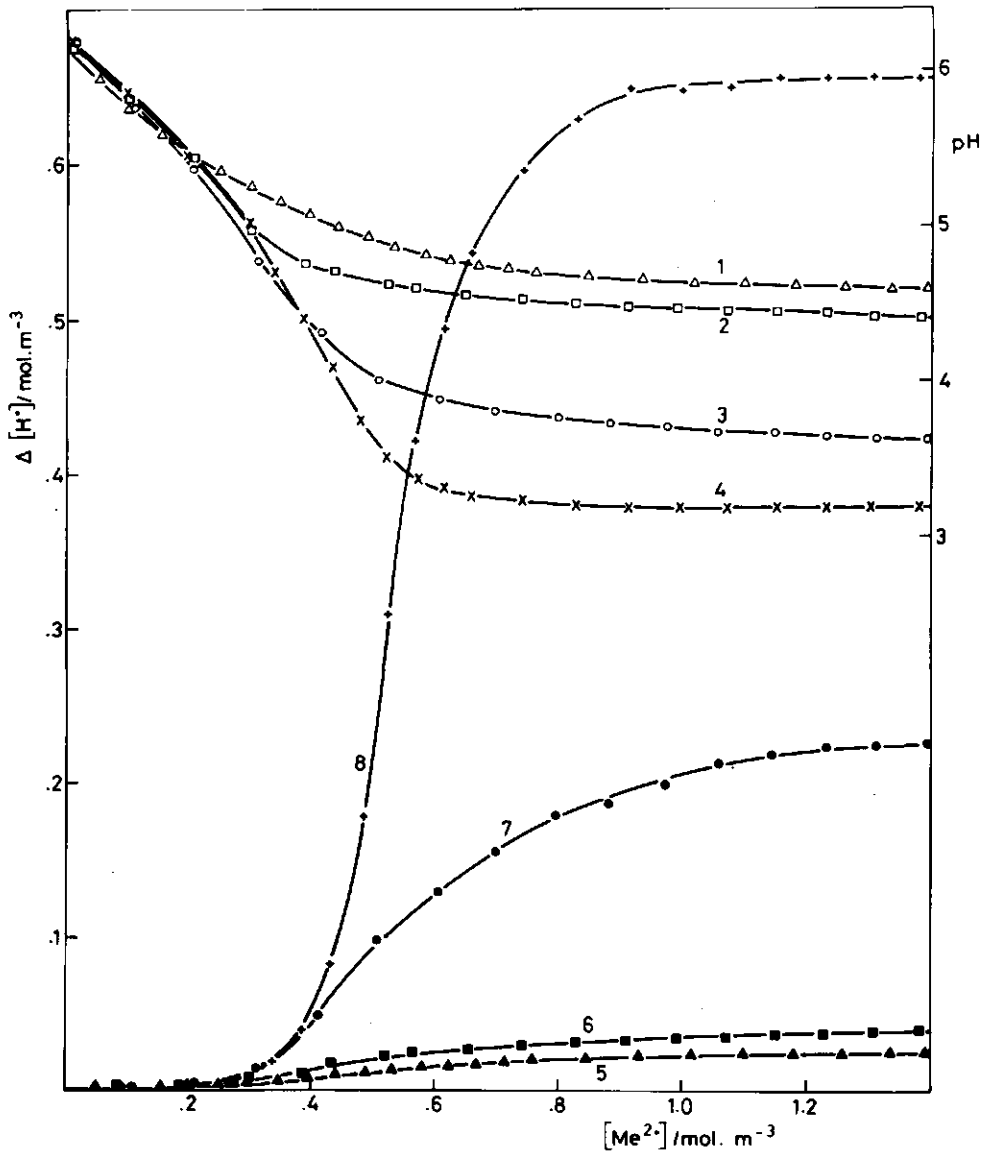

FIGURE 4.9.b The concentration of released protons, and the pH versus the concentration $M(NO_3)_2$, at α_n = 0.40. $[PAA]_i$ = 2.50 mol·m^{-3}. (1,5) Ba^{2+}; (2,6) Zn^{2+}; (3,7) Cd^{2+}; (4,8) Pb^{2+}.

plete association of the metal ions. Differences between the initial slopes β are attributed to differences in λ_M. At low M/L, the conductometric binding is identical for Ba, Zn, Cd and Pb. For values of M/L > 0.5 the $\Delta\kappa_T$ curves are different, reflecting the differences in covalent character of the M/PAA interactions.

In fig. 4.9.b, the maximum slopes $(d[H]/d[M]_a)_m$ are ~ 0.04 (Ba), 0.09 (Zn), 0.4 (Cd) and 2.6 (Pb). In this order the covalency increases, as expected. The low proton production in the Ba/PAA system demonstrates the predominantly electrostatic character of the interaction. The high proton production in the Pb/PAA system suggests the occurrence of j values larger than unity. It should be noted that extensive complex formation PbL_j may substantially enlarge the K_a value of carboxyl groups neighbouring the complexed groups.

In table 4.3, approximative values of K_{int} are collected for the formation of MPMApe, MPMA and MPAA, formulated in terms of 1:1 complexes, and calculated using eq. (4.5) for $\alpha_n = 0.40$.

TABLE 4.3 Approximative values of K_{int}(ML)

Polyacid	Zn	Cd	Pb
PMApe	0.9	1.7	$2.8 \cdot 10_2$
PMA	0.7	2.1	$1.1 \cdot 10_4^2$
PAA	$1.3 \cdot 10$	$9.2 \cdot 10^2$	$> 3 \cdot 10^4$

The values in table 4.3 are based on rather crude approximatations, especially due to the assumptions $d[M] = d[M]_a$, and the application of K_a for the acid strength. In chapter 5, more accurate values will be given for some of the systems, as a result of the polarographic experiments. Nevertheless, the table indicates order of increasing covalency: Zn < Cd < Pb, and PMApe ≤ PMA < PAA.

Larger values of K_{int} for M/PAA, as compared to M/PMA have also been found by *Yamashita et al.* (1979a,b). The difference can be attributed to several phenomena originating from the extra methyl group in PMA:

i The hydrophobic interaction between the methyl groups in PMA, and - even more pronounced - in PMApe, causes a rather stiff hypercoiled conformation of these polymers at low charge densities. Generally, binding constants of metal-polymer complexes are strongly dependent on the conformation of the polymer (*Kanedo & Tsuchida*, 1981). The polymer coil of PAA is more flexible, and readily able to adapt those conformations that are favourable to form complexes (*Nagata & Okamoto*, 1983).

ii The extra methyl groups in PMA create a different chemical environment of the functional groups. One of the features of this difference concerns the electron-repelling power of the methyl side-chains, which induces a displacement of the electrons in the carboxylate group. As a consequence, the potential at the locus of the binding will become more negative. This will facilitate further protonation rather than further metal binding.

iii Due to the less hydrophobic character of PAA, the amount of structure water around the polyacrylate ion is larger than around the polymethacrylate ion (*Conway*, 1981). Metal complexation involves replacement of bound water from the polyion (*Spegt et al.*, 1973). The corresponding gain in entropy is, as a rule, larger for MPAA than for MPMA.

Cooperation of these effects may very well explain the observed differences in K_{int}.

4.1.4 Critical data

An important result achieved in § 4.1.1 - § 4.1.3 is that for most of the systems investigated, the intrinsic binding constant is low. Consequently, the dramatic binding levels at low M/L are predominantly due to electrostatic interaction. Therefore, the conclusions for *low* M/L can be considered against the background of the CC and PB models. The main conclusions are:

i The maximum values of the slope β can only be explained by *complete* conductometric binding of the divalent metal ions.

ii At high α_n, monovalent ions are conductometrically bound, whereas at low α_n this is not the case. Moreover, the fraction bound increases with increasing α_n.

iii The value of R_c, that is the M/L ratio at which the binding of M ceases to be complete, increases with α_n.

An implication of conclusion (i) is that the bound ions are effectively immobilized at low M/L. In this respect, they behave as 'condensed' ions in CC. It is reasonable to assume that these bound ions are positioned in the direct vicinity of the polyion. Thus the CIV will refer to highly immobile ions.

A consequence of conclusion (ii) is that there exists a certain value of α_n, at which the conductometric binding of K^+ begins. This

would agree with the occurrence of critical values of ξ for condensation in CC. For the condensation of monovalent ions $\xi_{crit} = 1$. Since ξ_{str} is 2.95 for PMA and PAA, and 1.95 for PMApe, critical values of α_n are expected to be 0.33 and 0.51, respectively. Inspection of figs 4.1.a (Zn/PMApe), 4.3.a (Zn/PMA), 4.4.a (Cd/PMA) and 4.8.a (Cd/PAA) reveals that conductometric binding of K^+ only occurs at values of $\alpha_n > \alpha_n$(crit.). These observations support one of the basic concepts of the CC model, and concurrently affect the general validity of the sum-rule in PB.

Conclusion (iii) gives the opportunity to test the condensation criterion quantitatively. The CC model predicts that complete binding of divalent metal ions occurs until the effective charge density is equal to $\xi_{crit} = 0.5$, if 1:1 salt is absent. Thus R_c can be identified with the maximum value of θ_2, as given in eq. (2.17). Alternatively, if $R_c = \theta_2(max)$, then the value of the structural charge density parameter as calculated from experimental data ξ_{exp} should yield ~2.0 for PMApe and ~3.0 for PMA and PAA. With $R_c = \theta_2$ and $\xi_{exp} = \frac{1}{\alpha_n} \cdot \xi$, eq. (2.17) can be written as:

$$\xi_{exp} = [2 \cdot \alpha_n (1 - 2 \cdot R_c)]^{-1} \qquad (4.6)$$

In table 4.4, a number of values of R_c are collected. Due to the difficulty in determining R_c accurately, the error in the value of R_c

TABLE 4.4 Critical ratio R_c and the corresponding values of ξ_{exp} from conductometric data

	Zn			Cd			Pb		
	α_n	R_c	ξ_{exp}	α_n	R_c	ξ_{exp}	α_n	R_c	ξ_{exp}
PMApe	0.23	0.24	3.9-4.5						
	0.33	0.25	2.8-3.3						
	0.43	0.24	2.1-2.4	0.43	0.24	2.1-2.4	0.43	0.24	2.1-2.4
	0.63	0.30	1.8-2.2						
	0.83	0.36	1.9-2.5						
PMA	0.15	0.13	4.3-4.8						
	0.25	0.16	2.8-3.1	0.25	0.23	3.4-4.0	0.25	0.24	3.6-4.2
				0.35	0.26	2.7-3.2	0.40	0.27	2.5-3.0
	0.50	0.30	2.3-2.8	0.50	0.32	2.5-3.1			
	0.70	0.38	2.6-3.6	0.75	0.37	2.2-3.0			
PAA				0.20	0.09	2.9-3.2			
	0.40	0.31	3.0-3.7	0.40	0.32	3.1-3.9	0.40	0.34	3.5-4.5
				0.60	0.39	3.2-4.6			

may be about 0.02. The corresponding ranges of ξ_{exp} are given in the table.

Notwithstanding the scatter in the values of ξ_{exp}, some interesting trends can be observed in table 4.4:

i For high values of α_n, the ranges of the values of ξ_{exp} cover, in the case of PMApe and PMA, those predicted in the CC model.

ii For low values of α_n, say those below 0.3, the values of ξ_{exp} are much larger than ∿2.0 for PMApe and ∿3.0 for PMA. These large values are attributed to the compact conformation of PMApe and PMA at low α_n. The actual charge spacing may be half of that in the stretched conformation (*Liquori et al.*, 1959).

iii In the case of PAA, the values of ξ_{exp} appear to be larger than those for PMA, at high α_n. The difference between PAA and PMA can be due to the larger covalent character of the M/PAA interaction, as compared to M/PMA.

As the CC model is claimed to be applicable to purely electrostatic interaction of counterions with linear polyelectrolytes, the observed trends appear to agree with the predictions of the model.

4.2 POLAROGRAPHY

The results of the polarographic M/L-titrations are presented in the figs 4.10 - 4.17. The limiting currents i_ℓ are plotted versus the amount of added heavy metal nitrate. Each of the figures contains three i_ℓ-curves for metal/polyacid samples at different values of α_n. In addition, the calibration graph is included. This graph refers to the corresponding metal nitrate solution without polyacid, in the presence of 50 mol·m^{-3} KNO_3.

All figures have the same scale, enabling direct comparison. In § 3.3.3 it has been pointed out that the drop in the limiting current Δi_ℓ with respect to the calibration graph, is a measure of the extent of the metal association.

It should be noted that an excess of KNO_3 is present in the sample solutions.

4.2.1 Zn, Cd, Pb/PMA

The results of the M/PMA series are presented in the figs 4.10 - 4.14. In these figures is: 1. calibration graph; 2. α_n = 0.20; 3. α_n = 0.40; 4. α_n = 0.60.

Zn/PMA

The figs 4.10 - 4.12 refer to Zn/PMA systems at three levels of $[KNO_3]$, viz. 10, 50 and 100 mol·m^{-3}, respectively.

All polarograms of the Zn/PMA systems have the usual shape and well-defined limiting currents. *Cottrell* plots appeared to be linear, with only small intercepts of the ordinate. Indications of some reactant adsorption were obtained at $\alpha_n = 0.6$, over the range of M/L ratios where the slope of the i_ℓ-curves is about to change to approximately the value of the calibration curve (intermediate range).

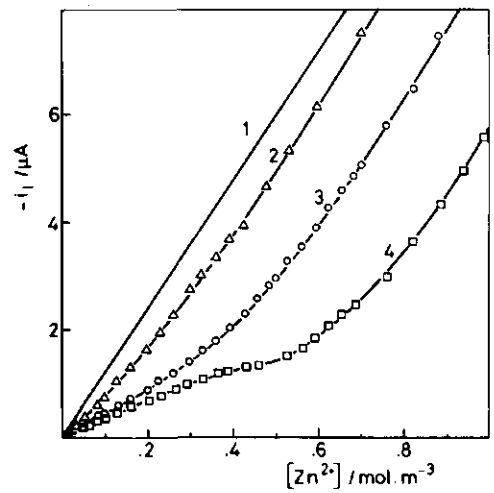

FIGURE 4.10

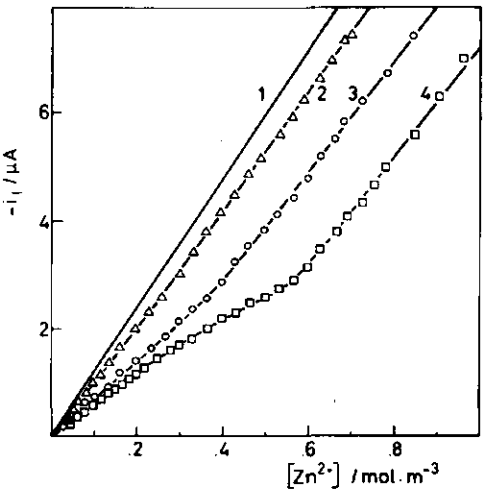

FIGURE 4.11

FIGURES 4.10-4.12 The limiting current for Zn/PMA versus the concentration $Zn(NO_3)_2$. $[PMA]_i = 2.50$ mol·m^{-3}. E_i = -850 mV vs. $Ag/AgCl,KCl_{sat}$; $t_p = 48$ ms; $t_d = 1$ s; $A = 0.993$ mm^2.
(1) calibration; (2) $\alpha_n = 0.20$; (3) $\alpha_n = 0.40$; (4) $\alpha_n = 0.60$.
$[KNO_3]$ = 10 mol·m^{-3} (Fig. 4.10), 50 mol·m^{-3} (Fig. 4.11), 100 mol·m^{-3} (Fig. 4.12).

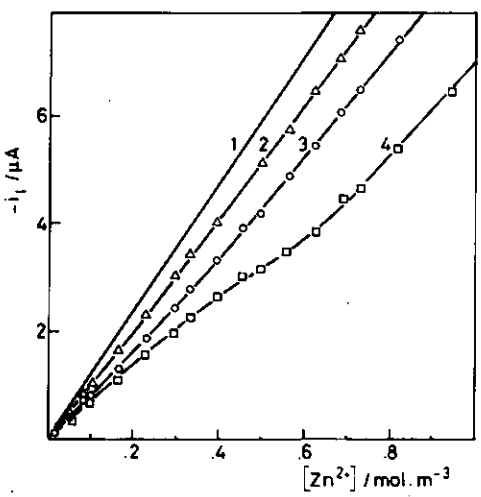

FIGURE 4.12

The curves in the figures demonstrate that for a given M/L-titration:

i At low M/L, the slope of the i_ℓ-curve is smaller than that of the calibration graph, indicating polarographic binding of the heavy metal ions.

ii At high M/L, the difference of the slope of the i_ℓ-curve with that of the calibration graph is small. This suggests that the binding of the ligands is approximately complete.

These trends may also be observed in voltametric analyses of low molecular mass metal-complexes (*Hanck & Dillard*, 1977). In these systems, the observed trends are generally attributed to the non- or quasi-lability of the complexes. However, in the present systems, small but definite shifts in the half-wave potentials were observed at *low* M/L, indicating polarographic lability of the metal/polyion complexes. Thus the average diffusion coefficient rather than the amount of electro-active species is lowered as a result of the binding with the polyion. The demonstrated lability allows the application of eq. (3.21) at low M/L, to quantify the binding. This will be established in the discussion.

An important feature of the i_ℓ-curves is that the range of M/L ratios over which the slope is low, generally increases with increasing α_n. In simple ligand systems, that range (the 'binding capacity') is mostly constant for a given total ligand concentration, and independent of α_n. The dependency of the metal binding on α_n in polyion systems emphasizes the electrostatic nature of the interaction.

The observed trends largely support the findings in the conductometric experiments, except for one important difference: the slopes of the i_ℓ-curves vary with α_n. From the maximum values of the slopes in the $\Delta\kappa_T$-curves, it was concluded that at low M/L complete binding occurred at all values of α_n. From the polarographic experiments, it appears that at given low M/L, the bound fraction of metal ions increases with increasing α_n. Thus, generally both free *and* bound metal ions will be present in the sample solutions. This phenomenon is connected with the presence of 1:1 salt in the polarographically investigated samples. K^+ ions, from added KNO_3, compete with Zn^{2+} in the electrostatic binding with the polyion. The lower the concentration KNO_3, the lower is the value of the slope of the i_ℓ-curve at low M/L. At high M/L, this dependency of the slope on c_1 is absent.

Obviously, the presence of 1:1 salt also affects the proton production when the M/L-titration proceeds. The initial pH is lower, and the decrease of the pH is both smaller and more gradual (not in figures) as compared to the corresponding systems without 1:1 salt. As a result, the proton production in the systems with added 1:1 salt is larger at low M/L and smaller at high M/L, as compared with the salt-free systems. The change of the slope of the proton production with M/L is smaller in the systems with added 1:1 salt. Effects of the presence of 1:1 salt will be discussed in more detail in chapter 6.

The indications of reactant adsorption, through slight pulse polarographic maxima discussed in § 3.3.5, will be related to the irregular form of the i_ℓ-curves sometimes obtained over the intermediate range of M/L ratios. A chain of processes will cause the i_ℓ-curves to become convex at intermediate M/L:

i At high α_n, the degree of metal binding is large, and thus the effective charge density of the polyion is low. As a consequence, the polymer coil tends to adopt a more compact conformation, hampering the kinetics of the exchange bound/free metal ions, and the drainage of the polymer coil.

ii Under these conditions (compact coil, high θ_2) reactant adsorption effects are facilitated.

iii A more compact conformation allows the formation of $M^{2+}(L^-)_2$ with ligands which are not direct neighbours in the chain. This process may result in flocculation of the metal/polyion complex.

The processes (i-iii) will be more pronounced in their effect if the metal/polyion interaction is more covalent. All processes result in a relative decrease of i_ℓ.

Cd/PMA

In fig. 4.13, i_ℓ-curves are presented for Cd/PMA at $[KNO_3]$ = 10 mol·m^{-3}. Comparing fig. 4.13 with fig. 4.10, it is evident that the Cd/PMA interaction is stronger than that of Zn/PMA under identical experimental conditions. Thus, in the presence of 1:1 salt, the polarographic binding appears to be dependent on the nature of the metal ion. Since the effective radii of Cd^{2+} and Zn^{2+} are approximately the same (*Creighton*, 1935; *Hunt*, 1963), the electrostatic binding of these metal ions is about the same. Alternatively, the ion-specificity originates from differences in chemical binding characteristics.

At low M/L, the polarograms of the Cd/PMA system have the usual

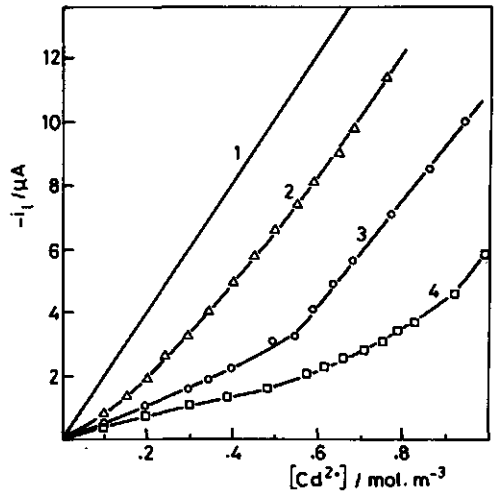

FIGURE 4.13 The limiting current for Cd/PMA versus the concentration $Cd(NO_3)_2$. $[PMA]_i$ = 2.50 mol·m^{-3}. $[KNO_3]$ = 10 mol·m^{-3}. E_i = -300 mV vs. $Ag/AgCl,KCl_{sat}$; t_p = 172 ms; t_d = 1 s; A = 2.61 mm^2; (1) calibration; (2) α_n = 0.20; (3) α_n = 0.40; (4) α_n = 0.60.

shape, showing a well-defined limiting current. In the range of intermediate M/L, a pulse polarographic maximum shows up at the onset of the wave. Apparently, a larger degree of metal binding provokes a more pronouced effect of (induced) metal ion adsorption.

The value of ΔE_{i_2} systematically decreases during the initial stage of the M/L-titrations. From this decrease, it is concluded that for low M/L, the Cd/PMA complexes can be considered as polarographically labile. A confirmation of the lability that simultaneously gives information on D_b/D_f, is the determination of the change of i_ℓ upon addition of excess of ligand to a given sample solution. In the case of sufficient excess of ligand, virtually all metal ions will be bound, and according to eq. (3.21) the limiting current will utimately yield a plateau value given by:

$$\frac{i_\ell^2}{i_o^2} = \frac{D_b}{D_f} \qquad (4.7)$$

For the Cd/PMA system tested by this procedure, the curve of i_ℓ versus [L] did asymptotically approach a certain plateau value, resulting in a D_b/D_f value of about 0.03. This value is in reasonable agreement with the corresponding value in table 3.3.

In fig. 4.14, the proton production is depicted as a function of the concentration $Cd(NO_3)_2$ for Cd/PMA at α_n = 0.40 in the absence and in the presence of KNO_3.

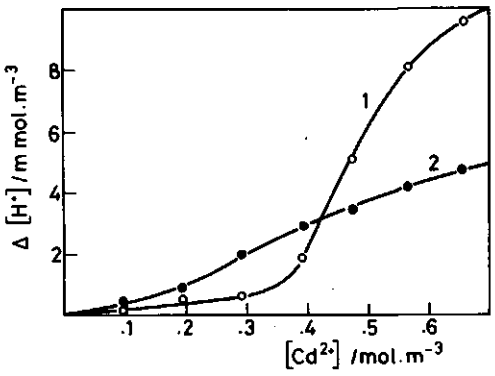

FIGURE 4.14 The concentration of released protons versus the concentration $Cd(NO_3)_2$. $[PMA]_i$ = 2.50 mol·m^{-3}; α_n = 0.40.
(1) no 1:1 salt added; (2) $[KNO_3]$ = 50 mol·m^{-3}.

From the curves in fig. 4.14, similar effects as described for Zn/PMA are demonstrated. Over the range of Cd^{2+} concentrations in fig. 4.14, the pH decreases from 7.00 to 4.98 for curve 1, and from 5.85 to 5.19 for curve 2, the latter decrease being more gradual. From the difference between the salt-free and added-salt curve, it appears that in the presence of added 1:1 salt, the reactions $M^{2+} + L^-$ and $M^{2+} + HL$ occur concurrently at low M/L, whereas only the former reaction occurs in the salt-free system. In the presence of excess of KNO_3 the reaction $K^+ + L^-$ competes effectively with $M^{2+} + L^-$.

Pb/PMA

In fig. 4.15, i_ℓ-curves are presented for Pb/PMA at $[KNO_3]$ = 50 mol·m^{-3}. The large values of Δi_ℓ demonstrate the strong Pb/PMA interaction. Over the range of Pb^{2+} concentrations given in fig. 4.15, $\Delta E_{\frac{1}{2}}$ systematically decreases over about 100 mV, at α_n = 0.60, whereas for Cd/PMA and Zn/PMA the decrease in $E_{\frac{1}{2}}$ is much less. These findings support the previously, in § 4.1.2, obtained conclusion, that the M/PMA interaction is increasingly stronger in the series Zn < Cd < Pb.

The polarograms of the Pb/PMA system show, even at low M/L, low α_n and large t_p, indications of reactant adsorption: a pulse polarographic maximum at the onset of the wave, and a slightly depressed limiting current. From a comparison with some SDC data it follows that the lowering of these NPP limiting currents is always less than about 5%. Thus the NPP limiting currents are still a reasonable measure of the Pb/PMA interaction. In the base-line, a hump is present at about

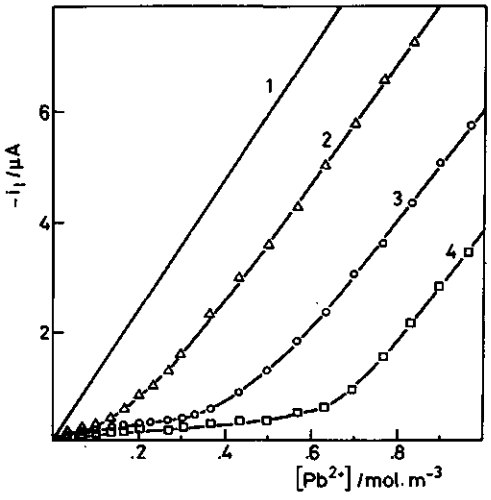

FIGURE 4.15 The limiting current for Pb/PMA versus the concentration $Pb(NO_3)_2$. $[PMA]_i$ = 2.50 mol·m^{-3}; $[KNO_3]$ = 50 mol·m^{-3}; E_i = -100 mV vs. $Ag/AgCl,KCl_{sat}$; t_p = 175 ms; t_d = 1 s; A = 1.63 mm^2; (1) calibration; (2) α_n = 0.20; (3) α_n = 0.40; (4) α_n = 0.60.

-400 mV vs. $Ag/AgCl,KCl_{sat}$ (not far from the p.z.c.), suggesting a potential dependence of the adsorption. A local maximum on the wave, at α_n = 0.40 and α_n = 0.60, positioned at about -700 mV vs. $Ag/AgCl,KCl_{sat}$ is possibly related to the appearance of a small second wave. This may be due to a splitting up of the reduction wave of the Pb-complex as a result of insufficient excess of ligand (*Elenkova & Nedelcheva*, 1976).

At high M/L, no maxima are present. Moreover, the slope of the i_ℓ-curve is about the same as that of the calibration graph. As suggested previously, at high M/L the (compact) polymer coil may be not well-drained, and the exchange process bound/free ions may be hampered. The contribution of the relatively large amount of free M^{2+} in the bulk to the limiting current will increase almost linearly with increasing M/L, and mask the adsorption effect.

4.2.2 Zn, Cd, Pb/PAA

The limiting currents for the M/PAA series are given in figs 4.16 - 4.18. These figures refer to $[KNO_3]$ = 50 mol·m^{-3}, and $\bar{M}$ = 300,000.

Three differences between M/PAA and M/PMA are generally observed:

i Corresponding values of $\Delta E_{\frac{1}{2}}$ are slightly larger for M/PAA. The values decrease with increasing M/L in the usual way.

ii The decrease of the pH in a M/L-titration is for M/PAA also somewhat larger than in the corresponding case of M/PMA. Moreover, the values of the pH are lower.

iii The M/PAA systems tend to coagulate at lower values of the concentration divalent metal nitrate, as compared to M/PMA. Sometimes the coagulation for M/PAA sets in at M/L ratios where the slope of the i_ℓ-curve is small.

These phenomena support the conclusion previously achieved in § 4.1.3, that, as a rule, the M/PAA interaction is stronger than for M/PMA.

Zn/PAA

In fig. 4.16, i_ℓ-curves are presented for Zn/PAA, at $[KNO_3]$ = 50 $mol \cdot m^{-3}$.

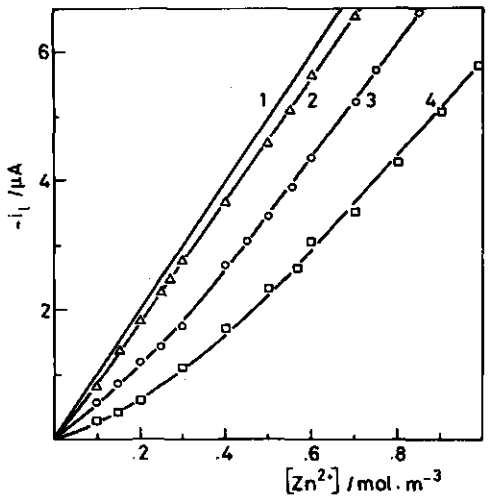

FIGURE 4.16 The limiting current for Zn/PAA versus the concentration $Zn(NO_3)_2$. $[PAA]_i$ = 2.50 $mol \cdot m^{-3}$; $\bar{M}$ = 300,000; $[KNO_3]$ = 50 $mol \cdot m^{-3}$; E_i = -750 mV vs. $Ag/AgCl,KCl_{sat}$; t_p = 175 ms; t_d = 1 s; A = 1.63 mm^2; (1) calibration; (2) α_n = 0.20; (3) α_n = 0.40; (4) α_n = 0.60.

The polarograms from which the curves have been constructed, have the usual shape. The limiting currents are well-defined. *Cottrell* plots at different values of α_n and M/L appeared to be linear, with only a small intercept on the ordinate axis. No adsorption maximum occurs at the onset of the polarographic wave. However, at α_n = 0.40 a small maximum is present at a pulse potential of about -1.2 V vs. $Ag/AgCl, KCl_{sat}$. During the M/L-titration, this maximum appears to be positioned at the onset of a small second wave that is growing with M/L. The value of the total limiting current never exceeds that of the first wave by more than 5%. At α_n = 0.60, similar phenomena occur at somewhat higher values of [Zn]. It is supposed that the reduction wave of the Zn/PAA system is split up due to lack of excess of ligand.

The larger decrease of the pH and the presence of the small second wave are interpreted as manifestations of an increased covalent char-

acter of the Zn/PAA interaction, as compared to Zn/PMA. This is in agreement with the findings from the conductometric experiments in the salt-free solutions.

Cd/PAA

In fig. 4.17, i_ℓ-curves are presented for Cd/PAA, at $[KNO_3]$ = 50 $mol \cdot m^{-3}$.

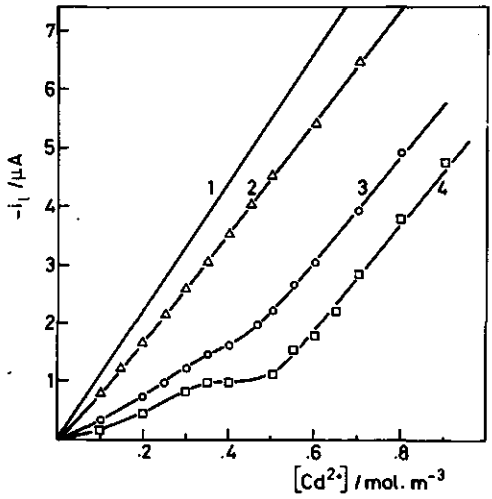

FIGURE 4.17 The limiting current for Cd/PAA versus the concentration $Cd(NO_3)_2$. $[PAA]_i$ = 2.50 $mol \cdot m^{-3}$; $\bar{M}$ = 300,000; $[KNO_3]$ = 50 $mol \cdot m^{-3}$; E_i = -300 mV vs. $Ag/AgCl,KCl_{sat}$; t_p = 172 ms; t_d = 1 s; A = 1.56 mm^2; (1) calibration; (2) α_n = 0.20; (3) α_n = 0.40; (4) α_n = 0.50.

For the Cd/PAA systems, the limiting currents are well-defined. The polarograms have the usual shape for values of α_n up to 0.40. At larger values of α_n, adsorption maxima appear, even at a t_p value as high as 175 ms, beginning at $[Cd]_a \cong 0.4$ $mol \cdot m^{-3}$. Moreover, the second wave, again starting at about -1.2 V vs. $Ag/AgCl,KCl_{sat}$ is now larger than in the case of Zn/PAA. At α_n = 0.50, the limiting current of the second wave amounts to about 10% of that of the first wave. At this value of α_n, and intermediate M/L, coagulation is also observed. The flat region in the i_ℓ-curve at α_n = 0.50 will be due to effects of induced metal ion adsorption and coagulation as a result of the strong interaction of Cd^{2+} with PAA and the low charge density of the polyion. These observations agree with the findings from the conductometric experiments that the intrinsic binding constant increases in the series CdPMA < ZnPAA < CdPAA.

From experiments with increasing ligand concentration, a D_b/D_f value of about 0.005 has been calculated for Cd/PAA, using eq. (4.7). This value agrees reasonably with the value given for M/PAA ($\bar{M}$ = 300,000) in table 3.3.

Pb/PAA

In fig. 4.18, i_ℓ-curves are presented for Pb/PAA, at $[KNO_3]$ = 50 $mol \cdot m^{-3}$. The limiting currents on polarograms recorded in the NPP mode

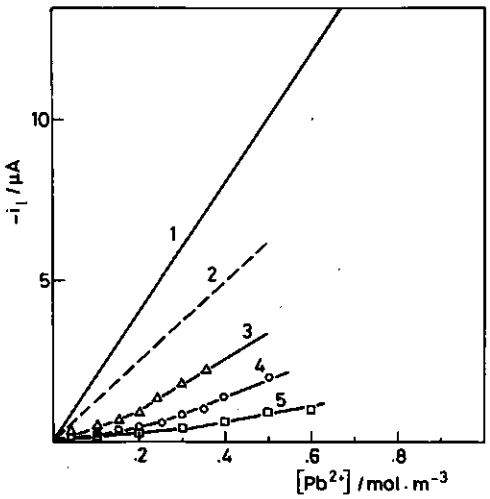

FIGURE 4.18 The limiting current for Pb/PAA versus the concentration $Pb(NO_3)_2$. $[PAA]_i$ = 2.50 $mol \cdot m^{-3}$; $\bar{M}$ = 300,000; $[KNO_3]$ = 50 $mol \cdot m^{-3}$; E_i = -100 mV vs. $Ag/AgCl,KCl_{sat}$; t_p = 172 ms; t_d = 1 s; A = 2.54 mm^2; (1) calibration; (2) α_n = 0; (3) α_n = 0.20; (4) α_n = 0.40; (5) α_n = 0.60.

were irregular at α_n = 0.40 and α_n = 0.60. At these α_n values, the SDC mode has also been applied to circumvent the strong induced metal ion adsorption effects. The i_ℓ-values from SDC were recalculated for the experimental conditions that correspond with those for the calibration graph. The Pb/PAA systems with added 1:1 salt are characterized by the occurrence of substantial coagulation. Fig. 4.18 is only presented to complete the M/PAA series.

Curve 2 refers to α_n = 0. Substantial binding of Pb^{2+} occurs even at very low charge densities of the polyion. Notwithstanding the irregularities in the systems, the curves 3-5 again reveal distinct ranges of low and high slopes, the ranges being related to the value of α_n.

The tendency to coagulate is observed to increase going from M/PMA to M/PAA on the one hand, and in the series Zn, Cd, Pb on the other. Thus, the tendency increases with increasing covalent character of the binding. In addition to this, the tendency increases with increasing $[KNO_3]$, when corresponding polarographic and conductometric results are compared.

4.2.3 Proton release

The release of protons in the polarographic M/L-titrations of the M/PAA systems at α_n = 0.40 are presented in fig. 4.19.

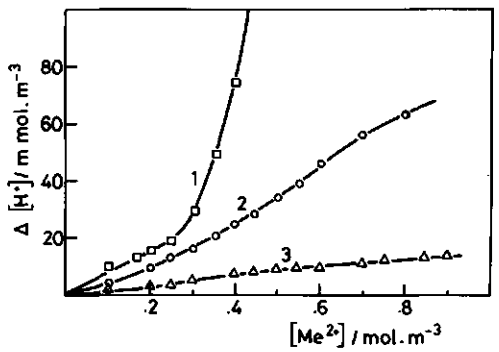

FIGURE 4.19 The concentration of released protons versus the concentration $M(NO_3)_2$. $[PAA]_i$ = 2.50 mol·m^{-3}; $\bar{M}$ = 300,000; $[KNO_3]$ = 50 mol·m^{-3}; α_n = 0.40; (1) Pb^{2+}; (2) Cd^{2+}; (3) Zn^{2+}.

The curves for Cd/PAA and Zn/PAA in fig. 4.19 show the same trend as for Cd/PMA in fig. 4.14: $[H^+]$ increases gradually, starting from the very onset of the titration. Only for the Pb/PAA system, a pronounced rise in the proton production is observed at a position which coincides with the change of the slope in the corresponding i_ℓ-curve. In contrast with the proton production in the salt-free solutions, the slope in fig. 4.19 at low M/L is dependent on the nature of the metal ion. Due to the presence of excess of KNO_3, K^+ ions compete effectively with M^{2+} in the electrostatic binding process. As à result, not all M^{2+} ions are electrostatically bound at low M/L. A fraction of the M^{2+} ions are involved in the proton substitution reaction.

Maximum values of the slope of the proton production curves, $(d[H]/d[M]_a)_m$, in the polarographic M/L-titrations are collected in table 4.5.

A familiar pattern is confirmed by the data tabulated: the maximum slope decreases with increasing α_n, it decreases with $[KNO_3]$, it increases in the series Zn, Cd, Pb, and it is higher for PAA than for PMA. Comparing the values for M/PMA at α_n = 0.20 in the table 4.5 with those at α_n = 0.25 in table 4.2 confirms the influence of added 1:1 salt.

TABLE 4.5 Maximum values of the slope of the proton production curves for M/PMA,PAA systems with 1:1 salt

	$[KNO_3]$ $mol \cdot m^{-3}$	$(d[H]/d[M]_a)_m$		
		α_n = 0.20	0.40	0.60
PMA				
Zn	10	0.022	0.007	0.003
	50	0.017	0.004	0.002
	100	0.012	0.002	0.001
Cd	10	0.040	0.015	0.010
Pb	50	0.190	0.105	0.042
PAA				
Zn	50	0.070	0.043	0.01
Cd	50	0.087	0.078	coag.
Pb	50	0.930	0.830	coag.

4.2.4 Zn, Cd, Pb/mono-, dicarboxylic acids

The intrinsic binding of M (and H) to polymeric acids is often considered to be similar to the binding to the monomeric analogues (*Begala & Strauss*, 1972; *Marinsky*, 1982). In the case of (meth)acrylic polyacids, 2-methylpropanoic (isobutyric) acid (*Travers & Marinsky*, 1974) or ethanoic (acetic) acid (*Jakubowski*, 1975) have been considered as the 'monomers'.

Therefore, the complex formation of Cd, Pb and Zn with a monocarboxylic acid, viz. 2-methylpropanoic acid, and, by way of comparison, the formation of the Cd-complex with a dicarboxylic acid, viz. butanedioic (succinic) acid, have been investigated polarographically. The sample solutions contained 0.50 $mol \cdot m^{-3}$ $M(NO_3)_2$, 10^{+3} $mol \cdot m^{-3}$ KNO_3 and different concentrations of acid. The acids were completely neutralized with KOH, and the pH of the solutions was sufficiently low to prevent metal hydrolysis.

All limiting currents of the single, reversible polarographic waves appeared to be diffusion controlled, in agreement with literature data on several other low molecular mass carboxylic acids used in complexation studies (*Klemencic & Filipović*, 1958; *Yadav et al.*, 1973; *Sharma et al.*, 1978).

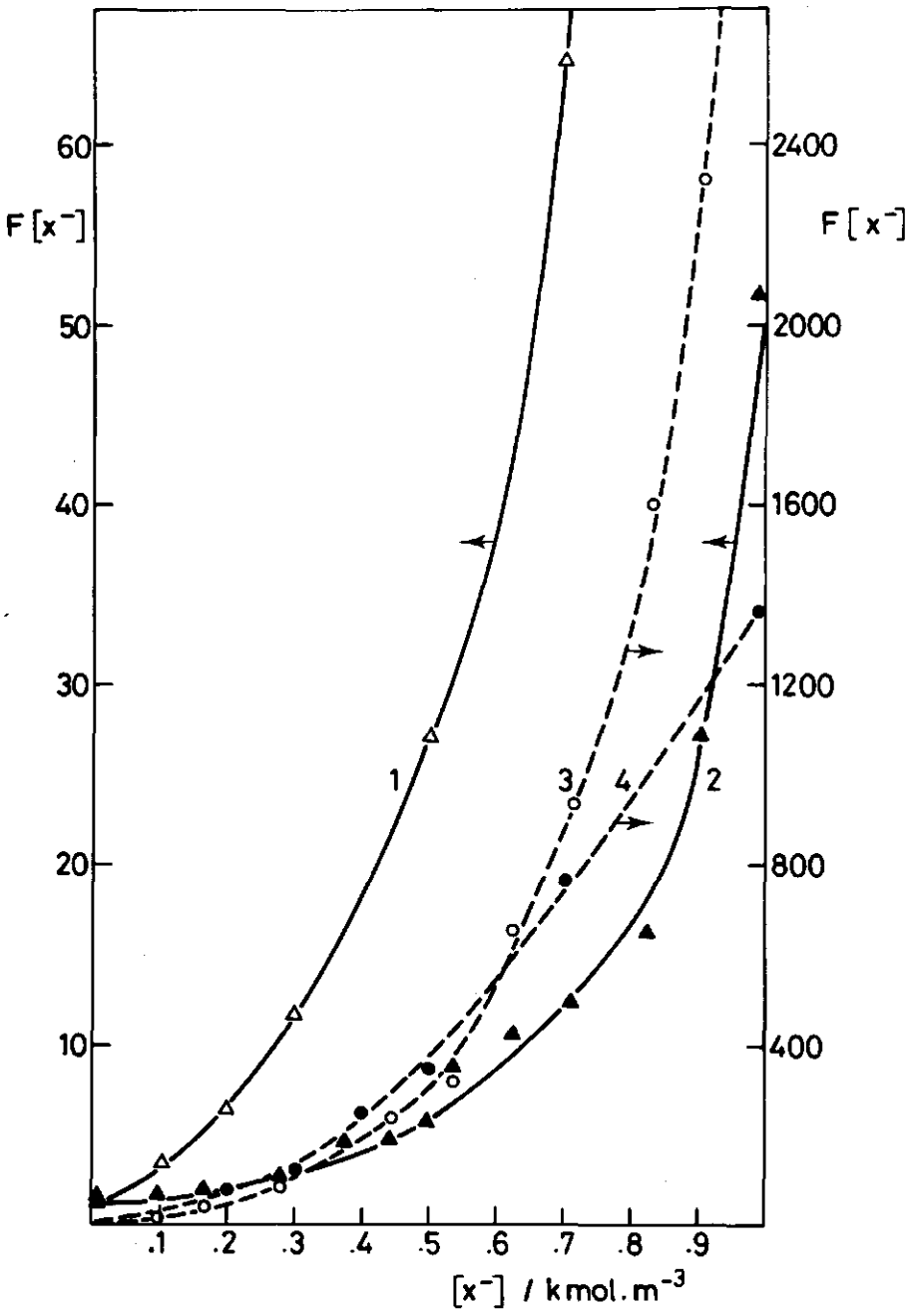

FIGURE 4.20 Initial $F[X^-]$ function, calculated by the method of DeFORD and HUME, for the complexation of 2-methylpropanoic acid with Cd^{2+} (1), Zn^{2+} (2), Pb^{2+} (3), and butanedioic acid with Cd^{2+} (4).

The results were interpreted following the method of *DeFord & Hume* (1951), and graphically analysed by the method of *Leden* (1941). These methods have been discussed in § 3.3.3. In fig. 4.20, the initial $F[X^-]$ curves are presented for the systems investigated. Extrapolation of the $F_n[X^-]$ curves, constructed using the initial $F[X^-]$ curves, to zero carboxylate ion concentration yielded values of the successive formation constants of the metal-complexes. These constants are collected in table 4.6. Values of K_j below 10^2 are based on relatively small shifts of $E_{\frac{1}{2}}$, and consequently the errors may be high, up to about 50% for the smallest K_j. Nevertheless, the orders of magnitude and the mutual differences are correctly represented, even for the weak Zn-complexes.

TABLE 4.6 Successive formation constants K_j of metal-complexes with simple acids

system	K_1	K_2	K_3
Zn/2-methylpropanoic acid	1.2	2.0·10	
Cd/2-methylpropanoic acid	1.6·10	2.9·10	9.6 ·10
Pb/2-methylpropanoic acid	$1.0 \cdot 10^2$	$3.4 \cdot 10^2$	$1.36 \cdot 10^3$
Cd/butanedioic acid	$1.5 \cdot 10^2$	$4.6 \cdot 10^2$	$1.20 \cdot 10^3$

Comparing the values of K_1, for the 2-methylpropanoic acid systems with the provisional values of $K_{int}(ML)$ in table 4.3, it appears that the order of magnitude fits for the M/PMApe and M/PMA systems rather than for the M/PAA systems.

It is noted that the value of K_1 for the binding of Cd^{2+} to a dicarboxylic acid is much larger than that for a monocarboxylic acid.

A number of interesting values of log K_1 and log K_2 of the systems investigated have been recalculated for zero ionic strength, using ionic strength dependencies of the activity coefficients of the metal ions as tabulated by *Robinson & Stokes* (1955). These values and a number of values of log K_j for metal-complex formation and protonation of monocarboxylate ligands, are collected in table 4.7.

Table 4.7 demonstrates that the log K_1 values for the binding of Zn^{2+} are generally low. The trend of decreasing log K_1 in the series Pb, Cu, Cd, Zn, Ba is clear. Moreover, there is a rather crude trend that low values of log K(H) are correlated with low values of log K(M). This trend would agree with the findings in § 4.1.1 - 4.1.3 that

TABLE 4.7 Stability constants for HL, ML and ML_2 complexes of monocarboxylate ligands L. Unless indicated otherwise, the data refer to zero ionic strength, 25°C, and have been cited from SILLÉN & MARTELL (1964)

Acid	log K_j						
	H	Cu	Pb		Cd	Zn	Ba
j =	1	1	1	2	1	1	1
methanoic	3.75	1.98	0.74	1.67[+]	0.48[++]	0.60[*]	0.60
ethanoic	4.76	2.24	2.23	2.88[+]	1.93	1.55[+++]	0.41
propanoic	4.87	2.22	2.34[+]	3.12[+]	2.89	1.01[**]	0.15
butanoic	4.82	2.14	2.28[+]	3.00[+]	-	1.00[**]	0.00
2-methylpropanoic	4.86	2.17	2.60[x]	3.13[x]	1.56[x]	0.39[x]	-
pentanoic	4.86	2.12	2.28[+]	3.18[+]	-	-	0.20
2-dimethylpropanoic	4.78	2.08	2.28[+]	3.18[+]	1.34[***]	-	-

x this study;
+ KLEMENČIĆ & FILIPOVIĆ (1958), I = 1.0 $mol \cdot dm^{-3}$;
++ HERSHENSON ET AL. (1957);
+++ ARCHER & MONK (1964);
* I = 2.0 $mol \cdot dm^{-3}$;
** I = 0.2 $mol \cdot dm^{-3}$;
*** I = 3.0 $mol \cdot dm^{-3}$.

K_{int}(MPMApe) ≤ K_{int}(MPMA) < K_{int}(MPAA). However, the existence of such a trend is not general (*Klemencić & Filipović*, 1958).

The finding that the value of K_1 for Cd/butanedioic acid is higher than that of Cd/2-methylpropanoic acid suggests that the values of the intrinsic binding in metal/polyacid systems may be larger than those for the monomeric acids. More accurate values of K_{int} for the polymer systems will be presented in chapter 5.

4.3 Cd-ISE POTENTIOMETRY

4.3.1 Cd/PMA

The interpretation of polarographic limiting currents of metal/polyion systems in terms of bound fractions of metal ions depends on the kinetics (labile?) of the equilibria involved, and on the mechanism (mass-action?) of the binding reaction, as discussed in chapter 3.

For low M/L, the polarographic lability of the systems investigated could be demonstrated. However, at high M/L, the kinetics of the exchange bound/free metal ions may be hampered due to a more compact polyion conformation. With respect to the mechanism of the binding, application of eq. (3.21) is only allowed if the ratio c_{bound}/c_{free} in

the diffusion layer is approximately the same as in the bulk. This assumption is reasonable for low M/L.

The range of M/L ratios over which application of eq. (3.21) is allowed, was tested with Cd-ISE potentiometry for a number of Cd/PMA systems.

M/L-titrations of Cd/PMA, at two levels of KNO_3 and three values of α_n, yielded the following characteristics:

i There is a strong potentiometric binding of Cd^{2+} with PMA at low M/L.

ii The fraction bound Cd^{2+} is strongly dependent on α_n and c_1.

iii At high M/L, a plateau value of the amount bound was reached for all the Cd/PMA systems investigated. For [PMA] = 2.5 $mol \cdot m^{-3}$ and [KNO_3] = 50 $mol \cdot m^{-3}$, the plateau values were positioned at 0.35 ± 0.03 and 0.45 ± 0.03 bound Cd^{2+} per ligand, at α_n = 0.40 and α_n = 0.60, respectively.

The third result is an important finding because it refers to M/L ratios for which the polarographic results are difficult to interpret.

4.3.2 Comparison with polarographic data

In fig. 4.21, the number of bound Cd^{2+} per ligand L^-, θ_2, determined by different methods, is plotted as a function of the total number of added Cd^{2+} per L^-. The data refer to Cd/PMA at α_n = 0.40. The θ_2 values of curves 1 and 2 have been calculated from polarographic limiting currents. In the case of curve 1, lability was assumed (eq. (3.21)), whereas in the case of curve 2, non-lability was assumed (eq. (3.13) with $c_b^* = 0$). Curve 3 refers to the Cd-ISE potentiometric results (eq. (3.37)).

The 1:1 salt level is lower for the polarographically determined curves, and therefore it may be expected that curves 1 and 2 are positioned at higher θ_2 than curve 3. For low M/L, this is only the case if lability is assumed. However, a plateau value at high M/L is only obtained if non-lability is assumed. Thus, as expected on theoretical basis (see § 3.3.3), eq. (3.21) for labile systems is only valid at low M/L.

At high M/L, the system behaves *as if* it is polarographically non-labile. A gradual change-over from curve 1 to curve 2, at intermediate M/L, would give the best fit with the potentiometric data of curve 3. The non-labile behaviour of the equilibrium at high M/L can be both

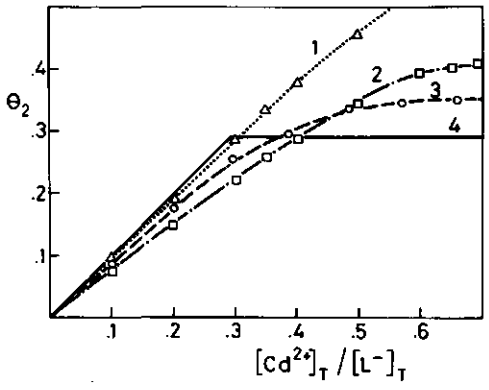

FIGURE 4.21 Values of θ_2 for Cd/PMA at α_n = 0.40, as a function of the number of Cd^{2+} added, per ligand. $[PMA]_i$ = 2.50 mol·m^{-3}. θ_2 is calculated from: (1) polarographic data assuming lability; $[KNO_3]$ = 10 mol·m^{-3}; (2) polarographic data, assuming non-lability; $[KNO_3]$ = 10 mol·m^{-3}; (3) Cd-ISE potentiometric data; $[KNO_3]$ = 50 mol·m^{-3}; (4) the condensation theory, using ξ_{str} = 3.0, assuming 1:1 salt absent.

kinetically and mechanistically explained. As pointed out before (in § 4.2.1) a compact conformation of the metal-polyion complex is expected at high M/L. The polyion 'sphere' is not well-drained, and the diffusion of 'free' metal ions inside the sphere will be affected. Unfortunately, *Cottrell* plots do not elucidate the hampered kinetics, since at intermediate and high M/L the limiting currents are also dependent on reactant adsorption effects. From a mechanistic point of view, it is reasonable to assume that at high M/L, where high θ_2 values occur, the ratio c_b/c_f does not change linearly with the distance to the mercury electrode in the diffusion layer. A decrease in c_f does not result in a approximately proportioned decrease in c_b.

It is concluded from the comparison of potentiometric and polarographic data that only at low M/L the limiting currents can be quantitatively evaluated with eq. (3.21).

Curve 4 in fig. 4.21 represents theoretical values of θ_2 according to te CC model for 1:1 salt-free systems (eq. 2.17). Although the plateau value depends on ξ_{str} selected, it seems that the agreement with experimental data is rather poor for high M/L. This point will be discussed in more detail in § 4.4.2.

4.4 FURTHER DISCUSSION

4.4.1 Coordination numbers

Covalenty bound counterions are attached to specific sites of the polyion. One of the characteristics of the corresponding metal complex

is the coordination number j. As mentioned in § 2.4.1, the occurrence of covalent binding with poly(meth)acrylic acids has been reported for a variety of metal ions. With respect to the systems investigated in the present study, the partially covalent character of the interactions has been sufficiently demonstrated by the proton production curves in § 4.1.1 - 4.1.3.

The assignment of coordination numbers for metal-polyion site-binding is hampered, predominantly by the uncertainty of the apparent acid strength at different degrees of complexation: classical *Bjerrum* and *Scatchard* plots do not work very well. The difficulties in the assignment of values to j are illustrated by the results in the literature for the most widely investigated systems: Cu/PMA and Cu/PAA. For both systems, the predominantly occurring complex has been reported to be: CuL_4 (*Kotliar & Morawetz*, 1955; *Gregor et al.*, 1955a,b), CuL_2 (*Kolawole & Mathieson*, 1977; *Marinsky et al.*, 1973), CuL (*Marinsky*, 1982; *Yamashita et al.*, 1979b).

The value of j is dependent on the spatial positions of the orbitals involved. The reported dependencies of j on the M/L ratio (*Kanedo & Tsuchida*, 1981), on α_n (*Yamashita et al.*, 1979a,b) and on the degree of cross-linking (*Marinsky*, 1982) can be understood in terms of local conformation and flexibility of the polyanion.

For the systems investigated in the present study, the existing literature data for the coordination numbers are contradicting. According to *Bolewski & Lubina* (1970) and *Mandel & Leyte* (1964a), j = 2 for Cd/PMA. *Jakubowski* (1975) and *Travers & Marinsky* (1974) give j = 1 for Zn/PMA, but *Bolewski & Lubina* (1969), *Mandel & Leyte* (1964a) and *Kolawole & Olayemi* (1980) report a j value of 2. For Cd/PAA, j = 1 (at low α_n) according to *Yamashita et al.* (1976), and for Zn/PAA j = 1 has been reported by *Travers & Marinsky* (1974). No values were found in the literature for Pb-containing systems.

Procedure applied

The following procedure has been applied to estimate values of j. The apparent *metal association* constant, $K_{app,j}$ and the apparent *acid dissociation* constant $K_{app,a}$ can be written as (see § 2.2.3 and § 2.3.2):

$$K_{app,j} = K_{int,j} \cdot e^{-2e\psi_s/kT} \quad \text{and} \quad K_{app,a} = K_a \cdot e^{+e\psi_s/kT} \qquad (4.8)$$

In eq. (4.8) it is assumed that $\psi_s(M^{2+}) = \psi_s(H^+)$. The following constants are defined:

$$K_1^* = K_{int,1} \cdot K_a^2 \qquad \text{and } K_2^* = K_{int,2} \cdot K_a^2 \tag{4.9}$$

From eqs (4.8-9) and the definitions of the apparent constants, it follows that:

$$K_1^* = \frac{[M]_b[H]^2}{[M]_f[HL]^2} \cdot [L] \qquad \text{and } K_2^* = \frac{[M]_b[H]^2}{[M]_f[HL]^2} \tag{4.10}$$

With respect to covalently bound metal ions, $[M]_b$ refers to 1:1 binding in K_1^* and to 1:2 binding in K_2^*. Now, B is defined as:

$$B = \frac{[M]_b[H]^2}{[M]_f[HL]^2} \tag{4.11}$$

where $[M]_b$ *refers to the experimentally determined amount of bound* metal ions. Two extreme cases are considered. If only complexes occur with j = 1, then a plot of B versus $[L]^{-1}$ should yield a straight line through the origin. If only complexes exist with j = 2, then B should be independent of $[L]^{-1}$.

In figs 4.22 and 4.23, plots of B versus $[L]^{-1}$ are presented for Zn- and Cd-containing systems, respectively. For curves 1 and 3 in these figures, [L] has been calculated assuming j = 1, whereas for curve 2 and 4, j = 2 has been assumed.

The data used in figs 4.22 and 4.23 originate from polarographic α_n-titrations. Analyses of data from M/L-titrations supported the dependencies shown. The curves demonstrate that for Zn,Cd/poly(meth)acrylic acids the coordination number j = 1 is more probable than j = 2. At high $[L]^{-1}$ there seems to be a tendency that j = 2 may occur in Cd-containing systems.

In the case of Pb-containing systems, the procedure applied did not work. At low $[L]^{-1}$ there is a considerable scatter in the values of B. For high values of $[L]^{-1}$, the trend in values of B suggested j = 1. The association of Pb with PMA and PAA is strong. As a consequence, [Pb] is small, and [H] is relatively large. Changes in these concentrations are difficult to determine sufficiently accurately. For low i_ℓ values, the results are sensitive to the selected value of D_b/D_f.

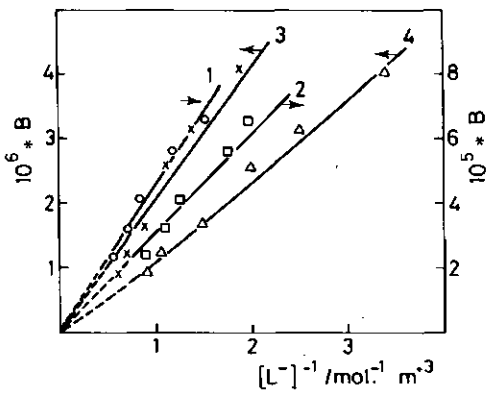

FIGURE 4.22 B, defined in eq. (4.11) as a function of $[L^-]^{-1}$, for Zn/PAA, assuming j = 1 (1); j = 2 (2), and for Zn/PMA, assuming j = 1 (3); j = 2 (4).

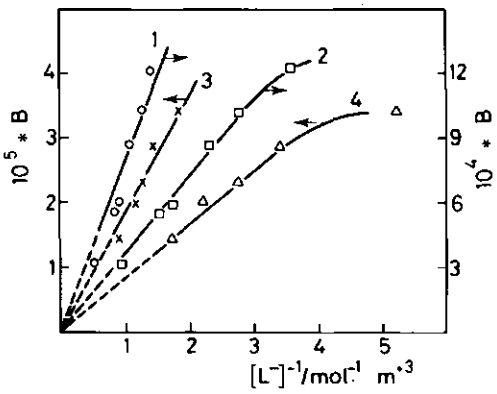

FIGURE 4.23 B, defined in eq. (4.11) as a function of $[L^-]^{-1}$, for Cd/PAA, assuming j = 1 (1); j = 2 (2), and for Cd/PMA, assuming j = 1 (3); j = 2 (4).

Moreover, Pb-containing systems tend to coagulate. Recent data for the (strong) interaction of Cu^{2+} with PMA and PAA yielded j = 1 (*Slota*, 1979; *Yamashita et al.*, 1979a,b; *Marinsky*, 1982). *Slota* (1979) used for Cu/PMA the same procedure as applied in the present work. Against the background of these data and our findings at high $[L]^{-1}$, we will provisionally set j = 1 for Pb/PMA,PAA.

It has been pointed out by *Marinsky* (1976) that for metal/polyelectrolyte systems, the frequently employed method of *Gregor* (see § 2.3.2) very often erroneously yields j = 2. The procedure applied in this work tends to favour j = 1. The procedure is based on independent chances for each ligand to meet a metal ion. Obviously, this is a crude assumption. Bidentate complex formation, in which possibly *neighbouring* ligands are involved, would be better described by using dimer concentrations $[L_2]$ instead of $[L]^2$, since the formation of the second bond is determined by the chance to establish the first bond, rather than the chance to meet a second independent ligand. If a dimer-mechanism controls the formation of ML_2, then the procedure applied would still yield j = 1. Nevertheless, if ML_2 is formed through dimer ligand groups, j = 1 would express the equilibrium mechanism better than j = 2.

In addition, a rather different argument advocates j = 1. Bidentate complex formation through dimers, in PAA- and PMA-containing

systems, would imply the formation of 8-membered rings, which are improbable.

4.4.2 Influence degree of binding

Henderson-Hasselbalch analysis

To demonstrate the dependency of the apparent metal association constant on M/L, polarographically determined M/L-titration data will be analysed using the *Henderson-Hasselbalch* (HH) formula. The HH-equation, usually applied to protolytic equilibria, see § 2.3.2, is the logarithmic form of the equation for the apparent equilibrium constant involved. In the present case of 1:1 metal ion binding by polyacid ligands:

$$pM = \log K_{app,1} + \log \frac{[L]}{[ML]} \qquad (4.12)$$

where L represents a free ligand and ML a bound metal ion. A modification of the HH-equation, often applied for polyacid systems, is:

$$pM = \log K_{av} + m \cdot \log \frac{[L]}{[ML]} \qquad (4.13)$$

where K_{av} is some 'average' association constant, and m an interaction parameter. For a number of protolytic equilibria of polyacids, such as H/PMA and H/PAA, the factor m appeared to be a constant larger than unity, if α_d is not too far from a value of 0.5 (*Katchalsky & Spitnik*, 1947). The magnitude of m is believed to depend on all factors (except for the degree of counterion binding) that control the electrostatic interaction, for instance ξ_{str}, α_n, c_1. It is noted that these factors also affect K_{av}.

In M/L-titrations at given ξ_{str}, α_n and c_1, the magnitude of m will be mainly related to the change in effective charge density of the polyion upon binding of counterions. Alternatively, m expresses the cooperativity of the ligands in counterion binding.

In fig. 4.24, pM is plotted versus log ([L]/[ML]) for Pb,Cd,Zn/PAA, PMA at α_n = 0.40. For not too low M/L, the curves are approximately linear, showing different values of K_{av} and m for the linear parts. In table 4.8, the values of m and log K_{av} of the curves are collected. From the tabulated values of m, it appears that these are larger than unity. This demonstrates the cooperativity of the binding sites: if an added metal ion has been bound, the effective charge density of the

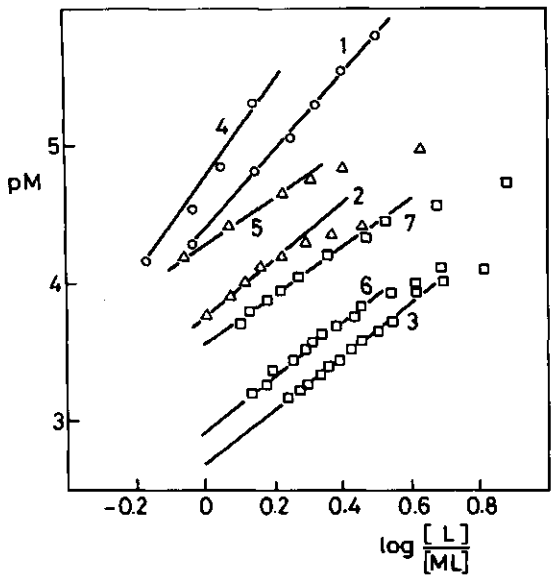

FIGURE 4.24 pM as a function of log ([L]/[ML]), at α_n = 0.40 for M/PAA: Pb^{2+} (1); Cd^{2+} (2); Zn^{2+} (3); and for M/PMA: Pb^{2+} (4); Cd^{2+} (5); Zn^{2+} (6,7); $[KNO_3]$ = 50 $mol \cdot m^{-3}$, except for Cd/PMA (5) and Zn/PMA (7): $[KNO_3]$ = 10 $mol \cdot m^{-3}$.

TABLE 4.8 Values of m and log K_{av} for Pb,Cd,Zn/PAA,PMA systems at α_n = 0.40 from polarographic M/L-titration data.

system	curve	$[KNO_3]$ $mol \cdot m^{-3}$	m	log K_{av}
PAA				
Pb	1	50	2.89	4.40
Cd	2	50	2.14	3.77
Zn	3	50	1.94	2.70
PMA				
Pb	4	50	3.57	4.77
Cd	5	10	1.72	4.28
Zn	6	50	2.00	2.90
Zn	7	10	1.69	3.58

polyion is diminished and a subsequently added metal ion will be bound less firmly.

At comparable levels of $[KNO_3]$, K_{av} and m increase in the series Zn < Cd < Pb. Apparently, a large covalent character of the metal/polyion interaction yields a more effective decrease of the effective charge density of the polyion. Comparing Pb,Zn/PMA with Pb,Zn/PAA, it appears that m and log K_{av} are somewhat larger for the PMA systems. This is possibly due to the slightly larger values of ξ in the case of

PMA as a result of the more compact conformation, as compared to PAA. This finding is not in contradiction with the result in § 4.1.3 that the intrinsic constants are larger for M/PAA than for M/PMA: K_{int} refers to the absence of an effective electric potential. For different 1:1 salt levels, m appears to increase with c_1, whereas log K_{av} shows the reverse dependence, at $\alpha_n = 0.40$. It is noted that at higher α_n values, different dependencies have been observed. Apparently, the 1:1 salt level affects both log K_{av} and log $\frac{[L]}{[ML]}$ in an α_n-dependent way. Effects of 1:1 salt are further discussed in chapter 6.

Electrostatic theories

From the analysis of the polarographic M/L-titration data using the empirical modified HH-equation, it is evident that for metal/polycarboxylic acid systems with added 1:1 salt, the binding parameters depend on the nature of the counterions, in contrast to the results for the salt-free systems at low M/L. Any ion specificity is not provided in purely electrostatic theories, such as the CC and the PB theory. Therefore, the best systems in this study to consider against the background of the electrostatic theories will be the Zn-containing systems, for which the covalent character is relatively low.

As pointed out in chapter 2, the CC model gives explicit expressions that relate the degrees of counterion condensation θ_1 and θ_2 to the concentrations of free monovalent and divalent metal ions c_1 and c_2. According to *Manning* (1978b), the following expressions are applicable to the electrostatic binding of metal ions with linear polyelectrolytes in dilute systems with relative excess of 1:1 salt:

$$\frac{\theta_2}{c_2} = \frac{e}{V_p} \cdot \frac{\theta_1^2}{c_1^2} \qquad (4.14)$$

$$\ln \frac{e \cdot \theta_1}{V_p \cdot c_1} = -2 \cdot \xi \cdot (1 - \theta_1 - 2 \cdot \theta_2) \cdot \ln (1 - e^{-\kappa b}) \qquad (4.15)$$

and:

$$V_p = e \cdot (1 - \xi^{-1})(\kappa b)^2 \cdot c_1^{-1} \qquad (4.16)$$

where e is the base number of the natural logarithm, and all other symbols have their usual meaning, previously introduced. The l.h.s. of eq. (4.14) is identified by *Manning* (1978b) as an 'association constant': $K_M = \theta_2/c_2$.

In fig. 4.25, theoretical values of K_M, calculated using eqs (4.14-16) are plotted (solid curves) as a function of θ_2 for c_1 = 50 mol·m^{-3}

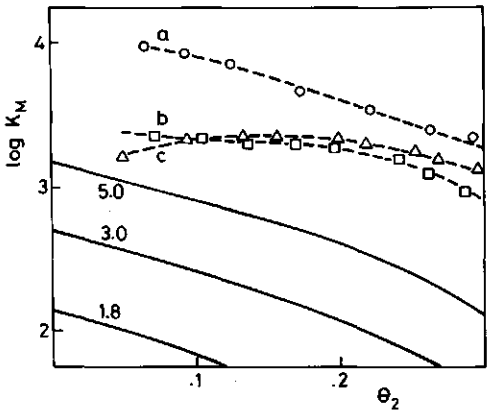

FIGURE 4.25 The dependency of log K_M on θ_2. Experimental values for Zn/PAA, α_n = 0.60 (a); Zn/PAA, α_n = 0.40 (b); and Zn/PMA, α_n = 0.4 (c). Solid lines: values according to MANNING (1978b) for ξ = 1.8, ξ = 3.0 and ξ = 5.0.

and different values of ξ. The theoretical curves show the decrease of log K_M with θ_2. In the CC model, this behaviour is explained by the decreasing gain in entropy with increasing θ_2 for the exchange of bound monovalent ions against divalent ions. Fig. 4.25 also contains experimental values of log K_M for Zn/PAA,PMA.

In the case of acrylic polyacids with α_n = 0.60, the theoretical value of ξ is 1.8. Comparing the theoretical and experimental curves of log K_M, it is evident that the predicted value are too low by about two orders of magnitude. Even if the value of ξ would be twice that calculated from ξ_{str}, as suggested by *Liquori et al.* (1959) for PAA, there remains one order of magnitude difference. *Meurer et al.* (1982) also noticed discrepancies between the experimental and predicted values of the amount of metal ions bound in Mn/PAA systems. On the other hand, data for Mg/dextran sulphate appeared to be well-predicted by eqs (4.14-16) (*Mattai & Kwak*, 1982).

The comparisons of the theoretical and experimental data suggest that covalent features of the systems, though small, have a great influence on the value of K_M. The introduction of any specificity in the CC model would imply an adjustment of V_p (*Manning*, 1977b), since the average distance separating a bound counterion and the polyion will decrease if additional short range interaction occurs. As a consequence, the radius of the condensation volume correspondingly decreases. From measurements of the relaxation rate of ^{23}Na in PAA sys-

tems, by *Kielman et al.* (1976), it appeared that the average distance separating bound Na^+ and the polyacrylate ion is about 0.5 nm, whereas the radius R_M of the cylindrical condensation volume V_p is much larger. The value of log K_M is sensitive to the value of R_M. Using, as a crude approximation, a value of 0.5 nm instead of 1.65 nm (ξ = 1.8) for R_M, the theoretical value of log K_M increases by a full order of magnitude.

A different argument that would account for the discrepancy between the theoretical and experimental values of K_M is the dependency of R_M on c_1. According to *Manning* (1978b), R_M is rather insensitive to c_1, whereas according to *LeBret & Zimm* (1984), R_M decreases with increasing c_1. The latter authors, using a Monte Carlo method to determine counterion distributions around polyions, found evidence that supports the predicted values of θ_2. However, the condensation volume was found to decrease with increasing c_1.

Apart from the demonstrated inapplicability of the CC model to predict log K_M for systems with some covalent character, the dependency of log K_M on θ_2 appears to be reasonably fitting for Zn/PAA (curves a and b in fig. 4.25). The decrease of log K_M with θ_2 can be considered as an expression of the cooperativity of the ligands. For Zn/PMA (curve c) the decrease in log K_M is somewhat less pronounced as compared to Zn/PAA. This is attributed to a gradual conformation change of PMA upon binding of Zn^{2+}. In that case, ξ_{eff} remains approximately constant over a range of θ_2 values.

In the PB model by *Guéron & Weisbuch* (1980), no 'association' constant or degree of 'association' is provided. The metal ions accumulated around the polyion are considered to be 'free and mobile'. The experimental results cannot be compared quantitatively with theoretical values of CIV_2. At low M/L, CIV_2 increases approximately linearly with the M/L ratio, whereas at intermediate M/L, the increase is less (*Meurer et al.*, 1982). This implies that if CIV_2 is considered as a measure of the electrostatically bound ions, the ratio CIV_2/c_2 decreases with M/L. This corresponds qualitatively with the change of K_M with θ_2.

Any ion-specificity in the PB model can be introduced by adjusting the charge density of the polyion, if uncharged covalent complexes occur. As a crude approximation, *Guéron & Weisbuch* (1980) suggest, considering the mass-action law for the local equilibrium concentrations:

$$K_{int} = \frac{[ML_{int}]}{CIV_2 \cdot [L]} \qquad (4.17)$$

Due to some covalent binding, the charge density of the polyion is reduced to a fraction y. CIV_2 is proportional to y^2, and $[ML_{int}]/[L]$ can be approximated by $(1-y)/y$ (*Guéron & Weisbuch*, 1980). Even for low values of K_{int}, the charge density is substantially affected by site-binding. For example, for a given system M/PMA (α_n = 0.60, c_1 = 50 $mol \cdot m^{-3}$ and c_2 = 1 $mol \cdot m^{-3}$), CIV_2 = 0.365 $mol \cdot dm^{-3}$ and CIV_1 = 0.955 $mol \cdot dm^{-3}$, according to the calculation scheme of *Weisbuch & Guéron* (1981). If an intrinsic binding constant of unity is assumed, the value of y in this example is 0.8. In other words, CIV_2 is reduced by about 36% as a result of the small covalent binding constant.

Apparently, covalent binding rapidly affects the purely electrostatic models, both CC and PB. Therefore, in many practical cases, it will be necessary to consider these models in combination with a covalent binding scheme, e.g. as indicated in § 2.2.3.

5 INFLUENCE DEGREE OF NEUTRALIZATION

5.1 CONDUCTOMETRY & POTENTIOMETRY

The conductometric α_n-titrations have been carried out by adding aliquots of a KOH solution of 100.0 mol·m^{-3} to a PAA or PMApe solution of about 2.5 mol·m^{-3} (exact data in figure legends) in which a fixed amount of metal nitrate was present. The conductometric as well as the pH-potentiometric responses have been determined. The results are presented by plots of pH versus α_n and/or pK_{app} versus α_d, and by plots of the change of the conductivity $\Delta\kappa$ versus α_n. The corresponding plots for the (divalent) metal-free solutions of the polyacids are given for comparison.

5.1.1 Acid strength

In fig. 5.1, curve 1 represents $pK_{app,a}$ of the metal-free PAA solution. The curve is slightly convex, the convexity decreases with increasing α_d. In the presence of 1.19 mol·m^{-3} KNO_3, corresponding to $[K^+]/[PAA] = 0.5$ (curve 2), the initial slope is diminished, and the values of $pK_{app,a}$ are lower. The features observed agree with the theoretical and experimental findings for PAA by *Nagasawa et al.* (1965). At a KNO_3 level of ~50 mol·m^{-3}, the curve (no 3) is concave at low α_d, whereas it is linear at high α_d. The slope of the linear part is approximately the same as in curves 1 and 2 at high α_d: $dpK_{app,a}/d\alpha_d \cong 2.5$.

In the presence of an amount of $Cd(NO_3)_2$ corresponding to $[Cd^{2+}]/[PAA] = 0.20$, the sample with ~50 mol·m^{-3} KNO_3 yielded curve 4. It appears that due to the presence of cadmium ions, the form of curve 4 is substantially different from that of curve 3, up to charge neutralization by Cd^{2+} at $\alpha_d \cong 0.4$. This reflects association of Cd^{2+} with the carboxylate groups of PAA. The apparent 'acid' strength parameter pK_{app} is much lower than for the divalent metal-free sample solution. These features, form of the curves of pK_{app} versus α_d, and the magnitude of the decrease with respect to $pK_{app,a}$ will be further investigated, qualitatively in § 5.1.3-4, and quantitatively in § 5.3.2.

The four curves, extrapolated to $\alpha_d = 0$, merge at the same limiting (intrinsic) value: $pK_a = 4.72$.

In fig. 5.2, the independency of $pK_{app,a}$ of the molecular mass is demonstrated for salt-free solutions of PAA of 10.40 mol·m^{-3}. The

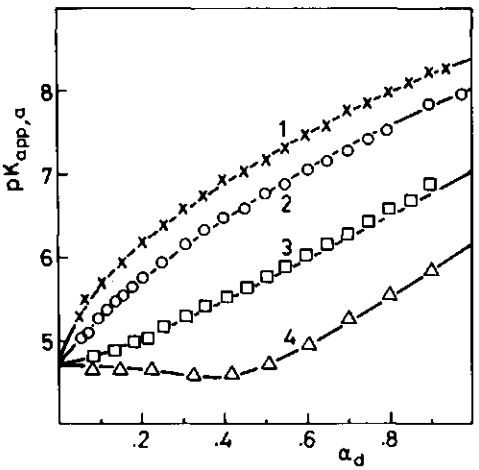

FIGURE 5.1 Dependence of $pK_{app,a}$ on α_d for PAA. [PAA] = 2.38 mol·m^{-3}. $\bar{M}$ = 300,000. 1. no salt; 2. $[K^+]$ = 1.19 mol·m^{-3}; 3. $[K^+]$ = 47.6 mol·m^{-3}; 4. $[K^+]$ = 47.6 mol·m^{-3} and $[Cd^{2+}]$ = 0.50 mol·m^{-3}

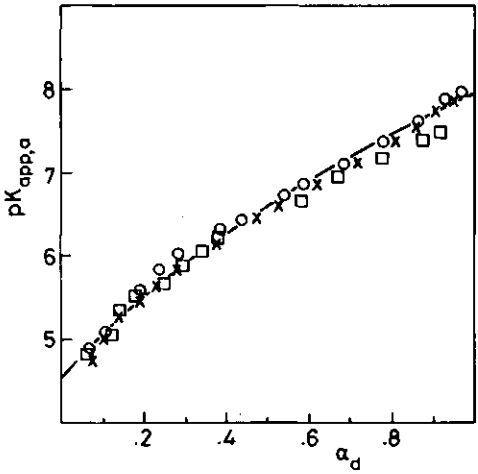

FIGURE 5.2 Dependence of $pK_{app,a}$ on α_d for different molecular mass samples of PAA. [PAA] = 10.40 mol·m^{-3}. $\bar{M}$ = 50,000, 150,000, 300,000. No salt added.

curves for samples of different molecular mass, viz. 50,000, 150,000 and 300,000, coincide. Additionally, the comparison of fig. 5.2 with curve 1 in fig. 5.1 demonstrates that the polyacid concentration markedly influences $pK_{app,a}$: at a four-fold increase in c_p, $pK_{app,a}$ decreases by log 4, on the average. Measurements at the 50 mol·m^{-3} KNO_3 level (not in figure) yielded the same independency of $pK_{app,a}$ of the molecular mass. All further results in this section 5.1 with respect to PAA, refer to $\bar{M}$ = 300,000.

In fig. 5.3, curves 1 and 2 refer to salt-free PMApe and PMA solutions, respectively. The initial steep rise of $pK_{app,a}$ is attributed to the relatively strong increase of electrostatic effects with increasing α_d for the compact conformations which are adopted at low α_d (*Leyte & Mandel*, 1964). In PMApe, more hydrophobic methyl groups are present per $-COO^-$ group than in PMA: the effect of the conformational transition is then more pronounced than in PMA. However, at high α_d, the average distance separating the $-COO^-$ groups is larger for PMApe, and the value of $pK_{app,a}$ is lower than for PMA, under comparable conditions.

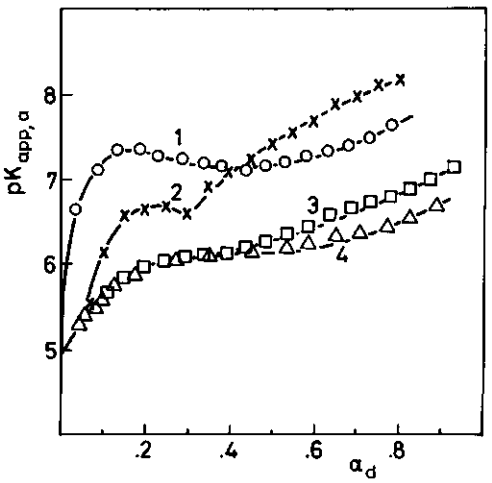

FIGURE 5.3 Dependence of $pK_{app,a}$ on α_d for PMApe and PMA. 1. [PMApe] = 2.38 $mol \cdot m^{-3}$, no salt; 2. [PMA] = 2.50 $mol \cdot m^{-3}$, no salt; 3. [PMA] = 2.54 $mol \cdot m^{-3}$, $[K^+]$ = 50.0 $mol \cdot m^{-3}$; 4. [PMA] = 2.56 $mol \cdot m^{-3}$, $[K^+]$ = 50.0 $mol \cdot m^{-3}$, $Ba(OH)_2$ used as the titrant.

Curves 3 and 4 refer to PMA in the presence of 50 $mol \cdot m^{-3}$ KNO_3. Moreover, for curve 4, $Ba(OH)_2$ was used as the titrant. Values of $pK_{app,a}$ are lower than in curve 2, and that decrease is more pronounced using $Ba(OH)_2$. In addition, the transition region is broadened in the salt-containing systems, in agreement with the results of *Nagasawa et al.* (1965) and *Crescenzi et al.* (1972). From extrapolation to $\alpha_d = 0$, pK_a(PMApe) and pK_a(PMA) are estimated to be 5.3 and 4.85, respectively.

5.1.2 K,Ba/PAA

The influence of the degree of neutralization on the conductometric and pH-potentiometric response is first investigated for K/PAA and Ba/PAA since these systems do not show substantial covalency. The main differences with systems in which covalent contribution to the binding is important, are indicated.

K/PAA

Fig. 5.4 gives the pH as a function of α_n. Curves 1-3 refer to the same samples as curves 1-3 in fig. 5.1: KOH was the titrant, and different levels of KNO_3 were applied. Indeed, the same features can be observed: the convexity of the curves decreases both with increasing α_n and increasing $[K^+]/[PAA]$, and the apparent acid strength increases with added salt.

Curve 4 refers to a solution of PAA in the presence of equimolar amounts of Pb and Zn, corresponding to $[M^{2+}]_T/[PAA] = 0.2$. This curve

shows some important differences with curves 1-3:

i At low α_n, the values of the pH are very low, and the curve is strongly concave.

ii At about $\alpha_n = 0.4$, where $[M^{2+}]_T \cong 2 \cdot [L^-]_T$, the value of the slope increases abruptly.

iii At high α_n, the slope is larger than for the curves 1-3.

Obviously, these differences are due to the presence of Pb and Zn. The features of curve 4 suggest (i) binding of M^{2+}, (ii) completion of the binding at charge neutralization, and (iii) a diminishing of the effective number of L^- due to (covalent) complex formation. Further evidence for these suggestions will be obtained from the conductometric responses.

In fig. 5.5, the change in the conductivity $\Delta\kappa$ of the same samples

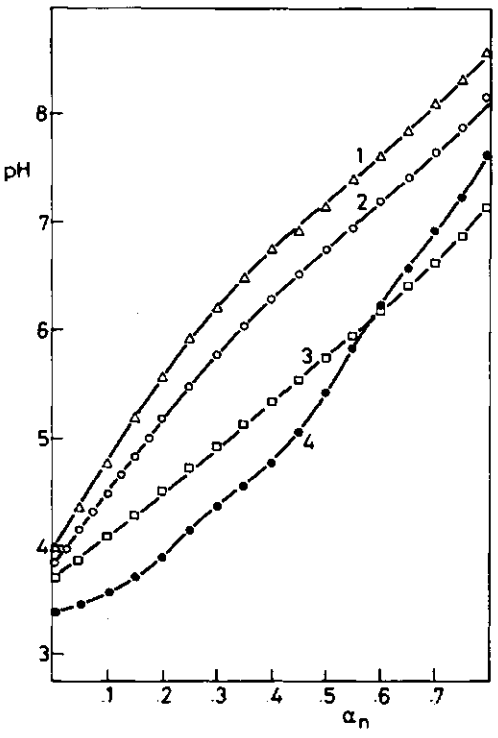

FIGURE 5.4 Dependence of the pH on α_n PAA. [PAA] = 2.38 mol·m^{-3}. 1. no salt; 2. [K^+] = 1.19 mol·m^{-3}; 3. [K^+] = 47.6 mol·m^{-3}; 4. [Pb^{2+}] = [Zn^{2+}] = 0.238

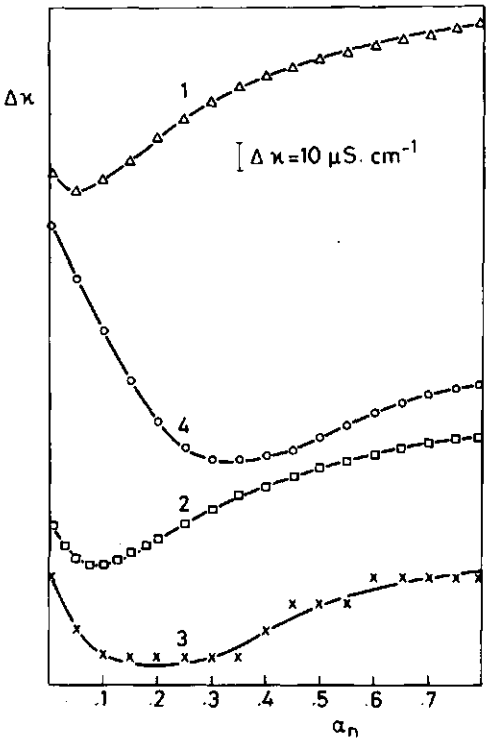

FIGURE 5.5 The conductivity difference $\Delta\kappa$ as a function of α_n for PAA. [PAA] = 2.38 mol·m^{-3}. 1. no salt; 2. [K^+]/[PAA] = 0.5; 3. [K^+]/[PAA] = 20; 4. [Pb^{2+} + Zn^{2+}]/[PAA] = 0.2

as in fig. 5.4 is presented as a function of α_n. The curves in fig. 5.5 consist of a descending and a rising branch. In the latter, a flattening of the curves is observed at high α_n. The position of the minimum appears to be dependent on the sample composition. In table 5.1, the values of the conductivity of the solution κ_s at $\alpha_n = 0.0$ and $\alpha_n = 0.9$ are given.

TABLE 5.1 Conductivities for the samples of fig. 5.5 at $\alpha_n = 0.0$ and $\alpha_n = 0.9$. Conditions: see figure legend.

No	$M(NO_3)_n$	$\frac{[M]}{[PAA]}$	$\kappa_s/\mu S \cdot cm^{-1}$	
			$\alpha_n = 0.0$	$\alpha_n = 0.9$
1	-	0.0	33.0	95.5
2	KNO_3	0.5	208	247
3	KNO_3	20	5540	5540
4	$Pb(NO_3)_2 + Zn(NO_3)_2$	0.2	232	174

The initial parts of the curves 1-3 represent predominantly the neutralization of (autodissociated) H^+ by added KOH (*Rinando & Daune*, 1967), corresponding with:

$$H^+ + L^- + K^+ + OH^- \longrightarrow H_2O + L^- + K^+ \qquad (5.1)$$

At not too high α_n (low charge density, low [OH]), where alkali metal cations are not conductometrically bound (see § 4.1.1-3), $\Delta\kappa$ for the salt-free sample (curve 1) can be expressed as:

$$\Delta\kappa = \lambda_H \cdot [H] + \lambda_p \cdot [L] + \lambda_K \cdot [K] - \kappa_s(\alpha_n = 0) \qquad (5.2)$$

where the concentrations refer to the conductometrically free species, and $\kappa_s(\alpha_n = 0)$ to the initial conductivity of the solution. The decrease in $\Delta\kappa$ is due to the decrease in [H], since both [L] and [K] increase as the α_n-titration proceeds. The concentrations in eq. (5.2) can be expressed in terms of α_d or α_n:

$$[H] = \frac{1-\alpha_d}{\alpha_d} \cdot K_{app,a}; \quad [L] = \alpha_d \cdot [PAA]; \quad [K] = \alpha_n \cdot [PAA] \qquad (5.3)$$

The position of the minimum corresponds to

$$d(\Delta\kappa)/d\alpha_n = 0 \qquad (5.4)$$

The combination of eqs (5.2), (5.3) and (5.4) with the approximation that in the minimum $\alpha_d \cong \alpha_n$ would yield, in a general form:

$$\alpha_n^2(\text{minimum}) \cong \frac{\lambda_H \cdot K_{app,a}}{(\lambda_p + \lambda_K) \cdot c_p} \qquad (5.5)$$

if $K_{app,a}$ were a constant. However, in the case of weak polyacids, $K_{app,a}$ is a function of α_n, so that the position of the minimum only gives an impression of the apparent acid strength. For a given acid, a change in the position of the minimum with changing sample composition reflects a change of the apparent acid strength.

For the systems with added KNO_3 (curves 2 and 3) the conductivity of the solution κ_s will be higher than for the salt-free solution. If no binding of K^+ ions occurs, eq. (5.5) remains qualitatively applicable. For increasing KNO_3 levels, the minimum in fig. 5.5 shifts to higher values of α_n, due to the screening which enlarges $K_{app,a}$. Simultaneously, κ_s increases with increasing 1:1 salt level. At low α_n, this increase is higher than at high α_n, due to the large amount of H^+ released at low α_n as a result of the screening. Ultimately, a very large amount of added 1:1 salt would result in a linear decrease of κ_s with increasing α_n, as found for strong (poly)acids, such as PSS (*Nagasawa*, 1974).

In the presence of divalent metal ions, the shift of the minimum (curve 4) is pronounced, even at low $[M^{2+}]/[PAA]$. Apparently, in this case screening is substantial due to (specific) counterion binding.

For $\alpha_n >> \alpha_n(\text{minimum})$, where H^+ ions no longer contribute measurably to κ_s, the conductivity difference $\Delta\kappa$ in curve 1 can be expressed as:

$$\Delta\kappa = \lambda_p \cdot [L] + \lambda_K' \cdot [K] - \kappa_s(\alpha_n = 0) \qquad (5.6)$$

where λ_K' refers to the ionic conductivity of the conductometrically free K^+ ions in the salt-free system. Although the analytical concentrations of L^- and K^+ increase linearly with increasing α_n, it appears from curve 1 in fig. 5.5 that $\Delta\kappa$ does not: the flattening of the curve demonstrates binding of K^+ and/or a decrease in λ_K'. The curve of the

conductivity becomes almost horizontal at $\alpha_n \cong 1$, see for example fig. 3.4. This suggests that binding of K^+ occurs. For $\alpha_n >> \alpha_n$(minimum), the neutralization reaction must be represented by:

$$LH + K^+ + OH^- \rightarrow L^-(K^+)_{\theta_1} + (1 - \theta_1) \cdot K^+ + H_2O \qquad (5.7)$$

where θ_1 is the number of K^+ bound per L^-. Using $[L] = [K] = (1 - \theta_1) \cdot \alpha_n \cdot [PAA]$, applying the concept of conductometric binding as elaborated in § 3.5.1, the conductivity difference for $\alpha_n >> \alpha_n$(minimum) is given by:

$$\Delta\kappa = (1 - \theta_1) \cdot \alpha_n \cdot [PAA] \cdot (\lambda_p + \lambda'_K) - \kappa_s(\alpha_n = 0) \qquad (5.8)$$

Comparing eq. (5.8) with curve 1 in fig. 5.5, it is suggested that θ_1 increases with α_n. The departure from linearity starts at about $\alpha_n = 0.35$.

Curve 2 of fig. 5.5 shows the same pattern as curve 1. However, $d(\Delta\kappa)/d\alpha_n$ is somewhat smaller for high α_n, because λ_p decreases with increasing 1:1 salt concentration (*van der Drift*, 1975). Even at a twenty-fold excess of KNO_3, in curve 3, where $\lambda'_K \cong \lambda_K$, a flattening of $\Delta\kappa$ is observed at high α_n, demonstrating conductometric binding of K^+. At this 1:1 salt level, the sensitivity of the conductometer to $\Delta\kappa$ is poor.

Against the background of curves 1-3, interesting observations can be made in curve 4:

i The decrease in $\Delta\kappa$ is almost linear up to about $\alpha_n = 0.2$. In § 4.1.3 it was concluded that Pb binds much stronger to PAA than Zn. It is reasonable to assume that the neutralization of H^+, released as a result of the binding of Pb, is responsible for the initial decrease in $\Delta\kappa$

ii The centre of the broad minimum is shifted to $\alpha_n \cong 0.35$, suggesting that the interaction with Zn takes place in the range $0.2 < \alpha_n < 0.4$.

iii The almost linear increase in $\Delta\kappa$ in the range $0.4 < \alpha_n < 0.6$ reflects further charging of the polyion without simultaneous binding of counterions.

iv The deviation from linearity for $\alpha_n > 0.6$ indicates conductometric binding of K^+. Due to the presence of (bound) Pb^{2+} and Zn^{2+}, the binding of K^+ has been shifted to larger values of α_n, as compared to the M^{2+}-free solution. This observation demonstrates the exis-

tence of a particular value of the effective charge density for the binding of monovalent counterions.

In curve 4, the consecutive binding of Pb^{2+}, Zn^{2+} and - after further polyacid charging - K^+, is remarkably manifest.

Ba/PAA

In figs 5.6 and 5.7, pH and $\Delta\kappa$ are plotted versus α_n for PAA in the presence of Ba^{2+}. For comparison, the Ba^{2+}-free curves are also given.

The interaction of Ba^{2+} with $-COO^-$ groups is almost purely electrostatic (*Rinaud & Milas*, 1970), as was concluded also in § 4.1.3. According to *Schwartz & François* (1981) Ba^{2+} remains hydrated in the $Ba^{2+}/-COO^-$ interaction. Thus Ba^{2+} can be considered as a model cation for electrostatic interaction.

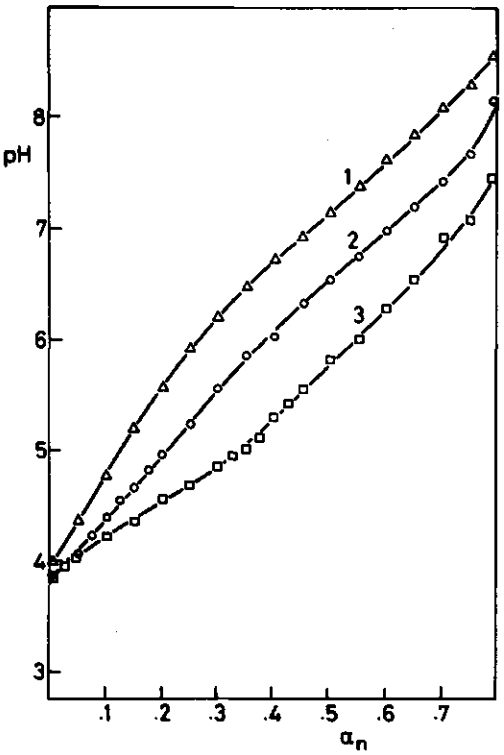

FIGURE 5.6 Dependence of the pH on α_n for Ba/PAA. [PAA] = 2.38 mol·m^{-3}. 1. no salt; 2. [Ba^{2+}] = 0.119 mol·m^{-3}; 3. [Ba^{2+}] = 0.469 mol·m^{-3}.

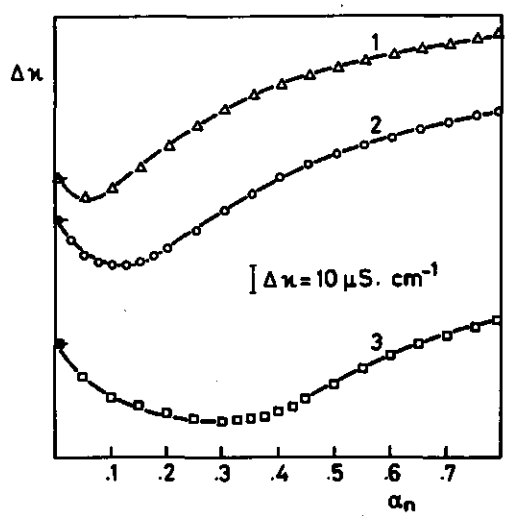

FIGURE 5.7 The conductivity difference $\Delta\kappa$ as a function of α_n for Ba/PAA. [PAA] = 2.38 mol·m^{-3}. [Ba^{2+}]/[PAA] = 0.00 (1); 0.05 (2); 0.20 (3).

The pH curves 2 and 3 can be viewed as being shifted to the right, in comparison with curve 1. For low and intermediate values of α_n, the shifts are approximately proportional to the ratios $[Ba^{2+}]/[PAA]$.

In fig. 5.7, the conductivity curves reveal almost the same features as discussed for fig. 5.5: a broadening and a shift of the minimum, and the shift of the K^+ binding to larger α_n. However, the initial decrease in $\Delta\kappa$ does not show the linearity as in curve 4 of fig. 5.5. Apparently, the stronger interaction Pb/PAA, as compared to Ba/PAA, caused the linearity, as was previously assumed.

The values of κ_s at $\alpha_n = 0.0$ and $\alpha_n = 0.9$ are 72.4 and 120 $\mu S \cdot cm^{-1}$, respectively, for $[Ba^{2+}]/[PAA] = 0.05$. For $[Ba^{2+}]/[PAA] = 0.20$, the values of κ_s are 170 and 183 $\mu S \cdot cm^{-1}$, respectively. Compared to the values for $[Pb^{2+} + Zn^{2+}]/[PAA] = 0.20$, the value at $\alpha_n = 0.0$ is lower: due to the binding of Pb^{2+}, more H^+ is released. However, the value at $\alpha_n = 0.9$ is larger: due to the (stronger) binding of Pb^{2+} (and Zn^{2+}) less M^{2+} ions and less $-COO^-$ groups contribute to the conductivity.

5.1.3 Zn, Cd, Pb/PAA

Zn/PAA

In fig. 5.8, the pH is plotted versus α_n for PAA in the presence of different levels of $Zn(NO_3)_2$. The curves are similar to those for added $Ba(NO_3)_2$ in fig. 5.6. However, for corresponding values of the ratio $[M^{2+}]/[PAA]$ and α_n, the decrease in pH, as compared to the M^{2+}-free system, is somewhat larger, as expected. Closer inspection of the curves reveals that at low α_n, the curves are slightly convex, and that at high α_n, they are almost parallel.

Representation of the data in the form of a plot of pK_{app} versus α_d (in fig. 5.9) demonstrates the features more pronouncedly. The value of pK_{app} (which refers to the apparent 'acid' strength of the polyacid in the *presence* of heavy metal ions) is calculated in the same way as $pK_{app,a}$ for the heavy metal-free systems, according to eq. (2.21). It appears that at low α_d, pK_{app} increases with α_d, and that the increase is levelling off from about $\alpha_d = 0.15$. The four curves merge at the same limiting value at $\alpha_d = 0$, corresponding to $pK_a = 4.72$. All values of pK_{app} pictured are higher than 4.72. These observations point at the predominantly electrostatic nature of the Zn/PAA interaction. At values of α_d sufficiently higher than $2 \cdot [Zn^{2+}]/[PAA]$, so that all Zn^{2+} present may have been bound, the slope $dpK_{app}/d\alpha_d$ is almost the same as that for the M^{2+}-free systems. Since the kinetics of the Zn/PAA

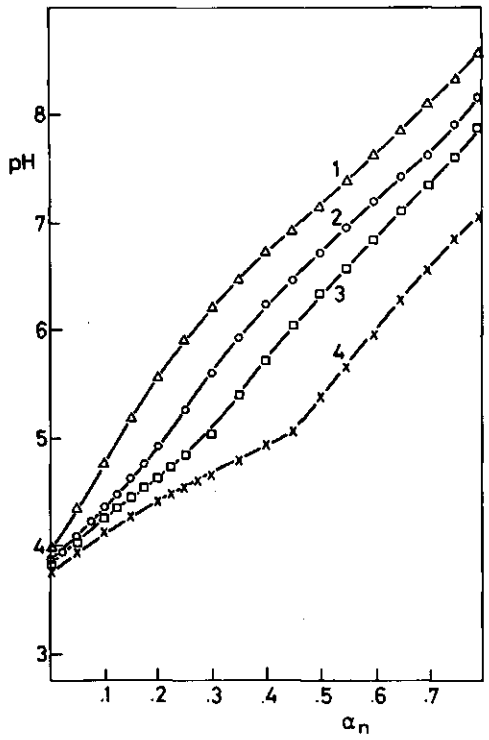

FIGURE 5.8 Dependence of the pH on α_n for Zn/PAA. [PAA] = 2.38 mol·m^{-3}. 1. no salt; 2. [Zn^{2+}] = 0.119 mol·m^{-3}; 3. [Zn^{2+}] = 0.238 mol·m^{-3}; 4. [Zn^{2+}] = 0.476 mol·m^{-3}.

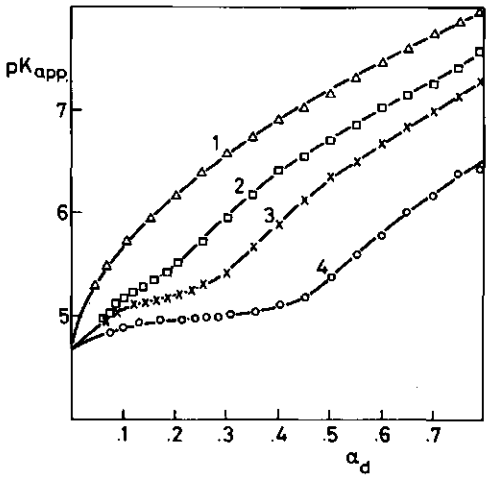

FIGURE 5.9 Dependence of pK_{app_3} on α_d for Zn/PAA. [PAA] = 2.38 mol·m^{-3}. 1. no salt; 2. [Zn^{2+}] = 0.119 mol·m^{-3}; 3. [Zn^{2+}] = 0.238 mol·m^{-3}; 4. [Zn^{2+}] = 0.476 mol·m^{-3}.

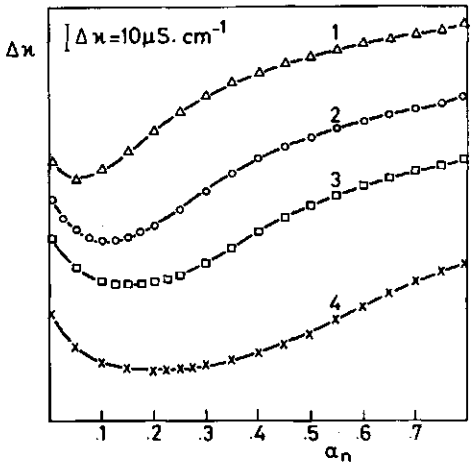

FIGURE 5.10 The conductivity difference $\Delta\kappa$ as a function of α_n for Zn/PAA. [PAA] = 2.38 mol·m^{-3}. [Zn^{2+}]/[PAA] = 0.00 (1); 0.05 (2); 0.10 (3); 0.40 (4).

equilibrium is fast, bound Zn^{2+} will be distributed randomly over the polyion chain. The equality of the slopes then indicates that the decrease of the charge density of the polyion as a result of covalent complex formation must be low.

In fig. 5.10, values of $\Delta\kappa$ are plotted versus α_n for the Zn/PAA system. Curve 2 is hardly distinguishable from the corresponding curve 2 in fig. 5.7 for added Ba^{2+}, stressing the lack of substantial covalency in the Zn/PAA interaction. The initial decrease in $\Delta\kappa$ is not linear, and this in in line with the assumption that in the mixed system (curve 4 in fig. 5.5) Pb^{2+} is preferentially bound over Zn^{2+}. Trends in the values of κ_s at $\alpha_n = 0.0$ and $\alpha_n = 0.9$ will be discussed at the end of this section, along with the corresponding trends for the Cd/PAA and Pb/PAA systems.

Cd/PAA

In fig. 5.11, the pH is plotted versus α_n for PAA in the presence of different levels of $Cd(NO_3)_2$. The curves differ from the corresponding curves for added $Zn(NO_3)_2$ in fig. 5.8. At low α_n, the curves tend to be concave, and at high α_n, the increase in pH with α_n is increas-

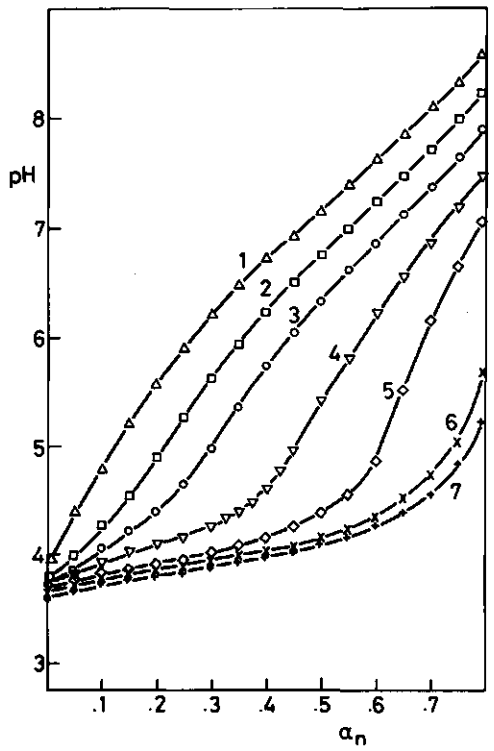

FIGURE 5.11 Dependence of the pH on α_n for Cd/PAA. [PAA] = 2.38 mol·m^{-3}. 1. no salt; 2. [Cd^{2+}] = 0.118 mol·m^{-3}; 3. [Cd^{2+}] = 0.235 mol·m^{-3}; 4. [Cd^{2+}] = 0.470 mol·m^{-3}; 5. [Cd^{2+}] = 0.705 mol·m^{-3}; 6. [Cd^{2+}] = 0.938 mol·m^{-3}; 7. [Cd^{2+}] = 1.175 mol·m^{-3}.

ingly steeper for higher $[Cd^{2+}]/[PAA]$ ratios.

Fig. 5.12, showing pK_{app} versus α_d, represents the differences with

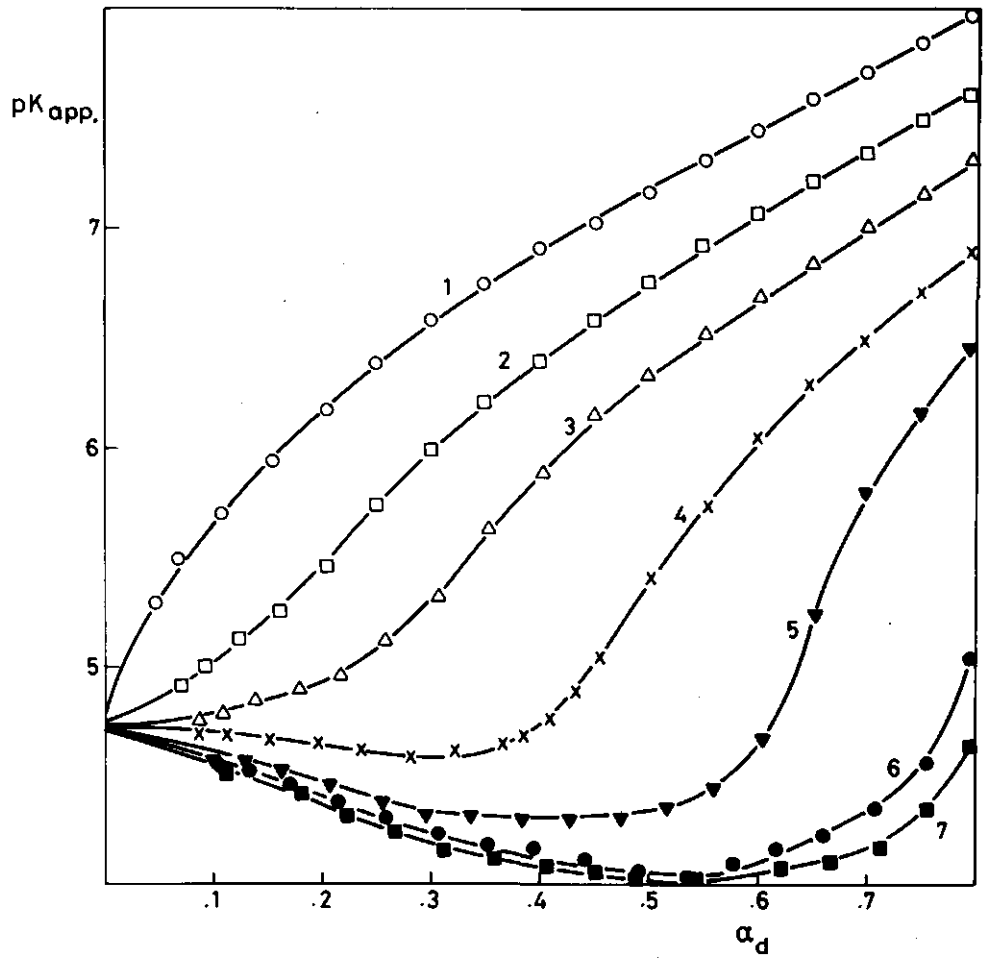

FIGURE 5.12 Dependence of pK_{app} on α_d for Cd/PAA. [PAA] = 2.38 $mol \cdot m^{-3}$; 1. no salt; 2. $[Cd^{2+}]$ = 0.118 $mol \cdot m^{-3}$; 3. $[Cd^{2+}]$ = 0.235 $mol \cdot m^{-3}$; 4. $[Cd^{2+}]$ = 0.470 $mol \cdot m^{-3}$; 5. $[Cd^{2+}]$ = 0.705 $mol \cdot m^{-3}$; 6. $[Cd^{2+}]$ = 0.938 $mol \cdot m^{-3}$; 7. $[Cd^{2+}]$ = 1.175 $mol \cdot m^{-3}$.

the Zn/PAA system (in fig. 5.9) more pronouncedly. For the ratios $[Cd^{2+}]/[PAA] > 0.1$ in fig. 5.12, pK_{app} initially decreases with α_n. This is attributed to the partially covalent character of the Cd/PAA interaction. Although log K_{int}(CdPAA) < pK_a(PAA), due to the relatively

large local concentration of Cd^{2+}, in comparison with H^+, further deprotonation of the polyacid is facilitated. The values of pK_{app} for Cd/PAA at low α_n are lower than the corresponding values for Zn/PAA. This difference will be quantitatively treated in terms of fractions covalent character of the interactions, in § 5.3.2. All curves in fig. 5.12 merge to the same limting value at $\alpha_d = 0$: $pK_a = 4.72$. This confirms that K_{int}(CdPAA) is relatively small. A second remarkable difference with the Zn/PAA system is the fact that for high α_d and large ratios $[Cd^{2+}]/[PAA]$, pK_{app} increases more strongly with increasing α_d. This is attributed to the larger covalent character of Cd/PAA interaction, as compared to Zn/PAA. The calculation of α_d is based on the number of deprotonated ligands. As a result of covalent complex formation CdL, the dependence of the polyion charge density on α_d is no longer linear. Thus the increase of the slope $dpK_{app}/d\alpha_d$, as compared to that of the M^{2+}-free system, is a measure of the covalent character of the M/PAA interaction.

In fig. 5.13, $\Delta\kappa$ is plotted versus α_n for the Cd/PAA systems. Qualitatively, the corresponding curves for Cd/PAA and Zn/PAA (in fig. 5.10) do not differ. Quantitatively, the minima for the Cd/PAA system are somewhat deeper and broader, in agreement with the larger binding strength.

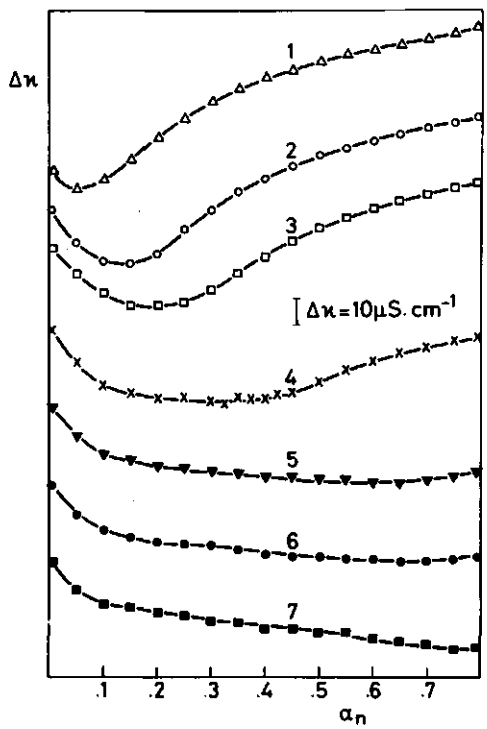

FIGURE 5.13 The conductivity difference $\Delta\kappa$ as a function of α_n for Cd/PAA. [PAA] = 2.38 mol·m^{-3}. $[Cd^{2+}]/[PAA]$ = 0.00 (1); 0.05 (2); 0.10 (3); 0.20 (4); 0.30 (5); 0.39 (6); 0.49 (7).

With increasing $[Cd^{2+}]/[PAA]$ ratio, the minimum in the $\Delta\kappa$ curve becomes very broad. In the flat region of the curves 4-7, $\Delta\kappa$ can be expressed as:

$$\Delta\kappa = \lambda_H \cdot [H] + \lambda_K \cdot [K] + \lambda_p \cdot [L] + \lambda_{Cd} \cdot [Cd] + \\ + \lambda_{NO_3} \cdot [NO_3] - \kappa_s(\alpha_n=0) \qquad (5.9)$$

For a given curve, $[NO_3]$ and $\kappa_s(\alpha_n=0)$ are constant. If no conductometric binding of Cd^{2+} would occur, the [K] and [L] would increase and [H] would decrease with increasing α_n. Using the pH values observed, the result would be an increase in $\Delta\kappa$. Thus the flat region demonstrates binding of Cd^{2+}. The extent of that region is related to $2\cdot[Cd^{2+}]/[PAA]$, suggesting ultimately charge neutralization by complete binding of Cd^{2+}. This agrees with the findings from M/L-titrations in § 4.1.3.

Pb/PAA

In fig. 5.14, the pH is plotted versus α_n for PAA in the presence

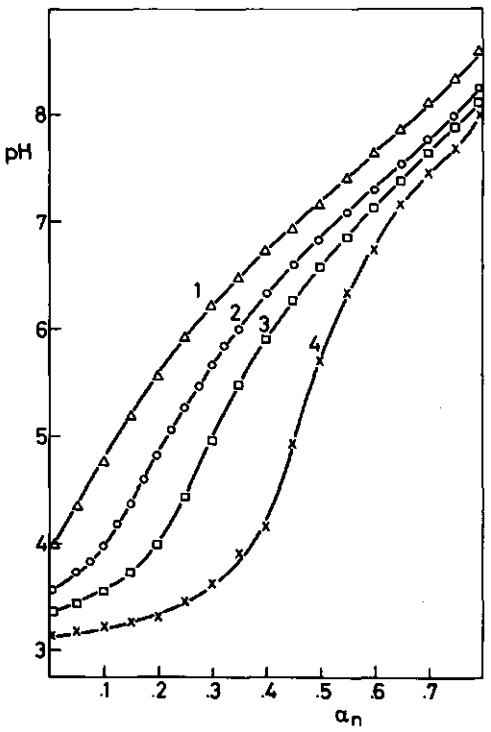

FIGURE 5.14 Dependence of the PH on α_n for Pb/PAA. [PAA] = 2.38 mol·m^{-3}. 1. no salt; 2. $[Pb^{2+}]$ = 0.119 mol·m^{-3}; 3. $[Pb^{2+}]$ 0.239 mol·m^{-3}; 4. $[Pb^{2+}]$ = 0.477 mol·m^{-3}.

of different levels of $Pb(NO_3)_2$. The differences between Pb/PAA and Zn/PAA are more pronounced than those between Cd/PAA and Zn/PAA. Even at $\alpha_n = 0$, a dramatic decrease in the pH is observed due to the presence of Pb^{2+}: the intrinsic binding of Pb^{2+} is about equally strong as the intrinsic binding of H^+, see § 4.1.3.

In fig. 5.15, the corresponding pK_{app} versus α_d curves are presented. Although some precipitation occurs in these systems, the trends in the data are in line with those expected in the series Ba, Zn, Cd, Pb. The rise in pK_{app} at high α_d is much stronger than for the other systems investigated. Extrapolation of pK_{app} for $\alpha_d \to 0$ is not possible: the covalent character of the Pb/PAA interaction seems dominant.

In fig. 5.16, the corresponding $\Delta\kappa$-curves are plotted versus α_n. The large release of H^+ due to the binding of Pb^{2+} results in an approximately linear decrease in $\Delta\kappa$ for $\alpha_n < 2\cdot[Pb^{2+}]/[PAA]$. The initially linear decrease in the mixed system $Pb^{2+} + Zn^{2+}$ (curve 4 in fig. 5.5) is now definitely attributable to the preferential binding of Pb^{2+} over Zn^{2+}. The extent of the linear decrease in $\Delta\kappa$ is proportional to $[Pb^{2+}]/[PAA]$, confirming complete binding of Pb^{2+}, as previously found in § 4.3.1. At high α_n, the flattening of the $\Delta\kappa$-curves, as a result of binding of K^+, is still clearly observed. For higher $[Pb^{2+}]/[PAA]$ ratios, the binding of K^+ shifts to higher values of α_n.

In table 5.2, the conductivities κ_s of the Zn,Cd,Pb/PAA sample solutions at $\alpha_n = 0.0$ and $\alpha_n = 0.9$ are compared at three levels of added metal nitrate. At $\alpha_n = 0.0$ the values for Pb/PAA are much larger, and those for Cd/PAA are only slightly larger than for Zn/PAA. This reflects the differences in covalent character between the systems. At $\alpha_n = 0.9$, all values of κ_s are fairly close for the three metals, except for Zn^{2+} at $[Zn^{2+}]/[PAA] = 0.20$, where $\kappa_s = 190\ \mu S\cdot cm^{-1}$. The corresponding value for Ba^{2+} is also high, $183\ \mu S\cdot cm^{-1}$. The lower values for Cd,Pb/PAA are possibly due to the effect of some precipitation.

TABLE 5.2 Conductivities of Zn,Cd,Pb/PAA systems for different values of α_n and ratios $[M^{2+}]/[PAA]$. Values of κ_s in $\mu S\cdot cm^{-1}$

metal	$[M^{2+}]/[PAA] = 0.05$		0.10		0.20	
	$\alpha_n = 0.0$	0.9	0.0	0.9	0.0	0.9
Zn	70.9	117	99.4	135	165	190
Cd	73.8	114	105	135	166	165
Pb	103	105	173	127	313	166

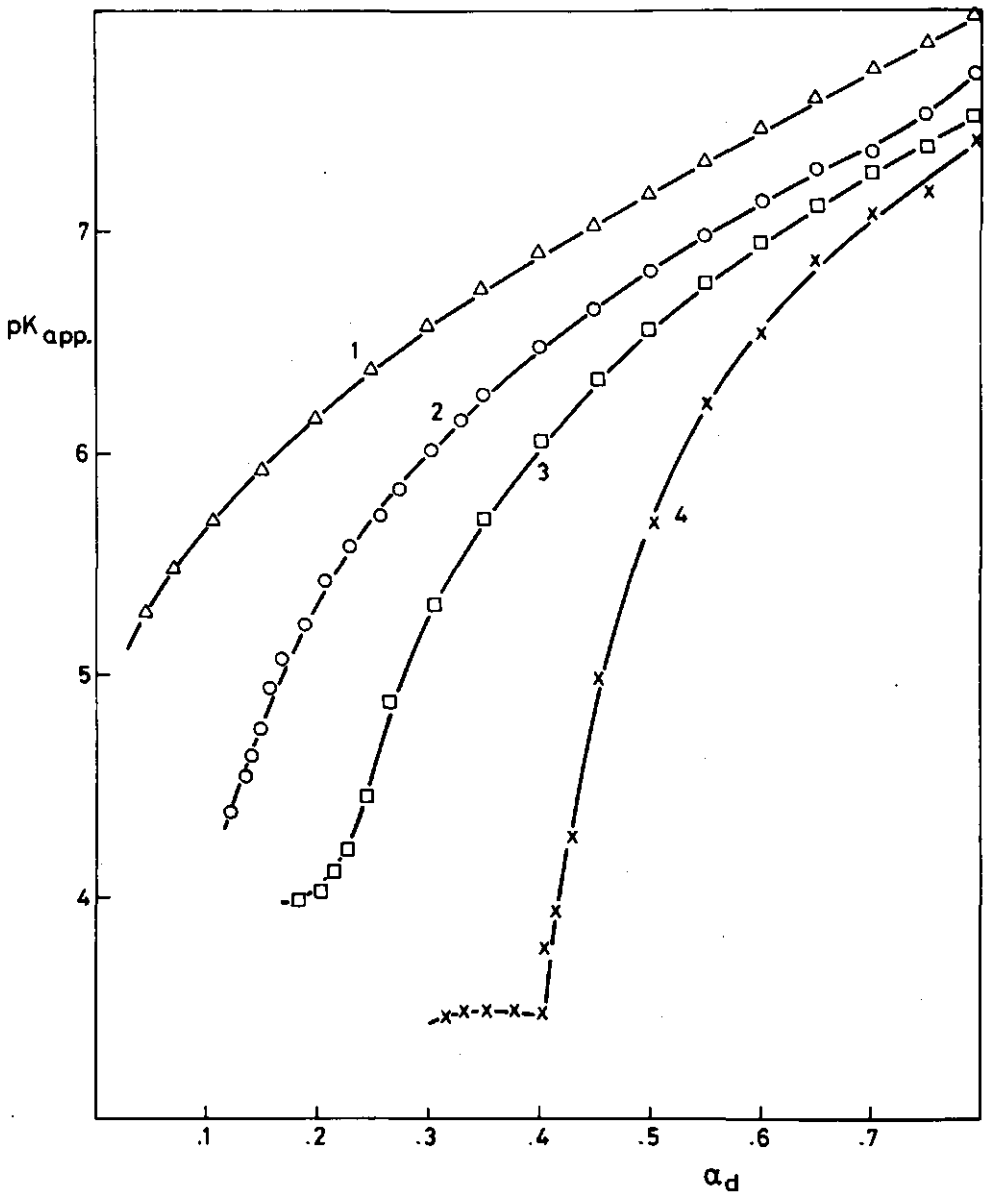

FIGURE 5.15 Dependence of pK_{app} on α_d for Pb/PAA. [PAA] = 2.38 mol·m^{-3}. 1. no salt; 2. [Pb^{2+}] = 0.119 mol·m^{-3}; 3. [Pb^{2+}] = 0.239 mol·m^{-3}; 4. [Pb^{2+}] = 0.477 mol·m^{-3}.

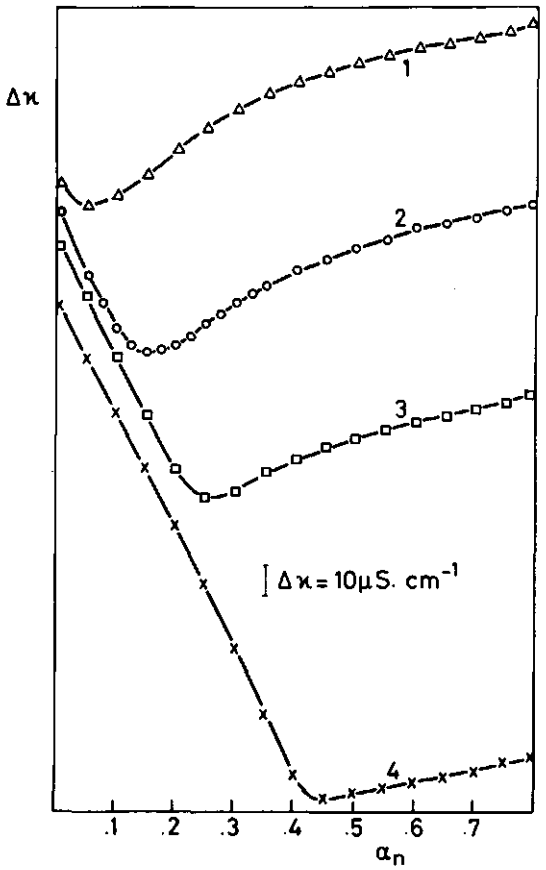

FIGURE 5.16 The conductivity difference Δκ as a function of α_n for Pb/PAA. [PAA] = 2.38 mol·m^{-3}. [Pb^{2+}]/[PAA] = 0.00 (1); 0.05 (2); 0.10 (3); 0.20 (4).

5.1.4 Cd,Pb/PMApe

A limited number of measurements has been performed using PMApe. In fig. 5.17 Δκ-curves are presented for M/PMApe systems, for three levels of $Cd(NO_3)_2$ and one level of $Pb(NO_3)_2$. The curves begin at α_n = 0.03, since PMApe coagulates at lower α_n, see § 3.2.4. Consequently, Δκ is equal to $\kappa_s(\alpha_n) - \kappa_s\ (\alpha_n = 0.03)$.

Due to the presence of the ester groups, the charge density of PMApe is lower than that of PMA, at corresponding values of α_n. As a result, the first signs of binding of K^+ are observed at higher values of α_n, i.e. about 0.5.

In the presence of Cd^{2+}, the minima in the Δκ-curves are not deep: PMApe is a weaker acid than PAA. In curve 5, binding of Cd^{2+} is now very clear. For $\alpha_n > \alpha_n$(minimum), the pH is higher than 5, and the flattening of the curve is unambiguously due to the binding of Cd^{2+}, up to $\alpha_n \cong 0.6$, where all Cd^{2+} ions have been bound.

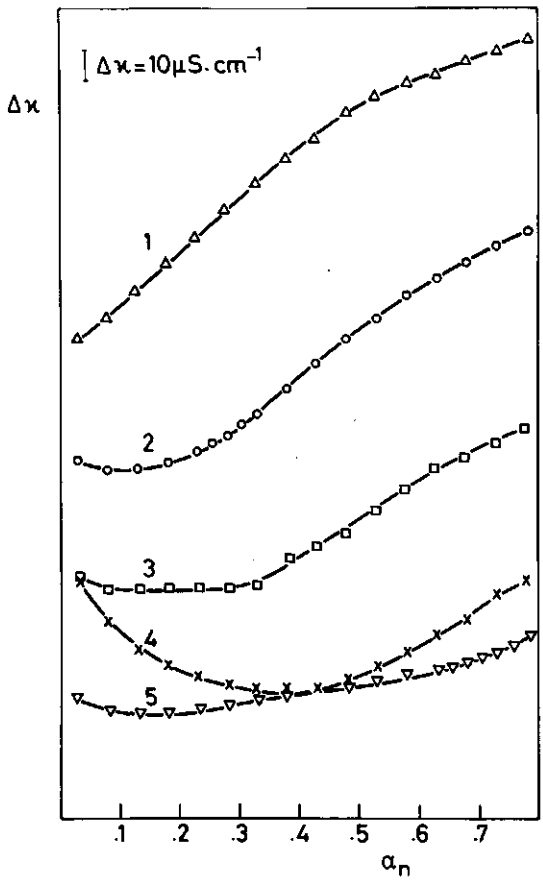

FIGURE 5.17 The conductivity difference Δκ as a function of α_n for M/PMApe. [PMApe] = 2.38 mol·$^{-3}$. [Cd^{2+}]/[PMApe] = 0.00 (1); 0.10 (2); 0.20 (3); 0.30 (5) [Pb^{2+}]/[PMApe] = 0.20 (4).

In the presence of Pb^{2+} (curve 4) the initial decrease in Δκ is more pronounced than for Cd^{2+}, which is in agreement with the finding in § 4.1.1 that K_{int} (PbPMApe)>K_{int}(CdPMApe).

In table 5.3, the conductivities κ_s of the systems at α_n = 0.03 and α_n = 0.83 are given.

TABLE 5.3 Conductivities of the M/PMApe samples of fig. 5.17. See figure legend

metal	$\frac{[M^{2+}]}{[PMApe]}$	κ_s / μS.cm^{-1}	
		α_n = 0.03	α_n = 0.83
-	0.00	15.6	118
Cd	0.10	75.5	157
	0.20	135	188
	0.30	189	216
Pb	0.20	179	183

In the absence of added salt, the value κ_s (α_n = 0.03) is lower than for PAA, because of the difference in acid strength. However, κ_s (α_n = 0.83) is higher than for PAA, which is partly due to the smaller amount of conductometrically bound K^+. The conductivities for Cd/PMApe and Pb/PMApe at α_n = 0.83 and corresponding $[M^{2+}]/[PMApe]$ ratio are almost equal. Apparently, differences in binding strength do not influence κ_s when all M^{2+} has been bound. This strengthens the assumption that the mobility of bound counterions in these cases is zero.

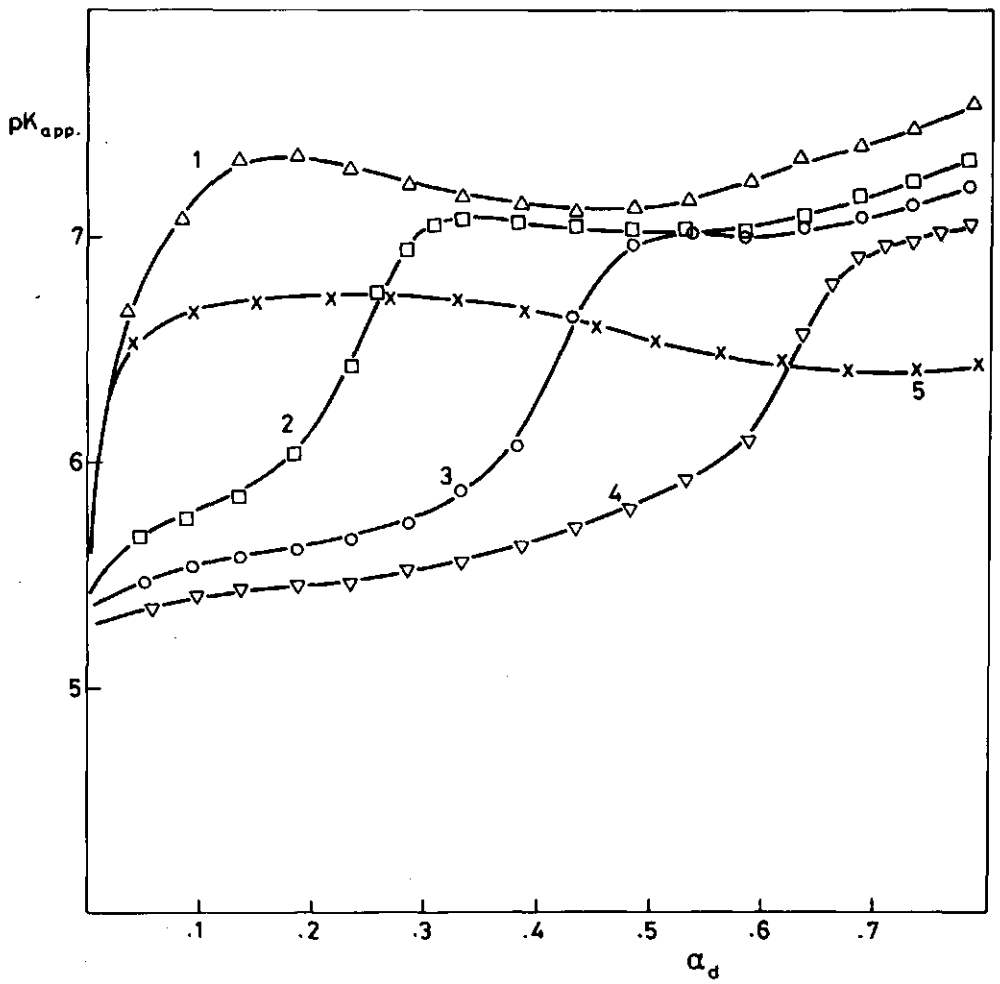

FIGURE 5.18 Dependence of pK_{app} on α_d for Cd/PMApe. [PMApe] = 2.38 mol·m^{-3}. 1. no salt; 2. $[Cd^{2+}]$ = 0.235 mol·m^{-3}; 3. $[Cd^{2+}]$ = 0.470 mol·m^{-3}; 4. $[Cd^{2+}]$ = 0.715 mol·m^{-3}; 5. no salt, $Ba(OH)_2$ as the titrant.

In fig. 5.18, pK_{app} versus α_d is presented for the Cd/PMApe systems. Additionally, pK_{app} versus α_d is given for $Ba(OH)_2$ as the titrant, in the absence of salt. Curve 1 refers to PMApe in the absence of $Cd(NO_3)_2$. A value for pK_a is difficult to obtain by extrapolation to $\alpha_d \to 0$. In the presence of increasing levels of $Cd(NO_3)_2$ (curves 2-4) the region of the substantial increase in pK_{app} with increasing α_d is shifted to higher α_d, as is the case with PAA in figure 5.12. Using these curves, the value of pK_a is estimated to be about 5.3.

For all values of α_d, pK_{app} is increasing with increasing α_d, in contrast to the Cd/PAA system. This indicates that the intrinsic binding strength for the CdPMApe complex is weak, and/or that a conformational change of the polyion may occur. If the latter occurs, it is much less pronounced than for the M^{2+}-free system.

The shapes of the pK_{app}-curves at high α_d, when all Cd^{2+} has been bound, are similar. This suggests that the binding is predominantly electrostatic, in agreement with the findings in § 4.1.1. Moreover, the shapes of the curves at high α_d indicate that for the remaining part of the polyion, for which no further binding of Cd^{2+} occurs upon deprotonation, a conformational transition takes place similar to that of the M^{2+}-free system. Comparing the ranges of the transition regions in curves 1-4, it appears that in the presence of increasing amounts of Cd^{2+}, a decreasing part of the polyion is involved in this transition. These features reveal that binding of divalent ions to PMApe stabilizes a more or less compact conformation of the polyion. As a result of the binding, the effective charge density of the polyion remains low. From the curve of the titration with $Ba(OH)_2$, it appears that a gradual conformation change may occur. However an abrupt opening of the polymer coil is inhibited. Curve 5 crosses the curves 2-4 at values of α_d where the binding of Cd^{2+} is considered to be complete. The stabilization of a more compact structure of PMApe was found for Ca, Mn and Ni by *Ralston et al.* (1981). The fact that no stabilization was found by these authors in the case of Cd is possibly due to the presence of excess of NaCl in their sample: $CdCl^+$ and $CdCl_2$ will have been formed, and monovalent cations do not stabilize the compact polyion conformation very pronouncedly. *Jakubowski* (1975) reported a stabilizing effect of the presence of Cu^{2+} on the compact conformation of PMA.

5.2 POLAROGRAPHY

The polarographic α_n-titrations have been carried out using the mixing procedure, described in § 3.1.2. Generally, the composition of the samples was: 2.5 mol·m^{-3} polyacid in the presence of M^{2+} at a ratio $[M^{2+}]/[\text{polyacid}] = 0.20$, and 50 mol·m^{-3} KNO_3. The partial neutralization was carried out with KOH. The molecular mass of PAA was 50,000.

The results are presented as plots of the pH, $(i_\ell/i_o)^2$ and $-\Delta E_{\frac{1}{2}}$ as a function of α_n, where i_ℓ and i_o are the NPP limiting currents for the sample and the corresponding polyacid-free solution respectively. This presentation was employed because of the applicability of eq. (3.21) for all the systems investigated, except Pb/PAA, as discussed in § 3.3.3.

5.2.1 Zn/PMA, PAA

In fig. 5.19, the results are presented for Zn/PMA (curves 1a, b, c) and Zn/PAA (curves 2a, b, c). The polarograms of the systems had a normal shape, and well-defined limiting currents. In the case of Zn/PAA, a small sign of a second wave was observed for $\alpha_n > 0.6$ with $E_{\frac{1}{2}} \cong -1.2$ V vs. $Ag/AgCl,KCl_{sat}$.

The increase in pH with α_n is for Zn/PAA less pronounced than in fig. 5.8, because of the twenty-fold excess of 1:1 salt in the polarographic experiments. Obviously, the pH for the Zn/PAA systems is lower than the corresponding values for the Zn/PMA system.

The curves of the current ratio $(i_\ell/i_o)^2$ show the following features:

i The current ratio decreases with increasing α_n: at low α_n somewhat more rapidly for Zn/PMA;

ii At low and intermediate α_n, the current ratio is lower for Zn/PMA than for Zn/PAA;

iii The curves show an intersection at about $\alpha_n = 0.67$, and show the tendency to become indistinguishable at low α_n.

Since the NPP method is sufficiently sensitive and accurate to consider the observations as significant, a detailed description of the binding processes is allowed.

The curves of $-\Delta E_{\frac{1}{2}}$ demonstrate that the systems are polarographically labile. Generally, the shift for Zn/PAA is slightly larger than it is for Zn/PMA. It is noted that shifts smaller than approximately

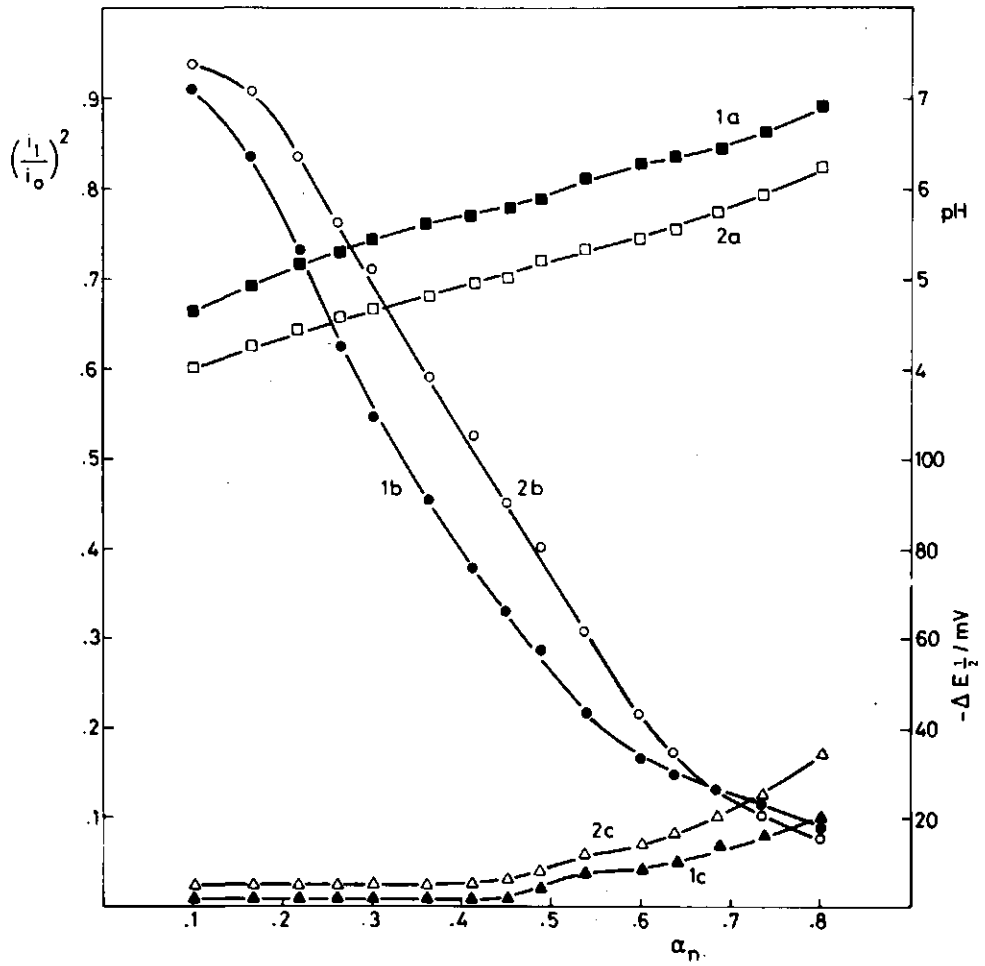

FIGURE 5.19 Results of polarographic experiments as a function of α_n for: 1. Zn/PMA, $\bar{M}$ = 26,000, and 2. Zn/PAA, $\bar{M}$ = 50,000. a. pH; b. $(i_l/i_o)^2$; c. $-\Delta E_{\frac{1}{2}}$/mV. [PMA] = 2.51 mol·m^{-3}; [PAA] = 2.52 mol·m^{-3}; [Zn^{2+}]/[polyacid] = 0.20; [KNO_3] = 50 mol·m^{-3}; E_i = -900 mV vs. Ag/AgCl, KCl_{sat}; t_p = 175 ms; t_d = 0.5 s; A = 1.35 mm^2.

5 mV are difficult to determine accurately. The slightly larger values of $-\Delta E_{\frac{1}{2}}$ for Zn/PAA confirm the conclusions of § 4.1.3 and § 5.1.3 that the intrinsic binding strength of MPAA is larger than that for MPMA. These findings are in agreement with literature data for several M/PAA and M/PMA systems mentioned in § 2.4.1. The curves of the current ratio

suggest that at intermediate values of α_n, Zn^{2+} is stronger bound to PMA. According to eq. (3.21) the ratio of polarographically free and bound metal ions, and the ratio of the diffusion coefficients of the polyion and the free metal ions determine the current ratio. It follows that the difference between Zn/PAA and Zn/PMA with respect to $(i_\ell/i_o)^2$ will be controlled by differences in:

i the diffusion coefficients of the polyions;
ii the intrinsic binding constants;
iii the charge densities of the polyions.

The values of D_b/D_f for PMA ($\bar{M}$ = 26,000) and PAA ($\bar{M}$ = 50,000) in table 3.3 are both 0.02, which is the rounded value of both 0.019 (PMA) and of 0.023 (PAA). Considering the small influence D_b/D_f on i_ℓ, see § 3.3.3, this small difference in D_b/D_f cannot explain the differences in $(i_\ell/i_o)^2$.

The intrinsic binding constants, and their difference, are relatively small for the systems involved. The difference in covalent behaviour may have an effect on the current ratio, but this effect would not be restricted to a certain range of α_n.

The third origin of the difference in the curves is the difference in charge density of the polyions, at equal values of α_n. The more compact conformation of PMA, that is stabilized in the presence of M^{2+}, explains the lower values of $(i_\ell/i_o)^2$ for Zn/PMA, as compared to those for Zn/PAA. Such a conformation effect has been noted with respect to R_c, in § 4.1.4 and with respect to pK_{app} in M/PMApe systems. This effect has also been indicated in literature for M/PMA interactions (*Kotliar & Morawetz*, 1955; *Yamashita et al.*, 1979a,b; *Jakubowski*, 1975). When almost all Zn^{2+} ions have been bound, and the PMA conformation changes with increasing α_n, the effect becomes smaller, and the differences in covalent character become more manifest: the curves intersect.

A quantitative analysis of the data, in terms of binding constants, will be given in § 5.3.3, along with the analyses for the other systems.

5.2.2 Cd/PMA, PAA

In fig. 5.20, the results are presented for Cd/PMA (curves 1a, b, c) and Cd/PAA (curves 2a, b, c). Generally, the polarograms of the systems had normal shapes with well-defined limiting currents.

Qualitatively, the characteristics of all the curves are similar to those for the Zn/PMA,PAA systems in fig. 5.19. Quantitatively, the differences between corresponding curves for Zn^{2+}- and Cd^{2+}-systems

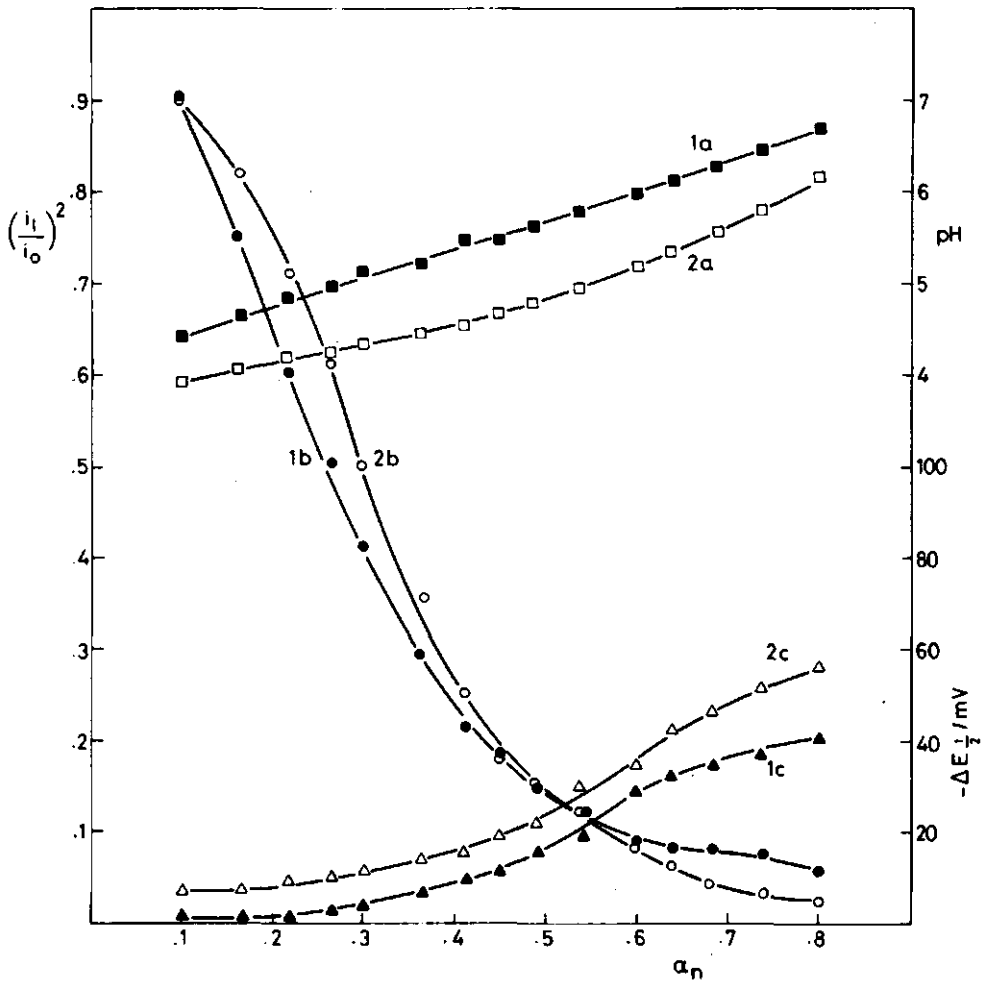

FIGURE 5.20 Results of polarographic experiments as a function of α_n for: 1. Cd/PMA, $\bar{M}$ = 26,000, and 2. Cd/PAA, $\bar{M}$ = 50,000. a. pH; b. $(i_l/i_o)^2$; c. $-\Delta E_{\frac{1}{2}}$/mV. [PMA] = 2.51 mol·m^{-3}; [PAA] = 2.52 mol·m^{-3}; [Cd^{2+}]/[Polyacid] = 0.20; [KNO_3] = 50 mol·m^{-3}; E_i = -500 mV vs. Ag/AgCl,KCl_{sat}; t_p = 175 ms; t_d = 0.5 s; A = 1.35 mm^2.

agree with the larger ability of Cd^{2+} to bind with the polyacids. The pH curves are positioned somewhat lower, and the increase in pH for Cd/PAA is more pronounced at high α_n. A plot of pK_{app} for Cd/PAA corresponding with curve 2a in fig. 5.20 has been given in fig. 5.1.

For Cd/PMA,PAA, the decrease of $(i_\ell/i_o)^2$ with α_n is stronger than for Zn/PMA,PAA. The difference between Cd/PMA and Cd/PAA is significant. The α_n value at which the curves intersect is lower than in the case of Zn^{2+}. This also demonstrates the stronger binding of Cd^{2+}, since the value of $(i_\ell/i_o)^2$ at the intersection point is about 0.13 for both the Zn^{2+}- and the Cd^{2+}- containing systems.

The shifts in $E_{\frac{1}{2}}$ are larger for Cd/PAA than for Cd/PMA at all values of α_n. This observation seems in contradiction with the differences between the curves 1b and 2b in fig. 5.20. However, $E_{\frac{1}{2}}$ pertains particularly to the behaviour of the metal ions *at* the mercury surface, just outside the electrical double layer, whereas i_ℓ is also controlled by the behaviour at some distance x from the electrode in the diffusion layer. The number of bound metal ions decreases for $x \to o$. Those metal ions that are bound through covalent linkages will persist in the bound state to smaller values of x, as compared to the purely electrostatically bound ions. In this situation, $E_{\frac{1}{2}}$ is more sensitive to the covalent nature of the binding than i_ℓ.

The curves 1b and 2b seem to intersect also at $\alpha_n \cong 0.1$. This may be explained by the fact that at very low α_n the charge densities are small, so that the differences in covalency are reflected more pronouncedly.

5.2.3 Pb/PMA, PAA

In fig. 5.21, the results are presented for Pb/PMA (curves 1a, b, c) and Pb/PAA (curves 2a, b, c).

The low values of $(i_\ell/i_o)^2$ in curve 2b are the consequence of considerable precipitation in the Pb/PAA system, as previously noted in the M/L-titration series for 1:1 salt containing systems, see fig. 4.18. If the values of curve 2b would have been plotted as i_ℓ/i_o instead of $(i_\ell/i_o)^2$, a curve approximately equal to curve 1b would have resulted. This indicates that the system behaves as an inert rather than as a labile equilibrium, with respect to the magnitude of the limiting current. Although the polarograms of the Pb/PAA system had normal shapes, the limiting currents of this system will not be further analyzed.

The polarograms of the Pb/PMA system show features of reactant adsorption, increasingly manifest with increasing α_n. Using SDC polarography, reliable values of i_ℓ were obtained up to $\alpha_n \cong 0.6$. For $\alpha_n > 0.6$ a bell-shaped maximum appeared at a fixed $E = -0.61$ V vs. $Ag/AgCl,KCl_{sat}$, probably due to formation of $Pb(OH)^+$, as pH > 5.5.

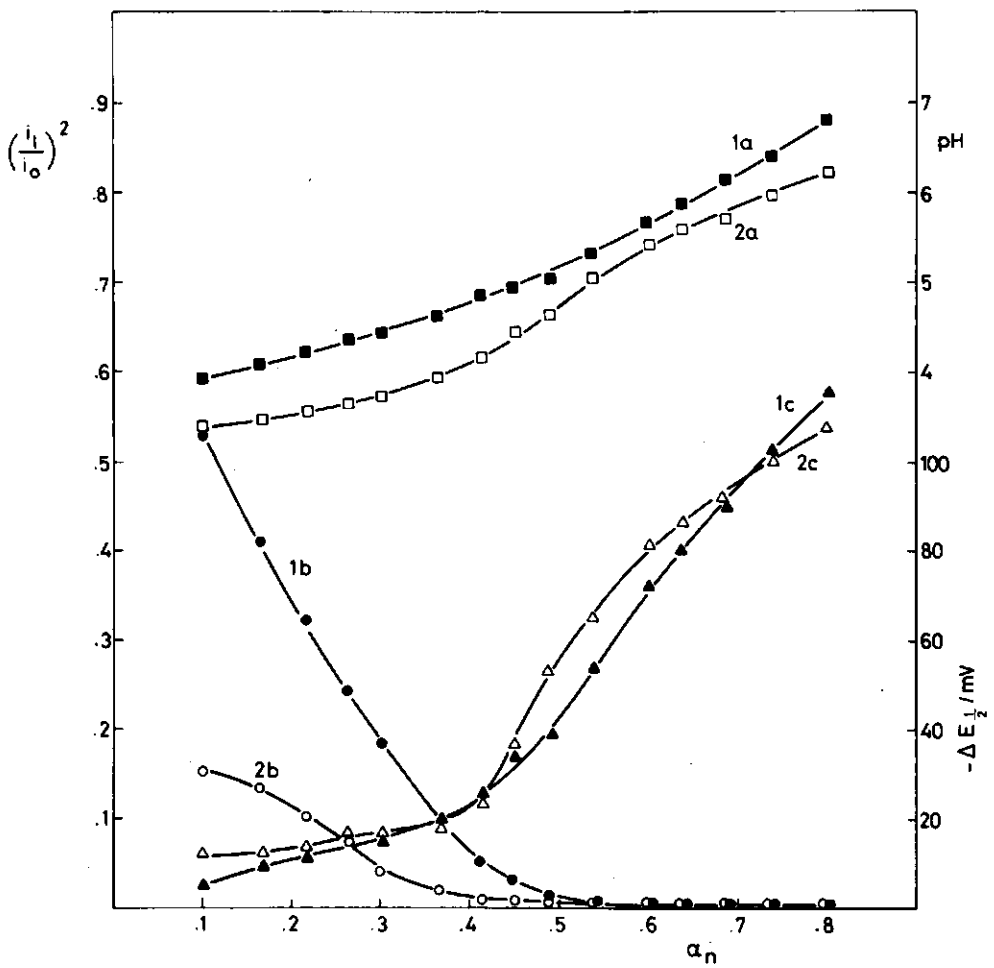

FIGURE 5.21 Results of polarographic experiments as a function of α_n for: 1. Pb/PMA, $\bar{M}$ = 26,000 and 2. Pb/PAA, $\bar{M}$ = 50,000. a. pH; b. $(i_l/i_o)^2$; c. $-\Delta E_{\frac{1}{2}}$/mV. [PMA] = 2.51 mol·m^{-3}; [PAA] = 2.52 mol·m^{-3}; [Pb^{2+}]/[polyacid] = 0.20; [KNO_3] = 50 mol·m^{-3}; E_i = -250 mV vs. Ag/AgCl,KCL_{sat}; t_p = 175 ms; t_d = 0.5 s; A = 1.35 mm^2.

The curves of the pH and of $-\Delta E_{\frac{1}{2}}$ are in agreement with the expected behaviour of Pb^{2+}, against the background of the increasingly covalent nature of the metal/polycarboxylic acid interaction in the series Zn, Cd, Pb. For the Pb/polyacid systems, the curves of the pH are positioned

much lower, and those of $-\Delta E_{\frac{1}{2}}$ much higher. The values of $-\Delta E_{\frac{1}{2}}$ are, on the average, somewhat larger for Pb/PAA, as compared to those for Pb/PMA. It is noted that the values of $-\Delta E_{\frac{1}{2}}$ for Pb/PAA only pertain to the part of the system that is not precipitated.

5.3 FURTHER DISCUSSION

5.3.1 Counterion condensation

The covalent contributions to the M^{2+}/polycarboxylic acid interaction are rather different for the different systems investigated. Still it is clear form the data in § 5.1.2-4, that the amount of M^{2+} ions bound is related to the degree of neutralization, stressing the influence of the polyion charge density. In a recent work of *Friedman & Manning* (1984) it is stated that polyelectrolyte effects help drive the site binding reaction.

From the conductometric M/L-titrations in § 4.1.1-3, it was demonstrated that the mobility of the conductometrically bound ions is approximately zero, which is in accordance with the condition for condensation in the CC model. The range of M/L-ratio over which complete binding of M^{2+} occurs has been demonstrated to agree with the predictions for condensation in the CC model.

From the conductometric α_n-titrations a number of observations support the theoretical criteria for condensation. For divalent ions, condensation occurs if $\xi > \frac{1}{2}$. In the case of PMA and PAA: $\alpha_d > 0.18$. For monovalent ions, the critical value of α_d is 0.36, in the case of PMA and PAA. With respect to the divalent heavy metal ions, the value $\alpha_d = 0.18$ only plays an observable role in the case of Zn^{2+}. In fig. 5.9, the value of the slope $dpK_{app}/d\alpha_d$ remains, in a given curve, at the lowest value from about $\alpha_d = 0.18$ up to where further binding of Zn^{2+} ceases due to depletion of free Zn^{2+}.

A critical value of α_d is more pronouncedly manifest for the binding of K^+ ions. For the M^{2+}-free systems, a deviation from linearity of the $\Delta\kappa$-curves starts at about $\alpha_n = 0.35$, see curve 1 in fig. 5.5. In addition to this, the curve of $pK_{app,a}$ versus α_d for PAA (see figs. 5.1 and 5.2) become approximately linear at $\alpha_n = 0.35$, in the M^{2+}-free systems. Moreover, the critical value increases with increasing amount of bound M^{2+}. This is clearly demonstrated in the Cd/PAA series in fig. 5.13. Additionally, the critical value of α_n increases in going from PAA to PMApe. Theoretically, K^+ condensation

would start at α_d = 0.53 for PMApe. In curve 1 of fig. 5.17, the deviation from linearity of the $\Delta\kappa$-curve starts at about α_n = 0.45. The difference with the theoretically expected value could be attributed to the not completely random esterification of PMApe, and to a slightly more compact conformation, due to the more hydrophobic character of PMApe, as compared to PAA.

The existence of particular values of α_n for the binding of K^+ demonstrates the applicability of the CC model to explain a number of features observed.

5.3.2 Acid dissociation constants

From the change of $\Delta\kappa$ in the conductometric α_n-titrations, it appears that the association of M^{2+} and M^+ occurs in *separate* regions of α_n, in agreement with the criteria for condensation. The values of $\Delta\kappa$ and of the concurrently determined pK_{app} appeared to be ion-specifically dependent on the intensity of the interactions. The CC model predicts whether a metal ion will be bound or not, rather than it predicts, the strength of the binding in the case of heavy metal ions.

To determine the fractional covalent contribution to the total change in free energy of the binding, values of pK_{app} of the different M^{2+}/polyacid systems can be compared with the value of $pK_{app,a}$ since pK_{app} appeared to be sensitive to the covalent character of the binding. This is illustrated in fig. 5.22 in which pK_{app} is plotted versus α_d for PAA in the presence of Cd, at $[M^{2+}]/[PAA]$ ratios of 0.3 and 0.4 respectively, and a 3:1 mixture of Cd and Zn, at $[M^{2+}]/[PAA]$ = 0.4. At low α_d, curve 2 is close to curve 1, whereas at high α_d it intersects curve 3. This demonstrates that Cd is preferentially bound over Zn, notwithstanding the only small difference in covalency.

The previously (in § 5.1.2) indicated preference of Pb over Zn is also clearly demonstrated by the behaviour of pK_{app} of the (Pb + Zn)/PAA system. In fig. 5.23, pK_{app} is again plotted for PAA in the presence of Zn (from fig. 5.9), Cd (from fig. 5.12) and Pb (from fig. 5.15). Additionally, pK_{app} is plotted for PAA in the presence of the 1:1 mixture of Pb and Zn. The curves 2-5 refer to $[M^{2+}]/[PAA]$ = 0.2. At low α_d, the shape of curve 4 resembles that of corresponding curve for Pb (curve 3 in fig. 5.15); at values of α_d between approximately 0.3 and 0.5 it resembles that of Zn (curve 3 in fig. 5.9). Moreover, at higher α_d, curve 4 is positioned inbetween curve 2 (Zn) and curve 5 (Pb).

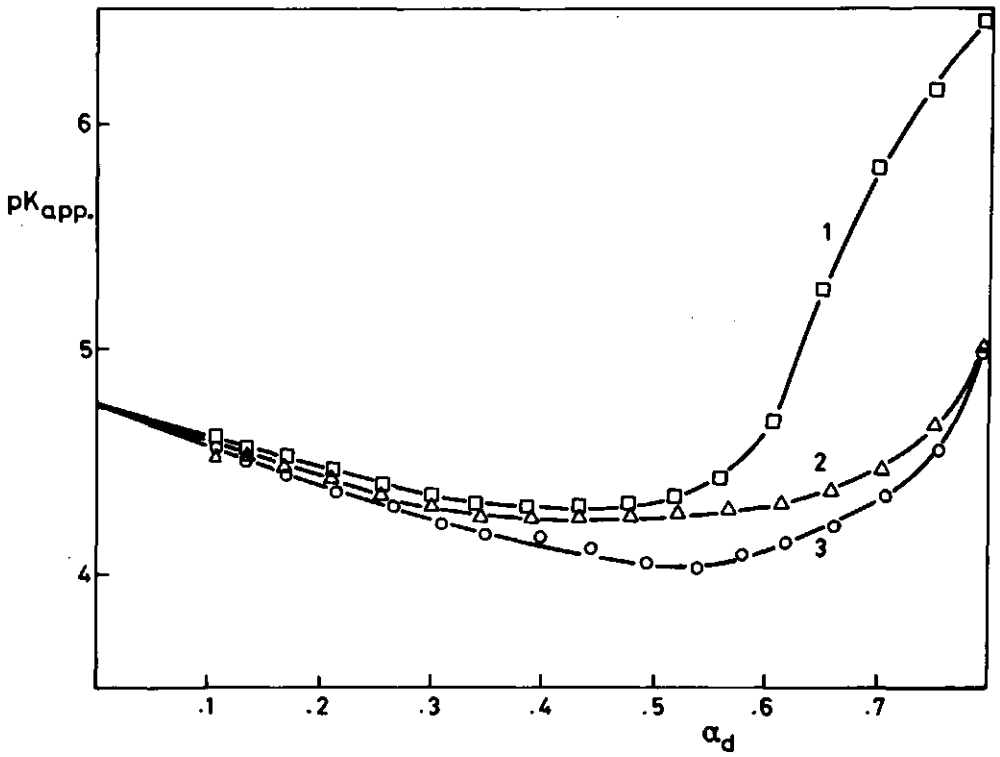

FIGURE 5.22 Dependence of pK_{app} on α_d for some Cd,Zn/PAA systems. 1. $[Cd^{2+}]$ = 0.705 mol·m^{-3}; 2. $[Cd^{2+}]$ = 0.705 mol·m^{-3} and $[Zn^{2+}]$ = 0.238 mol·m^{-3}; 3. $[Cd^{2+}]$ = 0.938 mol·m^{-3}.

To determine the fraction covalency of the binding using values of pK_{app}, the curves in fig. 5.23 may be further analyzed. To this end, the concept is adopted that has been previously employed in the evaluation of the H^+-production in the M/L-titrations (see § 4.1.1-3).

pK_{app} is a function of the (intrinsic) acid dissociation constant K_a, the (intrinsic) metal association constant K_{int} (ML), and the charge density of the polyion, controlled by α_d.

From the conductometric data (no 1:1 salt), it appeared that at values of α_d of about 0.4, most of the divalent metal ions have been conductometrically bound, in the case of $[M^{2+}]/[PAA]$ = 0.2. For the majority of the remaining RCOOH groups, the (intrinsic) acid dissociation constant will be K_a. In this respect it may be noted that at

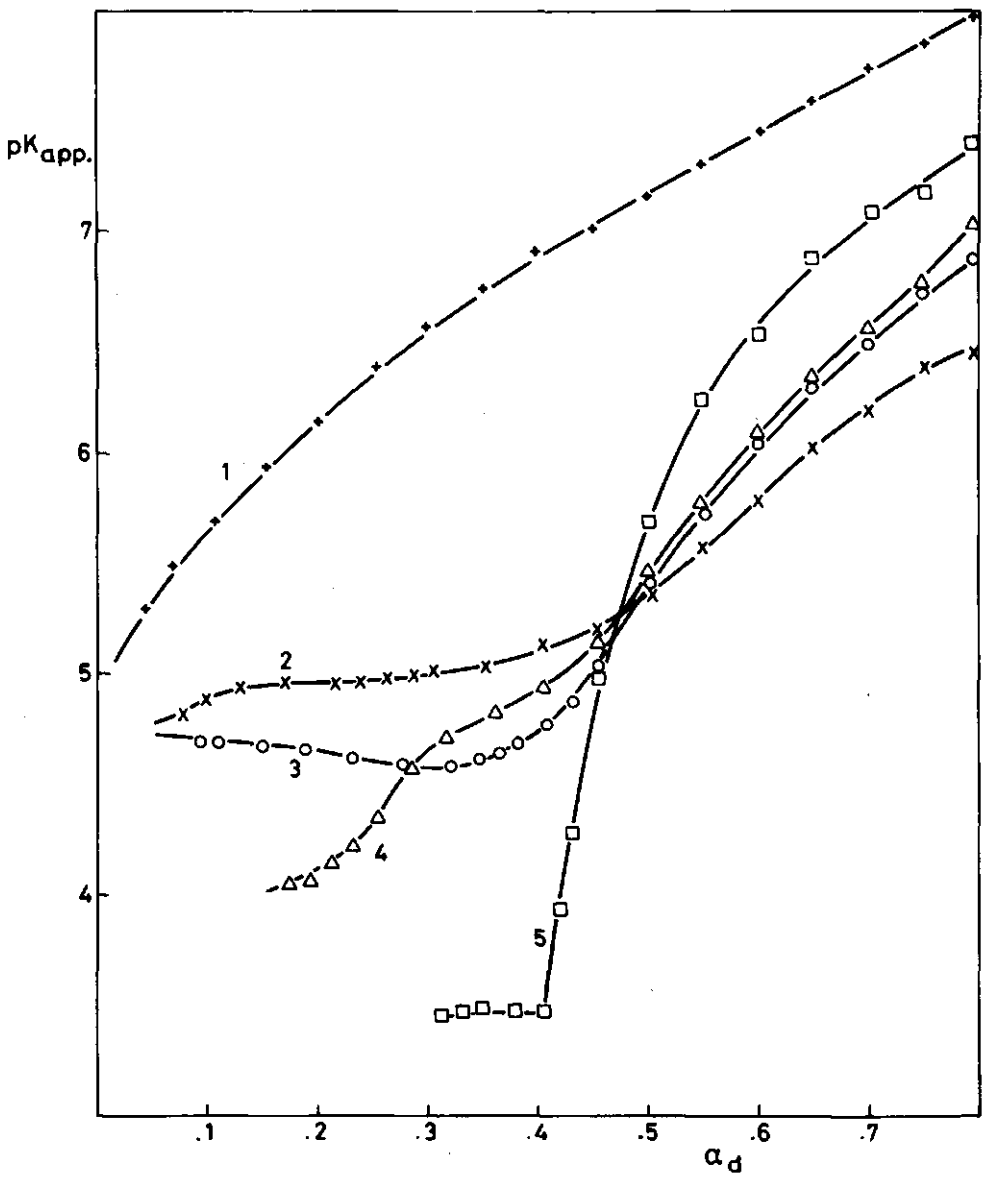

FIGURE 5.23 Dependence of pK_{app} on α_d for some Cd, Pb,Zn/PAA systems. 1. no salt; 2. $[Zn^{2+}] = 0.476\ mol \cdot m^{-3}$;3. $[Cd^{2+}] = 0.470\ mol \cdot m^{-3}$; 4. $[Zn^{2+}] = 0.238\ mol \cdot m^{-3}$ and $[Pb^{2+}] = 0.238\ mol \cdot m^{-3}$; 5. $[Pb^{2+}] = 0.477\ mol \cdot m^{-3}$.

values of α_d somewhat larger than 0.4, the curves 2-5 are very close: They intersect at a common point at about α_d = 0.47. At values of α_d below 0.47, the differences in pK_{app} are predominantly due to the effect of the covalency of the M^{2+}/polyacid interaction on the substitution of bound protons. At higher α_d, the differences are mainly connected with differences in the extent of the reduction of the polyion potential by covalent complex formation, and as a consequence of this, the differences in charge densities at equal values of α_d.

At a given α_d, the effective charge density of the polyion resulting from *deprotonation* by KOH and *electrostatic* binding of M^+ and of M^{2+}, will be the same for each of the systems in fig. 5.2.3. The charge density due to deprotonation by KOH and possible binding of K^+ is reflected in curve 1: pK_{app} (K). The effective charge density due to the electrostatic binding of M^{2+} is reflected in the apparent acid dissociation constant in the presence of Ba (not in figure): $pK_{app,a}$ (Ba), since Ba can be assumed to be bound almost purely electrostatically (*Rinando & Milas*, 1970). The corresponding values of $pK_{app,a}$ (Ba) can be calculated from curve 3 in fig. 5.6. Any further decrease in pK_{app} in the presence of metal ions M, to pK_{app} (M) originates from covalency. Thus the covalent contributions can be compared using:

$$\Delta pK_{app}\ (cov) = pK_{app,a}(Ba) - pK_{app}(M) \qquad (5.10)$$

The fractional covalent contribution may be indicated by:

$$\%\ cov = \frac{\Delta pK_{app}(cov)}{\Delta pK_{app}(tot)} \cdot 100\% = \frac{pK_{app,a}(Ba) - pK_{app}(M)}{pK_{app,a}(K) - pK_{app}(M)} \cdot 100\% \qquad (5.11)$$

In principle, eqs. (5.10) and (5.11) can be applied for any $\alpha_d < 0.45$ in fig. 5.23. The fractional covalency is not very sensitive to the choice of α_d. The value α_d = 0.32 will be chosen because at that value:

i pK_{app}(K) is neither affected by binding of K, nor by the suspension effect;

ii the absolute value of ΔpK_{app}(cov) is large;

iii no extrapolation is needed for pK_{app}(Pb).

In table 5.4, the covalency contributions for M/PAA are collected. The fractional covalency in the binding increases in the series Zn < Cd < Pb, up to more than 50% for Pb/PAA. The ratios of the values

of $\Delta pK_{app}(cov)$ can be compared to the ratios of the provisional values of log $K_{int}(ML)$ in § 4.1.3, as both parameters refer in a similar way to the covalent complex formation.

TABLE 5.4 Covalency contributions to the M/PAA interaction

	no salt	Ba	Zn	Cd	Pb
pK_{app}	6.64	5.24	5.02	4.56	3.47
$\Delta pK_{app}(tot)$	0	1.40	1.62	2.08	3.17
$\Delta pK_{app}(cov)$	-	0	0.22	0.68	1.77
% cov.	-	0	14	33	56

From the α_n-titrations it appeared that the ratios of $\Delta pK_{app}(cov)$ are (table 5.4): Zn : Cd : Pb ≅ (1) : (3) : (8), whereas from the M/L-titration the ratios of log $K_{int}(ML)$ obtained are (table 4.3): Zn : Cd : Pb ≅ (1) : (3) : (>4). The agreement is convincing, indicating the consistency of the models. The ratios of $\Delta pK_{app}(cov)$ can also be compared with the ratios of log K_1 (table 4.6) for the interaction with the monomer-like 2-metylpropanoic acid: Zn : Cd : Pb ≅ (1) : (4) : (7). These ratios are also in reasonable agreement with those from the α_n-titrations. Apparently, the differences in covalent behaviour in simple ligand systems and in uncharged polyacrylic ligand systems remain approximately the same in charged polyacrylic ligand systems. Comparisons with the polarographic results will be made in § 5.3.2.

The same kind of procedure can be applied to the results of the α_n-titrations for PMApe. In fig. 5.24, the pK_{app} curves for $[M^{2+}]/[PMApe] = 0.2$ are presented for Cd and Pb. The value $\alpha_d = 0.25$ was selected since at that value of α_d, $dpK_{app}(M)/d\alpha_d$ is at a minimum value. Moreover the conformation, as it occurs in the M^{2+}-free system, would be rather compact. The value of $pK_{app,a}(Ba)$ has not been measured and therefore it was estimated by applying the value of the ratio $\Delta pK_{app,a}(Ba)/(pK_{app,a}(K)-pK_a)$, as determined for PAA, to the PMApe system. The appropriate value of $pK_{app,a}(K)$ cannot be taken directly from curve 1 in fig. 5.24, since the interactions of Cd and Pb refer to the more compact conformation of PMApe. To estimate the value of $pK_{app,a}(K)$, the initial part of curve 1 has to be extrapolated for the compact conformation. This has been established using the HH-equation, see § 2.3.2.

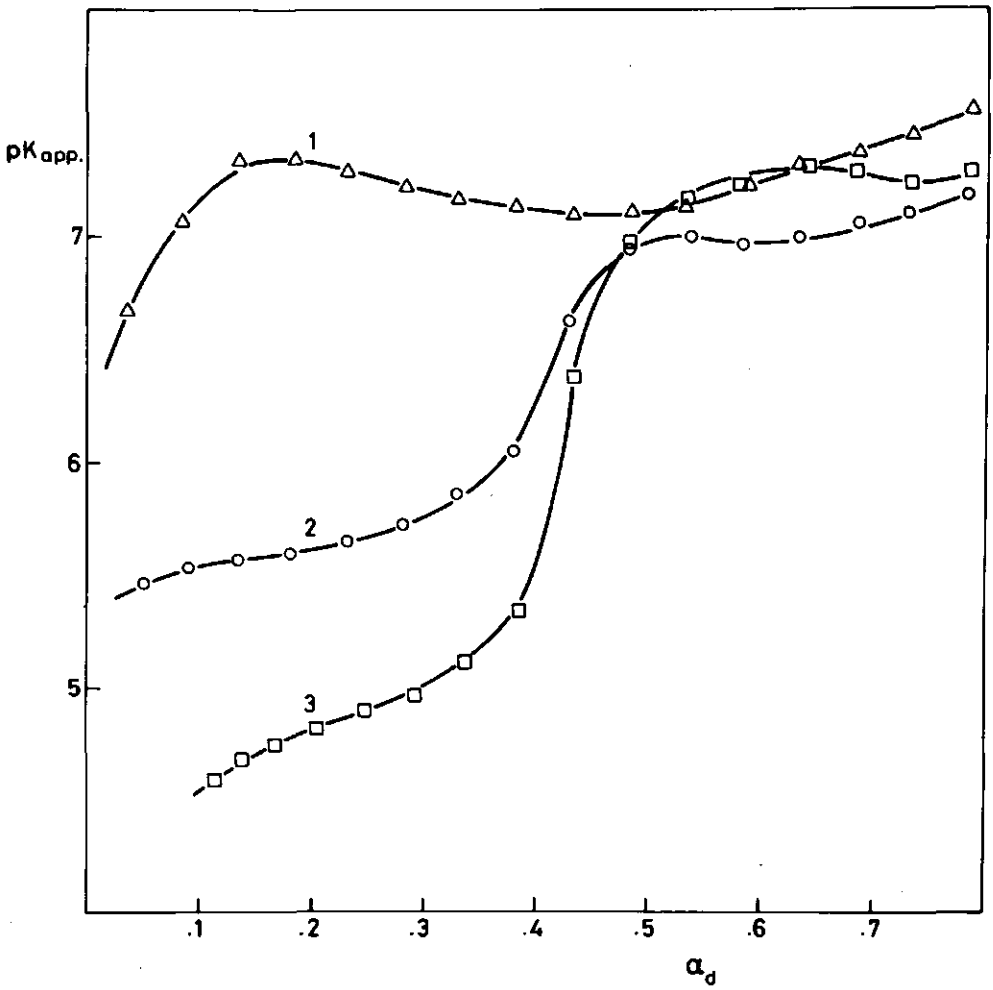

FIGURE 5.24 Dependence of pK_{app} on α_d for some Cd,Pb/PMApe systems. 1. no salt; 2. $[Cd^{2+}] = 0.470$ mol·m^{-3}; 3. $[Pb^{2+}] = 0.477$ mol·m^{-3}.

In table 5.5, the covalency contributions for M/PMApe are collected.

TABLE 5.5 Covalency contributions to the M/PMApe interaction

	no salt	Ba	Cd	Pb
pK_{app}	7.68	5.85	5.68	4.91
ΔpK_{app}(tot)	0	1.83	2.00	2.77
ΔpK_{app}(cov)	-	0	0.17	0.94
% cov.	-	0	9	34

From table 5.5, it appears that the ratio of the covalency contributions is Cd : Pb ≡ (1) : (6), which is identical to the ratio of the corresponding values of log K_{int} (ML). Moreover, a remarkable feature found in the M/L-titrations is now confirmed: covalency contributions in M/PMApe are smaller than in M/PAA. Simultaneously, the ratio of ΔpK_{app}(cov) for Cd and Pb is smaller in M/PMApe, as compared to M/PAA, but equal to that of the corresponding log K_{int}(ML) values in the case of M/PMA, see table 4.3. This suggests that, as pointed out in § 4.1.3, the different chemical environments of the $-COO^-$ groups, with the methyl group present in PMApe and PMA, may primarily cause the difference in fractional covalency contribution, as compared to PAA systems. In addition, the presence of the ester groups in PMApe may further influence the levels of log K_{int}(ML).

The values of ΔpK_{app}(tot) are for M/PMApe somewhat larger than for M/PAA at corresponding values of α_d. This is attributed to the high charge density in PMApe in the more compact conformation of the polyion. Apparently this conformation effect is large enough to compensate the decrease in charge density as a result of the partial esterification.

5.3.3 Metal association constants

From the values of $(i_\ell/i_o)^2$ in the figs. 5.19 - 5.21 and the corresponding pH values, the apparent association constants log K_1 have been calculated for a 1:1 binding formalism and a polarographically labile equilibrium. The actual pH was taken into account in the calculation of the free ligand concentration. The results are presented as a function of α_n in fig. 5.25. All the curves refer to the ratio $[M^{2+}]$/[polyacid] = 0.2. The values of log K_1 are in good agreement with those that can be calculated from the polarographic M/L-titration data in § 4.2.1-2, for corresponding values of M/L and α_n. Since the molecular mass of the PAA samples in the M/L-titrations was different from that in the α_n-titrations, the agreement confirms that the corresponding D_b/D_f values were reasonable estimates.

The curves in fig. 5.25 confirm the features of the systems as discussed on the basis of the corresponding curves in the figs. 5.19-21: an increase of the binding in the series Zn<Cd<Pb, an increase of the binding with increasing α_n, and a larger binding for Cd,Zn/PMA as compared to Cd,Zn/PAA at intermediate values of α_n. It is noted that for the Pb/PMA system, the curve becomes convex for high α_n (not in

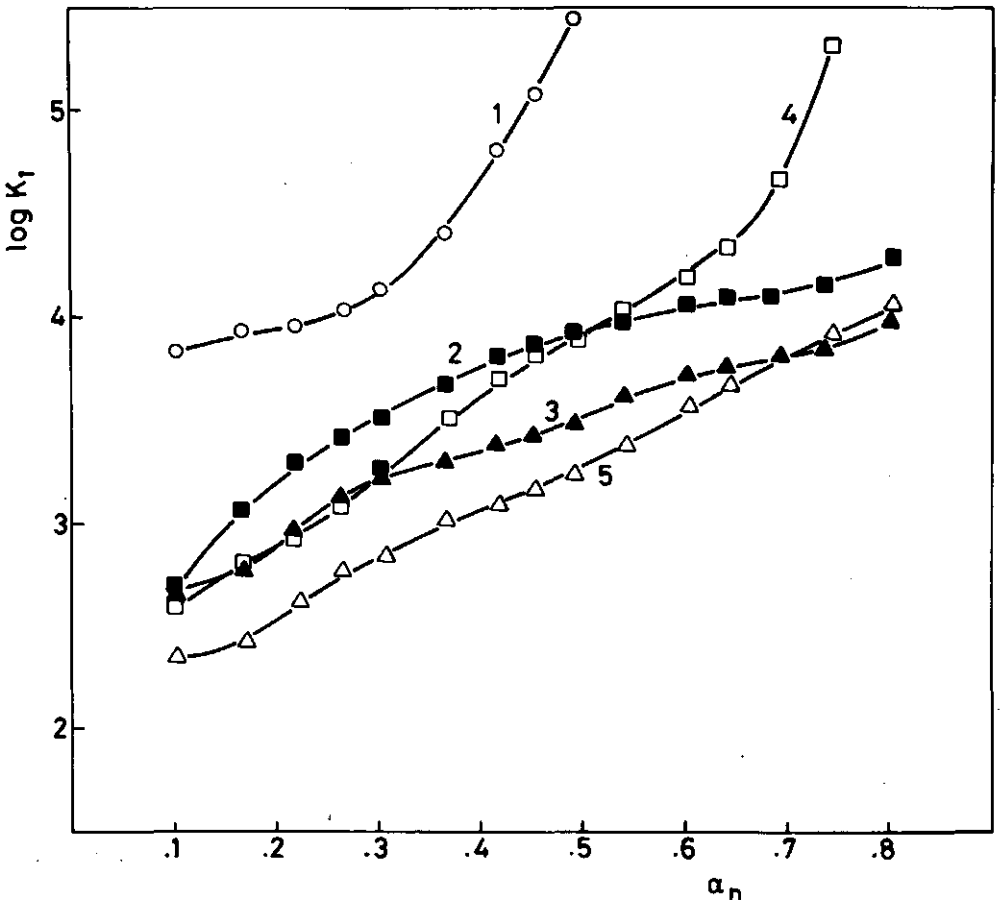

FIGURE 5.25 Dependence of log K_1 on α_n for Pb,Cd,Zn/PMA,PAA systems, from polarographic data. $[KNO_3]$ = 50 mol·m^{-3}. 1-3: M/PMA (D_b/D_f = 0.019); 4-5: M/PAA (D_b/D_f = 0.023). 1. Pb/PMA; 2. Cd/PMA; 3. Zn/PMA; 4. Cd/PAA; 5. Zn/PAA. See also legends of fig. 5.19-5.21.

figure). The corresponding limiting currents are too low to be analysed sufficiently accurately.

The magnitude of the increase of log K_1 with α_n is related to the number of charged ligands. In order to analyse the effect of the polyionic charge, log K_1 is also plotted as a function of α_{eff}, which is

a measure of the actual fractional charge:

$$\alpha_{eff} = \frac{[L^-]_{free}}{[L^-]_{free} + [HL]} \qquad (5.12)$$

where $[L^-]_{free}$ is the concentration of the free ligands, i.e. ligands which are not associated with polarographically bound ions. These plots are presented in fig. 5.26 for M/PMA and in fig. 5.27 for M/PAA. The open symbols represent values of log K_1 calculated on the basis of the *DeFord-Hume* method: eq. 3.25 has been applied for 1:1 complex formation, using $\Delta E_{\frac{1}{2}}$ and i_o/i_ℓ, only for $-\Delta E_{\frac{1}{2}} > 3$ mV. The curves in the figs. 5.26 and 5.27 allow a number of interesting conclusions.

Conformation

For Cd,Zn/PMA, the increase in log K_1 at low α_{eff} is much stronger than at high α_{eff}. It is suggested that this non-linear change of log K_1 with α_{eff} is due to a conformational transition of PMA, since it is not found for M/PAA. For the strongly covalent interaction in Pb/PMA, the compact conformation may persist at higher values of α_{eff}. It should be noted that $\alpha_{eff} < \alpha_d$ for the same degree of neutralization: the conformational transition begins at larger values of α_d than in the corresponding M^{2+}-free system. Although the bound metal ions will stabilize the compact conformation, the polymer will expand upon further deprotonation of the remaining -RCOOH groups. In that case, log K_1 no longer increases in proportion to the newly created charged sites, since the average distance separating bound and free functional groups simultaneously increases. The observation of a non-linear change of the binding strength with increasing charge density for PMA systems is supported by corresponding indications in literature (*Jakubowski*, 1975; *Gustavsson et al.*, 1978).

The curve for Cd/PAA in fig. 5.27 shows signs of a slight transition at about $\alpha_{eff} = 0.3$. Although a slight conformational change is not impossible (*Koda et al.*, 1982), the phenomena could also be due to slight precipitation effects.

$\Delta E_{\frac{1}{2}}$ versus i_ℓ

The values of log K_1 calculated using the *DeFord-Hume* method agree fairly well with those from i_ℓ and D_b/D_f. Generally, the former are slightly higher. As stated in § 3.3.3, the determination of $\Delta E_{\frac{1}{2}}$ is less accurate than that of i_ℓ. Nevertheless, the trends in the values of log K_1 using $\Delta E_{\frac{1}{2}}$ confirm that the increase with α_{eff} is different for M/PMA as compared to M/PAA.

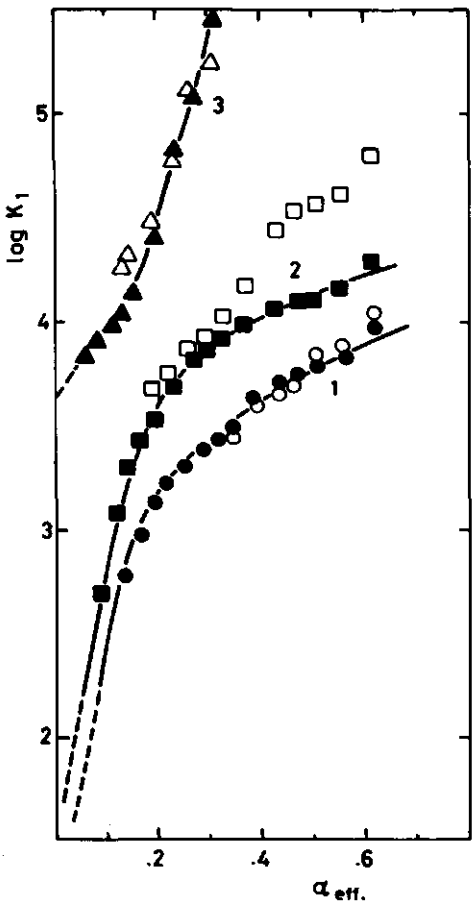

FIGURE 5.26 Dependence of log K_1 on α_{eff} for Zn,Cd,Pb/PMA systems, from polarographic data. $[KNO_3]$ = 50 mol·m^{-3}. Curves: from i_ℓ-data; open symbols: from $\Delta E_{\frac{1}{2}}$-data; 1. Zn/PMA; 2. Cd/PMA; 3. Pb/PMA.

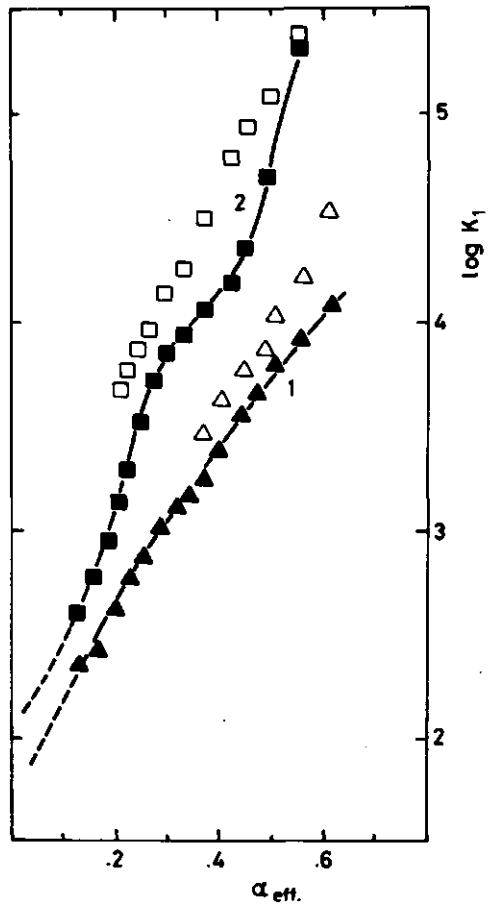

FIGURE 5.27 Dependence of log K_1 on α_{eff} for Zn,Cd/PAA systems from polarographic data. $[KNO_3]$ = 50 mol·m^{-3}. Curves: from i_ℓ-data; open symbols: from $\Delta E_{\frac{1}{2}}$-data; 1. Zn/PAA; 2. Cd/PAA.

dlog $K_1/d\alpha_{eff}$

For the M/PAA system, the change in log K_1 with α_{eff} can be compared with that of $dpK_{app,a}/d\alpha_d$ for the M^{2+}-free system (in fig. 5.1). For Zn/PAA, the slope dlog $K_1/d\alpha_{eff}$ is, on the average, 4.4, and for Cd/PAA it is 5.0, whereas in the M^{2+}-free system at the corresponding 1:1 salt level, $dpK_{app,a}/d\alpha_d$ is 2.5. Thus the model put forward by *Marinsky* (1976), as expressed in eq. (2.14) is reasonably applicable for M/PAA. This implies that the assumption $\psi_s(H^+) \cong \psi_s(M^{2+})$ is a fair approximation for the M/PAA system. The slope dlog $K_1/d\alpha_{eff}$ is a measure of the charging free energy. The value of 4.4 for the slope results in $\psi_s \cong 0.13$ V at $\alpha_d = 1$ (or $\xi \cong 2.9$).
The slight difference between the slopes for Cd/PAA and Zn/PAA may be attributed to the difference in covalency: a somewhat larger α_{eff} is needed to bind the less covalent Zn to the same extent as Cd.

$K_{int}(ML)$

In § 4.1.3, provisional values of K_{int} for the formation of the complex ML were determined on the basis of a crude model, using values of $(d[H]/d[M]a)_m$, pH and K_a at a certain α_n in the conductometric M/L-titrations. In this chapter, it appeared that important properties of the different systems are correctly represented by the provisional results, as far as the sequence of the values is concerned. However, to arrive at reliable absolute values of $K_{int}(ML)$, the fraction bound metal ions has to be determined, concurrently with the pH.

To find $K_{int}(ML)$, the curves in the figs. 5.26 and 5.27 can be extrapolated to $\alpha_{eff} = 0$. In the cases of Cd/PMA and Zn/PMA the extrapolation is difficult because of the large slopes.
In table 5.6 the results are collected. The values of log $K_{int}(ML)$

TABLE 5.6 Log $K_{int}(ML)$ from polarographic data

	Zn	Cd	Pb
PMA	1.1	1.5	3.6
PAA	1.7	2.1	-

for Zn/PAA and Cd/PAA from table 5.6, being 1.7 and 2.1, respectively, are in reasonable agreement with the corresponding values calculated from table 4.3, being 1.1 and 2.9 respectively. However, the values for the Zn,Cd/PMA systems calculated using the crude model in § 4.1.3, are much too low. The underestimation of $K_{int}(ML)$ will be due the

overestimation of K_a in eq. (4.5).

A comparison with the data for the simple acids in table 4.6 suggests that the M/PMA system is better described by the 2-methylpropanoic monomer than the M/PAA system.

A comparison with literature data from *Mandel & Leyte* (1964a) and *Bolewski & Lubina* (1969) is not very well possible, since a different reaction model, different coordination numbers and concentrations were employed. *Travers & Marinsky* (1974) gave values of log K_{int}(ML) for Zn/PMA and Zn/PAA of 1.2 and 1.4 respectively, at an ionic strength of 0.1 mol·dm^{-3}. For infinite dilution, a value of 1.4 for Zn/PMA has been given by *Jakubowski* (1975). These data are in good agreement with those found in the present study.

6 INFLUENCE ADDED 1:1 SALT

As pointed out in § 2.1.1, the effect of the presence of M^+ ions on the M^{2+}/polyacid interaction is two-fold. M^+ affects the activity coefficients of the species in solution, through its contribution to the ionic strength, *and* it may be bound to the polyion, possibly substituting bound M^{2+}. The first effect frequently leads to a $\sqrt{c_1}$ dependency of the apparent binding constant of the M^{2+} ions, whereas the latter effect has been predicted to result in a log c_1 dependency (*Alexandrowicz & Katchalsky*, 1963; *Neumann & Nolte*, 1980). Details of the dependency of the appararent binding constant on the concentration of added 1:1 salt, c_1, may give information on the nature of the binding of M^{2+}, and may reveal the dependency of the exchange bound M^+/M^{2+} on the sample composition.

6.1 POLAROGRAPHY

For a number of systems, viz. Cd,Pb/PAA and Cd,Pb/PMApe, c_1-titrations have been carried out at different values of α_n, and fixed M/L-ratio. The mixing procedure, see § 3.1.2, was applied for the M/PAA systems. However, in the case of Pb/PAA, coagulation occurred even at low c_1. Therefore, no useful series of results were obtained for this system, just like in α_n-titrations of Pb/PAA, as described in § 5.2.3. The addition procedure, see § 3.1.2, using monovalent metal nitrate solutions of high concentration, was applied for the M/PMApe systems. In the range of very low c_1 levels, conduction currents contributed to the polarographic limiting currents. The correction applied to find the pure diffusion currents has been explained in § 3.2.4.

The main results are presented as plots of log K_1 versus log $[KNO_3]_v^{-1}$. In line with the convention that K_1 is calculated in $mol^{-1} \cdot dm^3$ units, the subscript v refers to a value of $[KNO_3]_v^{-1}$ in the same units.

6.1.1 Cd/PAA

In fig. 6.1, results are given for Cd/PAA. Curves 1-3 refer to log K_1 for α_n values of 0.8, 0.6 and 0.3 respectively, and to a $[Cd^{2+}]/[PAA]$ ratio of 0.2.
The curves 2 refer to PAA samples of different molecular mass. Curve 4 represents the mean activity coefficient $\gamma_\pm$ of $Cd(NO_3)_2$ as a function of $[KNO_3]$, according to *Goldberg* (1981).

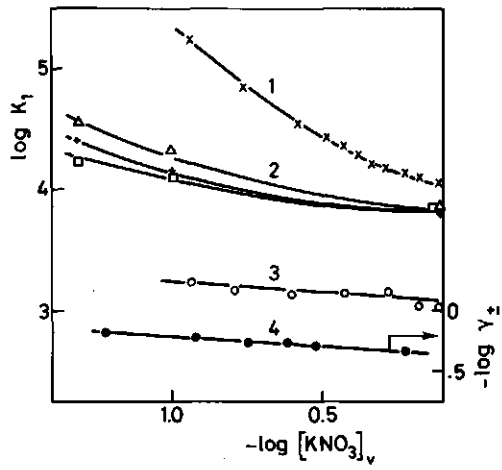

FIGURE 6.1 Influence of added KNO_3 on the apparent metal association constant for Cd/PAA, from polarographic data. [PAA] = 2.52 mol·m^{-3}; $[Cd^{2+}]/[PAA]$ = 0.20. 1. α_n = 0.80, $\bar{M}$ = 300,000; 2. α_n = 0.60, Δ : $\bar{M}$ = 150,000; + : $\bar{M}$ = 300,000; □ : $\bar{M}$ = 50,000; 3. α_n = 0.30, $\bar{M}$ = 300,000; 4. $-\log\gamma_{\pm}$ for $Cd(NO_3)_2$ (right hand ordinate axis).

All polarograms from which curves 1-3 have been constructed, had well-defined limiting currents, both in the NPP and in the SDC mode. Small sharp maxima showed up at the onset of the polarographic waves in NPP at α_n = 0.60 and low c_1 and at α_n = 0.80 at all c_1 levels.

The curves 1-3 demonstrate that over the range of $[KNO_3]$ studied, the slope $S_c = d\log K_1/d\log c_1^{-1}$:

i is positive for all values of α_n;
ii increases with increasing α_n;
iii tends to become equal to the value of $d \log K_1/d \log \gamma_{\pm}$ for increasing c_1 and for decreasing α_n;
iv is practically independent of the molecular mass of the polyion;
v is not constant for a given curve, but tends to become constant at low c_1.

An important conclusion from these observations is that at high α_n, the effect of electrostatic binding of M^+ on the value of K_1 overrules the effect of the presence of M^+ (and NO_3^-) on the activity coefficient of Cd^{2+}. In connotation with this conclusion, it is noted that over the range of $[KNO_3]$ studied, $-\Delta E_{\frac{1}{2}}$ decreases for high α_n (curve 1) from about 40 mV to 10 mV, and the pH decreases from about 5.9 to 5.5, whereas for curves 2 and 3 the changes in $-\Delta E_{\frac{1}{2}}$ and pH are much smaller.

An approximately linear decrease of $\log K_1$ with increasing $\log c_1$ for a M^{2+}/polyacid interaction is in agreement with different theoret-

ical models, whether of the CC type (*Oosawa*, 1971) or of the PB type (*Alexandrowicz & Katchalsky*, 1963). In the PB approach, the slope S_c is seen as a measure of the change of the potential at the binding site (*Bach & Miller*, 1967), and consequently S_c can also be related to the decrease in pH. In the CC approach, S_c reflects merely the exchange ratio bound M^+/M^{2+} (*Record et al.*, 1976). This will be further discussed in § 6.2.1.

The covalent features of the Cd/PAA interaction are reflected in the behaviour of log K_1 at relatively high c_1. S_c decreases with increasing c_1. According to *Lapanje* (1964) and *Lapanje & Oman* (1963), a more than 250-fold excess of KCl was needed to achieve a plateau value in a i_ℓ versus c_1 plot, for the Cd/PAA system, whereas only an approximately 100-fold excess of K_2SO_4 was needed for a Tl/PAA system. These authors concluded that the necessity of such a large excess has to be attributed to the partially covalent character of the Cd/PAA interaction. On the basis of the curves in fig. 6.1, and the demonstrated covalent character of Cd/PAA, see § 5.3.1, we are inclined to follow their conclusion. Both the electrostatic and the covalent contribution to K_1 will decrease with increasing c_1, the former contribution being much more sensitive to c_1 than the latter.

The increase of S_c with α_n at a given c_1 may be attributed to a changing ratio of bound M^+/M^{2+} with changing charge density of the polyion. In connotation with this, the ratio of unbound M^+ and M^{2+} that are partly present in the diffuse double layer, concurrently changes with α_n. In this respect it is noted that plots of log K_1 versus log c_1^{-1} may be different for different experimental strategies and conditions: the 1:1 salt level can be changed at constant $[M^{2+}]_T$ - like in fig. 6.1 - or at constant $[M^{2+}]_T/[M^+]_T$. Preliminary experiments using the latter strategy (by simple dilution of the system) yielded linear plots of log K_1 versus log c_1^{-1} for Cd/PAA at $\alpha_n = 0.60$ and $[Cd^{2+}]/[PAA] = 0.2$, with $S_c \cong 1.5$. At very low M/L, the results of both strategies may converge. General conclusions from details of plots of log K_1 versus log c_1^{-1} can only be drawn with reservation.

6.1.2 Cd, Pb/PMApe

Cd/PMApe

In fig. 6.2, results are presented for Cd/PMApe. The curves 1-3 refer to different values of α_n. For values of log c_1^{-1} higher than

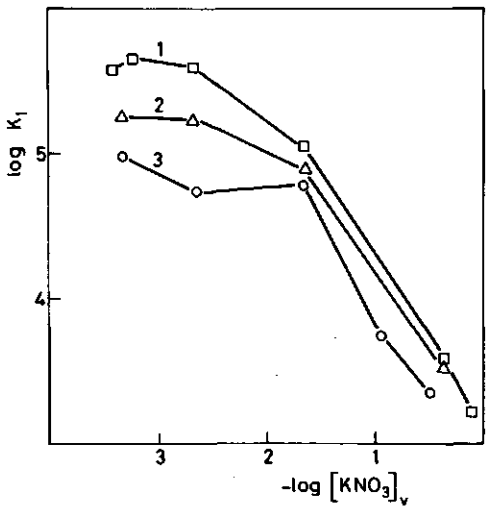

FIGURE 6.2 Influence of added KNO_3 on the apparent metal association constant for Cd/PMApe, from polarographic data. $[PMApe]_i$ = 1.50 mol·m^{-3}; $[Cd^{2+}]/PMApe\}$ = 0.7; 1. α_n = 0.9; 2. α_n = 0.75; 3. α_n = 0.6.

~ 1.7, a correction of i_ℓ for the conduction contribution was necessary. At very low c_1, the polarograms showed several maxima, but they reached a defined limiting value at more negative values of the pulse potential. Tests using the SDC mode confirmed the correctness of the NPP limiting currents. Due to the conduction contribution, the polarographic maxima, and the low concentrations of M^{2+}, the results will be less accurate than for the other polarographic experiments in the present study. However, the experiments with M/PMApe have been repeated a sufficient number of times, ensuring the reproducibility of the trends in the log K_1 versus log c_1^{-1} curves.

For Cd/PMApe these trends are:

i a slope S_c of about 1.1 for high c_1;

ii a decrease of S_c with decreasing c_1 at very low c_1;

iii replacement of K^+ by Li^+ (not in figure) leads to slightly higher values of K_1.

At values of c_1 around 0.1 mol·dm^{-3}, S_c is lower for Cd/PMApe than for Cd/PAA at α_n ~ 0.8, whereas it is somewhat higher at α_n = 0.6. The difference in S_c for different values of α_n are not significant in the case of Cd/PMApe. The differences between fig. 6.1 and fig. 6.2 at corresponding values of c_1, may be related to the difference in covalent character of the systems involved, in charge density of the polyions and/or in the $[Cd^{2+}]/[polyacid]$ ratios. More experiments are needed

to indicate the importance of each of these possibilities.

The surprising decrease of S_c with decreasing c_1, in the range of very low values of c_1 is partly explained, following a suggestion of *Oosawa* (1971), by the screening effects of ions that do not originate from added 1:1 salt, such as Cd^{2+}, and K^+ from added KOH. These screening effects override that of added 1:1 salt at very low c_1. In addition to this, the exchange reaction bound M^+/M^{2+} runs out due to depletion of M^+ for $c_1 \rightarrow 0$. It has been put forward by *Bach & Miller* (1967), for the case of Cd/DNA, that the slope S_c may decrease with decreasing c_1, due to the swelling of the polymer coil. This would reduce the increase in ψ_s with decreasing c_1. However, this argument would be also valid at intermediate values of c_1. We will discuss this subject further in § 6.2.1 in which the results are compared with predictions from the electrostatic models.

The fact that added $LiNO_3$ leads to somewhat higher values of K_1 as compared to an equal concentration of KNO_3 demonstrates that Li^+ less effectively competes with M^{2+}. This suggests that the electrostatic attraction of Li^+ is smaller than that of K^+, which may be due to a larger radius of Li^+. This would imply that Li^+ operates in some hydrated form. This finding does not agree with conclusions of *Crescenzi et al.* (1959, 1960) and *Eldridge & Treloar* (1970) for the Li/polycarboxylate interaction. However, the relatively large M/L-ratio applied for the Cd/PMApe system may have influenced the order: the fraction of M^+ that is bound will be relatively low, and consequently the effect of possible partial dehydration will be small.

Pb/PMApe

In fig. 6.3, results are presented for Pb/PMApe for different values of α_n. Several maxima have been observed on the polarographic waves, like in the case of Cd/PMApe. Generally, reasonably defined limiting currents were reached at more negative values of the pulse potentials. At high c_1, the maxima are small, or absent. Simultaneously, coagulation occurs at high c_1, limiting the range over which the influence of added 1:1 salt was studied.

The three curves are characterized by a very low value of S_c. The low values of S_c continue in the region of concentrations 1:1 salt, where corrections for conduction contributions are not needed. The low values of S_c are partly attributed to the stronger covalent character of the Pb/PMApe interaction, as compared to Cd/PMApe, and partly to the higher M/L-ratio applied. More experiments are needed to discrimi-

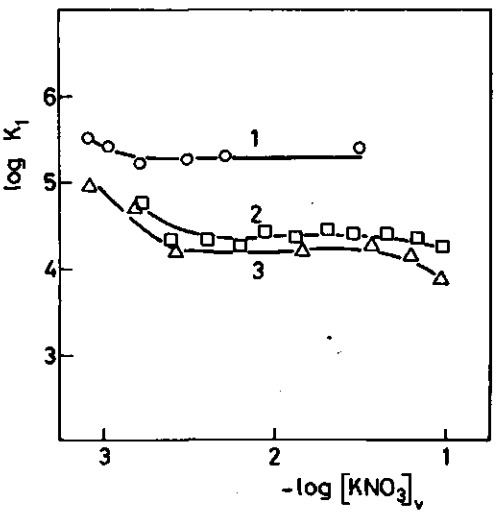

FIGURE 6.3 Influence of added KNO_3 on the apparent metal association constant for Pb/PMApe, from polarographic data. [PMApe] = 0.3 mol·m^{-3}; [Pb^{2+}]/[PMApe] = 1.0; 1. α_n = 0.8; 2. α_n = 0.45; 3. α_n = 0.2

nate between these possibilities.

Using $CsNO_3$ as the added 1:1 salt, no significant differences with KNO_3, neither with respect to the magnitude nor to the c_1-dependency of K_1 could be observed. This seems to stress the significance of the observation for added $LiNO_3$ in the case of Cd/PMApe, since the hydrated radii of K^+ and Cs^+ are almost equal (*Conway*, 1980). In addition to this, it has been reported by *Kurenkov et al.* (1979) that values of i_ℓ for Cd/PAA with [Cd^{2+}]/[PAA] = 1, where PAA had been neutralized by NaOH, were smaller than for the corresponding solutions where KOH had been used. The data support the conclusion that at high M/L, the Cd^{2+}/-COO^- association constant is increasingly lowered by the presence of M^+ in the order Li < Na < K ≅ C_s, that is with decreasing radius of the *hydrated* M^+ ion.

6.1.3 pH effects

Upon addition of 1:1 salt to partially neutralized PMA (*Mandel & Leyte*, 1964) and PAA (*Nagasawa*, 1971) the pH decreases. According to *Oosawa* (1971) and *Manning & Holtzer* (1963) using CC models, and according to *Nagasawa* (1971) using a PB model, the decrease in $pK_{app,a}$ (and pH) at a given α_d, is linear in log c_1. Experimentally and theoretically, the slope $dpK_{app,a}/dlogc_1^{-1}$ is unity at high α_d, and smaller than unity at low α_d.

In the presence of M^{2+}, the dependency of the pH on c_l is more complex. In the c_l-titrations of the M/PMApe systems, it has been observed that the initial additions of 1:1 salt caused a small rise (< 0.2 pH unit), whereas further additions led to a small decrease in pH. The higher the pH, the smaller the initial rise.

A rise in the pH as a result of increasing c_l can be attributed to a diminishing suspension effect (see § 3.4.3), and to a decrease of the activity coefficient of H^+ ions in the bulk. The subsequent decrease of the pH is attributed to the screening of the polyion charges.

In the M/PMApe systems studied, the changes in the pH with changing c_l were small, due to the high M/L-ratios applied. Therefore, the pH effects have been separately investigated for Cd/PAA at low M/L, and different values of α_n. Additionally, the pH effects for the corresponding Cd^{2+}-free systems have been determined. The results are presented in fig. 6.4.

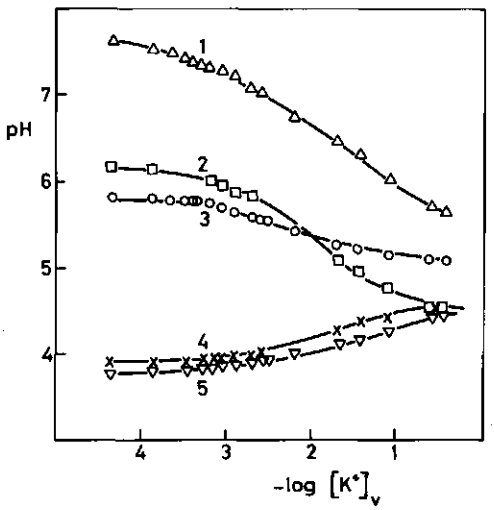

FIGURE 6.4 Influence of added KNO_3 on the pH of solutions of PAA in the presence and in the absence of $Cd(NO_3)_2$, and of a HNO_3 solution. 1. α_n = 0.60, no Cd^{2+}; 2. α_n = 0.30, no Cd^{2+}; 3. α_n = 0.60, $[Cd^{2+}]/[PAA]$ = 0.21; α_n = 0.30, $[Cd^{2+}]/[PAA]$ = 0.21; 5. HNO_3, pH_{init} = 3.76.

The curves 1 and 2 refer to the Cd^{2+}-free systems for α_n values of 0.6 and 0.3 respectively. At high α_n, the decrease in pH with increasing $\log[K^+]_v$ is approximately linear. The curves 3 and 4 refer to $[Cd^{2+}]/[PAA]$ = 0.21 for α_n is 0.6 and 0.3 respectively. Between the curves 3 and 4, an important difference is observed: the pH decreases with increasing c_l in the former, whereas it increases in the latter. The occurrence of this phenomenon seems to be related to the ratio $[Cd^{2+}]/[-COO^-]$, which is smaller than 0.5 for curve 3, and larger than 0.5

for curve 4. Since an increase in pH is not observed for Cd/PAA at α_n = 0.6, it is not reasonable to assume that a diminishing of the suspension effect would cause the rise in pH for the M^{2+}/polycarboxylate systems at higher M/L. Thus the increase in pH in curve 4, and in the M/PMApe experiments, is very likely to be a result of the decrease of the H^+ activity. If $[Cd^{2+}]/[-COO^-] > 0.5$ the polyion charges are effectively screened by Cd^{2+} present. Addition of K^+ affects in that case predominantly the activity coefficient of H^+ in the bulk, and a rise in pH with increasing c_1 is observed in curve 4.

To estimate separately this activity effect, a solution of HNO_3 with pH = 3.76 was investigated. The rise in pH upon addition of KNO_3 is plotted in curve 5. It is evident that the curves 4 and 5 are almost parallel, supporting the operation of the activity effect in curve 4.

6.2 FURTHER DISCUSSION

6.2.1 M^+/M^{2+} exchange

On *a priori* grounds, the influence of small ions on a highly charged polyion may be expected to be very complex (*Katchalsky*, 1971). Addition of 1:1 salt to a M^{2+}/polyacid system triggers a series of rearrangements of all charged entities. It affects the binding of divalent metal ions with the polyion mainly through the following interrelated but distinct mechanisms:

i Binding of M^+: the competition with M^{2+}, controlled by the polyionic charge density, will significantly contribute to the ion binding scheme (substitution effect);

ii Accumulation of free M^+ in the diffuse layer: the ratio M^+/M^{2+} of the mobile counterions, controlled by the effective charge density of the polyion will also influence the M^+/M^{2+} exchange (screening effect);

iii Regulation of the activity coefficients of M^{2+} and M^+: an increase in c_1 will lower these coefficients (activity effect);

iv Covalent binding of M^+ and/or NO_3^-: complex formations $M^+/-COO^-$ and M^{2+}/NO_3^- may interfere with the M^+/M^{2+} exchange equilibrium (covalency effect).

For highly charged polyions, the 1:1 salt effects (i) and (ii), controlled by ξ or ξ_{eff}, will be dominant. In connotation with this

it is noted that for extreme concentrations c_1, polyelectrolyte models based on smeared-out charges may fail: for very low c_1 due to end-effects and for very high c_1 due to insufficient field-overlap (*Nagasawa*, 1974). From curve 4 in fig. 6.1 it is evident that the change in log $\gamma_\pm$ for $Cd(NO_3)_2$ with log c_1, effect (iii), is small as compared to the change in log K_1 at high α_n. Covalency effects (iv) are not expected to be important for the alkali nitrates used in the systems investigated.

In § 2.2.2 the equilibrium constant K_{ex} for the exchange reaction in eq. (2.4) has been related to the apparent metal association constant $K_{app,1}$, in eq. (2.9).
If the effects of the mechanisms (ii)-(iv) are relatively small, which is likely to be the case at low c_1, low M/L and high α_n, then the slope S_c can be derived from eq. (2.9), in the short notation with K_1 and c_1:

$$S_c = - \frac{d\log K_1}{d\log c_1} \cong w \qquad (6.1)$$

In eq. (6.1) w is the number of bound M^+ ions that are exchanged for one bound M^{2+} ion. It has been pointed out by *Record et al.* (1976, 1978) that if a significant amount of M^+ is part of the diffuse layer, then the value of S_c is also significantly controlled by mechanism (ii), at higher c_1, M/L and lower α_n. In that case S_c is a measure of the number of M^+ released into the bulk upon binding of one M^{2+}.

For the Cd/PAA system at $\alpha_n = 0.8$ in fig. 6.1, it is evident that S_c may reach a value of about 2. At lower α_n and/or higher M/L, S_c decreases to values lower than 2. The fact that the exchange ratio bound M^+/M^{2+} is about 2 *only* at low $[M^{2+}]/[-COO^-]$ ratio, has also been found for carboxymethylcellulose systems (Ca + Na)/CMC (*Rinaudo & Milas*, 1972), for polystyrenesulphonate systems (Cu + Na)/PSS, for maleic acid copolymer systems (Cu + Na)/MAC (*Miyamoto & Imai*, 1980) and for dextran sulphate systems (Cu + Na)/DS (*Miyamoto*, 1981). Exchange ratios bound M^+/M^{2+} significantly larger than unity can be calculated from results for (Ca + Na)/PSS (*Kwak et al.*, 1976) and (Ca + Na)/MAC (*Shimizu et al.*, 1981), at low $[M^{2+}]/[-COO^-]$. Additionally, *Rinaudo & Milas* (1972) found a dependency of the exchange ratio on the polyion charge density.

It is interesting to note that *Kwak et al.* (1976) and *Shimizu et al.* (1981) consider their findings to be in full agreement with the CC theory, whereas the exchange ratio larger than unity found by *Miyamota & Imai* (1980) and *Miyamoto* (1981) at low $[M^{2+}]/[-COO^-]$ were at-

tributed to either covalency effects, or the inapplicability of the thin-rod model. It is further noted that the cited authors used different experimental strategies to realize variation of $[M^+]/[M^{2+}]$.

From the analysis of S_c, considering literature data for similar systems, it is concluded that for the (Cd + K)/PAA system, the exchange ratio is dependent on the $[Cd^{2+}]/[-COO^-]$ ratio, and may reach a value of 2, at high α_n and low c_1.

6.2.2 Comparison with models

As pointed out in § 2.2.4, both in the CC model of *Manning* and in the PB model of *Guéron* and *Weisbuch*, very large local concentrations of counterions occur in the vicinity of a highly charged polyion. The theories agree on two important points.

i In polyelectrolyte solutions with only one type of counterion, the local concentrations are largely independent of the bulk concentrations;

ii In mixed systems, there is a preference for accumulation of divalent ions over monovalent ions.

This preference (ii) has been expressed in rather similar equations. In the PB model (*Guéron & Weisbuch*, 1980; *Weisbuch & Guéron*, 1981) it has been derived that for low concentrations of divalent ions in the bulk, c_2:

$$\frac{CIV_2}{c_2} \cong \frac{CIV_1^2}{c_1^2} \tag{6.2}$$

In the CC model (*Manning*, 1978b), it has been derived that for low θ_2:

$$\frac{c_2(loc)}{c_2} \cong e \cdot \frac{c_1^2(loc)}{c_1^2} \tag{6.3}$$

In addition to this, both in the PB model and in the CC model, it is derived that the dependency of the local concentrations of divalent ions on c_1 is given by:

$$\frac{d\log CIV_2}{d\log c_1^{-1}} = \frac{d\log c_2(loc)}{d\log c_1^{-1}} \cong +2 \tag{6.4}$$

under the conditions that (in PB) c_2 and (in CC) θ_2 are very low and approximately constant. Our finding that S_c reaches a value of about 2 in the Cd/PAA system at high α_n agrees with the expressions in eq. (6.4), since $c_2(loc)$ is directly related to K_1.

It can be deduced from the PB model, that for higher values of c_2, the slope dlog CIV_2/dlog c_1^{-1} will be lower than 2, ultimately yielding a value of unity.

In the CC model, *Manning* (1978b) derives an expression for the case of high θ_2:

$$\frac{\text{dlog } c_2(loc)}{\text{dlog } c_1^{-1}} = 2 \cdot \xi \cdot (1-2\theta_2) \qquad (6.5)$$

For $c_1 \to 0$, θ_2 will increase, and according to eq. (6.5), $c_2(loc)$ will become less dependent, ultimately independent of c_1. The low values of S_c in the range of very low c_1 for the Cd/PMApe system in fig. 6.2 corroborate this aspect of the CC theory. A decrease of the dependency of the binding constant on c_1 has also been demonstrated for the systems (Mg + Na)/DS and (Ca + K)/DS by *Joshi & Kwak* (1981).

7 POLYELECTROLYTE EFFECTS OF HUMIC ACIDS

7.1 INTRODUCTION

7.1.1 Humic acid chemistry

Humic acids are the main constituents (80%) of soil organic matter (humus) and of dissolved organic matter in natural waters (*Hurst & Burges*, 1967; *Reuter & Perdue*, 1977). The ability of humic material to form salts and metal complexes has already been demonstrated by *Odén* (1912), who also divided humic material into brown, alkaline-soluble humic acid (HA) and yellow fulvic acid (FA) which is also soluble in acid solution (*Schnitzer & Khan*, 1976). Over the past century, many efforts have been undertaken to reveal the (physico-)chemical nature of humics and their metal complexes (*Flaig et al.*, 1975; *Stevenson*, 1982). Many experimental results seemed to be contradictory, and this has often been attributed to the idiosyncrasies of the 'local' sample. Nevertheless, it is now well-established that:

i HA and FA are polydisperse mixtures of random-copolymeric materials: more than 150 different 'monomeric' units have been identified (*Choudry*, 1981), and the average molecular mass in natural samples is generally in the range from about 1,000 to 100,000 (*Piret et al.*, 1960);

ii The functional groups in HA and FA are predominantly carboxyl and phenolic-hydroxyl groups (*Hayes & Swift*, 1978). The average total number of titratable groups is in the range of 8-24 mol/kg carbon for widely differing compositions (*Stevenson*, 1982). The acid capacity of FA is generally larger than that of HA (*Schnitzer & Ghosh*, 1979), and it decreases with increasing molecular mass (*Banerjee & Sengupta*, 1977);

iii The association of metal ions with the functional groups in HA and FA occurs predominantly through the carboxyl groups (*Vinkler et al.*, 1976; *Kerndorff & Schnitzer*, 1980). Is has been reported that trivalent metal ions (*Křibek et al.*, 1977), metal ions of the transition series (*Schnitzer*, 1969), the rare earth elements (*Nash & Choppin*, 1980), the alkaline earth (*Choppin & Shanbag*, 1981) and the alkali metals (*Gamble*, 1973) may be bound by humic material. However, binding constants of a given metal reported by different investigators, may differ up to 7 units of log K (*Buffle et al.*, 1984) for different samples and up to 5 units of log K (*Himes & Barber*, 1957) for the same sample of different pH values.

The binding of metals to HA and FA is of great agricultural and environmental importance. Humic material substantially contributes to the control of the pathways of metals in geosystems: it is able to extract metals from rocks and minerals (*Singer & Navrot*, 1976; *Rochus*, 1982), it keeps metal ions in solution, and transports them (*Zunino & Martin*, 1977a,b), it also deposits them again, depending on the local geochemical environment (*Putilina & Varentsov*, 1980). The stabilities of metal-humic complexes are generally higher than those of inorganic complexes of the metals (*Reuter & Perdue*, 1977) and those for adsorption of metal ions on clays (*Harding & Healy*, 1979; *Slavek & Pickering*, 1981). Humic material helps to control the bio-availability of metal ions at the plant root, and determines the fertility of soils to a great extent (*Stevenson*, 1982), due to the cation exchange and pH buffering capacities (*Gamble et al.*, 1983).

Levels of toxic metals (e.g. Pb, Cd) and toxic levels of nutrient metals (e.g. Zn) can only be predicted for a multi-component ecosystem if the relations between concentrations and chemical parameters are well-defined.

In this chapter we will focus on the possible importance of polyelectrolyte effects in the metal binding to humic and fulvic acids. More specifically, the question is considered to which extent the metal binding may be affected by the polyelectrolyte character of these ligands. To that end, the information on the synthetic polycarboxylic systems in the previous chapters will be used. Humic material is essentially polycarboxylic, and in fertile soils (pH levels from 6-7) most of the carboxylic groups are deprotonated.

7.1.2 Polyelectrolyte effects & mixture effects

The large dispersion in 'equilibrium constants' of the metal complexation for a given sample of humic material at different experimental conditions, has been attributed to the polyfunctional character of the material (*Gamble et al.*, 1980): although most of the functional groups are similar, they are assumed to be not entirely identical with respect to their chemical environment, and consequently every 'class' of groups will show its own equilibrium constant. Under different (experimental) conditions (pH, ionic strength, concentration of reactants), different classes of sites are involved in the equilibrium reactions. In this concept, the apparent association constant is seen to be a weighted average of the values of the association constants of all the

components. In the following we will denote this reason for variation of the apparent association constant: the *mixture* effect.

Although the mixture effect will certainly be operative in natural HA and FA, it is suspected, on a priori grounds, that a *polyelectrolyte* effect is also operative:

i A simple calculation learns that the number of charged sites *per molecule* can be large. For 9 moles of groups per kg carbon (our HA sample, see § 3.2.5) and a 50% carbon content (*Kuwatsuka et al.*, 1978), that number is 45, if $\bar{M}$ = 10,000. For this molecular mass, a coil diameter for HA of about 6 nm has been given by *Thurman et al.* (1982). Other authors reckoned with numbers of 15 (*Frimmel*, 1981) and 20 (*Brady & Pagenkopf*, 1978) for $\bar{M}$ = 3,000 in both cases. Using the polyion sphere model, and a uniform distribution of charges, these data result in an average charge separation of about 1 nm. A more realistic non-uniform distribution in space may lead to even shorter charge spacings along the backbone of the polyions (and thus to high charge densities);

ii The reduced specific viscosity of an HA solution increases upon dilution (*Rajalakshmi et al.*, 1959; *Piret et al.*, 1960; *Reuter & Perdue*, 1977; *Hayano et al.*, 1982), which is a typical polyelectrolyte effect;

iii The dependence of log $K_{app,j}$ on the ionic strength has been reported to be dramatically strong for Pb, Cd/HA (*Stevenson*, 1976);

iv There is binding of Na^+ and K^+ by the carboxylate groups of FA (*Gamble*, 1973).

These considerations strongly point at a polyelectrolyte effect in the M^{2+}/HA,FA interaction.

A number of authors mentioned the possibility of a polyelectrolyte effect in the binding of metals with humic material (*van Dijk*, 1960; *Banerjee & Mukherjee*, 1971; *Deb et al.*, 1976; *Arai & Kumada*, 1977; *Bloom & McBride*, 1979; *Gamble et al.*, 1980; *Ghosh & Schnitzer*, 1981; *Young et al.*, 1982; *Buffle et al.*, 1984), but to our knowledge, only *Marinsky et al.* (1980), *Nash & Choppin* (1980) and *Tuschal & Brezonik* (1984) explicitly employed a polyelectrolyte term ΔlogK (see eq. 2.11).

Nash & Choppin (1980) successfully employed eq. (2.14) for a Th^{4+}/HA system. A value d log K_1/d $pK_{app,a}$ of slightly smaller than 4 was found. *Marinsky et al.* (1980), working with peat in a two-phase system, concluded that for Cd, Pb, Zn, Ca, Cu/HA systems the mixture effect (in the cited study: heterogeneity effect) is more important than the

polyelectrolyte effect. However, with respect to Cu/HA this conclusion has been reversed later (*Marinsky et al.* 1982). *Tuschall & Brezonik* (1984) concluded from analogies between M^{2+}/HA and M^{2+}/polyasparatic acid with respect to the forms of the *Scatchard* plots of these systems, that polyelectrolyte effects will be important in all the systems.

Gamble et al. (1980) elaborated the mixture effect theoretically, and gave the following expression for the apparent equilibrium constant, as a number average of the individual equilibrium constants $K_{(r)}$ for each of the r classes of sites on humic material:

$$K_{app,j} = \frac{1}{[L^-]_f} \Sigma K_{(r)} \cdot [L^-]_{(r)} \qquad (7.1)$$

Eq. (7.1) has been elaborated for different experimental conditions and strategies (*Gamble et al.*, 1980; *Langford et al.*, 1983), for multiple exchange equilibria (*Gamble et al.*, 1983) and for the deprotonation equilibrium (*Gamble*, 1970). The problem now is that eq. (7.1) masks any polyelectrolyte effect, as long as variation of $K_{app,j}$ is interpreted only as the result of the differences in the *types* of sites exposed under different experimental conditions. According to *Buffle et al.* (1984) the polyelectrolyte effect is only important at high M/L ratios, whereas at low M/L the mixture effect dominates.

Possible polyelectrolyte effects of humic acids have also been analyzed on the basis of acid/base titration curves: *Young et al.* (1981) concluded that the increase of $pK_{app,a}$ with α_n can be satisfactorily interpreted in terms of purely electrostatic assumptions; *Varney et al.* (1981) stressed that electrostatic interaction are important in the protolytic behaviour of HA; *Davis & Mott* (1981) believed that electrostatics alone cannot account for the change of $pK_{app,a}$ with α_n; *Posner* (1964, 1966) stated that HA is not a polyelectrolyte, and that a Gaussian distribution of pK_a values in the mixture of acids accounts for the titration behaviour.

Summarizing, it must be concluded that the recent literature is most contradictory on the existence as well as on the importance of polyelectrolyte effects in cation binding by humic material. Moreover, the studies on polyelectrolyte effects in these natural systems are often tentative and circumstantial.

In the present study a number of conductometric and polarographic M/L-titrations are carried out on Cd,Pb,Zn/HA,FA systems for different values of α_n, on the analogy to those for the synthetic polycarboxylic acid systems. The polyelectrolyte effects observed in the latter sys-

tem are comparatively considered in the discussion of the results of the former.

7.2 LITERATURE DATA ON Cd,Pb,Zn/HA,FA

7.2.1 Characteristics of humic & fulvic acids

Composition and structure

The elemental composition, the functional groups and the major chemical structures of 'model' HA and FA are given in table 7.1. The data, from *Schnitzer & Ghosh* (1979) have been calculated on the basis of numerous analyses of HA and FA samples from widely differing soils, and agree with those from other studies (*Kuwatsuka et al.*, 1978; *Tsutsuki & Kuwatsuka*, 1978; *Stevenson*, 1982). An important difference between HA and FA is that FA contains more titratable groups per kg of material (*Silva et al.*, 1981). This accounts for the more hydrophilic character of FA. Generally, aquatic organic matter contains higher levels of carboxylic groups than soil organic matter (*Gillam & Riley*, 1982). FA is assumed to function sometimes as a precursor of HA (*Choudry*, 1981). HA and FA can be regarded as polycondensation products of random collections of benzenecarboxylic and phenolic acids. HA is highly condensed, whereas FA is rather poorly condensed (*Schnitzer & Khan*, 1976; *Hayes & Swift*, 1978). About 50% of the total carbon of HA is in aromatic structures, about 20% in carboxyl groups and about 30% in aliphatic or alicyclic structures (*Hurst & Burges*, 1967).

TABLE 7.1 Elemental composition, functional groups, and major chemical structures in model HA & FA

	HA	FA
% weight		
C	56.2	45.7
O	35.5	44.8
H	4.7	5.4
N	3.2	2.1
S	0.8	1.9
mol/kg		
COOH	3.6	8.2
phenolic OH	3.9	3.0
alcoholic OH	2.6	6.1
ketonic, quinonoid c=o	2.9	2.7
% weight		
aliphatic	24.0	22.2
phenolic	20.3	30.2
benzenecarboxylic	32.0	23.0
(SCHNITZER & GHOSH, 1979)		

Several structural formulas representing unit building blocks of humic material have been proposed. According to *Schnitzer & Ghosh* (1979), phenolic and benzenecarboxylic acids are linked by hydrogen bonds only. According to Fuchs (*Szalay & Szilágyi*, 1969), an HA unit contains may fused rings. Both extreme proposals have been criticized (*Choudry*, 1981; *Stevenson*, 1982). Intermediate constructions have been given by *Buffle* (1977) and *Green & Manahan* (1979). The building unit suggested by the latter authors is shown in fig. 7.1.

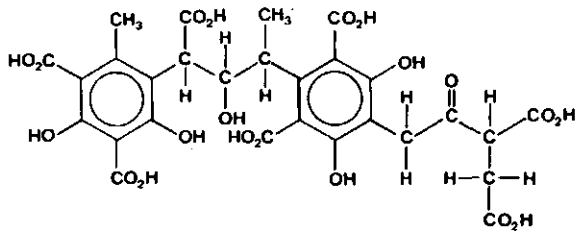

FIGURE 7.1 Model of the structure of a humic acid building unit.

Shape and Size

In solution, HA and FA are spherical random coils (*Hayes & Swift*, 1978; *Ghosh & Schnitzer*, 1980, 1981; *Visser*, 1982). They have an open structure (*Chen & Schnitzer*, 1976) and show some flexibility (*Hayano et al.*, 1982).

According to *Ritchie & Posner* (1982), the shape of HA is not affected by the pH. The size is believed to decrease with increasing pH, due to desintegration of the assumed aggregates in solution (*Wershaw & Pinckney*, 1971; *Sipos et al.*, 1978). However, an increase in size with increasing pH (*Varney et al.*, 1981), with decreasing concentration and decreasing ionic strength (*Ghosh & Schnitzer*, 1980, 1982) due to electrostatic effects has also been reported.

According to *Lapen & Seitz* (1982) the small FA molecules do not change size and shape with pH or ionic strength.

Data for the size of HA and FA in solution that were reported to correspond with certain molecular masses, show a wide spread (*Stevenson*, 1982). In table 7.2, a number of data are collected from different sources, that show a reasonable coherence.

TABLE 7.2 Radii of gyration of humics (orders of magnitude)

$\bar{M}$	r nm	reference
3,000	1	VARNEY ET AL., 1981
5,000	2	HAYES & SWIFT, 1978
10,000	3	THURMAN ET AL., 1982
20,000	4	RITCHIE & POSNER, 1982
70,000	7	FLAIG ET AL., 1975

Acid/base titrations

Acid/base titration curves of humics have been extensively studied. An important feature is the increase of $pK_{app,a}$ with α_n (*Young et al.*, 1982). As mentioned in § 7.1.2, this increase has been attributed alternatively to polyelectrolyte or mixture effects.

Several attempts have been made to distinguish classes of carboxylic groups, on the basis of conductometric or potentiometric results. *Schnitzer & Khan* (1976) claim that two types can be distinguished: ortho to phenolic OH (salicylic acid like) and adjacent to another carboxyl group (phtalic acid like). *Gamble* (1970), *Sposito et al.* (1977) and *Arai & Kumada* (1977a,b) found three classes of carboxylic sites. The phenolic OH groups are not deprotonated at pH<9. According to *Perdue et al.* (1980), distinction in classes is not realistic, since both polyelectrolyte and mixture effects are operational. We will discuss the classification further in § 7.4.1.

Values of the intrinsic pK_a for FA were reported to be slightly lower than 4 (*Davis & Mott*, 1981).

7.2.2 Metal binding

Literature data on binding of heavy metals with humic material are very abundant (*Flaig et al.*, 1975; *Stevenson*, 1982). It is generally observed that apparent association constants are strongly dependent on the concentrations of the reactants (*Beneš et al.*, 1976; *Saar & Weber*, 1979; *Gamble et al.*, 1980), on the ionic strength (*Schnitzer & Hansen*, 1970; *Deb et al.*, 1976; *Stevenson*, 1976; *O'Shea & Mancy*, 1978) and on the pH (*Schnitzer & Skinner*, 1966; *Cheam & Gamble*, 1974; *Lakatos et al.*, 1977; *Buffle et al.*, 1977; *Beveridge & Pickering*, 1980).

There is no consensus on a general order of metals with increasing binding constants for the M^{n+}/HA interaction. For example, the *Irving-Williams* series is followed according to *Khanna & Stevenson* (1962) and

Zunino & Martin (1977a,b), whereas it is not followed according to *Adhikari et al.* (1977) and *Schnitzer & Skinner* (1967).

Cd, Pb, Zn

With respect to the metals investigated in the present study, association constants for the interaction with humic material have been reported to decrease in the series Pb>Cd>Zn (*Guy & Chakrabarti*, 1976; *Takamatsu & Yoshida*, 1978; *Kerndorff & Schnitzer*, 1980; *Beveridge & Pickering*, 1980; *Slavek et al.*, 1982), whereas according to *Sposito et al.* (1981) and *Marinsky et al.* (1980) the order for Cd and Zn is reverse. In table 7.3, a number of literature values of log K_1 are given to indicate their orders of magnitude: a 1:1 binding (viz. 1 metal ion : 1 carboxylate group) is generally assumed for Pb (*Buffle et al.*, 1977; *Saha et al.*, 1979), for Cd (*Saar & Weber*, 1979; *Whitworth & Pagenkopf*, 1979) and for Zn (*Elgala et al.*, 1976; *Adhikari et al.*, 1977).

TABLE 7.3 Literature values of apparent association constants, for 1:1 complexes

	log K_1	
	low pH	high pH
Pb/HA pH	4.1 (SCHNITZER & HANSEN, 1970); 5.0	7.8 (ERNST ET AL., 1975); 7.8
Pb/FA pH	4.0 (SAAR & WEBER, 1980a); 4.0	6.3 (BUFFLE ET AL., 1977); 6.7
Cd/HA pH	3.3 (TAKAMATSU & YOSHIDA, 1978); 4.0	6.3 (WHITWORTH, 1982); 7.5
Cd/FA pH	3.0 (CHEAM & GAMBLE, 1974); 5.0	6.0 (BRADY & PAGENKOPF, 1978); 7.7
Zn/HA pH	2.6 (ADHIKARI ET AL., 1977); 4.0	5.2 (MANTOURA ET AL., 1978); 8.0
Zn/FA pH	1.7 (SCHNITZER & SKINNER, 1966); 3.5	4.0 (ELGALA ET AL., 1976); 7.0

Generally, the values for M^{2+}/HA are larger than for M^{2+}/FA. This is in agreement with the finding of *Guy & Chakrabarti* (1976) and *Křibek et al.* (1977) that the metal ions are bound by the higher, rather than by the lower molecular mass fraction of HA, which could be related to the interaction between the sites.

Depending on pH and M/L ratio, precipitation may occur: the M/L ratio at which precipitation starts, increases in the series Pb < Cd < Zn (*Verloo & Cottenie*, 1972; *Pagenkopf & Whitworth*, 1981). According to *Saar & Weber* (1980) a remarkable difference between Pb/HA,FA and Cd/HA,FA is that after precipitation binding of Pb continues, whereas the Cd precipitate is saturated.

Character of the binding

Sufficient evidence exists, mainly from infrared spectroscopy, that the carboxylate groups form the major binding sites (*Khanna & Stevenson*, 1962; *Khalaf et al.*, 1975; *Vinkler et al.*, 1975, 1976; *Adhikari & Hazra*, 1976; *Kerndorff & Schnitzer*, 1980; *Boyd et al.*, 1981). Thus the number of titratable groups generally determines the maximum binding capacity of humic material (*Stevenson*, 1976). The binding of heavy metals by humic material is partially covalent (*Martin & Reeve*, 1958; *van Dijk*, 1971; *Lakatos et al.*, 1977; *Prasad & Sinha*, 1981). According to *Slavek et al.*, (1982) ∿ 80% of Cd or Zn, and ∿ 50% Pb associated with humic acid is exchangeable using a variety of mineral acids.

The role of phenolic OH in the metal binding is not clear. According to *Zunino & Martin* (1977a,b), *Buffle et al.* (1977), *Gamble et al.* (1980), *Kerndorff & Schnitzer* (1980) and *Piccolo & Stevenson* (1982), phenolic OH, adjacent to a carboxylate group, forms a salicylate-like structure with M^{2+}. This configuration requires replacement of the phenolic proton. Phtalate-like structures, involving adjacent carboxylates, are also possible, but, according to *Takamatsu & Yoshida* (1978) and *Boyd et al.* (1981), less probable. Stability constants for the formation of heavy metal salicylates an phtalates are generally a few log units *lower* than those for humates and fulvates. For example, values of log K_1 for cadmium salicylate and for cadmium phtalate are about 3.5 and 2.5 respectively (*Martell & Smith*, 1977).

The number of protons released upon binding of one M^{2+} ion with HA or FA is generally much smaller than unity (*Khan*, 1969; *Buffle et al.*, 1977; *Saar*, 1980). On the basis of the analogy with our findings for the synthetic systems, this observation suggests the importance of electrostatic interactions.

Reactions of heavy metal ions with humic acids are predominantly entropically driven (*Adhikari & Chakrabarti*, 1977; *Nash & Choppin*, 1980; *Choppin & Shanbag*, 1982). This observation is also very similar to what has been reported for PMA and PAA.

With respect to the kinetics of the metal binding, it has been reported that in Cd,Zn/HA systems, equilibrium is reached within a few minutes (*Gardiner*, 1974b; *Bunzl et al.*, 1976). Charge neutralization reactions (*Pagenkopf & Whitworth*, 1981) and acid/base reactions with humic acid (*Borggaard*, 1974) are fast, whereas possible conformation changes, usually at high pH, are not.

7.3 RESULTS

Conductometric and polarographic M/L-titrations have been carried out on Cd,Pb/FA and Cd,Pb,Zn/HA systems. HA, as used in these experiments, refers to the Fluka sample described in § 3.2.5. FA, in these experiments, refers to the sample from the Mare aux Evées, and it has been described in § 3.2.6. The experimental procedures applied were identical to those applied in the study of the synthetic polyacid systems. The procedures are described in § 3.1.2.

7.3.1 Acid/base characteristics

The ligand concentration in solutions of humic material is expressed by the molarity of the charged groups which may be determined by potentiometric and conductometric acid/base titrations.

Typical examples of such titrations are presented in fig. 7.2 for FA and in fig. 7.3 for HA. In the potentiometric curves no sharp end-point is present: an arbitrarily selected pH value of 7 was used by *Posner* (1964) of 8 by *Martin & Reeve* (1958) and of 9 by *Banerjee & Mukherjee* (1971). The curves resemble those for synthetic polyacids. HA behaves as a weaker acid than FA.

Back-titrations with HNO_3 generally yield potentiometric curves that are positioned somewhat lower than those of titrations with KOH, predominantly at high α_n: the loop formed by these curves is always smaller for FA than for HA, and is increasingly smaller for HA if longer equilibrium periods are practised. These observations can be explained by slow conformation changes in the large HA molecules upon charging.

In the conductometric curves of figs. 7.2 and 7.3, an end-point is well-defined, and it corresponds with pH≅9. The minima in the curves have often been ascribed to a particular class of -COOH groups (*van Dijk*, 1960; *Banerjee & Mukherjee*, 1971; *Arai & Kumada*, 1977a,b), presumably those which are ortho to OH groups on aromatic rings (*Schnitzer*

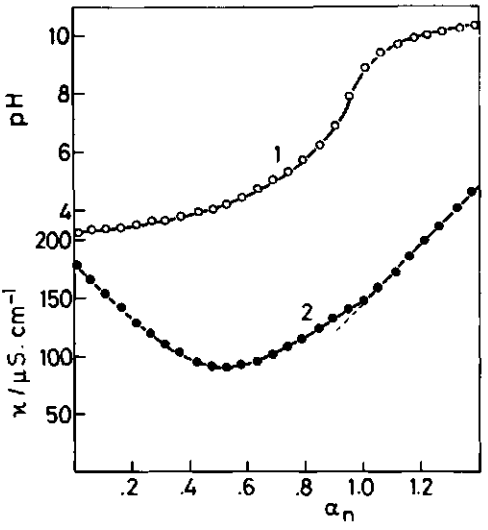

FIGURE 7.2 Conductometric and potentiometric acid/base titration curves for FA (Mare aux Evées). [FA] = 1.19 mol·m^{-3}; titrant: KOH; no 1:1 salt; 1. pH; 2. conductivity.

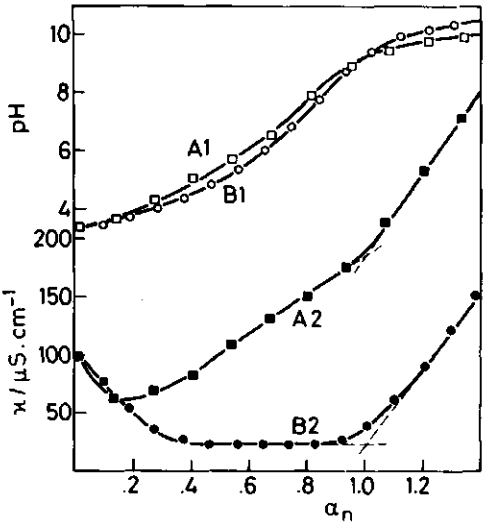

FIGURE 7.3 Conductometric and potentiometric acid/base titration curves for HA (Fluka sample). [HA] = 1.85 mol·m^{-3}; no 1:1 salt; titrant: (A) KOH; (B) $Ba(OH)_2$; 1. pH; 2. conductivity.

& Skinner, 1963; *Gamble*, 1970). However, the minima can also perfectly be explained in the case of only one type of -COOH group, in the same way as for PAA, see § 5.1.2. The minimum is deeper, and situated at higher α_n for FA, as compared to HA, whereas the fraction of -COOH groups ortho to OH is generally assumed to be larger in HA (*Hayes & Swift*, 1978).

Titration of HA with $Ba(OH)_2$ yields a flat region in the conductometric curve (B2). From a comparison with fig. 5.7, the conductometric curve for PAA in the presence of Ba^{2+}, it is clear that electrostatic interaction of Ba/HA could very well account for this feature. The flat region agrees with similar curves, for HA from woody bogpeat, obtained by *van Dijk* (1960), who observed a diminishing of the increase in κ at high α_n, using KOH as the titrant. In the discussion of the results for K/PAA, such a diminishing has been explained by the polyelectrolyte effect of PAA.

In fig. 7.4, $pK_{app,a}$, calculated according to the definition in eq. 2.21, is plotted versus α_n, for HA and FA.

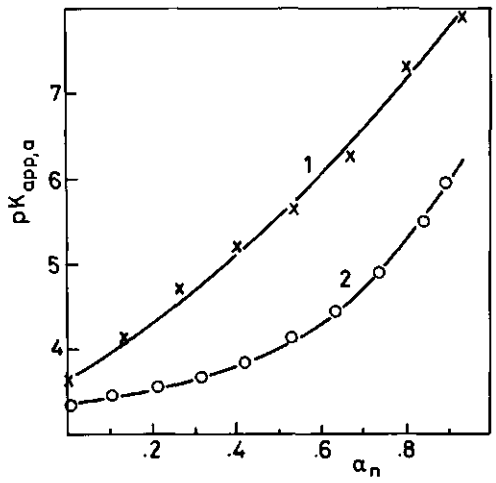

FIGURE 7.4 The dependence of the apparent acid dissociation constant $K_{app,a}$ of HA and FA on the degree of neutralization. 1. Fluka sample: [HA] = 1.85 $mol \cdot m^{-3}$; 2. Mare aux Evées sample: [FA] = 1.19 $mol \cdot m^{-3}$.

The initial slope $dpK_{app,a}/d\alpha_n$ is about four in the case of HA, and about unity in the case of FA. As far as polyelectrolyte effects are concerned, the difference can be explained by the relatively large fraction of small molecules in FA, that does not contribute to this effect. The strongly concave character of the FA curve may be related to a more pronounced manifestation of charge-charge interaction at high α_n. This would explain that for the remaining larger molecules, the polyelectrolyte effect is approximately the same as for HA, as could be inferred from the equality of the slopes at high α_n. 'Intrinsic' values of pK_a are about 3.4 and 3.7 for FA and HA respectively. It has been suggested by *Arai & Kumada* (1977a) that a 'monomer-like' unit could be represented by alginic acid, which has an intrinsic pK_a = 3.6.

In conclusion it can be stated that a polyelectrolyte effect, that is based on the close proximity of $-COO^-$ groups on the acid molecules, can explain the fundamental acid/base characteristics.

7.3.2 Cd, Pb/FA conductometry

The results of conductometric M/L-titrations of the Cd,Pb/FA systems are presented in the same way as the corresponding data for the synthetic polyacid systems in section 4.1.

Figs. 7.5.a and 7.5.b show the conductivity excess function $\Delta\kappa_T$ and the corresponding values of $\Delta[H^+]$ for Cd/FA and Pb/FA at given values of α_n.

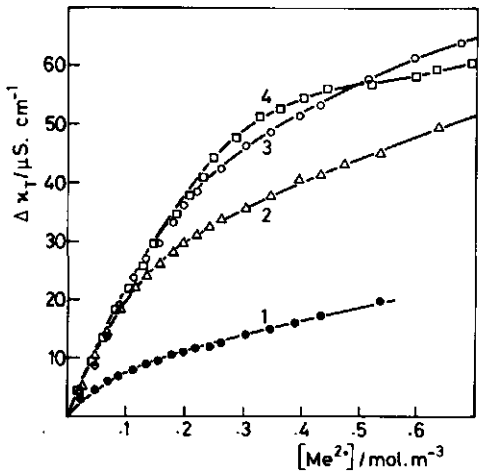

FIGURE 7.5.a The conductivity excess ΔK_T as a function of the amount $Cd(NO_3)_2$ or $Pb(NO_3)_2$; no 1:1 salt; $[FA]_i$ = 1.00 mol·m^{-3}; Cd: α_n = 0.60 (1), α_n = 0.80 (2), α_n = 1.00 (3); Pb: α_n = 0.80 (4).

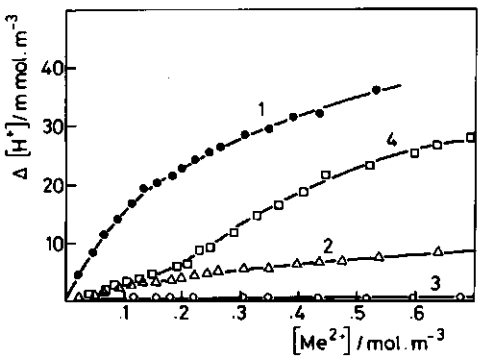

FIGURE 7.5.b The concentration of released protons as a function of the amount $Cd(NO_3)_2$ or $Pb(NO_3)_2$; no 1:1 salt; $[FA]_i$ = 1.00 mol·m^{-3}; Cd: α_n = 0.60 (1), α_n = 0.80 (2), α_n = 1.00 (3); Pb: α_n = 0.80 (4).

At $\alpha_n > 0.6$, $\Delta\kappa_T$ initially increases almost linearly with [M], demonstrating conductometric binding of Cd and Pb. At higher values of [M], the growth of $\Delta\kappa_T$ diminishes. The initial slope $\beta \cong 200$ S.cm^2·mol^{-1}, and this is larger than for the Cd,Pb/PAA,PMA systems. In section 4.1 it has been argued that in the case of complete conductometric binding, the slope can be approximated by

$$\beta \cong \lambda_M + 2\cdot\lambda_p \qquad (7.1)$$

According to *Arai & Kumada* (1977a), $\lambda_p \cong 50$ S·cm^2·mol^{-1} for the carboxylate group of humic material. Under the assumption that λ_K is not much altered by the presence of the fulvate ions, and using $\lambda_{Cd} \cong 100$ S·cm^2·mol^{-2}, the initial slope would correspond with a complete conductometric binding of Cd^{2+} at low M/L. In the case of Pb^{2+}, the initial

slope is expected to be somewhat larger than for Cd^{2+}, which is not the case. This might be due to the stronger covalence of the Pb^{2+}/ $-COO^-$ interaction, so that λ_p is diminished as a result of $PbCOO^+$ formation with isolated carboxylate groups.

The approximately complete conductometric binding by $-COO^-$ groups at low M/L can be explained by a polyelectrolyte effect resulting from small charge spacings for a number of these groups. In addition, it is clear from fig. 7.5.a that the values of $[Cd^{2+}]$, at which the slope decreases substantially, increase with increasing α_n, and thus with increasing charge density. However, it should be noted that these values of $[Cd^{2+}]$ are much smaller than $2\cdot[L^-]$, and that conductometric binding still continues at higher $[Cd^{2+}]$. These observations imply that not all $-COO^-$ groups of FA contribute to the polyelectrolyte effect in the same way. In fact the data suggest additional (chemical) binding of Cd^{2+} and Pb^{2+} to (isolated) $-COO^-$ groups, and stress that polyelectrolyte and mixture effects are concurrently operative.

The initial slope for $\alpha_n = 0.6$ (curve 1) is small. At this value of α_n, the initial value of the pH is 4.58. Upon addition of $Cd(NO_3)_2$ the proton production is sufficiently large as to cause a diminished growth of $\Delta\kappa_T$.

The proton production curves in fig. 7.5.b reveal the same pattern as for the synthetic systems, but are less pronounced: $\Delta[H^+]$ is the larger, the smaller α_n, and the curves for $\alpha_n = 0.8$ show an inflection point at which $\Delta[H^+]$ increases to grow. In § 4.1.1-3 it has been argued that the occurrence of an inflection point is a typical polyelectrolyte feature. In the case of a mixture of acids with different pK_a values, such an inflection point is not expected, unless the distribution of the pK_a values is very asymmetric. As FA will contain a fraction of small acid molecules, the proton production starts already at low M/L, whereas in the synthetic systems, $\Delta[H^+]$ is initially zero.

From curves 2 and 4 it is evident that the covalent character of the M/FA interaction decreases in the order: Pb > Cd. The maximum slopes $S_m = (d[H]/d[M]_a)_{max}$ are different for Pb and Cd. At $\alpha_n = 0.80$, $S_m = 0.07$ for Pb/FA and $S_m = 0.02$ for Cd/FA. It is noted that the ratio 0.07/0.02 is smaller than observed for the M/PMA systems at $\alpha_n = 0.40$.

From the $\Delta\kappa_T$-curves and the $\Delta[H^+]$ curves for Pb,Cd/FA it is concluded that the nearly complete conductometric binding of Pb and of Cd at low M/L evidence a polyelectrolyte effect in FA at natural pH levels. Differences between Pb and Cd binding are revealed at higher M/L, and are due to differences in covalent binding.

7.3.3 Cd,Pb/FA polarography

The results of the polarographic M/L-titrations for the Cd,Pb/FA systems are presented in fig. 7.6.

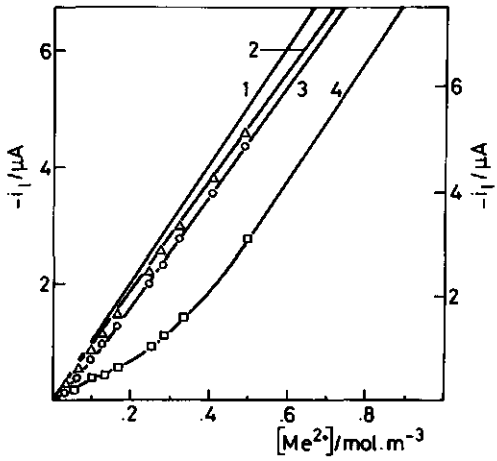

FIGURE 7.6 Limiting currents for M/FA as a function of the concentration $Cd(NO_3)_2$ or $Pb(NO_3)_2$; $[FA]_i$ = 0.95 $mol \cdot m^{-3}$ (Cd/FA); $[FA]_i$ = 1.00 $mol \cdot m^{-3}$ (Pb/FA); $[KNO_3]$ = 48 $mol \cdot m^{-3}$; E_i = -500 (Cd/FA)/-300 (Pb/FA) mV vs. $Ag/AgCl, KCl_{sat}$; t_p = 175 ms; t_d = 0.5 s; A = 1.63 mm^2; 1. calibration (right: Pb; left: Cd); 2. Cd/FA, α_n = 0.60; 3. Cd/FA, α_n = 0.80; 4. Pb/FA, α_n = 0.80.

The data are given in the same way as those of the synthetic polyacid systems in § 4.2.1-2. The polarograms had a normal shape. Only insignificant adsorption maxima were observed.

$E_{\frac{1}{2}}$ shifted to less negative values upon addition of $M(NO_3)_2$ which means that the systems behave pulse polarographically labile. There is sufficient support for this conclusion in literature for Cd/humic material (*O'Shea & Mancy*, 1976, 1978) and Pb/humic material (*Greter et al.*, 1979). For the given average molecular mass of 2,000 (*Buffle*, 1982), an average radius of gyration of the polyion r_p of about 1 nm would fit with the values in table 7.2. The corresponding value of D_b/D_f is 0.15. A test of this value using a large excess of ligand was not possible because of the low concentration of the FA stock solution. For Pb/FA at low M/L, the D_b/D_f value of 0.15 resulted in physically irrealistic values of the bound fraction. It was decided to calculate log K_1 *also* using D_b/D_f = 0.07 (which corresponds to $r_p \cong 2$ nm), since values of log K_1, calculated on this basis for Pb/FA, reasonably agreed with values of log K_1, calculated using $\Delta E_{\frac{1}{2}}$ according to the *DeFord-Hume* method. It is noted that the molecular mass of humics has been found to increase as more metal is complexed, probably partially due to the formation of bridges (*Ghosh & Schnitzer*, 1981).

In table 7.4, values of log K_1 and the corresponding pH, are given at different M/L-ratio, for both values of D_b/D_f.

TABLE 7.4 Log K_1 for Cd,Pb/FA, from polarographic data, and the corresponding pH

$\frac{[M^{2+}]_T}{[L^-]_T}$	$\frac{D_b}{D_f}$	Cd(α_n = 0.60) log K_1	pH	Cd(α_n = 0.80) log K_1	pH	Pb(α_n = 0.80) log K_1	pH
0.21 ±0.005	0.07	2.83	4.58	3.02	5.58	4.58*	5.17
	0.15	2.87		3.09		-	
0.42 ± 0.01	0.07	2.76	4.52	2.83	5.40	4.16	4.96
	0.15	2.82		2.90		4.74	
0.64 ± 0.03	0.07	2.54	4.40	2.69	5.35	3.84	4.74
	0.15	2.59		2.75		4.06	

* 4.61 (if $\Delta E_{\frac{1}{2}}$ is applied)

Table 7.4 shows that the uncertainty in D_b/D_f predominantly affects the large values of log K_1. Nevertheless, the trends in the data are clear: log K_1 increases with increasing α_n, with decreasing M/L, and in the order Cd < Pb. The values of log K_1 in table 7.4 are lower than usually found in literature - see table 7.3. This is due to the fact that in most studies the maximum concentration of sites is considered to be equal to the concentration of complexed sites at high M/L ('complexing capacity') for a given metal ions. This leads to a conditional binding constant. In the present study, the maximum concentration of sites is considered to be equal to the concentration of deprotonated groups: the choice of $[L^-]_T$ gives directly the association constant of metal binding, and fits to the aim to investigate the effect of the polyion charge. In passing it is noted that fig. 7.6 reveals that the 'complexing capacity' is lower for Cd than for Pb. Both complexing capacities are much smaller than the acidity of FA, which is a rather generally observed fact (*Lakatos et al.*, 1977).

7.3.4 Zn,Cd,Pb/HA conductometry

In figs. 7.7.a and 7.7.b, the conductivity excess $\Delta\kappa_T$ and the corresponding values of $\Delta[H^+]$ are given for different values of α_n for the Zn/HA system.

The pattern of the curves in fig. 7.7.a is very similar to those of the Zn/PMA,PAA systems: an initial linear part, showing a slope

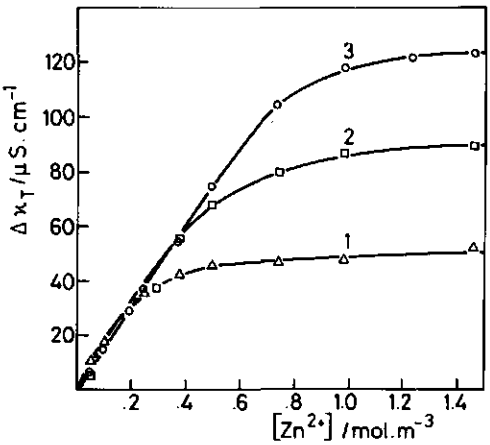

FIGURE 7.7.a The conductivity excess $\Delta\kappa_T$ as a function of the amount $Zn(NO_3)_2$; no 1:1 salt; $[HA]_i$ = 2.00 mol·m^{-3}; α_n = 0.40 (1); 0.60 (2); 0.80 (3).

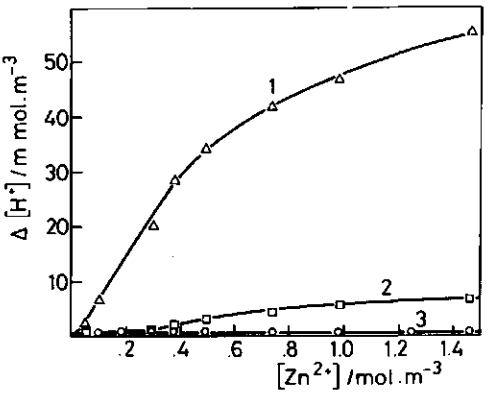

FIGURE 7.7.b The concentration of released protons as a function of the amount $Zn(NO_3)_2$; no 1:1 salt; $[HA]_i$ = 2.00 mol·m^{-3}; α_n = 0.40 (1); 0.60 (2); 0.80 (3)

$\beta \cong 150$ S·cm^2·mol^{-1}, a part with decreasing slope and a second linear part with *almost zero* slope. Moreover, this plateau starts at values of $[Zn^{2+}]$ where charge neutralization is about to occur, thus at larger $[Zn^{2+}]$ for larger α_n. The pattern of the proton production curves is also very similar to those of the poly(meth)acrylic systems: a rise in $\Delta[H^+]$ occurs only after $[Zn^{2+}]$ has exceeded a certain threshold value. It is stressed that these features are not observed in simple acid systems, but that they unequivocally demonstrate a polyelectrolyte effect of humic acids. It is more pronounced for humic than for fulvic acids. The discussion of the physical interpretation of the $\Delta\kappa_T$ and $\Delta[H^+]$ curves as given in § 4.1.1 for the Zn/PMApe system, remains valid for the present case.

The maximum value of the slope d[H]/d[Zn], at α_n = 0.40, is about 0.08, whereas the corresponding values for Zn/PMA and Zn/PAA were 0.01 and 0.09 respectively. When accounting for the different intrinsic acid strength of PAA, PMA and HA, it is expected that, K_{int}(Zn/HA) will have an order of magnitude of about 10-100.

In figs. 7.8.a and 7.8.b, the curves of $\Delta\kappa_T$ and $\Delta[H^+]$ are given for

Cd/HA, whereas in figs. 7.9.a and 7.9.b, the corresponding curves are given for Pb/HA.

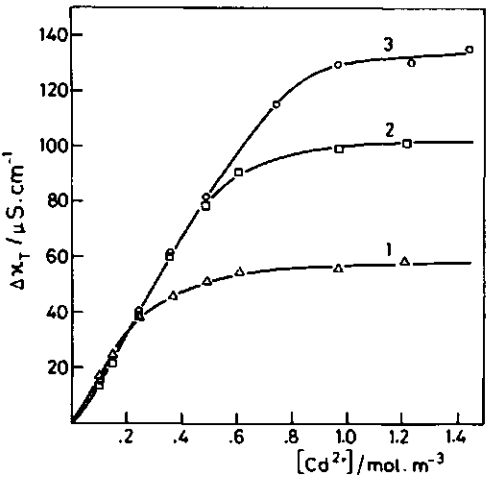

FIGURE 7.8.a The conductivity excess $\Delta\kappa_T$ as a function of the amount $Cd(NO_3)_2$; no 1:1 salt; $[HA]_i$ = 2.00 mol·m^{-3}; α_n = 0.40 (1); 0.60 (2); 0.80 (3).

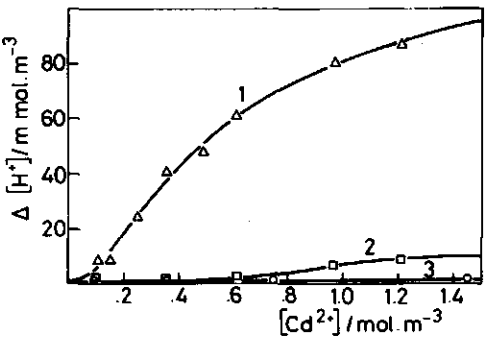

FIGURE 7.8.b The concentration of released protons as a function of the amount $Cd(NO_3)_2$; no 1:1 salt; $[HA]_i$ = 2.00 mol·m^{-3}; α_n = 0.40 (1); 0.60 (2); 0.80 (3)

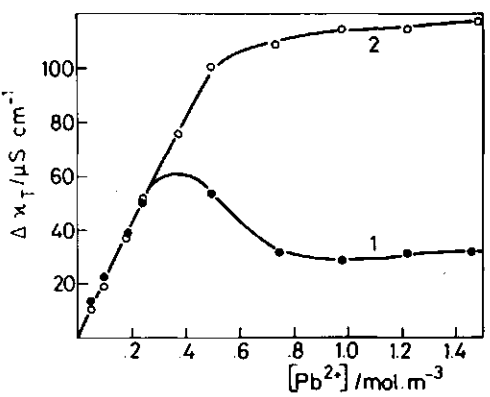

FIGURE 7.9.a The conductivity excess $\Delta\kappa_T$ as a function of the amount $Pb(NO_3)_2$; no 1:1 salt; $[HA]_i$ = 2.00 mol·m^{-3}; α_n = 0.40 (1); 0.60 (2).

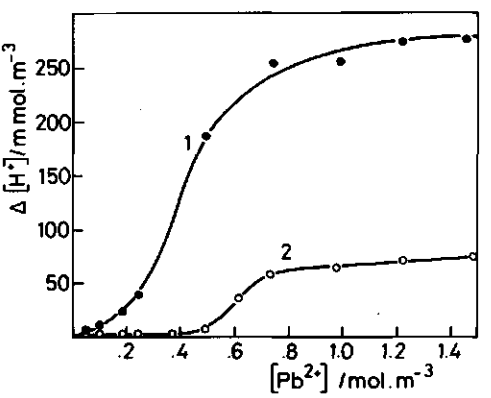

FIGURE 7.9.b The concentration of released protons as a function of the amount $Pb(NO_3)_2$; no 1:1 salt; $[HA]_i$ = 2.00 mol·m^{-3}; α_n = 0.40 (1); 0.60 (2).

The value of the initial slope β is about 165 $S \cdot cm^2 \cdot mol^{-1}$ for Cd/HA, and about 200 $S \cdot cm^2 \cdot mol^{-1}$ for Pb/HA. These values allow the conclusion that at low M/L almost complete conductometric binding of Cd and Pb occurs. The slope of the second linear part is almost zero in all cases: the increase in the amount bound at high M/L is small.

In the case of Pb/HA, at $\alpha_n = 0.40$, the $\Delta\kappa_T$ curve shows a maximum, positioned at M/L where Pb^{2+} saturates the available $-COO^-$ groups. In the case of Cd/HA such a maximum is absent. This observation suggests that intrinsic binding in M/HA is smaller for Cd than for Pb.

The proton production curves show the familiar pattern for polyacids: for a given α_n there is an inflexion point at a certain value of [M].

All these observations confirm the conclusion already drawn for Zn/HA, that HA shows a polyelectrolyte effect in the interaction with heavy metals. The effect is more pronounced for HA than for FA.

One particular feature of the M/PMA,PAA systems is the conductometric binding of K^+ at high α_n. This particular phenomenon has not been observed in the M/HA,FA systems. Apparently, the charge density of the humate and fulvate ions in the present study was not sufficiently large to show conductometric binding of monovalent ions. In terms of 'line' charge densities, this finding implies that at all values of α_n, $\xi < 1$, or $b > 0.7$ nm. In § 7.1.2, is has been estimated that b may be about 1 nm.

However, *Gamble* (1973) reported substantial binding of K^+ and Na^+ with humic material in his study. Evaluation of conductometric acid/base titration curves of other workers, for example *van Dijk* (1960) and *Chatterjee & Bose* (1952), also suggests binding of K^+ and Na^+. It is conceivable that a polyelectrolyte effect (or: the occurrence of small separations between charged groups) in humic material may differ from one sample to another. In the present study, HA shows stronger polyelectrolyte effects than the smaller FA entities. The findings of *Guy & Chakrabarti* (1976) and *Křibek et al.* (1977) that metal ions are preferentially associated with high molecular mass humic material, also suggests a relation between the (strength of the) polyelectrolyte effect and the size of the humic acid molecules.

The low values of the number of protons released per bound divalent metal ion, that are often reported in literature (*Khan*, 1969; *van Dijk*, 1971; *Shah et al.*, 1977; *Buffle et al.*, 1977; *Adhikari et al.*, 1978; *Saar*, 1980) can readily be understood applying the polyelectrolyte

option: an electrostatic contribution to the binding of a heavy metal ion with HA or FA, will result in a decrease of the apparent acid dissociation constant, yielding only 'fractional' release of protons.

Using the values of S_m from figs. 7.7-9.b at α_n = 0.40 for M/HA, being 0.08 (Zn/HA), 0.18 (Cd/HA) and 0.56 (Pb/HA), and a value of 3.7 for $\log K_a$ in eq. (4.5), it is estimated that K_{int}(ML) is about 8 (Zn/HA), 26 (Cd/HA) and 230 (Pb/HA). Although these data are only crude approximations, they have comparative value: the intrinsic binding M/HA decreases in the series Pb > Cd > Zn. Moreover the data demonstrate that binding strengths calculated on the basis of proton release are low.

7.3.5 *Zn,Cd,Pb/HA polarography*

In figs. 7.10-7.12, the results of the polarographic M/L-titrations for Zn/HA, Cd/HA and Pb/HA at different values of α_n are presented in the same way as for the synthetic polyacid systems.

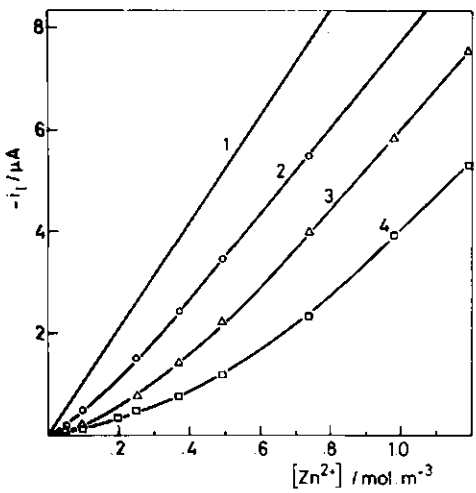

FIGURE 7.10 The limiting current for Zn/HA as a function of the amount $Zn(NO_3)_2$; $[HA]_i$ = 2.00 mol·m^{-3}; $[KNO_3]$ = 50 mol·m^{-3}; E_i = -800 mV vs. Ag/AgCl,KCl_{sat}; t_p = 175 ms; t_d = 1 s; A = 1.35 mm^2; 1. calibration; 2. α_n = 0.4; 3. α_n = 0.6; 4. α_n = 0.8.

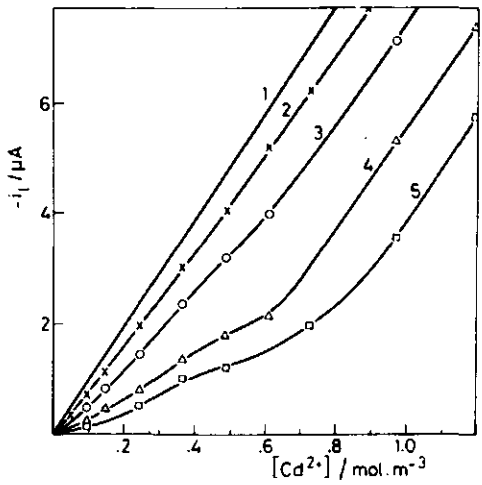

FIGURE 7.11 The limiting current for Cd/HA as a function of the amount $Cd(NO_3)_2$; $[HA]_i$ = 2.00 mol·m^{-3}; $[KNO_3]$ = 50 mol·m^{-3}; E_i = - 300 mV vs. Ag/AgCl, KCl_{sat}; t_p = 175 ms; t_d = 1 s; A = 1.35 mm^2; 1. calibration; 2. α_n = 0.2; 3. α_n = 0.4; 4. α_n = 0.6; 5. α_n = 0.8.

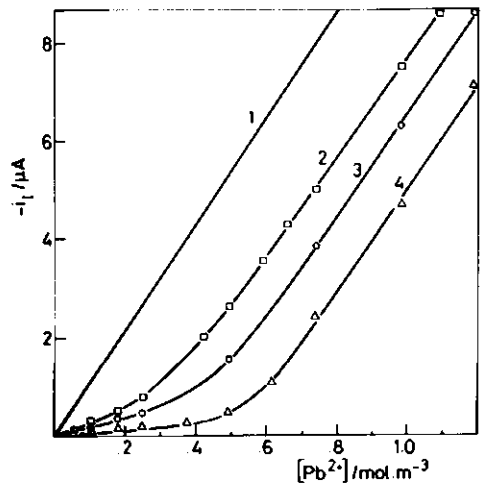

FIGURE 7.12 The limiting current for Pb/HA as a function of the amount $Pb(NO_3)_2$; $[HA]_i$ = 2.00 mol·m^{-3}; $[KNO_3]$ = 50 mol·m^{-3}; E_i = 0 mV vs. $Ag/AgCl,KCl_{sat}$; t_p = 175 ms; t_d = 1 s; A = 1.35 mm^2; 1. calibration; 2. α_n = 0.2; 3. α_n = 0.4; 4. α_n = 0.6.

The polarograms for Zn,Cd/HA generally showed a normal shape and a well-defined limiting current. Some indications of reactant adsorption have been observed, especially in the intermediate range of M/L-ratios, where coagulation is about to occur. In that range, the discarded mercury drops did not coalesce at the bottom of the polarographic cell. The polarograms for Pb/HA often showed clear signs of reactant adsorption at intermediate and high values of M/L, especially at large α_n. An example has previously been given, in fig. 3.3. Due to coagulation and adsorption phenomena, the number of i_ℓ values that is suited to be evaluated in terms of log K_1 is limited.

The polarographic activity of the humic material itself has been described by *Buffle & Cominoli* (1981). Faradaic contributions to the limiting current, due to the reduction of organic components, have also been observed for the HA and FA samples in the present study. However, under the experimental conditions, the values of $E_{\frac{1}{2}}$ of those reduction waves were more negative than -1.2 V vs. $Ag/AgCl,KCl_{sat}$: those waves did not affect the determinations of the proper values of i_ℓ for the reduction of the metal ions.

The characteristic features of the i_ℓ curves are essentially the same as those of the corresponding curves of the Zn,Cd,Pb/PMA,PAA systems. The discussion of these features in § 4.2.1-3, is *mutatis mutandis* valid for the polarographic results of the M/HA systems.

Most important is the dependency of the apparent binding of HA on α_n. For simple (monomeric) systems, the binding capacity is independent

on α_n. Thus, the polarographic results support the polyelectrolyte character of the HA sample as inferred from the conductometric and potentiometric data.

The initial slope of the i_ℓ-curves decreases with increasing α_n, indicating that the magnitude of the polarographically bound fraction depends on α_n, and that it is not complete at low M/L, as was the case in the absence of 1:1 salt.

Another consequence of the presence of 1:1 salt is the enlarged liability of the systems to coagulate and precipitate, as compared to the salt-free systems. In the case of Pb/HA, coagulation starts at values of [Pb] before the rounding in the i_ℓ-curves, whereas in the cases of Zn/HA and Cd/HA, the coagulation usually sets in at values of [M] where the change of the slope of the i_ℓ-curve is maximal.

The polarographic lability of the M/HA systems has often been reported (*Shuman & Woodward*, 1977; *Buffle et al.*, 1978; *Frimmel et al.*, 1981). For the M/HA systems of the present study, shifts of $E_{1/2}$ with M/L have been observed in all cases at low M/L, and a plateau value for i_ℓ was repeatedly reached using an increasing concentration of HA in a given Cd/HA system, at $\alpha_n = 0.6$.

From this plateau value, a value of D_b/D_f was calculated of about 0.05. This value has been used in the calculation of log K_1. It corresponds to $r_p \cong 3$ nm. Applying the information of table 7.2, an average molecular mass of 10,000 is estimated for the HA sample. For high values of α_n, and low values of M/L, the value of D_b/D_f sometimes gave irrealistic results for the Pb/HA system. However, in those cases, $\Delta E_{1/2}$ was sufficiently large to calculate a value of log K_1.

TABLE 7.5 Log K_1 for Zn, Cd, Pb/HA, from polarographic data, and the corresponding pH (in brackets)

$[M^{2+}]_T / [L^-]_T$	Log K_1					
	Zn		Cd		Pb	
	α_n=0.4	0.6	0.4	0.6	0.4	0.6
0.2	3.69 (4.70)	4.38 (5.88)	3.54 (4.65)	4.18 (6.03)	4.95* (4.35)	6.47* (5.74)
0.4	3.48 (4.57)	4.00 (5.68)	3.36 (4.46)	4.08 (5.75)	4.56* (4.00)	4.75* (5.08)
0.6	3.43 (4.50)	3.87 (5.50)	3.38 (4.38)	3.90 (5.53)	4.38 (3.74)	4.63 (4.63)

* using $\Delta E_{1/2}$

In table 7.5, a number of log K_1 values, at different α_n and at different M/L, are presented. Again, log K_1 increases with increasing α_n, and with decreasing M/L. Values of log K_1 for Zn/HA and Cd/HA hardly differ, in contrast to the M/PAA,PMA systems. In connection with this finding, it is noted that *Zunino et al.* (1979) reported that humic material may contain special groups, or arrangements of groups, which favour binding of Zn^{2+} at low M/L.

From a comparison of the values of log K_1 for Cd/HA and Cd/FA at α_n = 0.60 in the tables 7.4 and 7.5 it is evident that the binding strength for Cd/HA is larger than for Cd/FA. As the functional groups are probably similar, the difference suggests also a larger polyelectrolyte effect of HA, as compared to FA.

7.3.6 Cd/HA Cd-ISE potentiometry

In figs. 7.13 and 7.14, values of log K_1 for Cd/HA, from Cd-ISE potentiometric data, are plotted as a function of M/L at different values of α_n. Figs. 7.13 and 7.14 refer to KNO_3 levels of 50 mol·m^{-3}

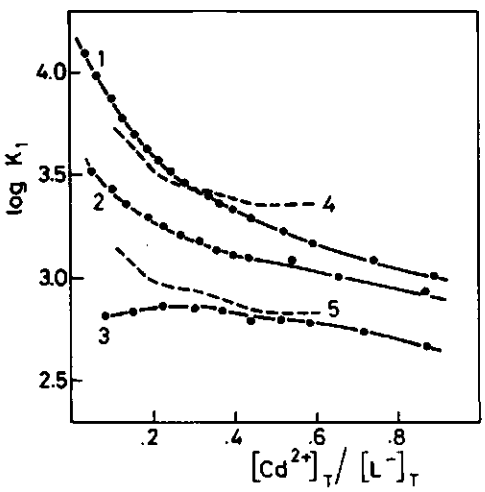

FIGURE 7.13 Log K_1 versus M/L for Cd/HA; $[KNO_3]$ = 50 mol·m^{-3}; Cd-ISE potentiometry, $[HA]_i$ = 2.81 mol·m^{-3} (1-3); polarography, $[HA]_i$ = 2.00 mol·m^{-3} (4,5); 1. α_n = 0.60; 2. α_n = 0.40; 3. α_n = 0.2; 4. labile, α_n = 0.4; 5. non-labile, α_n = 0.4.

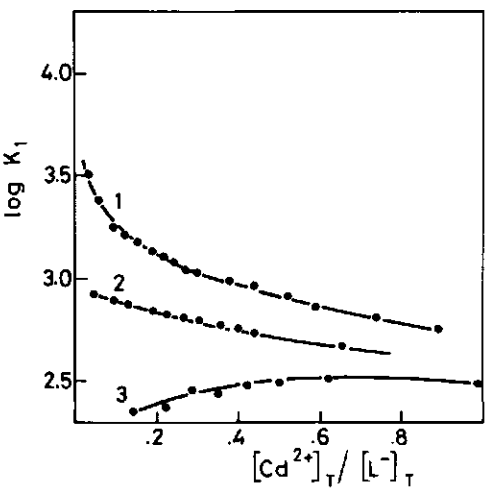

FIGURE 7.14 Log K_1 versus M/L for Cd/HA; $[KNO_3]$ = 200 mol·m^{-3}; Cd-ISE potentiometry; $[HA]_i$ = 2.81 mol·m^{-3}; 1. α_n = 0.60; 2. α_n = 0.40; 3. α_n = 0.20.

and 200 mol·m^{-3} respectively. In fig. 7.13, pulse polarographic data, for Cd/HA at α_n = 0.40, are also inserted, for both labile and non-labile equilibria. Polarographically non-labile behaviour is expected at high M/L, see § 4.3.1-2, in connection with precipitation.

From both figures, it is clear that the decrease in log K_1 with increasing M/L is stronger at higher values of α_n. This confirms the trends in the data in table 7.5. The difference in decrease of log K_1 stresses once again the polyelectrolyte character of the humic ligands.

At low M/L, log K_1 appears to be sensitive to the concentration 1:1 salt. At M/L = 0.1, values of S_c, as calculated from the differences between Cd-ISE potentiometric log K_1 values at equal values of α_n in figs. 7.13 and 7.14, are 1, 0.9 and 0.7 at α_n values of 0.60, 0.40 and 0.20 respectively. Such a strong dependency of log K_1 on log c_1^{-1} convincingly illustrates the polyelectrolyte character of the Cd/HA interaction.

Comparison of the log K_1 values at α_n = 0.40 from ISE data with those from NPP data reveals that the ISE results are inbetween those for labile-NPP and non-labile-NPP. For low values of M/L, the lability of Cd/HA has clearly been demonstrated, reactant adsorption does not significantly occur, and the NPP data are more accurate than the ISE data. For high values of M/L, reactant adsorption effects, and signs of precipitation have been observed. It is concluded that the kinetics of the M/HA equilibrium changes from labile to non-labile (on the pulse polarographic time scale) with increasing M/L.

7.4 FURTHER DISCUSSION

7.4.1 Log K_1 versus α_{eff}

In fig. 7.15, values of log K_1 for Zn,Cd,Pb/HA and Cd/FA are given as a function a α_{eff}, as defined in eq. (5.12). The values of log K_1 are averages over three polarographic determinations at very low M/L. In the cases where the Δi_ℓ-procedure did not work (high α, low M/L), the $\Delta E_{\frac{1}{2}}$-procedure was applied. The size of the circles in fig. 7.15 indicates the accuracy of the values of log K_1 and the corresponding value of α_{eff}.

The curves in fig. 7.15 are approximately linear for the Cd,Zn/HA systems. The linear increase of log K_1 with α_{eff} supports the polyelectrolyte option for HA. For Cd,Zn/HA the slope $d\log K_1/d\alpha_{eff}$ is inbetween 2 and 4. The corresponding slopes for Cd,Zn/PAA systems

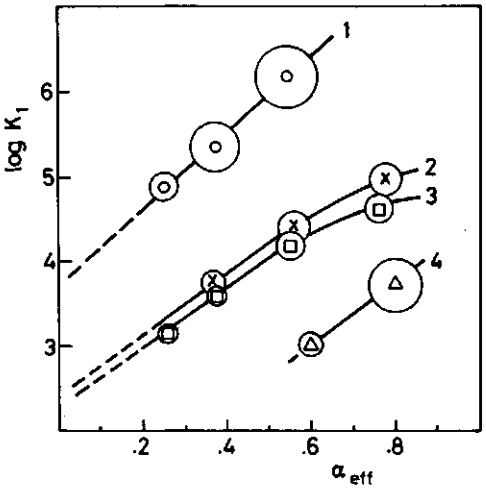

FIGURE 7.15 Log K_1 versus α_{eff} for M/HA,FA, from polarographic data. 1. Pb/HA, 2. Zn/HA; 3. Cd/HA; 4. Cd/FA.

(see fig. 5.27) were larger, about 4.4-5.0. Since the change in α_{eff} reflects the change in polyion charge density, the smaller slope for M/HA supports the previously (in § 7.3.1 and § 7.3.4) considered expectation that a polyelectrolyte effect of HA will be less than that of PAA.

Values of log K_1 for $\alpha_{eff} \rightarrow 0$ corresponding to log K_{int}(ML) are about 2.4, 2.4 and 3.8 for Zn/HA, Cd/HA and Pb/HA respectively. These values agree reasonably with values of log K_{int}(ML) given by *Marinsky et al.* (1980) for Zn,Cd,Pb/peat HA systems, viz. 2.8, 2.6 and 4.3 respectively. It is noted that the values of log K_{int}(ML) for Cd/HA are close to the corresponding values 2.5 for Cd/phtalic acid and 3.3 for Cd/malonic acid (*Sillén & Martell*, 1971).

Two facts remain to be explained:

i The average value of $d\log K_1/d\alpha_{eff}$ for Cd,Zn/HA systems is not about twice the average value of $dpK_{app,a}/d\alpha_n$ for the proton binding of HA;

ii The values of log K_{int}(ML), determined using S_m, are smaller than those determined from extrapolation of log K_1 to $\alpha_{eff} = 0$.

The fact that HA and FA are always mixtures of organic acids explains that $pK_{app,a}$ may cover a range of values: the difference, for example, between the (intrinsic) values of pK_a of phenolic acid and formic acid is about 5. However, the fraction of charged groups that is responsible for the polyelectrolyte effect is limited to those on the 'large' molecules. Thus, the dependency of $pK_{app,a}$ on α_n is only

in part the result of the polyelectrolyte effect. The average slope of log K_1 versus α_{eff} suggests that this part corresponds with a contribution of about one to two units of the slope $dpK_{app,a}/d\alpha_d$. This would mean that for the acid/base characteristics, the mixture effect may overrule the polyelectrolyte effect. The importance of the mixture effect is (inversely) related to the magnitude of the intrinsic binding: in the absence of substantial intrinsic binding, the contribution to the free energy of the binding is predominantly electrostatic. The intrinsic binding constants for proton association with different types of carboxylic acids are generally one to three orders of magnitude larger than for divalent metal ion association -see table 4.6. Thus, for a given sample of humic material, the mixture effect may control the resulting value of $pK_{app,a}$, whereas the polyelectrolyte effect may predominantly control the metal ion association.

These considerations solve the paradox that in some cases acid/base features of HA have been identified as definitely not polyelectrolytic (*Posner*, 1964), whereas in some other cases metal ion association features perfectly fit in polyelectrolyte behaviour (*Nash & Choppin*, 1980).

Using the values of $K_{int}(ML)$ determined for $\alpha_{eff} \to 0$, eq. (4.5) can be used in a different way, now to estimate an appropriate value of pK_a. It appears that the carboxylic groups with which the polyelectrolyte behaviour would be related, show values of pK_a in the range 4.7 - 5.3. It is noted that this range comprises the values of pK_a of PAA, PMA and PMApe.

7.4.2 Polyelectrolyte effects

Obviously, in a mixture of acids, such as a humic or fulvic acid sample, the distribution of cations over the functional groups with different intrinsic binding constants is always a factor that controls the resulting apparent association constant. The results in this chapter demonstrate that in addition to such a mixture effect, a polyelectrolyte effect is operative in the interaction of heavy metals with humic and fulvic acids at natural pH levels.

The following phenomena are manifestations of polyelectrolytic behaviour of the systems investigated:

i The approximately complete binding of M^{2+}, at low M/L and low c_1, directly related to α;

ii The decrease of log K_1 with increasing M/L, directly related to α_n;

iii The strong dependency of log K_1 on c_1, in relation to α_n;
iv The occurrence of an inflection point in the proton production curves, in relation to M/L.

The present electrochemical study shows that the analogies with the synthetic polyacids, PAA and PMA(pe), are striking. This confirms the analogies elucidated in a thermometric study of M/HA and M/PAA,PMA by *Khalaf et al.* (1975) and in an infrared spectroscopic study of M/HA and M/polymaleic acid by *Andersson & Russell* (1976).

A number of the characteristics of the systems investigated, for example a decrease of log K_1 with increasing M/L at a given α_n, could also have been understood in terms of the mixture effect. Nevertheless, special assumptions are needed in that case, viz. a number of *particular* configurations of different functional groups, and different binding capacities of humic material for different metals.

In conclusion, M/HA,FA systems cannot generally be described by a single intrinsic stability constant, or a particular set of intrinsic constants. An additional parameter is necessary to account for the polyelectrolyte effect, especially a low values of M/L, which are often met in nature.

That fact that polyelectrolyte effects substantially contribute to the binding of heavy metals by humic material, has important implications for the modelling of free M^{n+} concentrations in ecosystems. Some examples of these implications are:

i Upon dilution of the system, the bound fraction will hardly change, i.e. the metal 'complex' does not dissociate according to simple mass action;
ii The ionic strength dependency of the bound fraction if much stronger than expected on the basis of the *Debye-Hückel* approximation;
iii The relation between the pH of an HA system and its degree of dissociation is not simple in the presence of heavy metal ions.

Reports of apparent metal association constants for humic material should include a detailed description of the experimental conditions, and of the acid/base characteristics of the particular sample.

8 CONCLUSIONS

In this chapter, the main conclusions from the results on the interaction of Cd(II), Pb(II) and Zn(II) with polycarboxylic acids are summarized.

Poly(meth)acrylic acids

i At low M/L and in the absence of added 1:1 salt, the conductometric binding of M^{2+} to partially neutralized poly(meth)acrylic acids is virtually complete, irrespective the nature of M^{2+}. Upon conductometric binding of M^{2+}, alkali metal ions (from added base) that are conductometrically bound only at sufficiently high α_n, are exchanged.

ii The ranges of M/L and α_n values, over which complete conductometric binding of M^{2+} and additional binding of M^{+} will occur, are in reasonable agreement with counterion condensation criteria.

iii The character of the binding of the heavy metal ions is partially covalent and partially electrostatic. The covalent character increases generally in the series Zn < Cd < Pb, in accordance with the increasing covalence index, and as a rule it increases in the series PMApe $\leqslant$ PMA < PAA, that is with increasing intrinsic acid strength.

iv Bound divalent metal ions effectively stabilize the compact conformation of polymethacrylic acids. For $[M^{2+}]_T/[-COO^-]_T$ ratios lower than 0.5, a transition to a more open conformation may partially occur upon further deprotonation.

v At low M/L, the heavy metal-polyacid equilibria in the systems Cd,Zn,Pb/PMA and Cd,Zn/PAA are pulse polarographically labile. At high M/L, the equilibria become increasingly non-labile with increasing M/L. For Cd/PMA this conclusion has been supported by Cd-potentiometric data.

vi For the complex formation in the systems Cd,Zn/PMA,PAA, a coordination number of j=1 is likely.

vii Values of the apparent metal association constant K_1, from polarographic data, largely differ for different values of α_n, M/L and c_1. Intrinsic binding constants (low M/L, low c_1, $\alpha_{eff} \rightarrow 0$) for Cd,Zn/PMA,PAA systems are small. The values of log K_{int}(ML) are all lower than $\sim$2.1. For Pb/PMA, log K_{int}, assuming j=1, is $\sim$3.6. The values of the intrinsic binding constants increase in the

series Zn < Cd < Pb, and are as a rule slightly larger than the corresponding stability constants for the complex formation with 2-methylpropanoic acid, but of the same order of magnitude.

viii For Cd,Zn/PAA systems, log K_1 increases approximately linearly with α_{eff}. This increase is about twice that of $pK_{app,a}$ with α_d, demonstrating that $\psi_s(H^+) \cong \psi_s(M^{2+})$. The initially more rapid increase of log K_1 with α_{eff} for Cd,Zn/PMA, and the non-linearity of the increase for these systems are attributed to the compact conformation at low α_{eff} and the change in conformation respectively.

ix Log K_1 decreases with increasing M/L, demonstrating the cooperativity of the ligands. Although the dependence of the binding constant on the degree of binding is well-described by the counterion condensation model, the theoretical values of the binding strength for Zn/PMA,PAA systems, calculated on the basis of electrostatic interaction only, are too low by about two orders of magnitude.

x The dependence of log K_1 on c_1 varies considerably with α_n and M/L. For high α_n and low M/L, the slope S_c may reach a value of about two. For very low c_1, S_c tends to become zero.

Humic & fulvic acids

xi Against the background of the characteristics of the polyelectrolyte effect in the interaction of heavy metal ions with synthetic polycarboxylic acids, it is concluded that in the interaction of Cd^{2+}, Pb^{2+} and Zn^{2+} with FA (Mare aux Evées) and with HA (Fluka sample) the polyelectrolyte effect plays an important role at natural pH, in addition to the mixture effect.

xii At low M/L, the heavy metal-polyacid equilibria in the systems Cd,Pb/FA and Cd,Pb,Zn/HA are pulse polarographically labile.

xiii Values of the apparent metal association constants increase in the series Cd ≅ Zn < Pb, and are lower for FA than for HA. For Cd,Zn,Pb/HA, the 'intrinsic' metal association constants, assuming j=1, are about 2.4, 2.4 and 3.8 respectively.

xiv In modelling of ecosystems with respect to trace metal speciation, polyelectrolyte effects should be taken into account.

REFERENCES

Adhikari, M. & Hazra, G.C., 1976. J.Indian Chem.Soc. 53: 513-515.
Adhikari, M., Mukherjee, T.K. & Chakraborty, G., 1976. J.Indian Chem.Soc. 53: 1233-1235.
Adhikari, M. & Chakrabarti, G., 1977. J.Indian Chem.Soc. 54: 573-574.
Adhikari, M., Chakrabarti, G. & Hazra, G., 1977. Agrochimia 12: 134-139.
Adhikari, M., Roy, J. & Hazra, G., 1978. J.Indian Chem.Soc. 55: 332-336.
Akhmed'yanova, R.A., Kurenkov, V.F., Kuznetsov, E.V. & Myagchenkov, V.A., 1981. Vysokomol.Soedin. B23: 417-420.
Alexandrowicz, Z. & Katchalsky, A., 1963. J.Polymer Sci. A1: 3231-3260.
Anderson, C.F. & Record, M.T.Jr., 1980. Biophys.Chem. 11: 353-360.
Anderson, H.A. & Russell, J.D., 1976. Nature 260: 597.
Ansprach, W.M. & Marinsky, J.A., 1975. J.Phys.Chem. 79: 433-439.
Arai, S. & Kumada, K., 1977a. Geoderma 19: 21-35.
Arai, S. & Kumada, K., 1977b. Geoderma 19: 307-317.
Arai, S. & Kumada, K., 1981. Geoderma 26: 1-12.
Archer, D.W. & Monk, C.B., 1964. J.Chem.Soc. 3117-3122.
Arnold, R. & Overbeek, J.Th.G., 1950. Recl.Trav.Chim.Pays-Bas 69: 192.
Arnold, R., 1957. J.Coll.Sci. 12: 549-556.

Bach, D. & Miller, I.R., 1967. Biopolymers 5: 161-172.
Banerjee, S.K. & Mukherjee, S.K., 1971. Indian J.Appl.Chem. 34: 171-177.
Banerjee, S.K. & Mukherjee, S.K., 1972. J. Indian Soc. Soil Sci. 20: 91-94
Banerjee, S.K. & Sengupta, M., 1977. Fertilizer Technology 14: 279-282.
Barker, G.C., 1958. Anal.Chim.Acta 18: 118-131.
Barker, G.C. & Gardner, A.W., 1960. Z.Anal.Chem. 173: 79-83.
Barker, G.C. & Bolzan, J.A., 1966. Z.Anal.Chem. 216: 215-238.
Baxendale, J.H., Bywater, S. & Evans, M.G., 1946. J.Polymer Sci. 1: 237-244.
Begala, A.J. & Strauss, U.P., 1972. J.Phys.Chem. 76: 254-260.
Beneš, P., Gjessing, E.T. & Steinnes, E., 1976. Water Res. 10: 711-716.
Ben-Naim, A., 1980. 'Hydrophobic Interactions', Plenum Press, New York.
Berg, H. & Horn, G., 1981. Bioelectrochem.Bioenerg. 8: 167-178.
Beveridge, A. & Pickering, W.F., 1980. Water Air Soil Poll. 14: 171-185.
Bhat, G.A., Saar, R.A., Smart, R.B. & Weber, J.H., 1981. Anal.Chem. 53: 2275-2280.
Bhat, G.A. & Weber, J.H., 1982. Anal.Chim.Acta 141: 95-103.
Bhattacharya, A.K., 1972. Z.Anal.Chem. 262: 363-364.
Bloom, P.R. & MacBride, M.B., 1979. Soil Sci.Soc.Amer.J. 43: 687-692.
Bloys van Treslong, C.J., 1978. Recl.Trav.Chim.Pays-Bas 97: 13-21.
Böhm, J.T.C., 1974. Thesis, Agricultural University, Wageningen.
Böhm, J.T.C. & Lyklema, J., 1975. J.Colloid Interf.Sci. 50: 559-566.
Bolewski, K. & Lubina, M., 1969. Roczniki Chemii 43: 1531-1546.
Bolewski, K. & Lubina, M., 1970. Roczniki Chemii 44: 647-656.
Bolzan, J.A., 1975. J.Electroanal.Chem. 59: 303-309.
Bond, A.M. & Hefter, G., 1971. Electroanal.Chem. 31: 477-485.
Bond, A.M., 1980. 'Modern Polarographic Methods in Analytical Chemistry', Marcel Dekker Inc., New York.
Bond, A.M. & Jones, R.D., 1980. Anal.Chim.Acta 121: 1-11.
Borggaard, O.K., 1974. J.Soil Sci. 25: 189-195.
Bovendeur, J., van Buuren, J.C.L. & Jacobs, J.A., 1982. Z.Wasser Abwasser Forsch. 15: 181-186.
Boyd, S.A., Sommers, L.E. & Nelson, D.W., 1981. Soil Sci.Soc.Amer.J. 45: 1241-1242.
Brady, B. & Pagenkopf, G.K., 1978. Can.J.Chem. 56: 2331-2336.
Brandrup, J. & Immergut, E.H. (Eds), 1965. 'Polymer Handbook', Interscience Publ., New York.
Bratko, D. & Vlachy, V., 1982. Chem.Phys.Lett. 90: 434-438.
le Bret, M. & Zimm, B.H., 1984. Biopolymers 23: 271-312.
Brezonik, P.-L., Brauner, P.A. & Stumm, W., 1976. Water Res. 10: 605-612.
Brinkman, A.A.A.M. & Los, J.M., 1964. J.Electroanal.Chem. 7: 171-183.

Brinkman, A.A.A.M. & Los, J.M., 1967. J.Electroanal.Chem. 14: 269-296.
Buffle, J., Greter, F.-L., Nembrini, G., Paul, J. & Haerdi, W., 1976. Z.Anal.Chem. 282: 339-350.
Buffle, J., Greter, F.-L. & Haerdi, W., 1977. Anal.Chem. 49: 216-222.
Buffle, J., 1977. In: 'Conf.Proc. de la Commission d'Hydrologie Appliqué de l'A.G.H.T.M.', University of Orsay, pp. 3-10.
Buffle, J., Cominoli, A., Greter, F.-L. & Haerdi, W., 1978. Proc. Analyt.Div.Chem. Soc.Fourth Int. SAC Conf., pp. 59-61.
Buffle, J., 1979. La Tribune de Cebedeau 426: 165-176.
Buffle, J. & Greter, F.-L., 1979. J.Electroanal.Chem. 101: 231-251.
Buffle, J. & Cominoli, A., 1981. J.Electroanal.Chem. 121: 273-299.
Buffle, J., Deladoey, P., Zumstein, J. & Haerdi, W., 1982. Schweiz.Z.Hydrol. 44: 325-362.
Buffle, J. & Deladoey, P., 1982. Schweiz. Z.Hydrol. 44: 363-391.
Buffle, J., 1982. Personal communication.
Buffle, J., Tessier, A. & Haerdi, W., 1984. In: 'Complexation of Trace Metals in Natural Waters' (Kramer, C.J.M. & Duinker, J.C , Eds), Martinus Nijhoff/Dr. W. Junk Publ., The Hague.
Bunzl, K., Wolf, A. & Sansoni, B., 1976. Z.Pflanzenern.Bodenk. 139: 475-485.

Chatterjee, B. & Bose, S., 1952. J. Colloid Sci. 7: 414-427.
Cheam, V. & Gamble, D.S., 1974. Can.J.Soil.Sci. 54: 413-417.
Chen, Y. & Schnitzer, M., 1976. Soil Sci.Soc.Amer.J. 40: 682-686.
Chien, H.W. & Isihara, A., 1976. J.Polymer Sci.: Polymer Phys.Ed. 14: 1015-1019.
Choppin, G.R. & Shanbhag, P.M., 1981. J.inorg.nucl.Chem. 43: 921-922.
Choudry, G.G., 1981. Toxic.Environm.Chem. 4: 209-260.
Constantino, L., Crescenzi, V., Quadrifoglio, F. & Vitagliano, V., 1967. J.Polymer Sci. A2-5: 771-780.
Conway, B.E., 1981. 'Ionic Hydration in Chemistry and Biophysics', Elsevier Sci.Publ. Comp., Amsterdam.
Corner, T., 1981. Coll. & Surf. 3: 119-129.
Creighton, H.J., 1935. 'Principles of Electrochemistry', Vol. I, John Wiley & Sons Inc., New York.
Crescenzi, V., de Chirico, A. & Ripamonti, A., 1959. Ric.Sci. 29: 1424-1430.
Crescenzi, V., de Rosa, V. & Maldarella, D., 1960. Ric.Sci. 30: 1680-1687.
Crescenzi, V., Quadrifoglio, F. & Delben, F., 1972. J.Polymer Sci. A2-10: 357-368.
Crescenzi, V., Delben, F., Quadrifoglio, F. & Dolar, D., 1973. J.Phys.Chem. 77: 539-544.
Crescenzi, V., Delben, F., Paoletti, S. & Skerjanc, J., 1974. J.Phys.Chem. 78: 607-611.
Crow, D.R., 1968. J.Electroanal.Chem. 16: 137-144.
Crow, D.R., 1969. 'Polarography of Metal Complexes', Acad.Press, London.
Crow, D.R., 1982. Talanta 29: 733-742.

Daune, M., 1974. In: 'Metal Ions in Biological Systems', Vol. 3 (Siegel, H., Ed.), Marcel Dekker, New York, pp. 2-43.
Davis, H. & Mott, C.J.B., 1981. J.Soil Sci. 32: 379-391.
Davison, W. & Whitfield, M., 1977. J.Electroanal.Chem. 75: 763-789.
Deb, D.L., Kohli, C.B.S. & Joshi, O.P., 1976. Fertilizer Techn. 13: 25-29.
DeFord, D.D. & Hume, D.N., 1951. J.Amer.Chem.Soc. 73: 5321-5322.
Delben, F., Crescenzi, V. & Quadrifoglio, F., 1972. Eur.Polymer J. 8: 933-935.
Delben, F. & Paoletti, S., 1974. J.Phys.Chem. 78: 1486-1489.
Delville, A., 1980. Chem.Phys.Lett. 69: 386-388.
Delville, A. & Laszlo, P., 1983. Biophys.Chem. 17: 119-124.
Dhaese, A., 1977. Thesis, State University, Gent.
van Dijk, H., 1960. Sci.Proc.Royal Dublin Soc. A1: 163-176.
van Dijk, H., 1971. Geoderma 5: 53-67.
Dolar, D. & Peterlin, A., 1969. J.Chem.Phys. 50: 3011-3015.
Doty, P. & Ehrlich, G., 1952. Ann.Rev.Phys.Chem. 3: 81-108.
Drift, W.P.J.T. van der, 1975. Thesis, State University, Utrecht.

Dubin, P.L. & Strauss, U.P., 1975. In: 'Polyelectrolytes and their Applications' (Rembaum, A. & Sélégny, E., Eds), D. Reidel Publ. Comp., Dordrecht, pp. 3-30.
Dunsch, L., Feist, U. & Morgenstern, J., 1983. Acta Polymerica 34: 73-75.
Durrant, P.J. & Durrant, B., 1970. 'Introduction to Advanced Inorganic Chemistry', Sec.Ed., Longmans Ltd., London.

Eisenberg, H. & Fuoss, R.M., 1954. In: 'Modern Aspects of Electrochemistry', Vol. I (Bockris, J. O'M. & Conway, B.E., Eds), Butterworths, London, pp. 1-46.
Eisenberg, H., 1958. J.Polymer Sci. 30: 47-66.
Eisenberg, H., 1977. Biophys.Chem. 7: 3-13.
Eldridge, R.J. & Treloar, F.E., 1970. J.Phys.Chem. 74: 1446-1449.
Eldridge, R.J., 1973. Proc.Polymer Topics, May: 143-147.
Eldridge, R.J. & Treloar, F.E., 1976. J.Phys.Chem. 80: 1513-1516.
Elenkova, N.G. & Nedelcheva, T.K., 1976. J.Electroanal.Chem. 69: 385-395.
Elgala, A.M., El-Damaty, A.H. & Abdel-Latif, I., 1976. Z.Pflanzenern.Bodenk. 139: 293-300.
Ernst, R., Allen, H.E. & Mancy, K.H., 1975. Water Res. 9: 969-979.

Felber, B.J., Hodnett, E.M. & Purdie, N., 1968. J. Phys. Chem. 72: 2496-2500.
Felber, B.J. & Purdie, N., 1971. J.Phys.Chem. 75: 1136-1140.
Ficker, H.K., Ostensen, H.N., Schlossel, R.H., Scott, F., Spritzer, M. & Meites, L., 1978. Anal.Chim.Acta 98: 163-169.
Flaig, W., Beutelspacher, H. & Rietz, E., 1975. In: 'Soil Components', Vol. I (Gieseking, J.E., Ed.), Springer, Berlin, pp. 1-211.
Flanagan, J.B., Takahashi, K. & Anson, F.C., 1977a. J.Electroanal.Chem. 81: 261-273.
Flanagan, J.B., Takahashi, K. & Anson, F.C., 1977b. J.Electroanal.Chem. 85: 257-266.
Flato, J.B., 1972. Anal.Chem. 44: 75A-87A.
Florence, T.M., 1982. Talanta 29: 345-364.
Fonds, A.W., Brinkman, A.A.A.W. & Los, J.M., 1967. J.Electroanal.Chem. 14: 43-56.
Frei, Y.F. & Miller, I.R., 1965. J.Phys.Chem. 69: 3018-3023.
Friedman, R.A.G. & Manning, G.S., 1984. Biopolymers, in press.
Frimmel, F.H., 1979a. Vom Wasser 53: 243-247.
Frimmel, F.H., 1979b. Z.Wasser Abwasser Forsch. 12: 206-209.
Frimmel, F.H., 1981. Z.Wasser Abwasser Forsch. 14: 7-10.
Frimmel, F.H., Geywitz, J. & Quentin, K., 1981. Vom Wasser 57: 185-198.
Fuoss, R.M., 1948. Science 108: 545.

Gamble, D.S., 1970. Can.J.Chem. 48: 2662-2669.
Gamble, D.S., 1973. Can.J.Chem. 51: 3217-3222.
Gamble, D.S., Underdown, A.W. & Langford, C.H., 1980. Anal.Chem. 52: 1901-1908.
Gamble, D.S., Schnitzer, M., Kerndorff, H. & Langford, C.H., 1983. Geochim.Cosmochim.Acta 47: 1311-1323.
Gardiner, J., 1974a. Water Res. 8: 23-30.
Gardiner, J., 1974b. Water Res. 8: 157-164.
Ghosh, K. & Mukherjee, S.K., 1972. J.Indian Chem.Soc. 49: 89-94.
Ghosh, K. & Schnitzer, M., 1980. Soil Sci. 129: 266-276.
Ghosh, K. & Schnitzer, M., 1981. Soil Sci.Soc.Amer.J. 45: 25-29.
Ghosh, K. & Schnitzer, M., 1982. Geoderma 28: 53-56.
Gillam, A.H. & Riley, J.P., 1982. Anal.Chim.Acta 141: 287-299.
Goldberg, R.N., 1981. J.Phys.Chem.Ref.Data 10: 44-46.
Green, J.B. & Manahan, S.E., 1979. Anal.Chem. 51: 1126-1129.
Gregor, H.P., Luttinger, L.B. & Loebl, E.M., 1955a. J.Phys.Chem. 59: 43-39.
Gregor, H.P., Luttinger, L.B. & Loebl, E.J., 1955b. J.Phys.Chem. 59: 366-368.
Gregor, H.P., Gold, D.H. & Frederick, M., 1957. J.Polymer Sci. 23: 467-475.
Greter, F.-L., Buffle, J. & Haerdi, W., 1979. J.Electroanal.Chem. 101: 211-229.
Guéron, M. & Weisbuch, G., 1979. J.Phys.Chem. 83: 1991-1998.
Guéron, M. & Weisbuch, G., 1980. Biopolymers 19: 353-382.
Guéron, M. & Weisbuch, G., 1981. Biochimie 63: 821-825.
Guéron, M., 1982. In: 'Ionic Liquids, Molten Salts and Polyelectrolytes', (Bennemann, K.-H., Brouers, F. & Quitmann, D., Eds), Springer Verlag, Berlin, pp. 212-234.

Gunnarsson, G. & Guvtavsson, H., 1982. J.Chem.Soc., Faraday Trans. 1 78: 2901-2910.
Gustavsson, H., Lindman, B. & Bull, T., 1978. J.Amer.Chem.Soc. 100: 4655-4661.
Guy, R.D. & Chakrabarti, C.L., 1976. Can.J.Chem. 54: 2600-2611.

Hanck, K.W. & Dillard, J.W., 1977. Anal.Chim.Acta 89: 329-338.
Harding, I.H. & Healy, T.W., 1979. Prog.Water Techn. 11: 265-273.
Hart, B.T., 1981. Env.Techn.Lett. 2: 95-110.
Hayano, S., Shinozuka, N. & Hyakutake, M., 1982. Yukagaku 31: 357-362.
Hayes, M.H.B. & Swift, R.S., 1978. In: 'The Chemistry of Soil Constituents', (Greenland, D.J. & Hayes, M.H.B., Eds), J. Wiley & Sons, Chichester, pp. 179-320.
Hershenson, H.M., Brooks, R.T. & Murphy, M.E., 1957. J.Amer.Chem.Soc. 79: 2046-2048.
Himes, F.L. & Barber, S.A., 1957. Soil Sci.Soc.Amer.Proc. 22: 368-373.
Holtzclaw, K.M. & Sposito, G., 1979. Soil Sci.Soc.Amer.J. 43: 318-323.
Huizenga, J.R., Grieger, P.F. & Wall, F.T., 1950. J.Amer.Chem.Soc. 72: 2636-2642.
Hunt, J.P., 1963. 'Metal Ions in Aqueous Solution', Benjamin W.A. Inc., New York, p. 16.
Hurst, H.M. & Burges, N.A., 1967. In: 'Soil Biochemistry', Vol. I, (McLaren, D.A. & Peterson, G.H., Eds), Marcel Dekker Inc., New York, pp. 260-286.

Ikeuchi, H., Iwai, K., Kanedo, M., Maya, M. & Sato, G.P., 1979. Bull.Chem.Soc.Japan 52: 1863-1864.
Ilkovič, D., 1934. Coll.Czech.Chem.Commun. 6: 489-531.
Inoue, S., Yamaoka, K. & Miura, M., 1971. Bull.Chem.Soc.Japan 44: 1443.
Irving, H. & Williams, R.J.P., 1948. Nature 162: 746-747.
Irving, H. & Williams, R.J.P., 1953. J.Chem.Soc.: 3192-3210.
Ise, N., 1978. J. Polymer Sci.: Polymer Symp. 62: 205-226.
Ise, N. & Okubo, T., 1978. Macromolecules 11: 439-447.
Ise, N., Okubo, T. & Kunugi, S., 1982. Acc.Chem.Res. 15: 171-177.
IUPAC, 1952. J.Polymer Sci. 8: 257.

Jacobsen, E. & Lindseth, H., 1976. Anal.Chim.Acta 86: 123-127.
Jakubowski, A.F., 1975. Thesis, State University of Buffalo.
James, R.O., Stiglich, P.J. & Healy, T.W., 1975. Faraday Disc. 59: 142-156.
James, R.O. & Parks, G.A., 1982. Surface and Colloid Science 12: 119-216.
Janik, B. & Sommer, R.G., 1973. Biophys.J. 13: 449-461.
Jellinek, H.H.G. & Sangal, S.P., 1972. Water Res. 6: 305-314.
Jones, A.K., Johnson, M.S. & Bell, R.M., 1981. In: 'Heavy Metals in the Environment', CEP Consultants, Edinburgh, pp. 375-382.
Joshi, Y.M. & Kwak, J.C.T., 1980. Biophys.Chem. 12: 323-328.
Joshi, Y.M. & Kwak, J.C.T., 1981. Biophys.Chem. 13: 65-75.

Kačena, V. & Matoušek, L., 1953. Coll.Czech.Chem.Commun. 18: 294.
Kagawa, I. & Gregor, H.P., 1957. J.Polymer Sci. 23: 477-484.
Kanedo, M. & Tsuchida, E., 1981. Macrom.Rev. 16: 397-522.
Karenzi, P.C., Meurer, N., Spegt, P. & Weill, G., 1979. Biophys.Chem. 9: 181-194.
Katchalsky, A. & Spitnik, S., 1947. J.Polymer Sci. 2: 432-446.
Katchalsky, A., 1971. Pure Appl.Chem. 26: 327-373.
Kelkar, S.S. & Nemade, B.I., 1979. Indian J.Chem. 18A: 534-535.
Kerndorff, H. & Schnitzer, M., 1980. Geochim.Cosmochim.Acta 44: 1701-1708.
Khalaf, K.Y., MacCarthy, P. & Gilbert, T.W., 1975. Geoderma 14: 319-340.
Khan, S.U., 1969. Soil Sci.Amer.Proc. 33: 851-854.
Khanna, S.S. & Stevenson, F.J., 1962. Soil Sci. 93: 298-305.
Kharkats, Y.I., 1978. Elektrokhimiya 14: 969-970.
Kielman, H.S., van der Hoeven, J.M.A.M. & Leyte, J.C., 1976. Biophys.Chem. 4: 103-111.
Klemenčic, V. & Filipović, I., 1958. Croat.Chim.Acta 30: 99-101.
Koda, M., Namekawa, K. & Horinchi, T., 1982. Bull.Chem.Soc.Japan 47: 2011-2016.
Kodama, M. & Murray, R.W., 1965. Anal.Chem. 37: 1638-1643.
Kolawole, E.G. & Mathieson, S.M., 1977. J.Polymer Sci.: Polymer Chem.Ed. 15: 2291-2302.
Kolawole, E.G. & Mathieson, S.M., 1979. J.Polymer Sci.: Polymer Lett.Ed. 17: 573-578.

Kolawole, E.G. & Bello, M.A., 1980. Eur.Polymer J. 16: 325-332.
Kolawole, E.G. & Olayemi, J.Y., 1981. Macromolecules 14: 1050-1054.
Kolthoff, I.M. & Lingane, J., 1952. 'Polarography', Vol. 1 & 2, Interscience, New York.
Kotin, L. & Nagasawa, M., 1962. J.Chem.Phys. 36: 873-879.
Kotliar, A.M. & Morawetz, H., 1955. J.Amer.Chem.Soc. 77: 3692-3696.
Kowblansky, M. & Zema, P., 1981. Macromolecules 14: 1451-1456.
Kretz, R. & Völker, T., 1964. Landw.Forschung 17: 83-92.
Kreuter, J., 1983. Intern. J.Pharmaceutics 14: 43-58.
Kříbek, B., Kaigl, J. & Oružinský, V., 1977. Chem.Geol. 19: 73-81.
Kurenkov, V.F., Gazina, F.I. & Myagchenkov, V.A., 1977. Anal.Khim. 32: 712.
Kurenkov, V.F., Achmed'yanova, R.A. & Myagchenkov, V.A., 1979. Electrochimica Acta 24: 949-951.
Kurenkov, V.F., Akhmed'yanova, R.A. & Myagchenkov, V.A., 1981. Acta Polymerica 32: 612-615.
Kurucsev, T. & Steel, B.J., 1967. Rev.Pure Appl.Chem. 17: 149-157.
Kuwatsuka, S., Tsutsuki, K. & Kumada, K., 1978. Soil Sci.Plant Nutr. 24: 337-347.
Kwak, J.C.T. & Hayes, R.C., 1975. J.Phys.Chem. 79: 265-269.
Kwak, J.C.T., Morrison, N.J., Spiro, E.J. & Iwasa, K., 1976. J.Phys.Chem. 80: 2753-2761.

Lakatos, B., Meisel, J. & Mády, G., 1977. Acta Agron.Acad.Sci.Hung. 26: 259-271.
Langford, C.H., Gamble, D.S., Underdown, A.W. & Lee, S., 1983. In: 'Aquatic and Terrestrial Humic Materials' (Christman, R.F. & Gjessing, E.T., Eds.) Ann Arbor Science Publ., Michigan, pp. 219-237.
Lapanje, S. & Oman, S., 1962. Makromolekulare Chemie 53: 46-51.
Lapanje, S., 1964. Biopolymers 2: 585-592.
Lapanje, S. & Oman, S., 1965. Vest.Slov.Kemijsk.Drus. 12: 25-31.
Lapanje, S., 1966. Biopolymers 4: 85-89.
Lapen, A.J. & Seitz, W.R., 1982. Anal.Chim.Acta 134: 31-38.
Leden, I., Z., 1941. Z.Phys.Chem. 188: 160.
van Leeuwen, H.P., 1979a. Anal.Chem. 51: 1322-1323.
van Leeuwen, H.P., 1979b. J.Electroanal.Chem. 99: 93-102.
van Leeuwen, H.P., 1980. Anal.Chem.Symp.Series 2: 383-397.
van Leeuwen, H.P., 1981. In: 'Heavy Metals in the Environment', Int.Conf. Amsterdam 1981, CEP Consultants Ltd., Edinburgh, pp. 581-584 (1981).
van Leeuwen, H.P., Threels, W.F. & Cleven, R.F.M.J., 1981. Coll.Czech.Chem.Commun. 46: 3027-3937.
van Leeuwen, H.P., 1982. J.Electroanal.Chem. 133: 201-209.
van Leeuwen, H.P., Sluyters-Rehbach, M. & Holub, K., 1982. J.Electroanal.Chem. 135: 13-24.
Leyte, J.C. & Mandel, M., 1964. J.Polymer Sci. A2: 1879-1891.
Leyte, J.C., Zuiderweg, L.H. & van Reisen, M., 1968. J.Phys.Chem. 72: 1127-1132.
Lichtenbelt, J.W.Th., 1972. J.Electroanal.Chem. 37: 283-290.
Lind, C.J., 1978. Env.Sci. & Techn. 12: 1406-1410.
Linse, P., Gustavsson, H. & Lindman, B., 1981. J.magn.Res. 45: 133-141.
Liquori, A.M., Ascoli, F., Botré, C., Crescenzi, V. & Mele, A., 1959. J.Polymer Sci. 40: 169-178.
Loebl, E.M., Luttinger, L.B. & Gregor, H.P., 1955. J.Phys.Chem. 59: 559-560.
Loebl, E.M. & O'Neill, J.J., 1960. J.Polymer Sci. 45: 538-540.

Magdelenat, H., Turq, P. & Chemla, M., 1974. Biopolymers 13: 1535-1548.
Mandel, M. & Leyte, J.C., 1964a. J.Polymer Sci. A2: 2883-2899.
Mandel, M. & Leyte, J.C., 1964b. J.Polymer Sci. A2: 3771-3780.
Mandel, M., 1967. J.Polymer Sci. C16: 2955-2962.
Mandel, M., 1970. Eur. Polymer J. 6: 807-822.
Manning, G.S. & Zimm, B.H., 1965. J.Chem.Phys. 43: 4250-4259.
Manning, G.S., 1969a. J.Chem.Phys. 51: 924-933.
Manning, G.S., 1969b. J.Chem.Phys. 51: 934-938.
Manning, G.S., 1969c. J.Chem.Phys. 51: 3249-3252.
Manning, G.S., 1972. Ann.Rev.Phys.Chem. 23: 117-140.

Manning, G.S. & Holtzer, A., 1973. J.Phys.Chem. 77: 2206-2212.
Manning, G.S., 1974. In: 'Polyelectrolytes', Vol. I (Sélégny, E., Ed.), D. Reidel, Dordrecht, pp. 9-37.
Manning, G.S., 1975. J.Phys.Chem. 79: 262-265.
Manning, G.S., 1977a. Biophys.Chem. 7: 141-145.
Manning, G.S., 1977b. Biophys.Chem. 7: 95-102.
Manning, G.S., 1978a. Biophys.Chem. 9: 65-70.
Manning, G.S., 1978b. Q.Rev.Biophys. 11: 179-246.
Manning, G.S., 1979a. Biopolymers 18: 2357-2358.
Manning, G.S., 1979b. Acc.Chem.Res. 12: 443-449.
Manning, G.S., 1981a. Biopolymers 20: 2337-2350.
Manning, G.S., 1981b. J.Phys.Chem. 85: 870-877.
Mantoura, R.F.C.; Dickson, A. & Riley, J.P., 1978. Est.Coast.Mar.Sci. 6: 387-408.
Mantoura, R.F.C., 1981. In: 'Marine Organic Chemistry' (Duursma, E.K. & Dawson, R., Eds.), Elsevier Sci., Publ.Comp., Amsterdam, pp. 179-223.
Marinsky, J.A., 1966. In: 'Ion Exchange', Vol. I (Marinsky, J.A., Ed.), Marcel Dekker, New York, pp. 353-405.
Marinsky, J.A., Imai, N. & Lim, M.C., 1973. Israel J.Chem. 11: 601-622.
Marinsky, J.A. & Ansprach, W.M., 1975. J.Phys.Chem. 79: 439-444.
Marinsky, J.A., 1976. Coord.Chem.Rev. 19: 125-171.
Marinsky, J.A., Wolf, A. & Bunzl, K., 1980. Talanta 27: 461-468.
Marinsky, J.A., 1982. J.Phys.Chem. 86: 3318-3321.
Marinsky, J.A., Gupta, S. & Schindler, P., 1982. J.Colloid Interf.Sci. 89: 401-426.
Martell, A.E., 1975. Pure Appl.Chem. 44: 81-113.
Martell, A.E. & Smith, R.M., 1977. 'Critical Stability Constants', Vol. III, Plenum Press, New York.
Martin, A.E. & Reeve, R., 1958. J.Soil Sci. 9: 89-100.
Mattai, J. & Kwak, J.C.T., 1981. Biophys.Chem. 14: 55-64.
Mattai, J. & Kwak, J.C.T., 1982. J.Phys.Chem. 86: 1026-1030.
Meites, L., Campbell, B.H. & Zuman, P., 1977. Talanta 24: 709-724.
Meurer, B., Spegt, P. & Weill, 1982. Biophys.Chem. 16: 89-97.
Miller, I.R., 1965. J.Phys.Chem. 69: 2740-2743.
Miller, I.R. & Bach, D., 1968. Biopolymers 6: 169-179.
Miyamoto, S., 1979. Biophys.Chem. 9: 79-89.
Miyamoto, S. & Imai, N., 1980. Biophys.Chem. 11: 91-100.
Miyamoto, S., 1981. Biophys.Chem. 14: 341-346.
Morawetz, H., 1965. 'Macromolecules in Solution', Interscience Publ., New York.
Muzzarelli, R.A.A., 1973. 'Natural Chelating Polymers', Pergamon Press, Oxford.
Myagchenkov, V.A. & Kurenkov, V.F., 1976. Dep. Doc. No. Viniti, 265-276.
Myagchenkov, V.A., Kurenkov, V.F. & Frenkel, S.Y., 1977. Vysokomolek.Soedin. 19: 422-424.
Myagchenkov, V.A., Kurenkov, V.F., Sabirzyanova, E.M. & Akhmed'yanova, R.A., 1978. Vysokomolek.Soedin. 20: 1227.

Nagasawa, M. & Holtzer, A., 1964. J.Amer.Chem.Soc. 86: 531-538.
Nagasawa, M., Murase, T. & Kondo, K., 1965. J.Phys.Chem. 69: 4005-4012.
Nagasawa, M., 1971. Pure Appl.Chem. 26: 519-536.
Nagasawa, M., 1974. In: 'Polyelectrolytes', Vol. I (Sélégny, E., Ed.), D. Reidel, Dordrecht, pp. 57-77.
Nagata, I. & Okamoto, Y., 1983. Macromolecules 16: 749-753.
Nallet, F., Cotton, J.P., Nierlich, M. & Jannink, G., 1982. In 'Ionic Liquids', Molten Salts and Polyelectrolytes' (Bennemann, K.-H., Brouers, F. & Quitmann, D., Eds.), Springer Verlag, Berlin, pp. 175-183.
Nash, K.L. & Choppin, G.R., 1980. J.inorg.nucl.Chem. 42: 1045-1050.
Neumann, E. & Nolte, H., 1981. J.Bioelectrochem.Bioenerg. 8: 89-101.
Newman, J., 1966. I & EC Fundamentals 5: 525-529.
Newman, J., 1973. 'Electrochemical Systems', Prentice Hall, Englewood Cliffs.
Nieboer, E. & Richardson, D.H.S., 1980. Env.Pollution B1: 3-26.
Nishikawa, H. & Tsuchida, E., 1976. Bull.Chem.Soc.Japan 49: 1545-1548.
Noji, S. & Yamaoka, K., 1979. Macromolecules 12: 1110-1111.

Nürnberg, H.W. & Valenta, P., 1975. Phys.Chem.Sci.Res.Rept. 1: 87-136.
Nürnberg, H.W., 1978. Acta Universitas Upsaliensis 12: 270-307.

Oden, S., 1912. Ber.Deutsche Chem.Gesellsch. 35: 651-660.
Odijk, T., 1983. Chem.Phys.Lett. 100: 145-150.
Okada, S., Yoshizawa, S., Hine, F. & Asada, K., 1959. J.Electrochem.Soc.Japan (Overseas ed.) 27: E51-E52.
Olofsson, G. & Vlasenko, K., 1982. Acta Chem.Scand. A36: 485-488.
O'Neill, J.J., Loeble, E.M., Kandanian, A.Y. & Morawetz, H., 1965. J.Polymer Sci. A3: 4210-4204.
Oosawa, F., 1971. 'Polyelectrolytes', Marcel Dekker, Inc., New York.
Orlov, D.S. & Erosiceva, N.L., 1967. Vestnik Moskovsk.Univers.Biol.Pochv. 11: 84-95.
O'Shea, T.A. & Mancy, K.H., 1976. Anal.Chem. 48: 1603-1607.
O'Shea, T.A. & Mancy, K.H., 1978. Water Res. 12: 703-711.
Osteryoung, J.G., Christie, J.H. & Osteryoung, R.A., 1975. Bull.Soc.Chim.Belg. 84: 647-656.
Osteryoung, J.G. & Kirowa-Eisner, E., 1980. Anal.Chem. 52: 62-66.
Oth, A. & Doty, P., 1952. J.Phys.Chem. 56: 43-50.
Overbeek, J.Th.G., 1953. J.Colloid Sci. 8: 593-605.
Overbeek, J.Th.G., 1976. Pure Appl.Chem. 46: 91-101.
Oyama, N. & Matsuda, H., 1977. J.Electroanal.Chem. 78: 89-102.
Oyama, N., Shirato, T. & Matsuda, H., 1977. J.Electroanal.Chem. 81: 67-77.

Pagenkopf, G. & Whitworth, C., 1981. J.inorg.nucl.Chem. 43: 1219-1222.
Paleček, E., 1981. Bioelectrochem.Bioenerg. 8: 469-477.
Paoletti, S., Delben, F. & Crescenzi, V., 1976. J.Phys.Chem. 80: 2564-2568.
Parsons, R., 1980. Surface Sci. 101, 316-326.
Parry, E.P. & Osteryoung, R.A., 1965. Anal.Chem. 37: 1634-1637.
Perdue, E.M., Reuter, J.H. & Goshal, M., 1980. Geochim.Cosmochim.Acta 44: 1841-1851.
Piccolo, A. & Stevenson, F.J., 1982. Geoderma 27: 195-208.
Piret, E.L., White, R.G., Walther, H.C.Jr. & Madden, A.J.Jr., 1960. Sci.Proc.Dublin Soc. A1: 69-79.
Plochocka, K. & Wojnarovski, T.J., 1971. Eur.Polymer J. 7: 797-804.
Posner, A.M., 1964. Proc. 8th Congress of Soil Science, Bucharest, 161-174.
Posner, A.M., 1966. J.Soil Sci. 17: 65-78.
Prasad, B. & Sinha, M.K., 1981. Plant Soil 63: 439-448.
Prigogine, I. & Stengers, I., 1984. "Order out of Chaos, Man's new dialogue with nature", Bantam Books, New York.
Putilina, V.S. & Varentsov, I.M., 1980. Chem.Erde 39: 298-310.

Quadrifoglio, F., Crescenzi, V. & Delben, F., 1973. Macromolecules 6: 301-303.

Rajalakshmi, N., Sivarajan, S.R. & Vold, R.D., 1959. J.Coll.Sci. 14: 419-429.
Ralston, J. Lyklema, J. & van Vliet, T., 1981. J.Colloid Interf.Sci. 82: 53-61.
Ramaley, L., Dalziel, J.A. & Tan, W.T., 1981. Can.J.Chem. 59: 3334-3340.
Ramanathan, G.V. & Woodbury, C.P.Jr., 1982. J.Chem.Phys. 77: 4133-4140.
Rao, M.S.N. & Lal, H., 1958. J.Amer.Soc. 80: 3233-3226.
Record, M.T.Jr., Lohman, T.M. & de Haseth, P., 1976. J.Mol.Biol. 107: 145-158.
Record, M.T.Jr., Anderson, C.F. & Lohman, T.M., 1978. Q.Rev.Biophys. 11: 103-178.
Reuter, J.H. & Perdue, E.M., 1977. Geochim.Cosmochim.Acta 41: 325-344.
Richards, E.G., 1980. 'An Introduction to the Physical Properties of Large Molecules in Solution', Cambridge University Press, Cambridge, pp. 199-242.
Rinaudo, M. & Daune, M., 1967. J.Chimie Phys. 63: 1753-1760.
Rinaudo, M. & Milas, M., 1970. C.R.Acad.Sci.Paris C271: 1170-1172.
Rinaudo, M. & Milas, M., 1972. Eur.Polymer J. 8: 737-746.
Ritchie, G.S.P., Posner, A.M. & Ritchie, I.M., 1981. J.Electroanal.Chem. 123: 397-407.
Ritchie, G.S.P. & Posner, A.M., 1982. Soil Sci. 33: 233-247.
Ritchie, G.S. Posner, A.M. & Ritchie, I.M., 1982. J.Soil Sci. 33: 671-677.
Robinson, R.A. & Stokes, R.H., 1955. 'Electrolyte Solutions', Butterworths, London.
Rochus, W., 1982. Telma 12, 161-173.

Saar, R.A. & Weber, J.H., 1979. Can.J.Chem. 57: 1263-1268.
Saar, R.A., 1980. Thesis, University of New Hampshire.
Saar, R.A. & Weber, J.H., 1980a. Env.Sci. & Techn. 14: 877-880.
Saar, R.A. & Weber, J.H., 1980b. Geochim.Cosmochim.Acta 44: 1381-1384.
Saar, R.A. & Weber, J.H., 1982. Env.Sci.Techn. 16: 510A-517A.
Saha, S.K., Dutta, S.L. & Chakravarti, S.K., 1979. J.Indian Chem.Soc. 56: 1129-1134.
Sasaki, S. & Minakata, A., 1980. Biophys.Chem. 11: 199-216.
Saroff, H.A. & Mark, H.J., 1953. J.Amer.Chem.Soc. 75: 1420-1426.
Schmidtpott, H., 1980. Laborpraxis, January/February, 28-34.
Schnitzer, M. & Skinner, S.I.M., 1963. Soil Sci. 96: 86-93.
Schnitzer, M. & Skinner, S.I.M., 1966. Soil Sci. 102: 361-365.
Schnitzer, M. & Skinner, S.I.M., 1967. Soil Sci. 103: 247-252.
Schnitzer, M., 1969. Soil Sci.Soc.Amer.Proc. 33: 75-81.
Schnitzer, M. & Hansen, E.H., 1970. Soil Sci. 109: 333-340.
Schnitzer, M. & Khan, S.U., 1976. 'Humic Substances in the Environment', Marcel Dekker, New York.
Schnitzer, M. & Ghosh, K., 1979. J.Indian Chem.Soc. 56: 1090-1093.
Schwabe, K., Suschke, H,-D. & Wachler, G., 1980. Electrochim.Acta 25: 59-76.
Schwartz, T. & Francois, J., 1981. Makromolekulare Chemie 182: 2775-2787.
Shah, R.K., Chokshi, M.R. & Soni, K.P., 1977. J.Indian Chem.Soc. 54: 912-914.
Sharma, M.R., Chandra, H. & Kumar, A., 1978. Agra.Univ.J.Res.Sci. 27: 15-18.
Shimizu, T., Minakata, A. & Imai, N., 1981. Biophys.Chem. 14: 333-339.
Shuman, M.S. & Woodward, G.P.Jr., 1977. Env.Sci.& Techn. 11: 809-813.
Sillén, L.G. & Martell, A.E. 'Stability Constants of Metal Complexes', Special Publication No. 17, The Chemical Society, London (1964); Special Publication No. 25, The Chemical Society, London (1971).
Silva, S., Zanetti, B., Burzoni, E., Dell'Agnola, G. & Nardi, S., 1981. Agrochimia 25: 132-141.
Singer, A. & Navrot, J., 1976. Nature 62: 479-481.
Sipos, S., Sipos, É., Dékány, I., Deér, A., Meisel, J. & Lakatos, B., 1978. Acta Ágron.Acad.Sci.Hung. 27: 31-42.
Skogerboe, R.K., Wilson, S.A. & Osteryoung, J.G., 1980. Anal.Chem. 52: 1960-1962.
Slavek, J. & Pickering, W.F., 1981. Water Air Soil Poll. 16: 209-221.
Slavek, J., Wold, J. & Pickering, W.F., 1982. Talanta 29: 743-749.
Slota, P.Jr., 1979. Thesis, State University New York, Buffalo.
Sohn, M.L. & Hughes, M.C., 1981. Geochim.Cosmochim.Acta 45: 2393-2399.
Spegt, P., Tondre, C., Weill, G. & Zana, R., 1973. Biophys.Chem. 1: 55-61.
Spegt, P. & Weill, G., 1976. Biophys.Chem. 4: 143-149.
Sposito, G., Holtzclaw, K.M. & Keech, D.A., 1977. Soil Sci.Soc.Amer.J. 41: 1119-1125.
Sposito, G., Holtzclaw, K.M. & Levesque-Madore, C.S., 1981. Soil Sci.Soc.Amer.J. 45: 465-468.
Stevenson, F.J.S., 1976. Soil Sci.Soc.Amer.J. 40: 665-672.
Stevenson, F.J., 1982. 'Humus Chemistry', John Wiley & Sons, New York.
Stigter, D., 1975. J.Colloid Interf.Sci. 53: 296-306.
Strauss, U.P., 1958. J.Amer.Chem.Soc. 80: 6498-6500.
Subrahmanya, R.S., 1957. Proc.Indian Acad.Sci. A46: 443-453.
Subrahmanya, R.S., 1960. Adv.Polarography 2: 674-693.
Szalay, A. & Szilágyi, M., 1969. In: 'Advances in Organic Geochemistry 1968' (Schenck, P.A. & Havelaar, I., Eds.), Pergamon Press, Oxford, pp. 567-577.
Szymczak, J., Holyk, P. & Ander, P., 1975. J.Phys.Chem. 79: 269-272.

Takahashi, A., Kagawa, T. & Hayashi, Y., 1957. Kogyo Kagaku Zasshi 60: 1059.
Takamatsu, T & Yoshida, T., 1978. Soil Sci. 125: 377-386.
Tamamushi, R., 1980. J.Electroanal.Chem. 109: 353-356.
Tanford, C., 1951. J.Amer.Chem.Soc. 73: 2066-2070.
Thurman, E.M., Wershaw, R.L. & Pinckney, D.J., 1982. Org.Geochem. 4: 27-35.
Tondre, C., 1982. J.Chem.Soc. Faraday Trans.1: 78: 1795-1808.
Torrence, G., Amdur, S. & Marinsky, J.A., 1971. J.Phys.Chem. 75: 2144-2147.
Travers, C. & Marinsky, J.A. 1974. J.Polymer Sci.: Symp.Ser. 47: 285-297.
Trivedi, H.C., Patel, C.P. Patel, C.K. & Patel, R.D., 1978. Angew.Makromol.Chemie, 70: 39-48.

Tsuchida, E. & Nishide, H., 1977. Adv.Polymer Sci. 24: 1-87.
Tsutsuki, K. & Kuwatsuka, S., 1978. Soil Sci.Plant Nutr. 24: 547-560.
Tuschall, J.R. & Brezonik, P.L. 1984. In: 'Complexation of Trace Metals in Natural Waters' (Kramer, C.J.M. & Duinker, J.C., Eds.), Martinus Nijhoff/Dr. W.J. Junk, Publ., The Hague.

Ueberreiter, K. 1982. Coll.& Polymer Sci. 260: 37-45.

Valenta, P. & Nürnberg, H.W., 1980. Gewässerschutz Wasser Abwasser 44: 105-205.
Varney, M.S., Mantoura, R.F.C., Whitfield, M., Turner, D.R. & Riley, J.P., 1981. IMER-Manuscr. No. 487, Inst.Marine Env.Res., Plymouth.
Venugopal, B. & Luckey, T.P., 1975. In: 'Heavy Metal Toxicity, Safety and Hormology' (Luckey, T.P., Venugopal, B. & Hutcheson, D., Eds.), George Thieme, Stuttgart, pp. 4-73.
Verloo, M. & Cottenie, A., 1972. Pedologie 22: 174-184.
Veselý, J., Weiss, D. & Štulik, K., 1978. 'Analysis with Ion Selective Electrodes', Ellis Horwood Ltd., Chichester, pp. 198-199.
Vink, H., 1981. J.Chem.Soc.Faraday Trans.1: 77: 2439-2449.
Vink, H., 1982. Makromol.Chem. 183: 2273-2283.
Vinkler, P., Lakatos, B. & Meisel, T., 1975. Agrókemia és Talajtan 24: 137.
Vinkler, P., Lakatos, B. & Meisel, J., 1976. Geoderma 15: 231-242.
Visser, S.A., 1982. Pedologie 32, 163-174.
van Vliet, T. & Lyklema, J., 1978. J.Colloid Interf.Sci. 63: 97-105.
van Vliet, T. & Lyklema, J., 1979. J.Colloid Interf.Sci. 69: 332-333.
Vogelaar, E.F., 1980. Paramedica 7: 31-32.
Völker, Th., 1961a. Makromol. Chemie 44/46: 107-122.
Völker, Th., 1961b. Österr. Chem. Z. 62: 345-351.

Wall, F.T. & Doremus, R.H., 1954. J.Amer.Chem.Soc. 76: 1557-1560.
Wall, F.T. & Gill, S.J., 1954. J.Phys.Chem. 58: 1128-1130.
Wang, J.H., 1954. J.Amer.Chem.Soc. 76: 1528-1532.
Weisbuch, G. & Guéron, M., 1981. J.Phys.Chem. 85: 517-525.
Weiss, S., Diebler, H. & Michaeli, J. 1971. J.Phys.Chem. 75: 267-271.
van der Werff, M., 1981. Thesis, Free University, Amsterdam.
Wershaw, R.L. & Pinckney, D.J., 1971. Geol.Survey Res.Paper, 750-D, 216-218.
Whitworth, C. & Pagenkopf, G.K., 1979. J.inorg.nucl.Chem. 41, 317-321.
Whitworth, C.G., 1982. Thesis, Montana State University.
Wiegman-Ho, L. & Ketelaar, J.A.A., 1983. J.Dent.Res. 62: 105-108.
Williams, D.R., 1971. 'Metals of Life', van Nostrand Reinhold Company, London.
Wilson, S.A., Huth, T.C., Arndt, R.E. & Skogersboe, R.K.; 1980. Anal.Chem. 52: 1515-1518.
World Health Organization Report, 1982. 'Micropollutants in River Sediments', Euro Reports and Studies 61.

Yadav, R.P., Chandra, H. & Kumar, A., 1973. Agra University J.Res.(Sci.) 22: 83-88.
Yamada, R., Tamura, K., Harada, S. & Yasunaga, T., 1982. Bull.Chem.Soc.Japan 55: 3413-3416.
Yamashita, F., Komatsu, T. & Nakagawa, T., 1976. Bull.Chem.Soc.Japan 49: 2073-2076.
Yamashita, F., Komatsu, T. & Nakagawa, T., 1979a. Bull.Chem.Soc.Japan 52: 30-33.
Yamashita, F., Komatsu, T. & Nakagawa, T., 1979b. Bull.Chem.Soc.Japan 52: 1251-1254.
Yoshida, N., 1978. J.Chem.Phys. 69: 4867-4871.
Yoshida, N., 1982. Chem.Phys.Lett. 90: 207-210.
Young, S.D., Bache, B.W., Welch, D. & Anderson, H.A., 1981. J.Soil Sci. 32: 579-592.
Young, S.D., Bache, B.W. & Linehan, D.J., 1982. J.Soil Sci. 33: 467-475.

Zunino, H., Peirano, P., Aguilera, M. & Schalscha, E.B., 1975. Soil Sci. 119, 210-216.
Zunino, H. & Martin, J.P., 1977a. Soil Sci. 123: 65-76.
Zunino, H. & Martin, J.P., 1977b. Soil Sci. 123: 188-202.
Zunino, J., Aguilera, M., Caiozzi, M., Peirano, P., Borie, F. & Martin, J.P., 1979. Soil Sci. 128: 257-266.

SYMBOLS & ABBREVATIONS

Symbols

a	radius polyion cylinder
A	surface area
A'; A"	constant: in eq. (3.47); in eq. (3.37)
b	distance separating functional groups on polyion
b_1; b_2	constant: in eq. (3.14); in eq. (3.23)
B	$([M]_b \cdot [H]^2)/([M]_f \cdot [HL]^2)$
B'; B"	constant: in eqs. (3.12-14); in eq. (3.37)
c_1; c_2	concentration: monovalent metal ions; divalent metal ions
c_b; c_f	concentration (divalent) metal ions: bound; free
c_p	(overall) polyacid concentration: $-COO^-$ *and* -COOH groups
c_r	concentration of species r
c*	bulk concentration
D; D_r	diffusion coefficient; of species r
D_b; D_f	diffusion coefficient of (divalent) metal ions: bound; free
D_c; D_o	diffusion coefficient of uncondensed counterions: in the presence of polyacid; in the absence of polyacid
D_p	diffusion coefficient of the polyion
$\bar{D}$	mean diffusion coefficient
e	elementary charge; base number of Naperian logarithm
E	(pulse) potential
E_D; E_ℓ	potential: *Donnan*; liquid junction
E_i; $E_{1/2}$	potential: initial; half-wave
E_{st}	a standard potential of an electrochemical cell
$\Delta E_{1/2}$	shift in the half-wave potential
f	fractional coefficient in eq. (3.45)
F	*Faraday* constant
ΔG_{el};ΔG_{int}	contribution to the change in free energy of the metal association: electrical; intrinsic
$\Delta[H^+]$	proton production (in M/L-titrations)
i; i_r; i_m	current; current carried by species r; conduction current
i_c; i_f	charging current; faradaic current
i_d, i_ℓ	diffusion current; limiting current
Δi_ℓ	change of the limiting current
j	coordination number
k	*Boltzmann* constant
k_a; k_d	rate constant: association; dissociation

K_a	intrinsic acid dissociation constant
K_{app}	apparent acid dissociation constant in the presence of heavy metal ions
$K_{app,a}$	apparent acid dissociation constant in the absence of heavy metal ions
$K_{app,j}$	apparent metal association constant
K_1; K_2	short notation for $K_{app,j}$: j=1; j=2
K_1^*; K_2^*	$K_1 \cdot K_a^2$; $K_2 \cdot K_a^2$
K_{av}	'average' acid dissociation (or metal association) constant in HH-equation
K_{ex}	equilibrium constant of the M^+/M^{2+} exchange reaction
K_h	hydrolysis constant of metal-aquo complex
$K_{int,j}$	intrinsic metal association constant
K_M	apparent metal association constant in *Manning's* formulary
$[L]$;$[L]_f$	ligand concentration: carboxylate groups; free carboxylate groups
m	prelogarithmic factor in HH-equation
$[M]_a$	concentration of the added divalent metal ions
$[M]_b$;$[M]_f$	metal ion concentration: bound; free
$\bar{M}$	average molecular mass
n	valence; number of electrons transferred in reduction metal ions; degree of polymerization
N_A	number of *Avogadro*
P	$\exp[(nF/RT)(E-E_{\frac{1}{2}})]$ in eq. (3.6)
r	radius; ionic species; class of sites
r_b	radius of the cylinder containing bound ions
r_f	effective radius of the free metal ions
r_p	radius of gyration of the polymer coil
R	gas constant; relative concentration 1:1 salt
S_c	$d\log K_1/d\log c_1^{-1}$
S_m	$(d[H]/d[M]_a)_{max}$
t	time
t_d	drop period
t_p	effective pulse duration
t_{pp}	pre-pulse period
t_{ps}	sampling period
t_{pt}	total pulse period
t_{pw}	waiting period during pulse, before sampling
t_r	transference number
T	*Kelvin* temperature

u, v, w	stoichiometric coefficients in reaction eq. (2.4)
V_p	volume, per charged ligand, containing condensed ions
w	weight
x	distance from the electrode; from the polyion
$\langle x^2 \rangle$	mean-square displacement
z	charge
z_c; z_r	charge of counterion; charge of species r
α_d	degree of dissociation
α_{eff}	effective degree of dissociation
α_n	degree of neutralization
α_s	linear expansion coefficient
β	slope of $\Delta\kappa_T$ versus $[M]_a$ curve
$\gamma_\pm$; γ_r	mean activity coefficient; activity coefficient of species r
δ	diffusion layer thickness
ε	bulk dielectric constant
η	viscosity
θ_n	number of bound n-valent metal ions per L^- (degree of association)
κ	*Debye* screening parameter
κ_s	conductivity of solution s
$\Delta\kappa$	change of the conductivity of the sample solution
$\Delta\kappa_b$	change of the conductivity of the blank solution
$\Delta\kappa_p$	change of the conductivity of the polyion-containing solution (in M/L-titrations)
$\Delta\kappa_T$	conductivity excess: $\Delta\kappa_b - \Delta\kappa_p$
λ_r; λ'_r	equivalent ionic conductivity of species r: in the absence; in the presence of polyacid
λ°_c	limiting equivalent ionic conductivity of counterion
λ_p	equivalent ionic conductivity of polyion
μ_r	chemical potential of species r
ξ	charge density parameter of linear polyion
ξ_{crit}; ξ_{eff}	charge density parameter: critical value; effective value
ξ_{exp}; ξ_{str}	charge density parameter: experimental value; structural value
τ	(arbitrarily short) period of time
τ_b; τ_f	period of time in which a metal ion is bound; free
ϕ	potential in electrolysis cell
ψ; ψ_s	potential in polyion domain; potential at the binding site on the polyion

Abbreviations

C	conductometry
CC	counterion condensation
CIV_n	concentration of n-valent metal ions in the vicinity of the polyion
CMC	carboxymethylcellulose
DC	direct current polarography
DH	*Debye-Hückel*
DME	dropping mercury electrode
DNA	deoxyribonucleic acid
DOC	dissolved organic carbon
DPP	differential pulse polarography
DS	dextran sulphate
FA	fulvic acid
HA	humic acid
HH	*Henderson-Hasselbalch*
I	ion-selective potentiometry
ISE	ion-selective electrode
K	monovalent metal ion, if not stated otherwise
L	ligand: $-COO^-$ group, if not stated otherwise
l.h.s.	left hand side
loc	local
M	metal ions: divalent, if not stated otherwise
MAC	maleic acid copolymer
NPP	normal pulse polarography
P	polarography
PAA	poly(acrylic acid)
PB	*Poisson-Boltzmann*
PMA	poly(methacrylic acid)
PMApe	partially esterified poly(methacrylic acid)
PP	pulse polarography
PSS	poly(styrene sulphonate)
p.z.c.	point of zero charge
RPP	reverse pulse polarography
sat	saturated
SCE	saturated calomel electrode
SDC	sampled direct current polarography
SMDE	static mercury drop electrode
TOC	total organic carbon

SUMMARY

(1)
Since polycarboxylic acids are weak, their charge density increases with increasing deprotonation. Heavy metal ions can be *physically* bound to the polyions formed, as a result of the strong electrostatic attraction. The effect of the charge density on this binding is defined as the polyelectrolyte effect. Heavy metal ions can also be *chemically* bound to carboxylate groups. Knowledge of the metal/polyacid interaction in which chemical *and* physical binding are important, is far from complete. Such knowledge would be of theoretical interest but also of practical importance. Humic acids (and fulvic acids as well), decay products of plants, can be considered as natural polycarboxylic acids. These acids are mixtures of macromolecules that contain different types of functional groups, mainly carboxylic, that are able to bind heavy metal ions. To a great extent, humic material controls the transport processes and the bioavailability of metal ions in soils and natural waters. The binding in metal/humic acid systems strongly varies with changing conditions. This phenomenon has usually been attributed to a mixture effect, a result of the polyfunctional character of humic acids. In the past, no systematic investigations have been specially aimed at the question whether or not a polyelectrolyte effect is operative in the change of the binding with the conditions. To predict correctly trace metal concentrations in ecosystems, it is necessary to know the relative importance of chemical and physical binding, since they follow different laws. In this thesis, polyelectrolyte effects are characterized for a number of synthetic polycarboxylic acids as model substances, in order to establish the relevance of such effects in the interaction of heavy metal ions with humic acids.

(2)
In several theoretical models for metal/polyacid interaction, the binding of ions is defined and interpreted in largely different ways. In a literature review of experimental work on ion binding to synthetic polycarboxylic acids, several controversies are noted.

(3)
The acids investigated are: poly(acrylic acid), PAA, poly(methacrylic acid), PMA, partially esterified poly(methacrylic acid), PMApe, a humic acid sample, HA, from a brown coal containing soil and a fulvic acid

sample, FA, from the Mare aux Evées (Fontainebleau). Moreover, 2-methylpropanoic acid has been investigated. Cadmium, lead and zinc have been selected as heavy metals. Three electrochemical methods have been applied, viz. pulse polarography, conductometry and potentiometry. Information from each method on the binding characteristics was partly completing and partly confirming that from the other methods. The experimental variables, viz. the metal/polyion ratio (M/L), the degree of neutralization (α_n) and the amount of added 1:1 salt (c_1), have been selected because of their influence on the effective polyion charge density, and their importance in practice.

(4)
From the experiments with the synthetic polyacids, it appears that at low M/L, and $c_1 = 0$, the conductometric binding is virtually complete, irrespective the nature of the metal ion. However, the chemical contribution to the binding energy is different for each system. It increases in the series Zn < Cd < Pb, and PMApe ≤ PMA < PAA. In the presence of 1:1 salt, the binding is not complete. The apparent metal association constant K_1 decreases with increasing M/L, indicating cooperativity of the carboxylate ligands. Values of M/L for which complete binding occurs reasonably agree with predictions form the counterion condensation theory. For the complex formations, a coordination number $j = 1$ is likely.

(5)
Values of K_1 are strongly dependent on α_n. For M/PAA systems, log K_1 increases linearly with the effective degree of dissociation, whereas for M/PMA systems that increase is not linear, as a result of a conformation transition of PMA. When the effective degree of dissociation approaches zero, the values of K_1 become of the same order of magnitude as those for monocarboxylic acids. For high values of the effective charge density, conductometric binding of monovalent metal ions has been demonstrated, in agreement with the counterion condensation criteria.

(6)
For the synthetic systems, the decrease of K_1 with increasing c_1 is much stronger than expected for a pure chemical binding of the metal ions. From the dependence of K_1 on c_1 it can be inferred that at high α_n and low M/L, the exchange ratio bound monovalent metal ions and

bound divalent metal ions is about 2.
However, this ratio is strongly dependent on the values of α_n and M/L. For very low values of c_1, K_1 becomes rather independent of c_1.

(7)
In chapter 7, the characteristics of the polyelectrolyte effects, as described for the synthetic polycarboxylic acid systems, are compared with the results of the interaction of heavy metal ions with humic and fulvic acids. It is shown that a polyelectrolyte effect, in addition to a mixture effect, substantially contributes to the binding of cadmium lead and zinc ions to humic and fulvic acid. The chemical binding increases in the series Cd $\cong$ Zn < Pb, and is weaker for FA than for HA.

(8)
The conclusions in this thesis result in the recommendation that in modelling of ecosystems with respect to trace metal speciation, polyelectrolyte effects should be taken into account.

SAMENVATTING

Titel: ZWAAR-METAAL/POLYZUUR INTERACTIE; een electrochemische studie van de binding van Cd(II), Pb(II) en Zn(II) aan polycarbonzuren en humuszuren.

(1)
Polyzuren zijn polymeren waarvan elk segment een zuurgroep bevat. Bij poly*carbon*zuren kunnen die groepen alle, maar ook voor een deel, worden geneutraliseerd, waarbij negatief geladen carboxylaatgroepen ontstaan. Naarmate de neutralisatiegraad toeneemt, wordt de ladingsdichtheid van het polyion groter. Positief geladen zware-metaalionen kunnen, door electrostatische aantrekking, *fysisch* worden gebonden aan het polyion. De invloed van de ladingsdichtheid op deze binding wordt het polyelectrolyteffect genoemd. Zware-metaalionen vertonen ook vaak *chemische* binding met carboxylaatgroepen, waarbij complexen worden gevormd. De kennis van de interactie van metaalionen met polyzuren waarbij chemische *en* fysische binding belangrijk zijn, is nog zeer onvolledig. Deze kennis is niet alleen van theoretisch maar ook van praktisch belang. Humuszuren (en de ermee verwante fulvinezuren), afbraakprodukten van plantaardig materiaal, kunnen als natuurlijke polycarbonzuren worden beschouwd. Deze zuren zijn mengsels van macromoleculen, die verschillende typen groepen, maar voornamelijk carbonzuurgroepen, bevatten die zware-metaalionen kunnen binden. Ze zijn van groot belang voor het transport van metalen in de bodem en in oppervlaktewater, en bepalen in hoge mate de bodemvruchtbaarheid. De binding van zware-metaalionen met humuszuren is sterk afhankelijk van de omstandigheden. Dit werd veelal toegeschreven aan een mengseleffect, een gevolg van de polyfunctionaliteit van deze zuren. Er is in het verleden vrijwel geen systematisch en doelgericht onderzoek verricht naar de vraag of ook een polyelectrolyteffect van invloed is op de genoemde afhankelijkheid van de binding. Voor het voorspellen van concentraties metaalionen in ecosystemen is het noodzakelijk de mate van chemische dan wel fysische binding te kennen, omdat verschillende wetmatigheden gelden. In dit proefschrift worden eerst voor een aantal synthetische polycarbonzuren, als modelstoffen, polyelectrolyteffecten gekarakteriseerd, om vervolgens het mogelijke belang van zulke effecten bij de interactie van zware-metaalionen met humuszuren te kunnen vaststellen.

(2)
De binding van metaalionen aan polyzuren wordt in diverse theoretische modellen zeer verschillend gedefinieerd en geïnterpreteerd. In een literatuuroverzicht van experimenteel werk met betrekking tot metaalionbinding aan synthetische polycarbonzuren, worden diverse controversen gesignaleerd.

(3)
De onderzochte zuren zijn: poly(acrylzuur), PAA, poly(methacrylzuur), PMA, partieel veresterd poly(methacrylzuur), PMApe, een humuszuur, HA, afkomstig uit een bruinkoolhoudende bodem, en een fulvinezuur, FA, uit de Mare aux Evées (Fontainebleau). Bovendien is ook een monocarbonzuur bestudeerd. Als zware-metaalionen zijn de tweewaardige ionen van cadmium, lood en zink geselecteerd. Drie electrochemische methoden zijn toegepast, t.w. pulspolarografie, conductometrie en potentiometrie. Ze leverden elkaar aanvullende dan wel bevestigende informatie over de bindingskarakteristieken op. De experimentele variabelen, t.w. de metaal/polyion verhouding (M/L), de neutralisatiegraad (α_n) en de hoeveelheid toegevoegd 1:1 zout (c_1), zijn geselecteerd omdat deze elk de effectieve ladingsdichtheid van het polyion kunnen beïnvloeden, en van praktisch belang zijn.

(4)
Uit de experimenten met de synthetische polyzuren blijkt dat bij lage M/L, en $c_1 = 0$, de conductometrisch bepaalde binding vrijwel volledig is, onafhankelijk van de aard van het metaalion. De chemische bijdrage aan de binding is voor elk systeem echter verschillend. Ze loopt op in de series Zn < Cd < Pb en PMApe $\leqslant$ PMA < PAA. Bij aanwezigheid van 1:1 zout is de binding niet volledig. De schijnbare bindingsconstante K_1 neemt af met toenemende M/L, hetgeen wijst op coöperativiteit van de liganden. Met een van de theoretische modellen, de tegenioncondensatie theorie, kunnen M/L waarden waarbij de volledige binding optreedt redelijk worden voorspeld. Voor de complexvorming lijkt een coördinatiegetal j=1 goed te voldoen.

(5)
De neutralisatiegraad heeft sterke invloed op de bindingssterkte. Voor de M/PAA systemen neemt log K_1 lineair toe met de effectieve dissociatiegraad, terwijl voor de M/PMA systemen die toename niet-lineair verloopt als gevolg van een conformatieovergang van dit polyion. Als de effec-

tieve dissociatiegraad tot nul nadert, worden van waarden van K_1 alle van dezelfde orde van grootte als die voor niet-polymere carbonzuren. Voor hoge waarden van de effectieve ladingsdichtheid is ook binding van éénwaardige metaalionen conductometrisch aantoonbaar, conform de tegenioncondensatie theorie.

(6)
Door toevoeging van 1:1 zout aan de synthetische systemen worden de waarden van K_1 veel sterker verlaagd dan op grond van een chemische binding alleen kan worden verwacht. Uit de c_1-afhankelijkheid van de K_1 waarden kan worden afgeleid dat bij hoge α_n en lage M/L, gebonden een- en tweewaardige ionen in de verhouding 2:1 worden uitgewisseld. Deze verhouding is sterk afhankelijk van de waarden van α_n en M/L. Bij zeer lage waarden van c_1 wordt K_1 onafhankelijk van c_1.

(7)
In hoofdstuk 7 wordt de kennis van de polyelectrolyteffecten, opgedaan met de systemen met de synthetische polyzuren, gebruikt bij het bestuderen van de interactie van zware-metaalionen met humuszuren en fulvinezuren. Duidelijk blijkt dat een polyelectrolyteffect, naast een mengseleffect, substantieel kan bijdragen tot de binding van de ionen van cadmium, lood en zink. De chemische binding neemt toe in de reeks Cd $\cong$ Zn < Pb, en is kleiner voor FA dan voor HA.

(8)
De conclusies in dit proefschrift monden uit in de aanbeveling dat bij de analyse van ecosystemen met betrekking tot de speciatie van zware metaalionen rekening dient te worden gehouden met polyelectrolyteffecten.

DANKWOORD

Aan belangrijke gedeelten van het experimentele werk werd meegewerkt door Wim Threels, en - in het kader van hun ingenieursstudie - Egbert Brouwer, Hans van Grinsven, Henri Spanjers en Chris Velzeboer. Op initiatief van Siewert Oost werden enkele metingen uitgevoerd door examenkandidaten van de Analistenschool Amsterdam. Voor deze bijdragen wil ik allen danken.

Het fulvinezuur werd beschikbaar gesteld door de afdeling Analytische Chemie van de Universiteit van Genève. Pour les échantillons de l'acide fulvique, pour l'hospitalité à son laboratoire et pour les discussions enrichissantes, je voudrais remercier Jacques Buffle très cordialement.

De figuren werden getekend en verzorgd door Gerrit Buurman. De tekst werd corrigerend in machineschrift overgebracht door Inga Diraoui en Dory Neijenhuis. Adviezen betreffende de engelse taal werden gekregen van Yvonne Hameleers. Ik ben hen veel dank verschuldigd.

Herman van Leeuwen, die bereid was als co-promotor op te treden, heeft het onderzoek intensief en enthousiasmerend begeleid, waarvoor ik hem zeer dankbaar ben.

Hans Lyklema, die bereid was als promotor op te treden, begeleidde alert de groei van het manuscript, en voorzag het consciëntieus van verrijkende kritiek. Ik wil hem daarvoor van harte danken.

Overigens zou het werkstuk niet tot stand zijn gekomen zonder de uitgebalanceerde stimulering door Margo Huismans.

LEVENSOVERZICHT

Op aanbeveling van het college van dekanen volgt hier een kort levensoverzicht van de schrijver.

Hij werd geboren op 27 januari 1948 te Heerlen, en groeide op in Born. Het HBS-B diploma werd in 1964 behaald aan het Bisschoppelijk College "St. Jozef" te Sittard. Daarna begon hij met de ingenieursstudie aan de Technische Hogeschool Eindhoven, aan de afdeling Scheikundige Technologie. Het afstudeerwerk werd verricht in de vakgroep Anorganische Chemie & Katalyse. De studie werd in 1976 afgesloten met het behalen van het ingenieursdiploma en de onderwijsbevoegdheden voor Natuur- en Scheikunde. Daarna heeft hij tot 1978 onderzoek verricht naar de kristalliniteit van koolhydraten, in de sectie Proceskunde van de vakgroep Levensmiddelentechnologie van de Landbouwhogeschool Wageningen. Aansluitend was hij tot 1980 docent Natuur- en Scheikunde aan het Bisschoppelijk College "St. Jozef" te Weert. Vervolgens werd in de vakgroep Fysische & Kolloïdchemie het onderzoek uitgevoerd naar de interactie van zware metalen met polyzuren waarvan dit proefschrift het resultaat is. Vanaf 1984 is hij werkzaam aan een onderzoek naar de anisotropie van de groei van silicium en gallium arsenide bij chemische depositie uit de gasfase, aan de Katholieke Universiteit Nijmegen, in dienst van de organisatie voor Zuiver Wetenschappelijk Onderzoek.